



Food and Agriculture
Organization of the
United Nations

2019

REMOTE SENSING FOR SPACE-TIME MAPPING OF SMOG IN PUNJAB AND IDENTIFICATION OF THE UNDERLYING CAUSES USING GEOGRAPHIC INFORMATION SYSTEM (R-SMOG)





PUNJAB

FAO in collaboration with
Department of Agriculture Punjab
investigates the crop residue burning
practices of farmers.

©FAO

2019

REMOTE SENSING FOR SPACE-TIME MAPPING OF SMOG IN PUNJAB AND IDENTIFICATION OF THE UNDERLYING CAUSES USING GEOGRAPHIC INFORMATION SYSTEM (R-SMOG)

The designations employed and the presentation of material in this information product do not imply the expression of any opinion whatsoever on the part of the Food and Agriculture Organization of the United Nations (FAO) concerning the legal or development status of any country, territory, city or area or of its authorities, or concerning the delimitation of its frontiers or boundaries. Dashed lines on maps represent approximate border lines for which there may not yet be full agreement. The mention of specific companies or products of manufacturers, whether or not these have been patented, does not imply that these have been endorsed or recommended by FAO in preference to others of a similar nature that are not mentioned.

The views expressed in this information product are those of the author(s) and do not necessarily reflect the views or policies of FAO.

ISBN 978-92-5-131960-4

© FAO, 2020



Some rights reserved. This work is made available under the Creative Commons Attribution-NonCommercial-ShareAlike 3.0 IGO licence (CC BY-NC-SA 3.0 IGO; <https://creativecommons.org/licenses/by-nc-sa/3.0/igo/legalcode>).

Under the terms of this licence, this work may be copied, redistributed and adapted for non-commercial purposes, provided that the work is appropriately cited. In any use of this work, there should be no suggestion that FAO endorses any specific organization, products or services. The use of the FAO logo is not permitted. If the work is adapted, then it must be licensed under the same or equivalent Creative Commons licence. If a translation of this work is created, it must include the following disclaimer along with the required citation: "This translation was not created by the Food and Agriculture Organization of the United Nations (FAO). FAO is not responsible for the content or accuracy of this translation. The original [Language] edition shall be the authoritative edition."

Disputes arising under the licence that cannot be settled amicably will be resolved by mediation and arbitration as described in Article 8 of the licence except as otherwise provided herein. The applicable mediation rules will be the mediation rules of the World Intellectual Property Organization <http://www.wipo.int/amc/en/mediation/rules> and any arbitration will be conducted in accordance with the Arbitration Rules of the United Nations Commission on International Trade Law (UNCITRAL).

Third-party materials. Users wishing to reuse material from this work that is attributed to a third party, such as tables, figures or images, are responsible for determining whether permission is needed for that reuse and for obtaining permission from the copyright holder. The risk of claims resulting from infringement of any third-party-owned component in the work rests solely with the user.

Sales, rights and licensing. FAO information products are available on the FAO website (www.fao.org/publications) and can be purchased through publications-sales@fao.org. Requests for commercial use should be submitted via: www.fao.org/contact-us/licence-request. Queries regarding rights and licensing should be submitted to: copyright@fao.org.

CONTENTS

Prologue	vii
Foreword	viii
Acknowledgments	ix
Contributors	xi
Acronyms	xii
Executive summary	xiv
Introduction and scope of prevailing smog problem in Pakistan	xix
Report overview	xxii
Section I—Focus group discussions for crop residue burning practices	2
Section II—Climatological modeling of smog	15
2.1 A brief introduction to atmospheric pollutants playing role in smog formation	15
2.2 Optical properties of different atmospheric pollutants	16
2.3 Climatology and seasonal air masses entering Punjab	16
2.4 Smog source identification in smog dominated regions with a focus on Punjab province of Pakistan	17
2.5 Spatial source identification using MODIS deep blue imagery	27
2.6 Seasonal dynamics and trends of smog (period: 2008–2017)	33
2.7 Results & findings of climatological modeling	38
Section III—Remote sensing analysis and numeric MODELING	40
3.1 Data acquisition and their characteristics	40
3.2 Data processing	43
3.3 Results of remote sensing analysis	45
SECTION IV—Sectoral emission inventory of air pollutants in Punjab	62
4.1 Fuel combustion—power, industry, and transport	62
4.2 Results	64
4.3 Conclusions & recommendations	73
References	77
Appendices	87

FIGURES

1.1. Map showing areas surveyed for crop residue burning practices	3	
1.2. Map showing the percentage of basmati rice residue burnt by the farmers	5	
1.3. Map showing percentage of non—basmati rice residue burnt by the farmers	6	
1.4. Map showing percentage of wheat residue burnt by the farmers	7	
1.5. District wise chart for percentage of crop residue burnt	8	
1.6. District wise chart for a comparison of crop residue burning in basmati rice	8	
1.7. District wise chart for a comparison of crop residue burning in non—basmati rice varieties	9	
1.8. District wise chart for a comparison of crop residue burning in wheat	10	
1.9. District wise percentage of community members whose health was affected by smog in 2016 (%).	11	
1.10. District wise percentage of communities that experienced smog in 2016	11	
1.11. Cost (rs. /acre) a farmer will bear if stopped crop burning	12	
1.12. Farmers would stop crop residue burning if given subsidy/incentive of rs/acre	12	
2.1. Five—day daily backward trajectories ending at lahore from 2010 to 2014 with trajectory colors representing values of α measured at lahore. The trajectories are shown season wise (a) winter (b) pre—monsoon (c) monsoon and (d) post—monsoon. The position of lahore is represented by the black dots.	18	showing the occurrence frequency of different aerosols in (a) winter (b) pre—monsoon (c) monsoon (d) post—monsoon (source: <i>zafar et al., 2018</i>)
2.1.1. Five—day daily backward trajectories ending at lahore from 2015 to 2017 with trajectory colors representing values of α measured at lahore. The trajectories are shown season wise (a) post—monsoon (b) winter	19	
2.2. Point source locations (period: 2008—2017)	19	
(a) for post—monsoon	19	2.4. Classification of point sources in to dust, biomass burning/urban—industrial, mixed and maritime pollutants (period: 2008—2017)
(b) for winter at 2000 m.	20	(a) post—monsoon 22
2.3. Gaussian distributions fitted to the aerosol sources found around lahore from 2010 to 2014 for α	21	(b) winter. 23
		2.5. Graphical representation of aerosol sources 26
		2.6. seasonal spatial source locations (in %) of 'bu' and 'dust' aerosols. (period: 2008—2014).
		(a) post—monsoon 27
		(b) winter 28
		For both seasons, top figures represent t values, middle figs represent foo for 'bu' type pollutants and bottom figs as 'dust type pollutants.
		2.7. (a) upper panel (post—monsoon) left—right (2008—2014)—2017 29
		(b) lower panel (winter) left—right (2008—2014)—2017 29
		2.8. Different extreme smog events in the post—monsoon from 2008—2017. (l.h.s) t values have been plotted against anthropogenic aerosol optical depth (α). 33
		2.9. Wind speeds in October (period: 2008—2017) from 1000 hpa—800 hpa (upper left to lower right). 34
		2.10. Wind speeds in 1000 hpa—800 hpa (upper left to lower right).January (period: 2008—2017) from 35
		2.11. Upper panel indicates trends of winter t values from 2008—2017, lower panel indicate trends of α values from 2008—2017. 36
		2.12. Upper panel indicates trends of winter t values from 2008—2017, lower panel indicates trends of α values from 2008—2017. 38
		3.1. Raw (left) and processed (right) active fires data (viirs) of punjab, pakistan for a sample time. Number fire events significantly reduced when a confidence level of 95% or above is selected. 43
		3.2. General methodology 44
		3.3. Seasonal average of aod from 2008—2013. 45
		3.4. Seasonal average of aod from 2014—2018. 45
		3.5. Seasonal average of aod from 2008—2018. 45
		3.6. Seasonal average of ozone from 2008—2013. 46

3.7. Seasonal average of ozone from 2014–2018	46	4.5. Industrial sector emissions (NO _x , NMVOCs, CO) during 2008–2017 – Punjab	68
3.8. Seasonal average of ozone from 2008–2018	46	4.6. Transport sector emissions (NO _x , NMVOCs, CO) during 2008–2017 – Punjab	68
3.9. Seasonal average of SO ₂ from 2008–2013	47	4.7. NO _x , emissions in Punjab – by sector	68
3.10. Seasonal average of SO ₂ from 2014–2018	47	4.8. Average share (10 years) of NO _x in Punjab by sector	69
3.11. Seasonal average of SO ₂ from 2008–2018	47	4.9. NMVOCs, emissions Punjab – by sector	69
3.12. Seasonal average of NO ₂ from 2008–2013	48	4.10. Average share (10 years) of NMVOCs in Punjab – by sector	69
3.13. Seasonal average of NO ₂ from 2014–2018	48	4.11. CO emissions in Punjab – by sector	69
3.14. Seasonal average of NO ₂ from 2008–2018	48	4.12. Average share (10 years) of CO in Punjab by sector	69
3.15. Calipso derived aerosol types and altitude for the year 2009–10	49	4.13. SO _x emissions in Punjab – by sector	70
3.16. Calipso derived aerosol types and altitude from 2008–18	49	4.14. Average share (10 years) of SO _x in Punjab by sector	70
3.17. Calipso derived aerosol types and altitude from 2008–2013	49	4.15. PM _{2.5} emissions in Punjab – by sector	70
3.18. Calipso derived aerosol types and altitude from 2014–2018	49	4.16. Average share (10 years) of PM _{2.5} in Punjab – by sector	70
3.19. Classification of fire events from October 2008 to February 2013 (left) and from October 2014 to February 2018 (right)	50	4.17. Gains model results – PM _{2.5} ambient concentration over Punjab	71
3.20. Active fire status from October 2008 to February 2018	51	4.18. Rice production in 11 districts from 2008–2017	71
3.21. Unique day fire events frequency from 2008–2018	51	4.19. Total rice production of all 11 districts in Punjab	71
3.22. Hotspot analysis for the period from October 2008 to February 2018	52	4.20. Emissions from rice residue burning in 11 districts	72
3.23. Five-year hotspot analysis for 2008–2013 (left) and 2014–2018 (right)	53	4.21. Rice production (total) in Punjab from 2008–2017	72
3.24. Hotspot analysis and rice crop	54	4.22. Emissions (total) from rice residue burning in Punjab from 2008–2017	72
3.25. Top 10 fire events trajectories (2008–2018)	55	4.23. Sectoral emissions in Punjab (cumulative)	73
3.26. Top 10 fire events trajectories 2016 and 2017	56	4.24. Sectoral emissions shares in Punjab	74
3.27. Vertical extent of air pollution on 18 October 2011	57	Tables	
3.28. Vertical extent of air pollution on 9 November 2016	57	2.1. Different types of aerosol sources (coarse mode/dust, fine mode/urban–industrial, mixed type, and background type)	24
3.29. Residual plot for the numerical model	60	2.2. Percentage wise types of aerosol sources	25
4.1. Fuel consumption trend of power sector – punjab (2008–2017)	67	3.1. Sources, format, temporal and spatial resolutions of data acquired.	40
4.2. Fuel consumption trend of industrial sector – Punjab (2008–2017)	67	3.2. Numerical modeling results for prediction of smog.	59
4.3. Fuel consumption trend of transport sector – Punjab (2008–2017)	67	4.1. District wise rice production of Punjab (2008–2017) (000 tonnes)	63
4.4. Power sector emissions (NO _x , NMVOCs, CO) during 2008–2017 – Punjab	67	4.2. List of thermal plants located in 11–districts of Punjab province	65

Appendices

a. Number of focus group discussions conducted by tehsil and district	87
b. List of union councils surveyed during the focus group discussions	89
c. Year wise mapping of AOD (2008–2018)	93
d. Year wise mapping of ozone (2008–2018)	96
e. Year wise mapping of SO ₂ (2008–2018)	99
f. Year wise mapping of NO ₂ (2008–2018)	102
g. Year wise mapping of fire events (2008–2018)	105

PREFACE

In order to respond to governments' priority needs, FAO globally supports the member countries by making its resources and technical expertise available to provide assistance in all areas pertaining to FAO's mandate covered by Strategic Framework. FAO Pakistan undertook an initiative in the form of Technical Cooperation Programme R–SMOG to support Government of Punjab for the investigation of the causes of smog in Punjab. Modern geospatial technologies, remote sensing, and advanced climatological modelling techniques have been employed to provide a comprehensive piece of knowledge for the decision makers and policy makers in order to understand the seasonal dynamics of smog, its formation and sectoral contributions.



As a way forward, it is foreseen that the Government Institutions will be well-informed with research-based resources to better understand the causes of smog in order to alleviate detrimental health and environmental effects. Given that the Government is cognizant of the harmful health and environmental effects of smog, the results and findings of R–SMOG will be useful for devising appropriate policies and action plans. This will also aid to the increased capacity of Government institutions at the provincial level for design and implementation of the appropriate policies and strategies for climate change adaption and mitigation.

Ms Mina Dowlatchahi

A handwritten signature in blue ink, appearing to read 'Mina Dowlatchahi'.

FAO–Country Representative, Pakistan

FOREWORD

The Punjab Agriculture Department is mandated to sustain food security and contribute towards the national economy. It aims to make agriculture cost—effective and knowledge—based sector with emphasis on farmer's welfare as well as maintenance of the yield potentials. Having said that, the Punjab Agricultural Department has made significant progress in transforming the cropping sector of Punjab and is making grave efforts to make the agriculture sector more productive and sustainable along with the promotion of environmentally safe agricultural practices. However, in recent years, smog in Punjab has emerged as a serious problem and crop residue burning is considered one of the key contributor in the formation of smog. Therefore, the Punjab Agricultural Department has requested FAO Pakistan to provide technical assistance in order to investigate the real contribution of smog caused by crop residue burning practices in Punjab.



With the technical support of FAO Pakistan, the Punjab Agricultural Department hopes to utilize the findings of this report by identifying the causes of smog and help in formulating appropriate policies and action plans for mitigation of smog. The technical support provided by FAO Pakistan for planning and implementing high—end sophisticated geospatial research is highly valuable. The extensive piece of research on the causes of smog and seasonal dynamics would serve as the basis for devising appropriate agriculture policies and action plans for reducing the formation of smog caused by the agriculture sector.

Mr Wasif Khurshid

A handwritten signature in blue ink, appearing to read 'Wasif Khurshid', with a long horizontal stroke extending to the right.

Secretary Agriculture Punjab,
Government of Punjab

ACKNOWLEDGEMENTS

The TCP R-SMOG project is the outcome of a combined effort of many stakeholders and specialists, mainly from national organizations such as the Department of Agriculture Punjab, Global Change Impact Studies Center (GCISC), Ministry of Climate Change Pakistan, Agriculture Delivery Unit (ADU), Department of Agriculture Punjab, COMSATS University Islamabad, academia and individual consultants. The request was initiated from the office of the Secretary of Agriculture, Government of Punjab in 2017 to carry out a geospatial research on the causes of smog and its relation to crop residue burning in Punjab. The project was planned and executed by a coordination team from FAO led by Mr. Nasar Hayat (Assistant FAO Representative–Head of Programme, FAO Pakistan) and including Ms. Mehwish Ali (GIS Officer, FAO Pakistan) and Dr. Robina Wahaj (Lead Technical Officer, FAO). The technical support from Dr. Robina Wahaj and the assistance for timely execution of the activities is highly appreciated. We are also thankful to Ms. Angeliki Dimou (Former Head Information Management Unit, FAO Pakistan) for the initial support for the project planning. From the Department of Agriculture Punjab, Ms. Humera Qasim (Climate Change Advisor, Department of Agriculture, Punjab) coordinated the project activities and her continuous support is highly commendable.

The project was technically led and managed by Ms. Mehwish Ali (GIS Officer, FAO), who also contributed for the technical review and development of the report, remote sensing and spatial analysis, creation of maps and integration of the technical editorial comments on the report. The support from Dr. Douglas Clark (Air Quality Specialist, AirQuality.dk, Denmark) is highly appreciated for improving and refining the methodology of the technical work.


The technical assistance provided by the Global Change Impact Studies Center (GCISC), Ministry of Climate Change is extremely remarkable. The valuable technical contributions of Ms. Qudsia Zafar (Senior Scientific Officer) Mr. Kaleem Anwar Mir (Scientific Officer), Ms. Anum Mir (Research Assistant), Ms. Mahnoor Kausar (Research Assistant) and Mr. Shahbaz Mehmood (Head, Climatology & Environment) under the leadership of Mr. Muhammad Arif Goheer (Head, Agriculture & Coordination) are highly acknowledged. Their technical

contributions in this regard are largely in the following two research areas:

- (1) Climatological modelling for smog – point sources identification along with the smog dynamics study;
- (2) Development of sectoral emission inventory of air pollutants in Punjab – sector– specific contribution to smog formation.

Dr. Imran Shahzad (a Remote Sensing and GIS expert from Department of Meteorology, COMSATS) highly contributed in the Remote Sensing analysis for the remote sensing analysis for the mapping of the fire events occurring in transboundary regions of Punjab and also the effects of other aerosols and dust particles in the atmosphere. Initial work on remote sensing analysis and mapping was also done by Dr. Saad Saleem Bhatti (Remote Sensing Specialist). Mr. Raja Ajmal Jahangir (Statistician, FAO) assisted in designing the questionnaires and performing the statistical analysis of the focus group discussions. The technical support of Mr. Yasir Riaz (Assessment Officer, UNOCHA) for the improvement of the data collection tool and for carrying out the training for data collection is also valuable. The support of Mr. Muhammad Afzal, Mr. Tahir Masood and Mr. Habib Wardag is also acknowledged for the training of enumerators and facilitating the focus group discussions. Ms. Areesha Asghar (GIS Assistant, FAO) helped in the development of mapping products and layouts.

An in depth technical review of the report was done by the team of experts from Geospatial Unit, CBDS, FAO Headquarters, Italy led by Dr. Douglas Muchoney (Senior Environment Officer, Head of Geospatial Unit, CBDS, FAO Headquarters, Italy). Editorial changes are carried out with the valuable feedback from Dr. Douglas Muchoney, Mr. Peter Moore (Forestry Officer, FOA Headquarters, Italy), Ms. Gianluca Franceschini (Geospatial data analyst, CBDS, FOA Headquarters, Italy). Besides this, Mr. Muhammad Arif Goheer (Head of Agriculture, Forestry & Land Use Section, Global Change Impact Studies Centre) and Mr. Shahbaz Mehmood (Head of Climatology & Environment Section, Global Change Impact Studies Centre) also provided editorial support.



Mr. Shahid Ahmed (Graphic Designer – FAO Pakistan) has designed the report and carried out the development of the graphic layout. Efforts of Ms. Amber Pervaiz (Programme Development Specialist, Consultant, FAO Pakistan) for the professional editing and improvement of the report are also acknowledged.

The development of this report would have been difficult without the leadership and guidance provided by Ms. Mina Dowlatchahi (FAO Country Representative–Pakistan) and Mr. Nasar Hayat (Former, Assistant FAO Representative–Pakistan).

CONTRIBUTORS

Project Coordination Team

Ms. Mehwish Ali (GIS Officer, FAO Pakistan)

Mr. Nasar Hayat (Assistant FAO Representative—Head of Programme, FAO Pakistan)

Dr. Robina Wahaj (Lead Technical Officer, FAO)

Ms. Humera Qasim (Climate Change Advisor, Department of Agriculture, Punjab)

Technical Team

Ms. Mehwish Ali (GIS Officer, FAO Pakistan)

Dr. Imran Shahzad (Associate Head — Department of Meteorology, COMSATS University, Islamabad, Pakistan)

Ms. Qudsia Zafar (Senior Scientific Officer, Climatology & Environment Section, Global Change Impact Studies Centre)

Mr. Kaleem Anwar Mir (Scientific Officer, Climatology & Environment Section, Global Change Impact Studies Centre)

Dr. Saad Saleem Bhatti Remote Sensing Specialist, Asian Institute of Technology, AIT)

Dr. Douglas Clark (Air Quality Specialist, AirQuality.dk, Denmark)

Mr. Raja Ajmal Jahangeer (Statistician, FAO Pakistan)

Mr. Muhammad Afzal (Information Management Assistant, FAO Pakistan)

Ms. Areesha Asghar (GIS Assistant, FAO Pakistan)

Editorial Team

Mr. Douglas Muchoney (Senior Environment Officer, Head of Geospatial Unit, CBDS, FAO Headquarters, Italy)

Mr. Peter Moore (Forestry Officer, FOA Headquarters, Italy)

Mr. Gianluca Franceschini (Geospatial data analyst, CBDS, FOA Headquarters, Italy)

Ms. Mehwish Ali (GIS Officer, FAO Pakistan)

Mr. Muhammad Arif Goheer (Head of Agriculture Section, Global Change Impact Studies Centre)

Mr. Shahbaz Mehmood (Head of Climatology & Environment Section, Global Change Impact Studies Centre)

Ms. Amber Pervaiz (Programme Development Specialist, Consultant, FAO Pakistan)

Design and Layout

Mr. Shahid Ahmad (Graphic Designer, FAO Pakistan)

ACRONYMS

AERONET	Aerosol robotic network
AOD	Aerosol optical depth
ARL	Air resources laboratory
EOS	Earth observing system
CALIPSO	Cloud–aerosol lidar and infrared pathfinder satellite observations
DU	Dobson unit
ECMWF	European center for medium range weather forecasts
EDGAR	Emission database for global atmospheric research
FIRMS	Fire information for resource management system
FRP	Fire radiative power
GDAS	Global data assimilation
GIS	Geographic information science
GUI	Graphical user interface
HYSPLIT	Hybrid single–particle lagrangian integrated trajectory model
IDL	Interactive data language
IDW	Inverse distance weighted
IPCC	Intergovernmental panel on climate change
LULC	Land use land cover
MODIS	Moderate resolution imaging spectroradiometer
MW	Megawatts
NASA	National aeronautics and space administration
NCEP	National centre for environmental prediction
NetCDF	Network common data form
NOAA	National oceanic and atmospheric administration
NRT	Near real-time
OMI	Ozone monitoring instrument
OLS	Ordinary least square
OLI	Operational land imager
ONDJF	October, November, December, January, February
OTC	Ozone total column
SMOG	Smoke and fog
SPM	Suspended particulate matter
Suomi–NPP	Suomi national polar-orbiting partnership
TIRS	Thermal infrared sensor
TM	Thematic mapper
UV	Ultra-violet
VIIRS	Visible infrared imaging radiometer suite
VOCs	Volatile organic compounds

Chemical Formulae

CH ₄	Methane
CO	Carbon monoxide

CO_2	Carbon dioxide
NH_4^+	Ammonium
NO	Nitric oxide
NO_2	Nitrogen dioxide
NO_3^-	Nitrate
O_3	Ozone
SO_4^{2-}	Sulfate

EXECUTIVE SUMMARY

FAO has created the Technical Cooperation Programme (TCP) to make its technical expertise available to member countries upon request, drawing from FAO's core resources. The Technical Cooperation Programme on Remote Sensing for Spatio-Temporal mapping of Smog (R-SMOG) in Punjab was initiated in 2017 upon the request of the Government of Punjab. The key objective of the R-SMOG is to evaluate the relationship between Smog and the rice residue burning practices by farmers in the Rice belt of Punjab. The findings of the R-SMOG will assist to generate scientific evidences to study the causes of Smog and to adopt adequate mitigation and adaptation strategies. It will also promote the development of appropriate strategies and necessary action plans.

The R-SMOG is a first of its kind comprehensive geospatial research which integrates Spatio-temporal mapping of smog viz-a-viz climatological modelling, study of seasonal trends and dynamics and estimates an inventory of sectoral emissions. The scientific study has generated significant data and results, within the limits of unavailability of ground based air quality data and monitoring.

The term 'smog' was first coined in the early 20th century in London to describe the low-hanging pollution that covered the city. Smog is formed as a result of chemical reactions among suspended particles in lower part of the atmosphere, less than 5km above the ground and constitutes a mixture of air pollutants including ozone, dust particles, smoke particles, volatile organic compounds (VOCs), nitrous oxides and oxides of Sulphur. In Pakistan, the problem of smog has been increasing in intensity especially in the province of Punjab in recent years. Smog began to get noticed as a major problem in the late 1990s in upper Punjab, mainly in the industrial belt around Lahore, and generally in the winter months (December and January). In recent years, it has spread to a broader swath of the country including southern Punjab and Sindh. For the years 2015, 2016 and 2017 its intensity was observed even during the months of October and November. Punjab is the country's most vibrant province which contributes almost 60% to the annual growth of industrial goods and services. The anthropogenic emissions are mainly contributed from

industrial and vehicular emissions and biomass burning activities. During the episodes of Smog in Punjab, visibility conditions are often reported as extremely poor, and have at times resulted in economic losses due to disruptions in transport, e.g. air and road transport. Apart from this, the intense smog in Punjab in the past few years has also caused serious respiratory diseases and other health issues such as eye infections and allergies.

Smog is not only a local problem of Pakistan but has emerged as a regional problem affecting India and China as well and debates pertaining to this crisis are going on regarding burning of rice stubble as a significant contributor to smog. It has been reported that increase in the area of non-basmati varieties and decrease in the area of basmati varieties has taken place in the previous few years, and non-basmati varieties produce a lot more stubble. Farmers owing to the less expensive methods, burn crop residues generated by rice in order to get rid of the stubble, as they have only three to four weeks to prepare for the wheat crop. The smoke resulting from this rice stubble burning normally stays in the lower troposphere (below 5 km) and is transported to the northern Punjab along southerly winds during the post-monsoon season.

RESIDUE BURNING PRACTICES OF FARMERS

In order to understand the crop residue burning practices of farmers in Punjab, focus group discussions were organized in 11 rice growing districts namely Faisalabad, Gujranwala, Gujrat, Hafizabad, Kasur, Lahore, Mandi-Bahauddin, Nankana Sahib, Narowal, Sheikhupura, and Sialkot. The Focus group discussions were conducted in collaboration with the agriculture specialists from Department of Agriculture Punjab and the district extension officers. The findings of the focus group discussions helped understand the trends in residue burning practices.

- Crop residue burning is a common practice in the districts especially for rice in the month of November. The main reasons for burning crop residue are to get rid of trash/residue, the difficulty in soil preparation, desire to

save labor cost, to eradicate weeds and pests and to facilitate cultivation and timely sowing of the next crop.

- For Rice crop, 20-23% of the farmers reported that crop residue burning has increased in the last years. Overall, farmers reported burning of crop residue for the past 16 years, ranging from 5 to 30 years.
- An important fact is that in the past farmers used crop residues as fodder for their animals before starting burning of residues. This is no longer widely practiced.
- As reported by 44% of farmers it was observed that the decision to burn a field is taken after mainly considering the dryness of the crop residue.
- Regarding the timings for crop residue burning, it was reported by 80% of the farmers that Crop residue burning is practiced during daylight, out of which between 28-48% of farmers burn the crop residue between 11 am-12 pm. In one field, crop residue burning lasts mostly for 0.5-1 hour as reported by 27 percent farmers.
- According to farmers, burning of crop residue particularly of rice when it is wet/green and contains moisture, increases the amount of smoke.
- About 44% of farmers informed that there has been an increase in the cultivation of non-basmati rice varieties in the last two years.
- About 84% of farmers informed that there has been an increase in the use of combined harvester in the last five years.
- Around 37% of respondents were of the view that there has been an increase in waste material.
- 70-80% of respondents reported that small industries have increased while 50-60 percent think that the number of automobiles/vehicles have increased since the last 5 to 10 years.

FARMERS' RESPONSE TO BAN ON RESIDUE BURNING

- 42% of the farmers would agree to accept the ban provided that alternative methods for cleaning the field to facilitate the tillage operations are made available. These farmers also demanded Government to provide subsidy or better technology for incorporation of crop residue.
- 46% of the farmers would oppose the ban as they face a huge problem in land preparation and ploughing and in their view they have no other alternative.

CLIMATOLOGICAL MODELLING, SEASONAL DYNAMICS AND SMOG SOURCE IDENTIFICATIONS

Hybrid Single Particle Lagrangian Integrated Trajectory (HYSPLIT) model, developed by NOAA's Air Resources Laboratory was used to find 5-day air-back source trajectories to assess transport of air parcels. AERONET and MODIS data were used for characterizing the optical properties and size distribution of atmospheric aerosols. Besides the source analysis, monthly wind dynamics using ERA-Interim from ECMWF at pressure levels (1000, 975, 950, 900, 850 & 800) hPa have also been examined. The detected sources and wind speeds at different heights are studied in conjunctions with different extreme smog events. The model simulations showed seasonal variations in air parcel trajectories originating from different locations. In winter, most of the air parcels were arriving from west and south-west, in pre-monsoon the westerly and south westerly air masses also became southerly, and monsoon exhibited eastern transport of air masses along with westerly and southerly air masses while post-monsoon predominantly exhibited south-westerly air masses. This trajectory analysis also demonstrates the western disturbances originating from the Mediterranean Sea in winter, dust storms associated with the southerly air masses carrying along dust aerosols from the deserts of Thar and Cholistan in pre-monsoon, easterly and southerly monsoon currents originating from the Bay of Bengal, and the Arabian Sea in monsoon and dry season as a result of south westerly air-masses with no moisture in the post-monsoon.

ASSESSMENT AND MAPPING OF REGIONAL POINT SOURCE LOCATIONS

Assessment and mapping of aerosol point sources indicate that 65% of the aerosol sources were detected within Pakistan which means most of the sources are located within Pakistan and sources of smog needs to be managed and controlled within the country as a matter of priority.

Biomass burning, and mixed-type pollutants were found mostly originating from within Pakistan in the smog dominated zone, however, sources were also detected in neighboring regions such as India, Afghanistan, and Iran with Indian contributions mainly constituting to fine mode 'biomass/urban' type pollutants.

On a seasonal basis, winter was found to comprise more sources than post-monsoon due to the greater season length, however, more "biomass/urban" type pollutant sources were found in the post-monsoon. Trend analysis showed higher concentration during the recent years i.e. 2015–2017, which is also confirmed by the spatial source locations found by the satellite data. The satellite pictures of smog dominated area show that burning activities in winter take place in different locations than the post-monsoon. In the high-pressure system, accumulation of pollutants is evident, therefore, if burning and combustion activities are controlled, the smog problem can be controlled.

REMOTE SENSING FOR ACTIVE FIRES MAPPING AND HOTSPOT ANALYSIS

With the advancements in satellite remote sensing methods, mapping of thermal anomalies and active fires has become possible through sensors aboard satellites. Availability of real-time data has improved, along with the mapping of thermal anomalies. There are different data products available for fire detection at different resolutions. Visible Infrared Imaging Radiometer Suite (VIIRS) Active Fire detection product is one of the few data products that record active fires and thermal anomalies using satellite-based sensors. In the current study VIIRS and MODIS

fire data products have been employed to map the active fires and later on develop a hotspot analysis of frequent fire areas during the months of October, November, December and January.

A comparison of total fire events from 2008–2018 shows that the number of fire events is significantly higher in the months of October and November which complements the fact that more crop residues burning activities are carried out in these months to prepare land for next sowing. Daily MODIS data products were also used to classify the active fire areas by using temperature and FRP (fire radiative power) in megawatts (MW). The fire data for a confidence level of 95% and above, has been used for this study. FRP aided in quantifying burned biomass and the amount of radiant energy released per unit of time by burning vegetation. The point data of fire were interpolated to estimate the effect of fire. It is observed from the detection of seasonal fire events that there is a considerable spatio-temporal variation in locations and intensities of the fire events. Spatio-temporal hotspot analysis for ten years shows that many fire events occurred in the Indian administered Punjab. The fire events in Pakistan's Punjab are relatively less intense. These observations and analyses demonstrate the importance of aerosols and their transboundary impacts.

SECTORAL EMISSION INVENTORY

Though formation of smog is supported by fires and crop burning activities, emissions from transport and industrial sector have a major contribution towards the formation of smog. Therefore, it was considered to perform a sectoral emission inventory in order to compare and analyze the sectoral contributions. This was achieved by estimating the emissions of gases such as SO_x , NO_x , CO, NVOMCs and $\text{PM}_{2.5}$ from transport sector, Industrial sector and agriculture (crop residue burning).

Since the burning activity of rice residue occurs in October and November every year, the resultant air pollutant emissions from this burning activity would also be occurring only in these two months. On the other hand, power, industry, and transport runs all over the year, the resultant air pollutant

emissions from these sectors would also be occurring during the twelve months. Assuming that energy sector activities operate uniformly in a year, the total emissions are disaggregated into per month emissions. This gives a realistic comparison of sectoral air pollutant emissions and share in Punjab.

Sectoral emission inventory for Punjab shows that the major portion of total air pollutant emissions are coming from the transport sector (269 GG) and it holds 43% share in all sectors (power, industry, transport, and crop residue burning – CRB). The second key sector responsible for air pollutant emissions in Punjab is industry whose share is 25% and amounts 154 GG. The sector at number three is agriculture (mainly considering rice residue burning). It accounts for 20% (121 GG) of total air pollutant emissions with respect to other sectors. The emissions from residue burning of other crops have not been estimated due to the fact that since smog usually happens in October and November and these two months only involves burning of rice residue. The last sector is a power which amounts 74 GG and contributes 12% in total emissions. Collectively, the main sectors responsible for air pollutant emissions in Punjab are power, industry, and transport which together hold 80% contribution in air pollutant emissions and aids in the formation of photochemical smog in Punjab. The contribution of agriculture sector (crop residue burning) is significant to the seasonal smog phenomenon in Punjab, although it is the third sector by emissions following transport and industrial sector.

RECOMMENDATIONS

Based on the conclusions, the key sectoral recommendations are proposed with regard to the reduction of air pollutant emissions from fuel combustion process and crop residue burning:


1. SO_x and NO_x emissions from combustion processes in power stations and industry needs to be controlled. In the case of controlling VOCs and CO emission in power and industry sector, there are a number of ways in which the combustion efficiency could be increased, and emissions could be reduced.

2. In order to control air pollutant emissions from road transport, options available include changes in engine design and fuel quality better inspection and maintenance of vehicles is discussed. Long run recommendations include investment in public transport to reduce aggregate fuel consumption, shift to cleaner fuels and renewable energy.

3. For reducing crop residue burning, some of the key control measures could include:

- a) Awareness raising amongst the farming communities about the negative impacts of crop biomass burning and importance of crop residues incorporation in the soil for maintaining sustainable agricultural productivity.
- b) Support to be provided by the government to help farmers to purchase machines that can harvest with less residues, to adopt relevant climate smart practices to help increase yields and to use residues as fertilizer, animal feed supply, biogas production, or sell for use in different industries instead of being burnt.
- c) Avoid usage of combine harvesters and promote no till and zero till methods of cultivation.
- d) Responsibilities of local and central governments should be defined to improve coordination and cooperation between departments; to carry out various forms of information and education; to monitor fire spots by meteorological and environmental satellite; and to strengthen the inspection of illegal activities, etc.
- e) There is a need for crop residue-based renewable energy planning. A number of such initiatives are being undertaken in the neighboring countries to utilize the potential of crop residues for bio-energy generation.

4. There is an urgent need of the collection of high-quality data in various districts of Punjab, especially those which cover the rice belt, on a regular basis. It is suggested that air-quality monitoring stations may be installed throughout Punjab province, and air samples of winter smog and post-monsoon smoky haze should be taken. More evidence needs to be collected regarding



sources and transport pathways of emissions of fine mode aerosols affecting northern Punjab.

5. Establishment of an early–warning systems for potentially severe smog incidents and smog monitoring network is also recommended.

6. Finally, since smog is a regional problem, which also affects neighboring countries (e.g., India, Iran, and Afghanistan), there is a need for inter–country collaboration on data and information exchange as well as collaborative strategies.

INTRODUCTION

Scope of prevailing smog problem in Pakistan

Smog is one of the several forms of air pollutants that cause harm to human functioning. It is normally a combination of several types of pollutants (nitrogen oxides, sulphur oxides, aerosols, smoke or particulates, etc.) with fog.

Industrial/vehicular emissions and forest/crop burning are some of the common sources of these pollutants. Formation of smog, however, is not dependent only on the presence or increase of these pollutants, but certain meteorological/ weather conditions also help these pollutants suspend in the lower atmosphere because of which the pollutants form a dense visible layer of smog. This causes serious health implications (inhalation of higher than normal levels of pollutants and affects logistics operations (reduction of visibility. This study attempts to use satellite remote sensing data to examine the smog and its behavior in relation to a variety of air pollutants, with a focus on crop residue burning practices in Punjab province of Pakistan and India.

Among other sources of pollutants, fire (generated through biomass burning and/or crop residual burning) is one of the important components used in emission and climate modeling and is also important for land management issues especially in case of natural hazards such as forest burning. A variety of greenhouse gases are emitted into the atmosphere when vegetation is burnt, and some of the chemically reactive gases also influence the chemical processes within the troposphere. Biomass burning has shown a strong relationship with the regional and global distributions of troposphere ozone and has been related to acid deposition in tropical regions (NASA, 2017). Other studies also point out that intensive biomass burning is a major source of emission of gases such as Nitric oxide (NO), Carbon dioxide (CO₂), Carbon monoxide (CO), Ozone (O₃), Methane (CH₄), and various gases containing Nitrogen, Sulfur, and other Non-methane hydrocarbons (NASA, 2017). Not only this, but the aerosols concentration is also increased because of extensive biomass burning. The effects of smoke aerosols on clouds and climate have also been indicated in several studies. Smoke tends to interact with the clouds in a variety of ways, and due to the dark color of soot particles, they can constrain the cloud formation by inverting the convection process.

With the advancements in satellite remote sensing methods, thermal anomalies or active fires can be detected through sensors aboard satellites. Not only the availability of data has improved, but also the methods for mapping thermal anomalies have enhanced over the time. Mapping of thermal anomalies/crop burning has been done using a variety of data sources – a few relevant literature references include *Korontzi, McCarty, Loboda, Kumar, & Justice, 2006; McCarty et al., n.d.; Singh & Kaskaoutis, 2014; and Sukhinin et al., 2004*. Near real-time (NRT) Suomi National Polar-orbiting Partnership (Suomi-NPP) Visible Infrared Imaging Radiometer Suite (VIIRS) Active Fire detection product is one of the few data products that

record active fires and thermal anomalies using satellite-based sensors. Compared to the usually coarser spatial resolution satellite fire detection product ($\geq 1\text{km}$), the VIIRS provides an improved 375 m spatial resolution that provides a greater response over fires of relatively small areas (Schroeder, Oliva, Giglio, & Csiszar, 2014). The 375 m product complements the baseline Suomi-NPP/VIIRS 750 m active fire detection and characterization data, which was originally designed to provide continuity to the existing 1 km Earth Observing System Moderate Resolution Imaging Spectroradiometer (EOS/MODIS) active fire data record (EOSDIS, 2016). The active fire data is acquired globally, at a daily time interval.

Formation of smog has been found to be related to air pollution, and some researchers have also examined and evaluated this relationship (Ma, Hu, Huang, Bi, & Liu, 2014; SIFAKIS, 1998). Some studies also point to the development of indices using remotely sensed data for detection and mapping of fog, which could indirectly be used for assessing the presence of smog (*Güls & Bendix, 1996; Torregrosa, Combs, & Peters, 2016; Wen et al., 2014*). Several other research studies also point to the direct or indirect smog mapping approaches employing remote sensing and other data sources, and have also found some degree of relationship between crop residue burning and concentration of atmospheric particles such as particulate matter PM_{2.5} and PM₁₀, as well as with the pollutants such as carbon monoxide, Sulphur dioxide and nitrogen dioxide (*Acharya & Sreekes, 2013; Alam, Qureshi, & Blaschke, 2011; Badarinath, Kharol, Sharma, & Roy, 2009; Kaskaoutis et al., 2014; Khokhar, Yasmin,*

Chishtie, & Shahid, 2016; Samina Bibi, Alam, Bibi, Khan, & Haq, 2015; Sharif, 2015; Tariq & Ali, 2015; Tariq, Zia, & Ali, 2016; Ul-Haq, Tariq, Ali, Rana, & Mahmood, 2017; Ul-Haq et al., 2015).

The literature points to some sort of relationship between aerosol optical depth (AOD) and biomass burning (Vadrevu, Ellicott, K.V.S. Badarinath, & Vermote, 2011). The AOD can be derived from a variety of data sources, such as Aerosol Robotic Network (AERONET) (ground-based instrument) or MODIS (satellite-based instrument). Around 450 AERONET radiometers are in operation worldwide (Tariq et al., 2016), while MODIS uses a different set of algorithms to retrieve aerosol concentrations over land and oceans. Cloud-Aerosol Lidar and Infrared Pathfinder Satellite Observations (CALIPSO) is another data source that provides information about the altitude of aerosols. While all the sources provide data with a good level of accuracy, the MODIS aerosol retrieval algorithm has recently been improved in order to correct systematic biases in the MODIS algorithm used previously (Remer et al., 2005).

Fog has been mapped and characterized in several research studies. One such study attempts to use multi-satellite data and ground-based observations on aerosol properties and solar irradiance in the north Indian region to study the fog conditions (Badarinath et al., 2009). The study found a considerable increase in AOD and a decrease in total solar irradiance in the study area during the fog period. Another study employed the MODIS data to examine the temporal variations of AOD over central India (Asha B. Chelani, 2015). The study found a significant relationship between population change and AOD levels, thus suggesting some sort of impact of urban agglomeration in AOD in the study area. In another study, the effects of crop residue burning on aerosol properties were examined in northern India (Kaskaoutis et al., 2014). This study used MODIS data (along with ground-based sensors) for AOD measurement and found that biomass burning over densely populated and polluted areas were of concern as it contributed to the deterioration of the environment. The MODIS images also showed thick smoke and hazy aerosol layer in the atmosphere during the crop residue burning period. The winter fog episodes during 2012–2015

over Pakistan were examined in a study using MODIS, Ozone Monitoring Instrument (OMI) and CALIPSO data with the aim to map the spatial distribution of aerosols during the foggy periods (Khokhar et al., 2016). This study found that the major constituents of winter fog in Pakistan were the smoke and absorbing aerosols. Another study examined the NO₂ patterns and anomalies over a large area of Indus, Ganges, Brahmaputra, and Meghna river basins, and found that the highest seasonality was found over Meghna Basin due to large variations in meteorological conditions and large-scale crop-residue burning (Ul-Haq et al., 2017). The study also found some anomalies in NO₂ levels that could be linked to intense crop-residue burning events. OMI data was used to obtain NO₂ concentration in this study.

CO₂ emissions, that can be somewhat attributed to crop residue burning, could be assessed using satellite remote sensing data. One study examined the spatiotemporal variations of CO₂ emissions through satellite remote sensing over Pakistan and neighboring regions (Zia ul-Haq, Salman Tariq, & Muhammad Ali, 2017). The data from Atmospheric Infrared Sounder (AIRS), together with the anthropogenic emission data from the Emission Database for Global Atmospheric Research (EDGAR), was used in this study. Similar sort of activity was undertaken to analyse the spatiotemporal variations of CO emissions through satellite remote sensing data over Pakistan (Ul-Haq et al., 2015). Mapping and analysis of the CO emissions could also be useful in studying its relationship with crop residue burning.

A.1 A brief introduction to smog associated problems in Punjab

In Pakistan, the problem of smog has been increasing in intensity especially in the province of Punjab in recent years. Smog began to be identified as a major problem in the late 1990s in upper Punjab, mainly in the industrial belt around Lahore, and generally in the winter months (December and January). In recent years, it has spread to a broader swathe of the country, including southern Punjab and Sindh. For the years 2015, 2016 and 2017 its intensity was observed even during the months of October and November. Punjab is the country's most vibrant province which contributes almost

60% to the annual growth of industrial goods and services (Hussain *et al.*, 2012). The anthropogenic (man-made) emissions mainly come from high industrial emissions, vehicular emissions and biomass burning activities (Biswas *et al.*, 2008; Alam *et al.*, 2012). Visibility conditions in Punjab are often reported as poor e.g. visibility falls up to 200 m reducing even up to 50m (Yasmeen *et al.*, 2012), the main cause of which are the intense polluted conditions in Punjab leading to increased risk of cardiovascular and respiratory diseases.

According to the World Health Organization (WHO) estimates, in 2015, almost 60 000 Pakistanis died from the high level of fine particles in the air, one of the world's highest death tolls from air pollution. On Nov 6, 2016, DAWN News reported the intense haze conditions in Lahore (capital of Punjab) due to impending smog. They reported that NASA (the National Aeronautics and Space Administration) has pointed out the crop stubbles burning which might be the major reason for a smog blanket in New Delhi, and also in Lahore, as their map showed several places in West Punjab that had thermal emissions. They quoted environmentalist and researcher Noman Ashraf that issue of crop stubble burning was being misinterpreted. "This is nothing new in the region and has been happening for decades. But this recent spike is because farmers in East Punjab, who had originally been selling their wheat stalks for biomass plants, burnt their agri-waste this year after their requested price was turned down by the biomass plants."

(Source: <https://www.dawn.com/news/1294579>
date of access: Oct 17, 2018)

In 2017, the poor visibility situation in Punjab was reported by 'Pakistan Today' on third of November, when motorway officials provided visibility conditions as reduced from 50 meters up to 25 meters from Lahore to Bhera and up to the Vehari district, where 12 people got injuries in traffic accidents due to visibility problems

(Source: <https://www.pakistantoday.com.pk/2017/11/03/smog-continue-s-to-wreak-havoc-in-punjab/>
date of access: Nov 8, 2018).

On Nov 10, 2017, The New York Times referred to Lahore 'as

one huge airport smokers' lounge' "You can see and smell the smoke all day; you can actually touch the filth," said Amna Manan, a 26-year-old manager for a multinational company in Lahore. They reported the state of Lahore as a city of 11 million where half the time, people are scared to breathe in (Source:

<https://www.nytimes.com/2017/11/10/world/asia/lahore-smog-pakistan.html>
date of access: Oct 17, 2018).

An independent activist, Abid Omar, who has installed his own air quality monitors and started publishing air pollution data, reported that in the recent few years, the level of dangerous PM_{2.5} particles (i.e., particles with a diameter of less than 2.5 micrometers) in Lahore had reached 1 077 micrograms per cubic meter, compared with the WHO prescribed safe limit of 30 mcg/cu.m.

Pertaining to this looming crisis, a strong debate is going on regarding burning of rice stubble as a significant contributor to smog, as excessive smoke produced as a result of burning is thought to travel in a trans-boundary transport. It has been reported previously that increase in the area of non-basmati varieties and decrease in the area of basmati varieties has taken place in the previous few years, in which non-basmati varieties produce a lot more stubble (BOS 2017). Farmers owing to the less expensive methods, burn these in order to get rid of the stubble, as they have only three to four weeks to prepare for the wheat crop. The smoke resulting from rice stubble burning normally stays in the lower troposphere (below 5 km) and is transported to northern Punjab along southerly winds during the post-monsoon season.

There is an interest in the trans-boundary dimension of the problem as well. Rice stubble burning takes place both in Pakistani Punjab and Indian Punjab in the post-monsoon season when deep smoke engulfs the cities in the Gangetic region, including Lahore and Delhi. In a newspaper interview, the former DG PMD, Dr. Qamar-uz-Zaman Chaudhry argued that the increasing intensity of smog has been caused mainly by the transport of pollutants from India, while the former DG PEPA, Mr. Asif Shuja Khan, placed responsibility on dust storms from the West. Therefore, the R-Smog project is an

OBJECTIVES

attempt to find out precursors and sources of smog by considering the time of rice stubble burning activities.

Considering the prevailing Smog in winters, FAO Pakistan was requested by Department of Agriculture Punjab in 2016 to undertake a Geospatial research-based project to investigate the causes of Smog. This project attempts to uncover the relationships among smog/fog formation, crop residue burning, and a variety of air pollutants in Pakistan and Indian administered Punjab, during the period from October 2008 to February 2017. The project entails two key objectives:

1. Provide a scientific evidence to identify the relationship between smog and crop residue burning in Punjab and determine the sectoral contribution of crop residue burning in the formation of smog.
2. Propose policy recommendations based on the findings of the R-SMOG project for the necessary steps to be undertaken to reduce the contribution of agriculture-related practices towards smog.

REPORT OVERVIEW

Section I

Describes the results of focus group discussions undertaken to learn about the crop residue burning practices of farmers in the rice wheat belt of Punjab.

Section II

Discusses the details about types of atmospheric pollutants contributing to smog formation and the seasonal dynamics and trends of Smog in Pakistan.

Section III

Describes remote sensing analysis performed for a period of ten years. It also includes the data used, including satellite imagery from VIIRS, MODIS, CALIPSO and Landsat sensors.

Section IV

Describes the sectoral inventory of major air pollutants.

SECTION I

FOCUS GROUP DISCUSSIONS FOR CROP RESIDUE BURNING PRACTICES

Key messages

1 Farmers burn crop residues generated by rice cultivations as it is the fastest and the least expensive method to prepare the field for the next planting season.

2 An important fact is that in the past farmers used crop residues as fodder for their animals before starting burning of residues. This is no longer widely practiced.

3 Upto 88% of the farmers would accept to respect a law banning burning of crop residues provided that alternative methods for management of crop residues are made available.

Section I

Focus group discussions for crop residue burning practices

Focus group discussions¹ were organized in the rice growing districts of Punjab to investigate the crop residue burning practices of farmers in Punjab. A training workshop for Agriculture officers/extension officers from Agriculture Department Punjab and Agriculture Extension Department Punjab to conduct Focus Group Discussions with the farmers was planned. Data collection was carried in the following 11 districts of Central-East Punjab which are part of Wheat-Rice Systems namely Faisalabad, Gujranwala, Gujrat, Hafizabad, Kasur, Lahore, Mandi Bahauddin, Nankana Sahib, Narowal, Sheikhupura, and Sialkot.

A total of 123 FGDs were conducted in 38 Tehsils of 11 rice growing districts in Punjab (Faisalabad, Gujranwala, Gujrat, Hafizabad, Kasur, Lahore, Mandi Bahauddin, Nankana Sahib, Narowal, Sheikhupura, and Sialkot). In each district, FGDs were conducted in 2–5 Tehsils depending upon the size of the district. In each Tehsil, 2–3 FGDs were conducted. The selection of districts, tehsil, and UCs was done in consultation with the Agriculture Department of Government of Punjab. The map shows the UC's surveyed for the Focus Group Discussions. For a list of districts and Tehsils, and UCs where FGDs were conducted please refer to Appendix B.

Some of the key findings of the Focus Group Discussions (FGDs) summarized at district level are in the following section. On average, there were 401 farming households in each village where an FGD was conducted. In each FGD, on average 17 farmers participated. The farming households cultivated 1 867 acres of land on average, highest 3 380 in Hafizabad, whereas lowest 1 021 acres in Lahore.

Crop cultivation

Basmati Rice:

Overall, on average, basmati rice is grown on 819 acres in the selected districts; lowest 52 acres in Faisalabad, highest 1 867 acres in Mandi Bahauddin. Average yield (maund/acre) reported is 34 maunds, highest (44 maunds) in Hafizabad and lowest (31 maunds) in Gujrat district.

¹ The objective of the Focus Group Discussions is to gather information on the crop residue burning practices, and to identify reasons of crop residue burning. Preliminary findings reported are based on the responses in the FGDs in the selected areas and may not represent the situation of the entire district.

Non-Basmati Rice:

Non-basmati rice varieties are grown on 619 acres in the selected districts on an average. Average yield (maund/acre) is 45 maunds, which is highest (46 maunds) in Hafizabad and Kasur, and lowest (42 maunds) in Mandi Bahauddin and Narowal districts.

Maize:

Maize is grown on 181 acres in the selected districts on an average; whereby 17 acres in Hafizabad and 532 acres in Kasur. Cultivation of maize is not reported in Mandi Bahauddin and Narowal district. Average yield (maund/acre) is 272 maunds, highest (523 maunds) in Lahore, lowest (41 maunds) in Kasur.

Sugarcane:

Sugarcane is grown on 288 acres in the selected districts on an average. Cultivation of sugarcane is not reported in Gujranwala, Sialkot and Narowal districts. Average yield (maund/acre) is 737 maunds, highest (900 maunds) in Lahore, 850 maunds in Gujrat, lowest (520 maunds) in Hafizabad district.

Wheat:

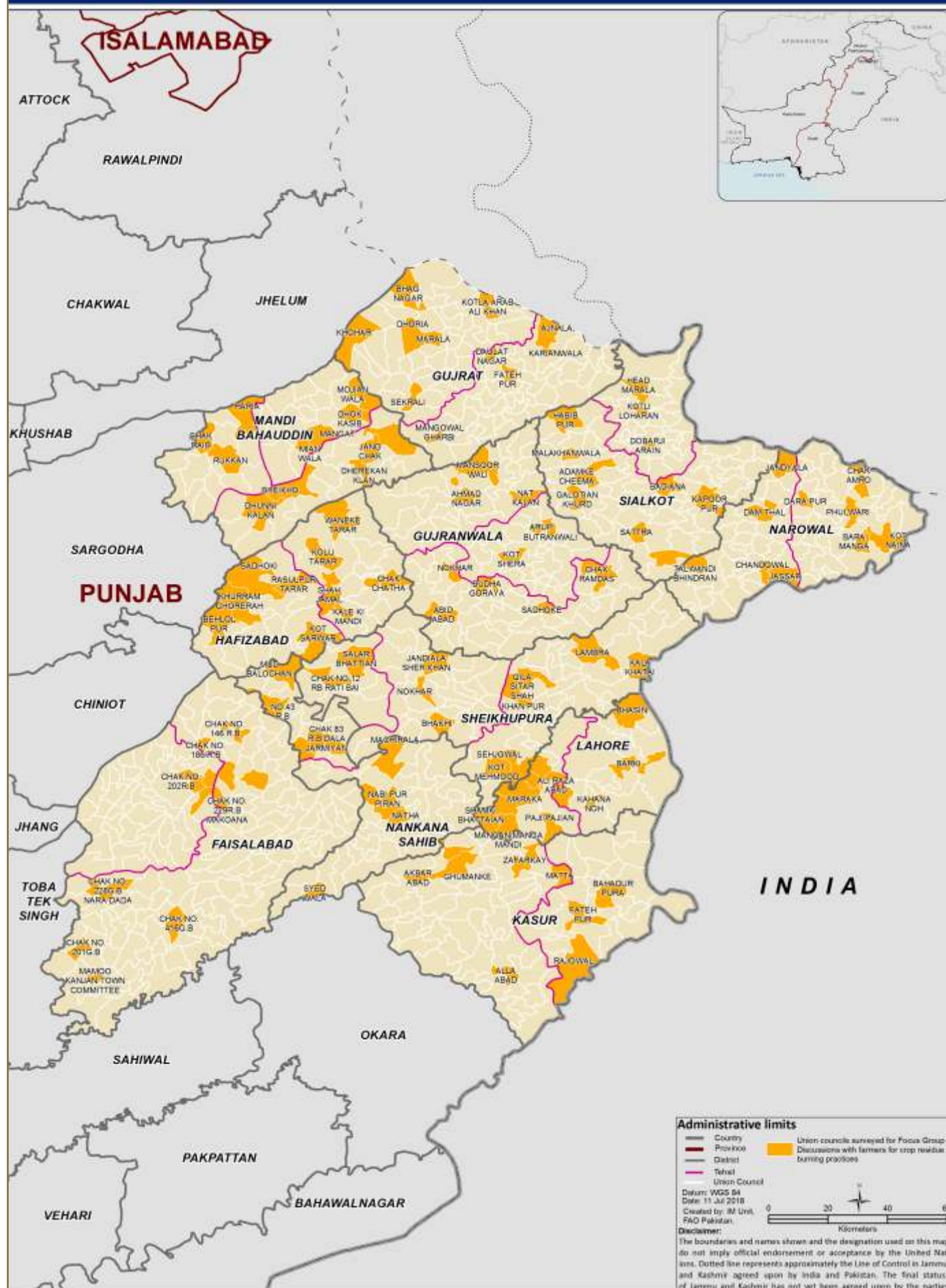
Wheat is grown on 1 357 acres in the selected districts on an average; whereby 743 acres in Lahore whereas 2 730 acres in Hafizabad. Average yield (maund/acre) reported is 35 maunds, highest (49 maunds) in Lahore, lowest (29 maunds) in Narowal district.

1- Crop residue burning

After harvesting, burning of crop residue is quite a common practice in the selected districts. Different crops produce different types of residues. Rice and wheat produce straws, maize produces stalks while sugarcane produces trashes. The removed residue of crops is used for multiple purposes including for animal feed, fuel for brick kilns, and fuel in small industry. Some of it is burnt and other is sold out.

Basmati rice:

For Rice crop, according to the results of FGDs, an average of 66% of crop area of basmati rice is burnt, which is lowest



1.1. Map showing areas surveyed for crop residue burning practices
Source: Adapted from United Nations World map, February 2020.

Section I

Focus group discussions for crop residue burning practices

(15%) in Lahore and highest (78%) in Narowal. Crop residue burning of basmati rice was not reported in Faisalabad district. There are also variations in burning of crop area within one district. Between 70–100% of crop area in Kamoki, Pindi Bhattian, Mandi Bahauddin, Nankana Sahib, Narowal, Shakargarh, Ferozwala, Sheikhupura, Pasrur, and Sialkot tehsils are burnt by the farmers. Rice residue produced by cutting basmati is 32 maunds/acre with highest rice residue reported in Kasur (42 maunds/acre). The ratio of paddy to straw is 48%.

When inquired about the uses of removed residues of basmati rice, it was found out that 60% of the removed residue of basmati rice is burnt by farmers. The practice of residue burning is lowest (7%) in Lahore and highest (95%) in Nankana Sahib. The burning of the residue of basmati rice is more prevalent (70% and above) in Pindi Bhattian, Nankana Sahib, Sanglahill, Shahkot, Narowal, Zafarwal, Shakargarh, Ferozewala, Daska, Pasrur, and Sialkot tehsils. On average, 29.8 acres of Basmati Rice crop residue is burnt in one day.

Non-basmati rice:

The burning of the residue of other Rice varieties is prevalent in all the districts except in Faisalabad and Gujrat districts. Overall, on average, 61% of the crop area of non-basmati Rice varieties is burnt; which is the lowest (12%) in Lahore and highest (88%) in Hafizabad. Between 70–100% of crop area of non-basmati rice varieties is burnt by farmers in Noshehra Virkan, Hafizabad, Pindi Bhattian, Nankana Sahib, Ferozewala, Sheikhupura, and Sialkot tehsils.

Rice residue produced by cutting other rice varieties is 27 maunds per acre which were reported highest (51 maunds) in Kasur. The ratio of paddy to straw is 48%.

When inquired about the uses of removed residues of other Rice varieties, it was found out that 58% of the removed residue of basmati rice is burnt by farmers. The practice of residue burning is lowest (7%) in Lahore and highest (95%) in Nankana Sahib. The burning of the residue of non-basmati Rice varieties is more prevalent in Kamoki, Pindi Bhattian, Nankana Sahib, Sanglahill, Shahkot, Narowal, Zafarwal, Ferozewala, Daska, Pasrur, and Sialkot tehsils. On average, 35.5 acres of non-basmati Rice varieties are burnt in one day.

Wheat:

The burning of the wheat residue was reported in all the districts except in Faisalabad, Gujrat and Kasur districts. Overall on average, 61 of crop area (acres) of Wheat is burnt, which is the lowest (2%) in Faisalabad and highest (89%) in Hafizabad district. Between 70–100% of crop area of wheat is burnt by farmers in Kamoki, Noshehra Virkan, Wazirabad, Hafizabad, Pindi Bhattian, Malikwal, Mandi Bahauddin, Phalia, Safdarabad, Daska, Pasrur, Sambrial, and Sialkot tehsils. Crop residue produced by wheat is 28 maunds per acre which were reported as the highest (49 maunds/acre) in Lahore. The ratio of paddy to straw is 52%.

When inquired about the uses of removed residues of wheat, it was found out that 41% of the removed residue of wheat was burnt by the farmers. The practice of residue burning of Wheat is lowest (3%) in Lahore and highest (84%) in Nankana Sahib.

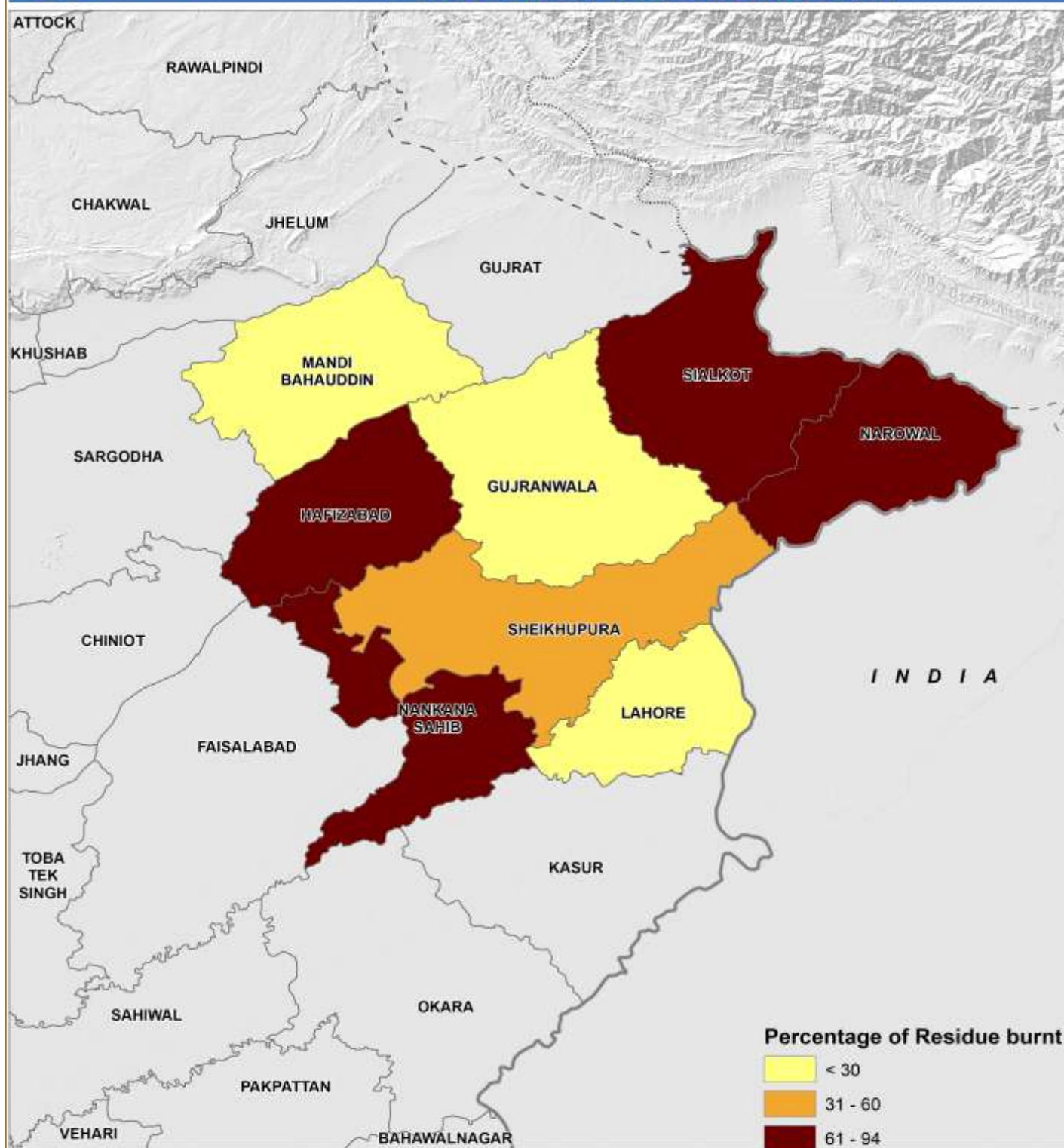
The burning of the residue of wheat is more prevalent in Nankana Sahib, Sanglahill, Shahkot, Zafarwal, Daska, and Pasrur tehsils. As reported by the farmers, on average, 119.1 acres of wheat are burnt in one day.

Maize:

The burning of maize crop residue area was only reported in Faisalabad, Kasur, and Nankana Sahib Districts. Overall, on average, 32% of crop area (acres) of maize is burnt; which was the lowest (15%) in Nankana Sahib and highest in Kasur (100%).

Crop residue produced by maize is 45 maunds per acre which were reported highest (72 maunds/acre) in Kasur.

When inquired about the uses of removed residues of maize, it was found out that 34% of the removed residue of maize is burnt by farmers. The practice of residue burning of maize is lowest (10%) in Faisalabad and highest (40%) in Nankana Sahib.



Map Legend

Administrative limits

- Country
- Province
- District

Data sources

FAO, Department of Agriculture Punjab

Disclaimer

The boundaries and names shown and the designation used on this map do not imply official endorsement or acceptance by the United Nations. Dotted line represents approximately the Line of Control in Jammu and Kashmir agreed upon by India and Pakistan. The final status of Jammu and Kashmir has not yet been agreed upon by the parties.

About Map

The map shows the information collected by farmer communities via Focus Group Discussions about percentage of Non Basmati Rice Residue burnt.

Map scale and Datum

Nominal scale: 1:2,557,000 at A3

Datum: WGS 84

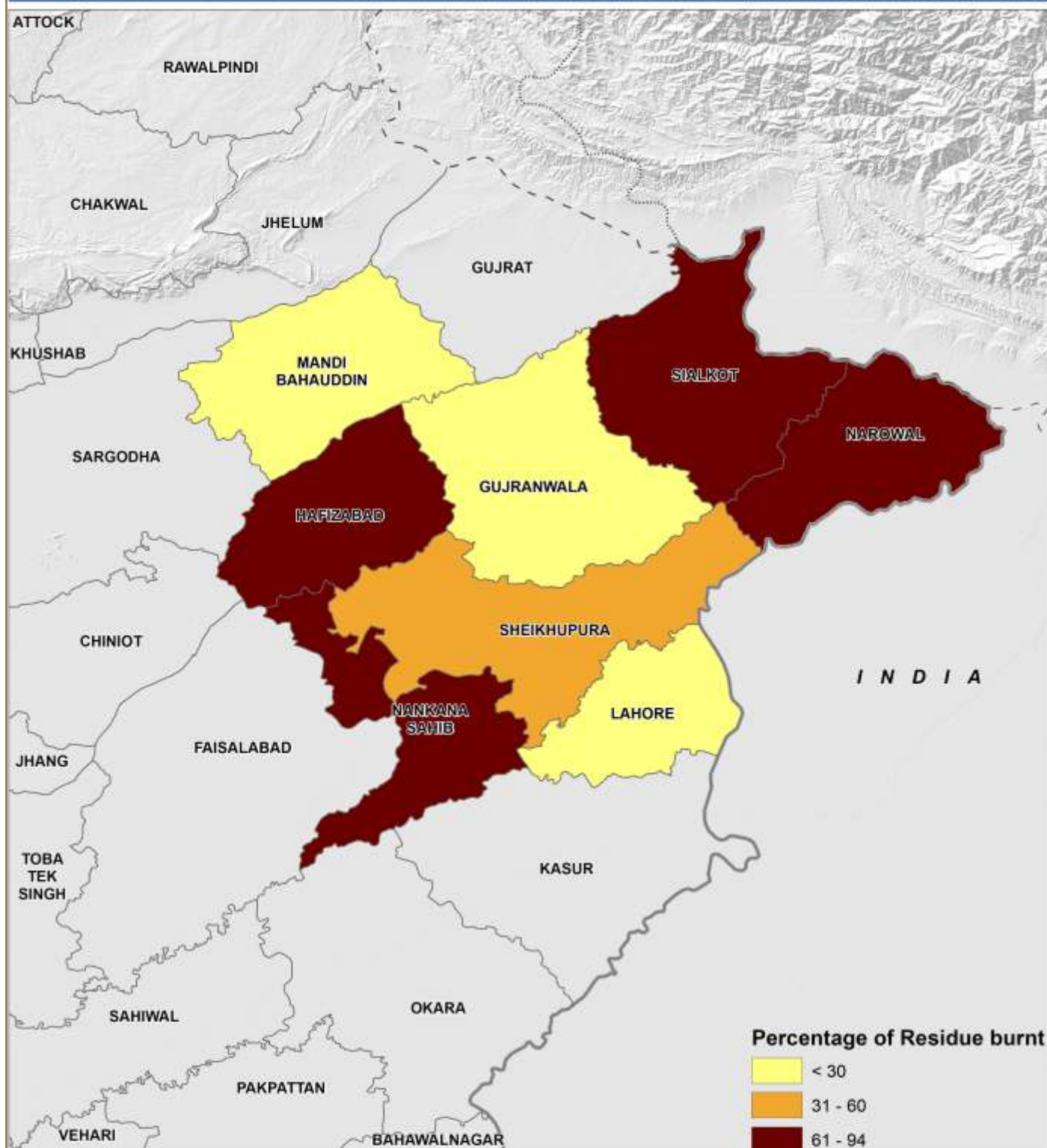
0 10 20 30 40 50
Kilometers

Date: 10 Sept 2018

Created by: IM Unit, FAO Pakistan



1.2. Map showing percentage of Basmati Rice Residue burnt by the farmers
Source: Adapted from United Nations World map, February 2020.



Map Legend

Administrative limits
Country
Province
District

Data sources

FAO, Department of Agriculture Punjab

Disclaimer

The boundaries and names shown and the designation used on this map do not imply official endorsement or acceptance by the United Nations. Dotted line represents approximately the Line of Control in Jammu and Kashmir agreed upon by India and Pakistan. The final status of Jammu and Kashmir has not yet been agreed upon by the parties.

About Map

The map shows the information collected by farmer communities via Focus Group Discussions about percentage of Non Basmati Rice Residue burnt.

Map scale and Datum

Nominal scale: 1:2,557,000 at A3

Datum: WGS 84



Date: 10 Sept 2018

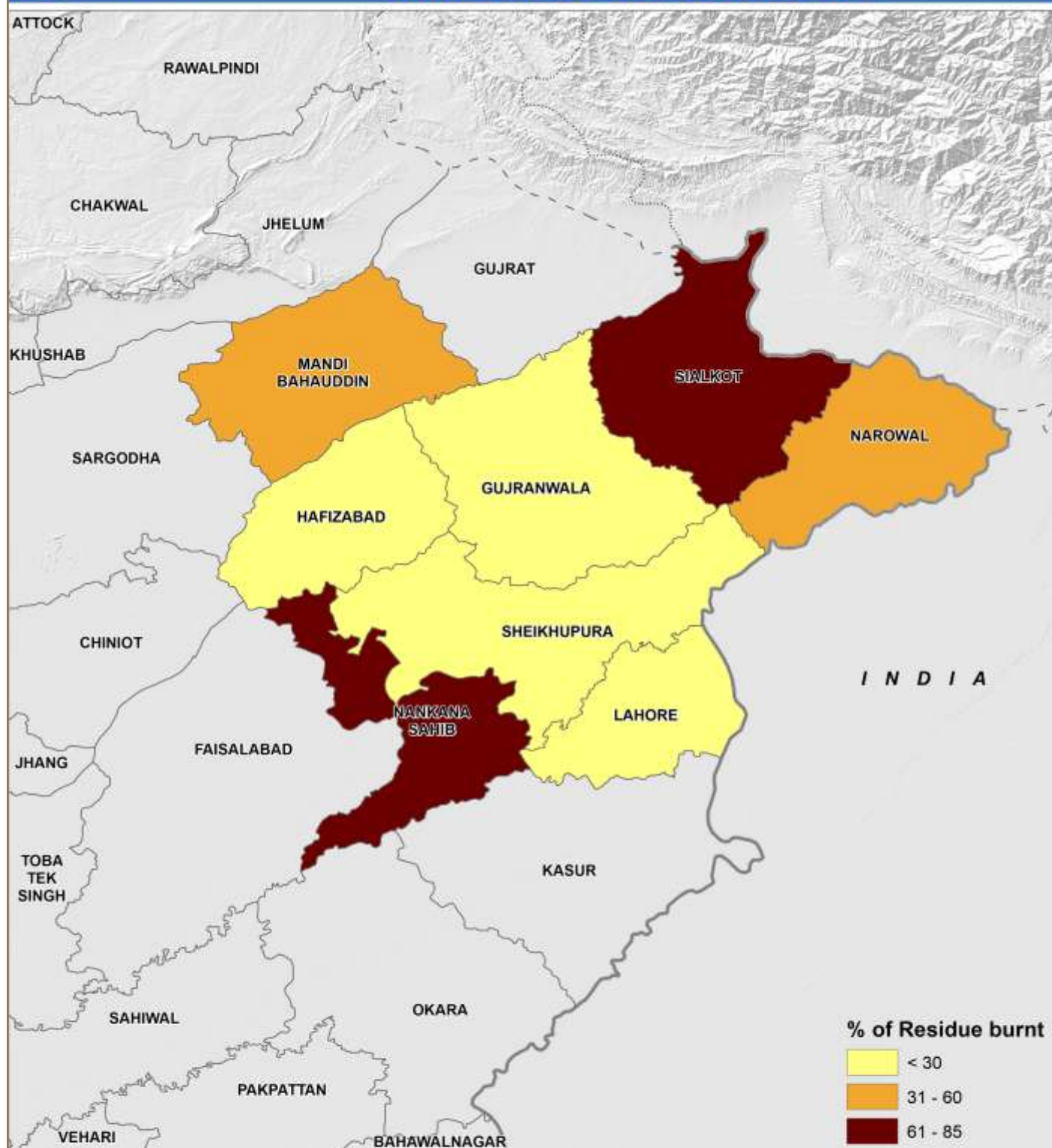
Created by: IM Unit, FAO Pakistan



1.3. Map showing percentage of Non-Basmati Rice Residue burnt by the farmers
Source: Adapted from United Nations World map, February 2020.



PERCENTAGE OF WHEAT RESIDUE BURNT FOCUS GROUP DISCUSSIONS 2017



Map Legend

Administrative limits

- Country
- Province
- District

Data sources

FAO, Department of Agriculture Punjab

Disclaimer

The boundaries and names shown and the designation used on this map do not imply official endorsement or acceptance by the United Nations. Dotted line represents approximately the Line of Control in Jammu and Kashmir agreed upon by India and Pakistan. The final status of Jammu and Kashmir has not yet been agreed upon by the parties.

About Map

The map shows the information collected by farmer communities via Focus Group Discussions about percentage of Wheat Residue burnt.

Map scale and Datum

Nominal scale: 1:2,557,000 at A3

Datum: WGS 84

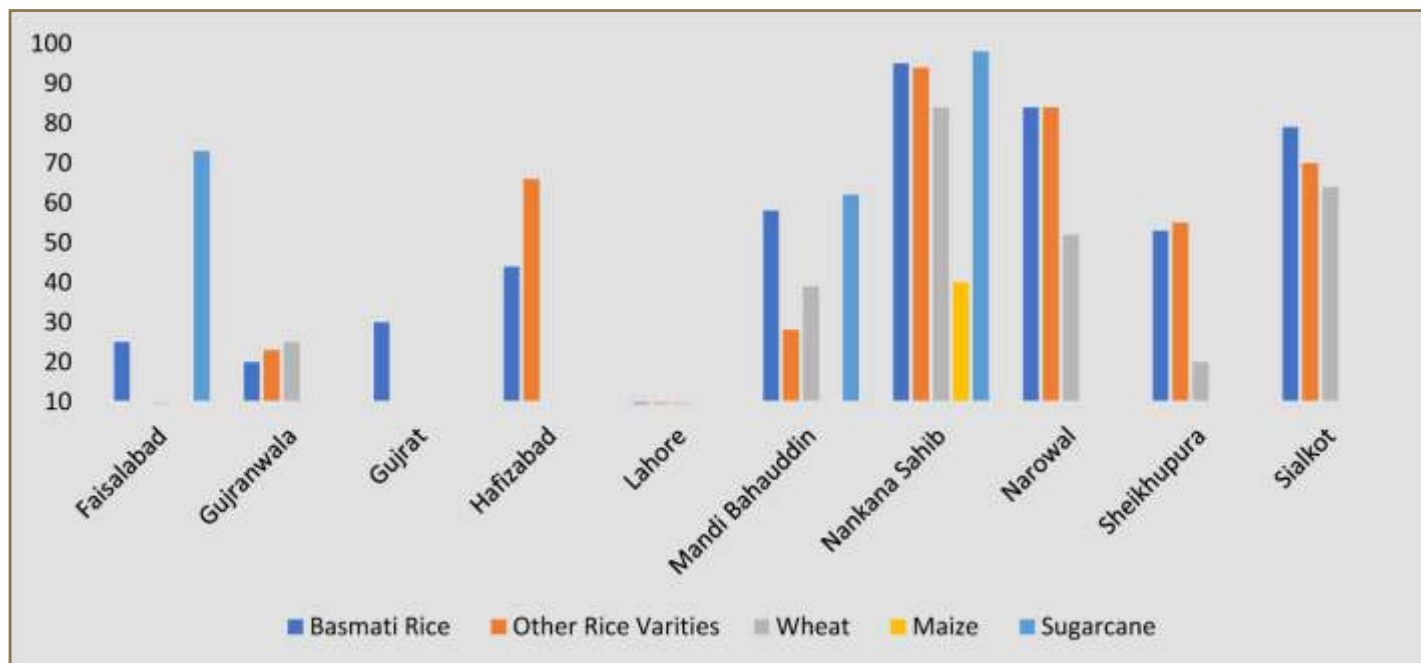


Date: 10 Sept 2018

Created by: IM Unit, FAO Pakistan



1.4. Map showing percentage of Wheat Residue burnt by the farmers
Source: Adapted from United Nations World map, February 2020.



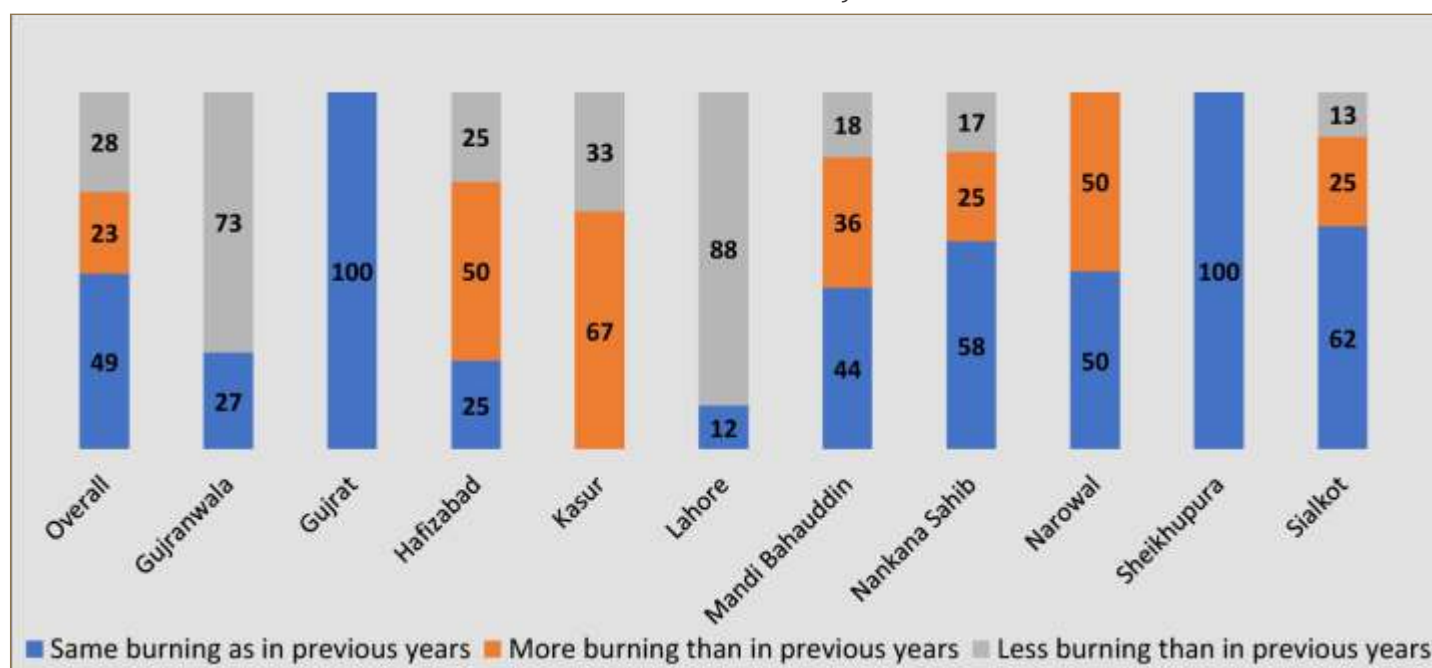
1.5. District wise chart for percentage of crop residue burnt

Sugarcane:

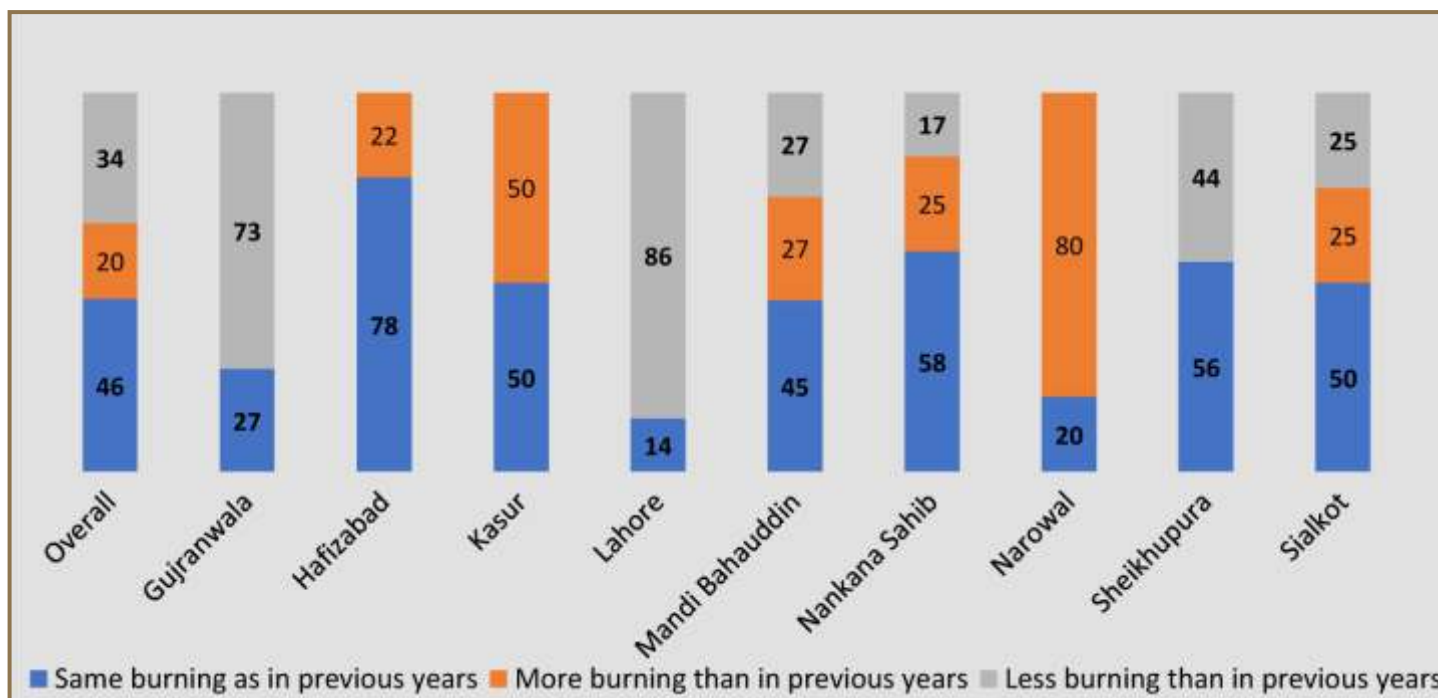
The burning of the residue of sugarcane was only reported in Faisalabad, Mandi Bahauddin and Nankana Sahib Districts. On an average, 78% of crop area of sugarcane is burnt, which is the lowest (70%) in Nankana Sahib and highest (88%) in Faisalabad district. Between 70-100% of crop area of

sugarcane is burnt by the farmers in Faisalabad, Jaranwala, Sumundri, Tandlianwala, Malikwal, Mandi Bahauddin, Phalia, Sanglahil, and Shahkot tehsils.

When inquired about the uses of removed residues of sugarcane, it was found out that 78% of the removed residue of sugarcane is burnt by farmers. The practice of residue burning of sugarcane is lowest (62%) in Mandi Bahauddin and highest (98%) in Nankana Sahib.



1.6. District wise chart for percentage of crop residue burning in Basmati Rice



1.7. District wise chart for a comparison of crop residue burning in Non-Basmati Rice varieties

The burning of the residue of sugarcane is more prevalent (70% and above) in Chak Jhumra, Jaranwala, Tandlianwala, Malikwal, Nankana Sahib, Sanglahill and Shahkot tehsils. On average, 36.2 acres of sugarcane is burnt in one day.

Crop residue burning compared to previous years

Basmati rice:

For basmati rice, 49% of the farmer communities reported the same burning in 2016 as in the previous years. 23% of the farmers reported more burning, whereas 28% reported less burning compared to the previous years. Farmers in Kasur, Hafizabad, and Narowal reported more burning in 2016.

Non-basmati rice:

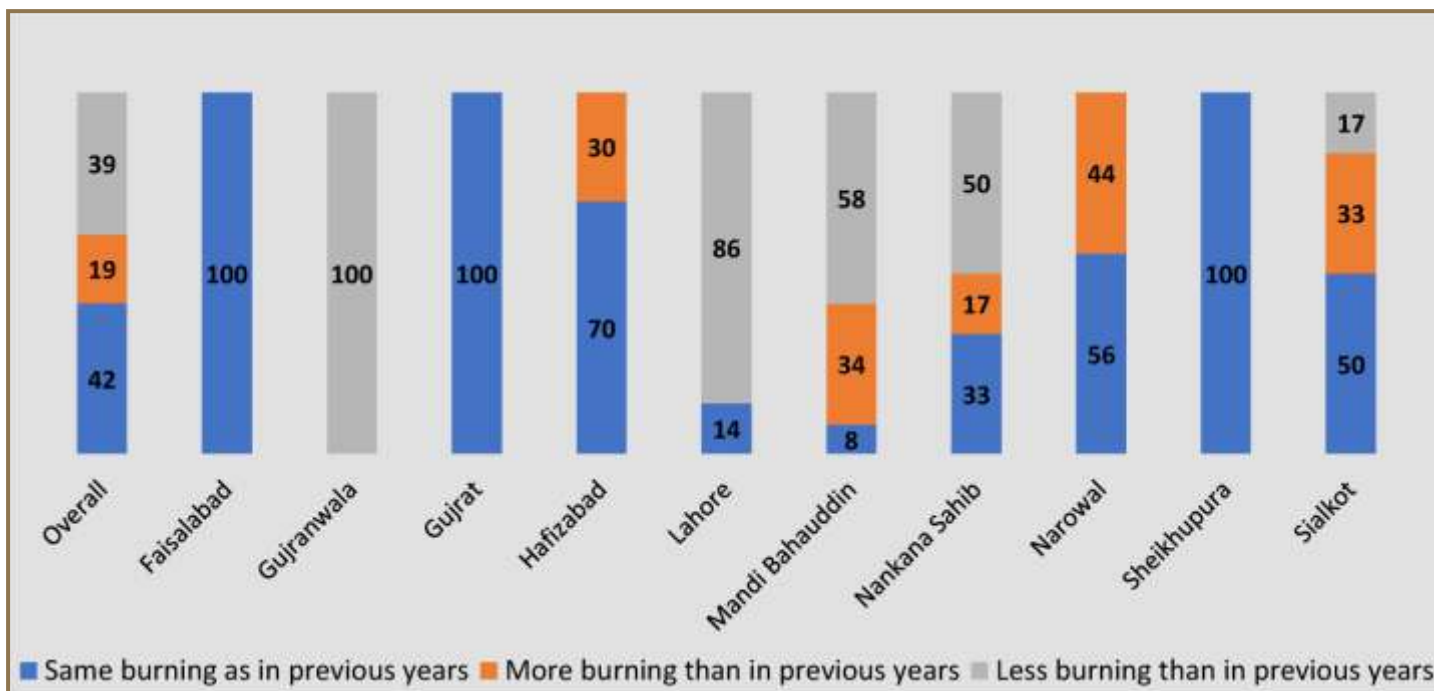
For non-basmati Rice varieties, 46% of the farmer communities reported the same burning in 2016 as in previous years. 20% of the farmers reported more burning, whereas 34% reported less burning compared to the previous years. Farmers in Kasur and Narowal reported more burning in 2016.

Wheat:

For Wheat crop, 42% of the farmer communities reported the same burning in 2016 as in previous years last year. 19% of the farmers reported more burning, whereas 39% reported less burning compared to previous years. Farmers in Narowal, Mandi Bahauddin, and Sialkot reported more burning in 2016.

Some other facts related to residue burning are as follows:

- The main reasons for burning crop residue reported by farmers are to get rid of trash/residue, the difficulty in soil preparation, desire to save labour cost, to eradicate weeds and pests and to facilitate cultivation and timely sowing of the next crop.
- Overall, farmers reported burning of crop residue for the past 16 years, ranging from 5 to 30 years.
- An important fact is that before starting burning of crop residue, farmers used to use crop residue as fodder for their animals.
- As reported by 44% of farmers it was observed that the decision to burn a field is taken after mainly considering the dryness of crop residue.



1.8. District wise chart for a comparison of crop residue burning in Wheat

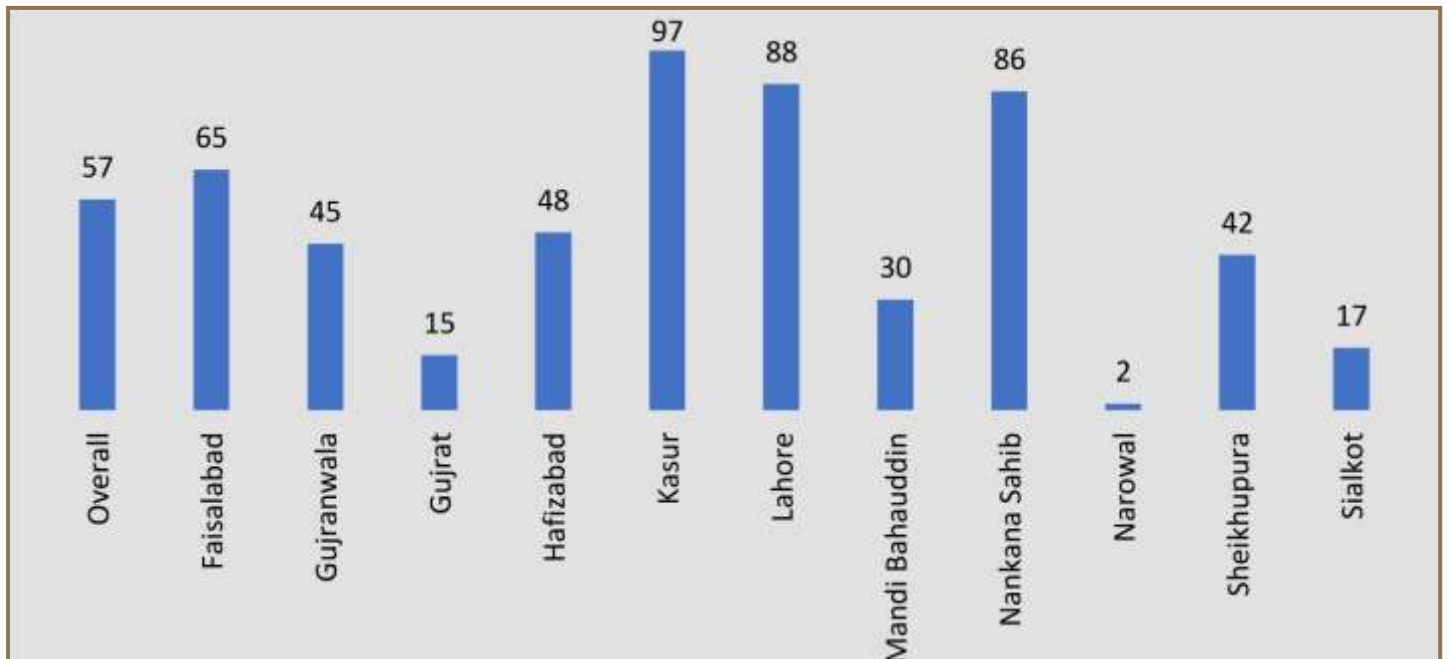
- Regarding the timings for crop residue burning, it was reported by 80 percent of the farmers that Crop residue burning is practiced during daylight, out of which between 28–48% of farmers burn the crop residue between 11 am–12 pm. In one field, crop residue burning lasts mostly for 0.5–1 hour as reported by 27 percent farmers.
- According to farmers, burning of crop residue particularly of rice when it is wet/green and contains moisture, increases the amount of smoke.
- About 44% of farmers informed that there has been an increase in the cultivation of non-basmati rice varieties in the last two years.
- About 84% of farmers were informed that there has been an increase in the use of combined harvester in the last five years.
- Around 37% of respondents were of the view that there has been an increase in waste material.
- 70–80% of respondents reported that small industries have increased while 50–60 percent think that the number of automobiles/vehicles have increased since the last 5 to 10 years.

2– Experience/impact of smog

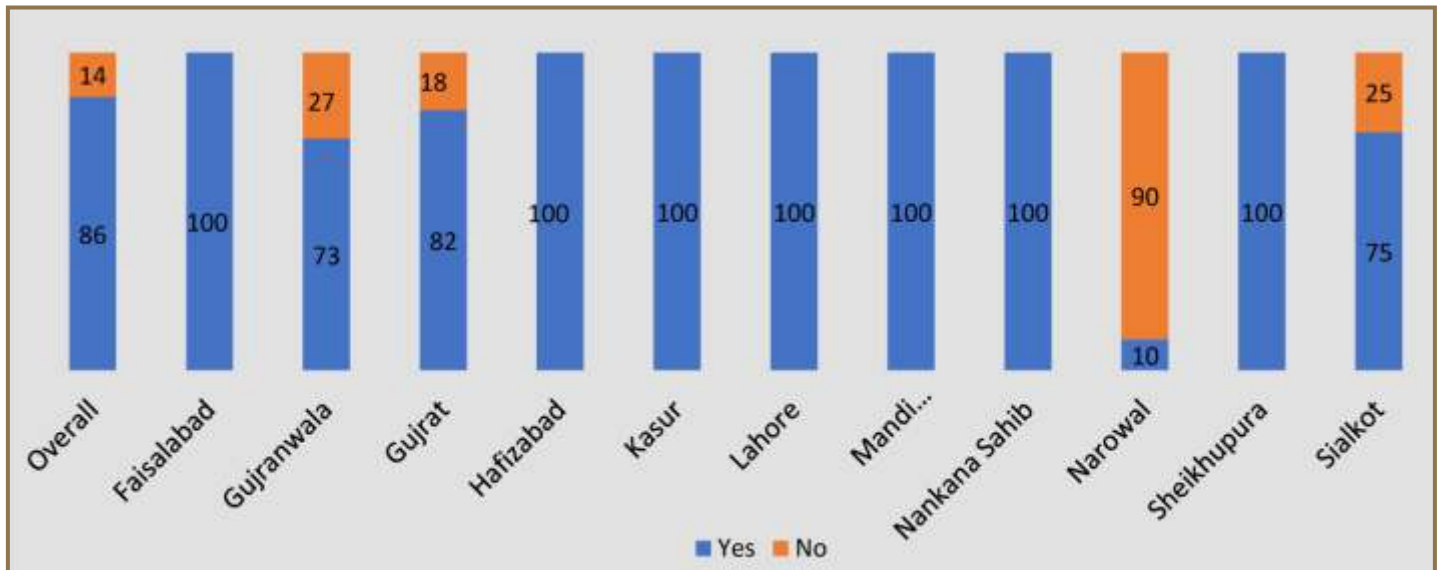
Based on the survey around half of the majority of farmers agreed that crop burning causes the formation of smog. Around 86% of respondents reported experiencing smog in 2016 which includes 100% of the farmers from Faisalabad, Hafizabad, Kasur, Mandi Bahauddin, Nankana Sahib and Sheikhupura districts. Smog was reported intense in the months of

November–December 2016. 81% of the farmers also reported smog was experienced by other villages in their UCs. Further, 83 percent of respondents considered the intensity of smog was higher in 2016 compared to 2015. In all the districts, the intensity of smog was higher in 2016 compared to the intensity of smog in 2015 except in Kasur and Narowal, where it was the same as in 2015.

The overwhelming majority of the respondents agreed that smog caused health problems in their areas. Overall, the health of 57% of community members was reported to be affected by smog. Throat problem, breathing/respiration problems, cough, flu, eye infections, allergy, and asthma were reported as major health problems caused by smog in all the districts.



1.9. District wise percentage of community members whose health was affected by smog in 2016 (%).

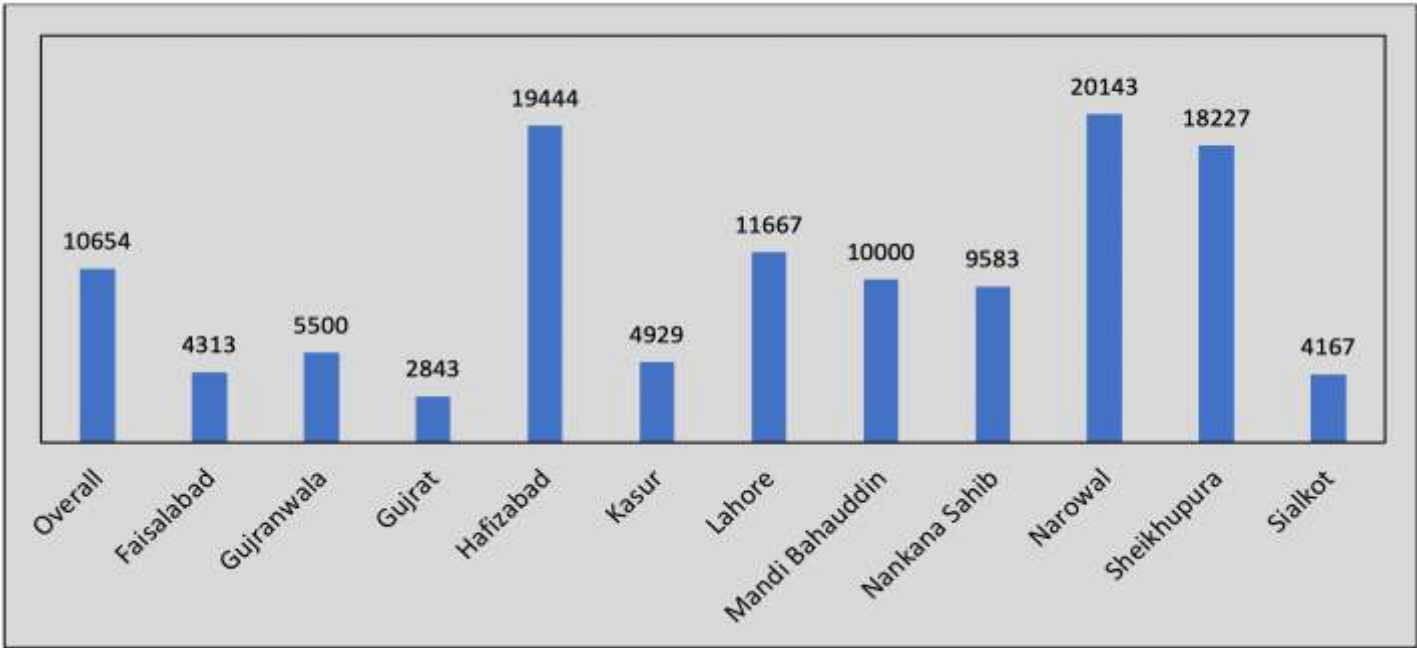


1.10. District wise percentage of communities that experienced Smog in 2016

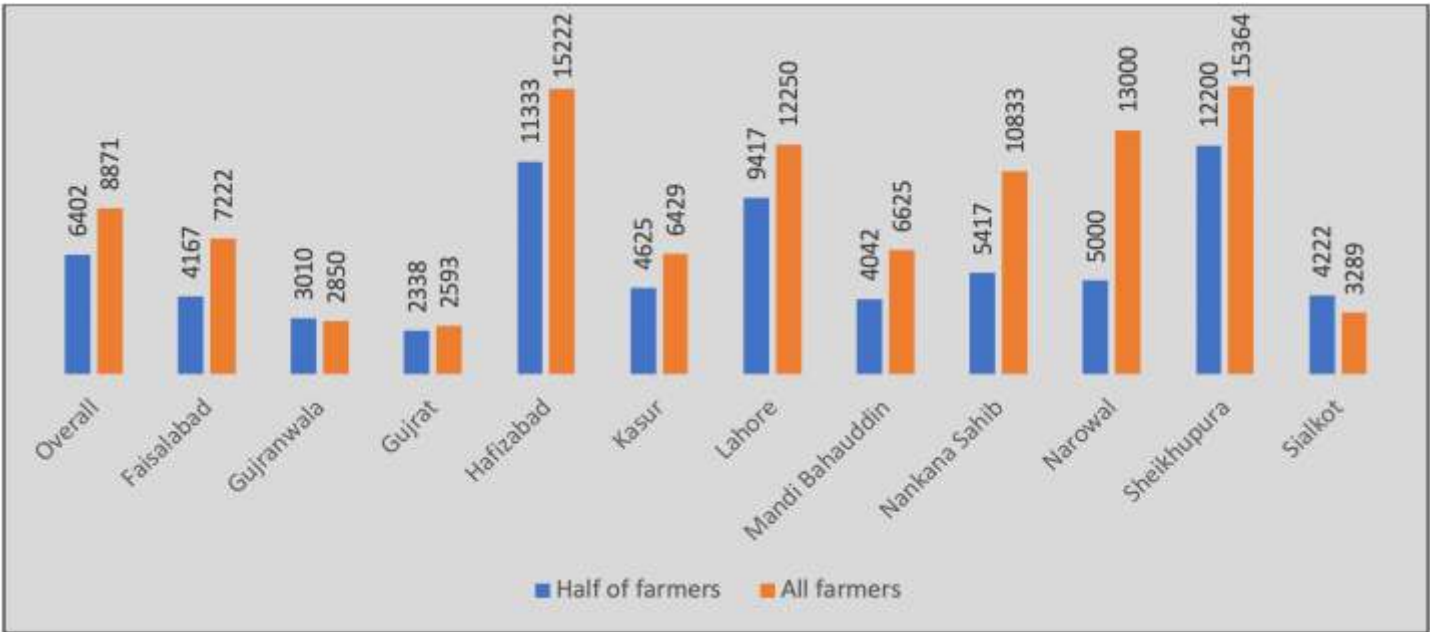
Cost and incentive to farmers to stop crop burning

The farmers were also asked about the incentives in order to stop crop residue burning. As reported in the FGDs, a farmer would accept a cost of Rs. 10 654/acre if crop burning is to be

stopped. Half and all farmers would stop crop burning if provided an economic incentive of Rs. 6 400 and Rs. 8 800 per acre respectively. The demand for incentives was the highest by farmers in Sheikhupura (Rs. 12 200 and Rs. 15 364 per acre respectively).



1.11. Cost (Rs./acre) a farmer will bear if stopped crop burning



1.12. Farmers would stop crop residue burning if given subsidy/incentive of Rs./acre

3– Suggestions by farmers to reduce crop residue burning

The farmers offered the following main suggestions to reduce the crop residue burning:

- Use it as fodder or incorporate it into the soil.
- Provide suitable machinery to cut the residue at ground level and the machine which can separate the grains from straw/stems and bury the residues. It was also mentioned to provide special machinery such as (Kabuta), special harvester and chopper for rice residue management. It was also suggested to plough the Crop residue by disc harrow.
- Awareness among farmers about health, environmental issues and about care of environment Provision of special harvester for rice and wheat on subsidy.

4– What farmers would do if crop residue burning is banned by the Government

The responses by farmers, on the question of the possible ban by the Government on crop burning, are categorized into two groups mainly:

- 42% of the farmers agreed to accept the ban and demand for alternate methods for cleaning the field to facilitate the tillage operations. These farmers also demanded Government to provide subsidy or better technology for incorporation of crop residue.
- 46% of the farmers refused to accept the ban and said that they will protest against such laws as there face a huge problem in land preparation and ploughing due to straw and stems and there is no other alternate other than burning. They will stop the cultivation of such crops which produce residues.

SECTION II

CLIMATOLOGICAL MODELLING OF SMOG

Key messages

1 Assessment and mapping of regional aerosol point sources indicates that the 65% of the aerosol sources are detected within Pakistan. Smog sources need to be managed and controlled within the country as a matter of priority.

2 If burning and combustion activities in winter and post-monsoon periods are controlled, the smog levels can also be quickly reduced.

SECTION II

Climatological modelling of smog

2.1 A brief introduction to atmospheric pollutants playing a role in smog formation

Before the phenomenon of smog is discussed further, it is useful to describe various types of atmospheric aerosols (suspended particulates which can either be naturally occurring such as dust, pollen, sea salt, volcanic ash, and carbon particles from natural fires, or anthropogenic (man-made i.e. from combustion sources in urban areas including soot, carbon particles, ammonia, sulphate and nitrate compounds).

Atmospheric particulates or aerosols can be found suspended in the air at different heights owing to their composition and size. They are divided into two main types; namely primary and secondary. Primary aerosols are emitted or injected directly into the atmosphere i.e. dust, pollen, vehicular exhaust, industrial emissions, biomass burning activities etc. and secondary aerosols are formed in the atmosphere by chemical reactions on the primary aerosols, such as the creation of sulfuric acid droplets and sulphate particles from an initial injection of sulphur dioxide gas from volcanic eruptions etc. Both primary and secondary particulates can have either natural or anthropogenic sources or a combination of both.

Smog is an example of a secondary aerosol formed as a result of chemical reactions in the lower part of the atmosphere. As discussed above, smog is a mixture of different pollutants, including oxides of nitrogen (NO_x), oxides of sulphur (SO_x), carbon monoxide (CO), particulate matter (PM), volatile organic compounds (VOC) and the ozone. In these pollutants, NO_x in the presence of sunlight undergoes chemical reactions to create ozone. Ozone is the major factor behind the build-up of smog. Hence pollutants such as carbon monoxide are emitted directly from combustion activities of vehicles, industry and biomass burning which act as the primary aerosols, while ground-level ozone formed in the air from Nitrogen oxide emissions act as the secondary aerosol in the build-up of smog. There is extensive scientific literature present on different modes of atmospheric aerosols. Here, discussed briefly, atmospheric aerosols are categorized into

different modes depending upon their size distribution. Generally, three modes are expressed in terms of their radii namely 'aitken mode', 'accumulation mode' and 'coarse mode'. The aitken mode (particle size $< 0.1 \mu\text{m}$) consists primarily of combustion particles emitted directly into the atmosphere and particles formed in the atmosphere by gas-to-particle conversions. They are usually found near highways and other sources of combustion. Because of their high number concentration, especially near their source, these small particles coagulate rapidly. Consequently, aitken particles have relatively shorter lifetimes in the atmosphere and end up in the accumulation mode.

The accumulation mode ($0.1 \mu\text{m} < \text{particle size} < 2.5 \mu\text{m}$) includes combustion particles, smog particles, and coagulated aitken-mode particles. Particles in this mode are small but they coagulate too slowly to reach the coarse-particle mode. Hence, they have a relatively long lifetime in the atmosphere and they account for most of the visibility effects of atmospheric aerosols. The nuclei and accumulation modes together constitute 'fine-mode' particles.

The coarse-particle mode (particle size $> 2.5 \mu\text{m}$) consists of windblown dust, large salt particles from sea spray, and mechanically generated anthropogenic particles such as those from agriculture and surface mining. Because of their large size, the coarse particles readily settle out or impact on the surface, so their lifetime in the atmosphere is only a few hours. In our analysis, we take two broad categories from literature as mentioned above namely 'fine-mode' particles (size $< 2.5 \mu\text{m}$) and 'coarse-mode' particles (size $> 2.5 \mu\text{m}$). Particle sizes with radii less than $2.5 \mu\text{m}$ are generally called $\text{PM}_{2.5}$ while with radii less than $10 \mu\text{m}$ are called PM_{10} (which also include $\text{PM}_{2.5}$). Particles with diameter $< 0.01 \mu\text{m}$ represent freshly formed particles near to the combustion source and are categorized as 'ultra-fine' particles in the Aitken mode.

$\text{PM}_{2.5}$ has the greatest potential to affect human health. Because of their small size $\text{PM}_{2.5}$ can be drawn deep into the lungs upon inhalation. Approximately 70% of all particulates

emitted by biomass burning are less than 2.5 microns in diameter. PM_{10} (dust, pollen, mold etc.) are bigger particles and quickly settle down by gravity or are washed out by rain. $PM_{2.5}$ (combustion, organic compounds, metals etc.) are smaller particles which remain in the atmosphere for a longer time (a couple of days to weeks). Due to their small sizes, they can be transported over longer distances. Their longer stay in the atmosphere, also makes the possibility of different photochemical and physiochemical processes, thereby altering their composition and characteristics. Therefore, the third category as 'mixed type', which defines those particles do not fall under fine-mode and the coarse-mode category.

2.2 Optical properties of different atmospheric pollutants

Smog makes the atmosphere appear thick and dark or yellow in colour (depending upon the colour of pollutants present in the atmosphere). It can occur any time during the year in the presence of air pollutants, however, the most noticeable times are from October to March, when lower temperatures and high atmospheric stability lead to reduced dispersal rates of pollutants. In order to get information about concentration, size distribution and variability of aerosols in Punjab, during the smog period, two types of optical properties have been used namely, aerosol optical depth τ and Angstrom wavelength exponent (α).

Aerosol optical depth is a dimensionless number that is related to the amount of aerosols distributed within a vertical column of atmosphere over the observation location. Aerosol particles in the atmosphere can block sunlight by absorbing or by scattering. τ is used as a quantitative measure of the extinction of solar radiation by aerosol scattering and absorption. Heavy aerosol loadings can lead to τ higher than 0.3. In intense polluted days in Lahore, $\tau > 1$ has also been reported.

Angstrom wavelength exponent (α) provides additional information on the particle size, aerosol phase function and the relative magnitude of aerosol radiances at different wavelengths. α is an exponent that expresses the spectral dependence of aerosol optical thickness (τ) with the

wavelength of incident light (λ).

(α) can be calculated from the spectral distribution of AODs following Ångström power law (Ångström, 1929) as:

$$\tau(\lambda) = \beta \lambda^{-\alpha(\lambda)},$$

where $\tau(\lambda)$ is the AOD at a particular wavelength λ (in μm) and β is the turbidity coefficient (at $1 \mu\text{m}$). Typical values of α estimated from different measured in the $0.44\text{--}0.87 \mu\text{m}$ wavelength regime are found to vary from 1 to 3 for fresh smoke particles, which is dominated by accumulation-mode aerosols to nearly zero for the atmosphere dominated by coarse-mode aerosols such as dust and sea salt [Holben *et al.*, 2001; Eck *et al.*, 2001]. α can be computed following the Volz method using any pair of wavelengths λ_1 and λ_2 as

$$\alpha = -\frac{d \ln \tau}{d \ln \lambda} = -\frac{\ln \left(\frac{\tau_1}{\tau_2} \right)}{\ln \left(\frac{\lambda_1}{\lambda_2} \right)},$$

where τ_1 and τ_2 are the AODs at wavelengths λ_1 and λ_2 . α has been used in many studies as a tool to quantify particle size distribution from spectral distribution of and for extrapolating throughout the shortwave spectral region [e.g., Smirnov *et al.*, 2002].

2.3 Climatology and seasonal air masses entering Punjab

The climate of Punjab ranges from semi-arid to hyper-arid. Receptor site of Lahore ($31^{\circ}23'$; $74^{\circ}22'$)E being in northern Punjab enjoys a semi-arid climate, while the deserts of Cholistan and Thal come under the hyper-arid category. Punjab receives frequent dust storms (DS) in the months April–June followed by monsoon rains from July–September. Hottest temperatures are recorded in the months of June and July with mean daily maximum temperature often exceeding 40°C . The rainy season is followed by the dry months of October and November. Cold weather persists December to March when the mercury falls as low as -2°C on some of the days.

Looking at wind directions, during winter (December–February), western disturbances (from northwest and

Southwest) cause light to moderate rain and foggy conditions (Hameed et al., 2000), followed by pre-monsoon (April–June) during which air masses come from the southwest and the south resulting in dust storms (DS) and heat waves. The rainy monsoon (July–September) follows onwards, bringing along heavy downpour under influence of southerly and southeasterly air masses (Rasul and Chaudhry, 2010) while the post-monsoon (October–November) is characterized as the dry season in which air masses usually come from the west. This makes Lahore particularly a sensitive receptor site in terms of long-range transport of different types of aerosols coming from remote locations carried along seasonal air masses.

The long-range transport of different types of atmospheric suspended particles (aerosols) on a regional basis, arriving Lahore (representing northern Punjab) originating from various source locations around the receptor site have been previously discussed in detail in a study carried out by GCISC (Zafar et al., 2018). The results of the study showed that for the year as a whole, 61 percent of the particles originated from within Pakistan (mostly concentrated within Punjab) and 39 percent from other regional sources. A classification criterion was further established to identify aerosols as dust, anthropogenic (fine-mode; mixed-mode) and maritime aerosols. Based on their findings, they established winter (December, January, February and March) and post-monsoon (October, November) seasons as the months during which most of the anthropogenic aerosols were transported to Punjab, from various locations both inside and outside of Punjab.

This study discusses the regional sources of anthropogenic aerosols (responsible for smog formation) for a period of ten years (2008–2017) on a seasonal basis i.e. for winter and post-monsoon.

The study entails in identifying different types of pollutants originating from within Pakistan focusing Punjab of Pakistan and regional countries. In the absence of any ground network of air quality observations, international data sources to study smog precursors have been utilized mainly taking into consideration optical properties of aerosols i.e. aerosol optical depth (τ) and Ångström Wavelength Exponent (α) in order to quantify their concentrations and types.

2.4 Smog source identification in smog dominated regions with a focus on Punjab province of Pakistan

2.4.1 Data and methodology

2.4.1.1 Hysplit air-parcel trajectory model

Hybrid Single Particle Lagrangian Integrated Trajectory (HYSPLIT) model, developed by NOAA's Air Resources Laboratory was used to create 5-day air-back trajectories for the study period (2008–2017) to assess transport and sources of air pollutants. HYSPLIT has been widely used in the research community for analyzing transport of air masses using forward and backward trajectories. The trajectories were created for the whole study period at the height of 2 000 m (2 km) taking Lahore as representative of smog dominated zone in Punjab. Lahore site has been selected based on availability of ground observations, hereby called as receptor site.

2.4.1.2 AERONET

The ground-based observations used for the study (period: 2008–2017) are (a) sun-photometer data for aerosol-monitoring, obtained from AERONET (AErosol RObotic NETwork) Level 1.5 (cloud-screened) (Holben et al., 1998; Smirnov et al., 2000), (τ) (500 nm) and (α) (measured between 440 and 870 nm), installed in Lahore, and operated by the

National Aeronautics and Space Administration (NASA) (<https://aeronet.gsfc.nasa.gov/>);

Both AERONET and MODIS provide a powerful method for characterizing the optical properties and size distribution of atmospheric aerosols and have been extensively used to study the optical properties of aerosols at the global level (Holben et al., 1998).

The trajectories were further associated with ground-based sun-photometer (AERONET) data of aerosol size distribution, to assess transport pathways of different aerosol types such as dust and anthropogenic arriving at the receptor site.

2.4.1.3 ERA–Interim

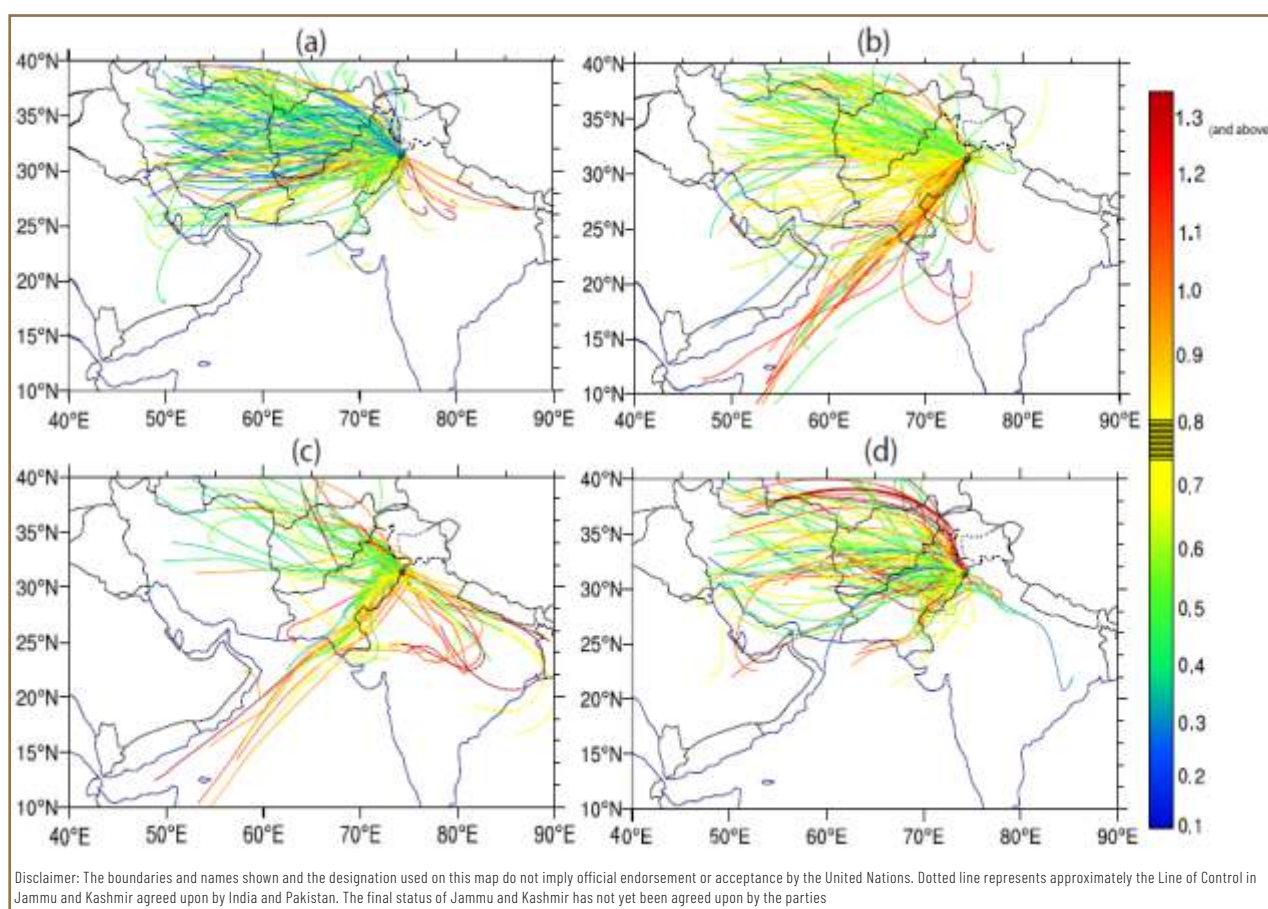
Besides the source analysis, monthly wind dynamics using ERA-Interim from ECMWF at pressure levels (1 000, 975, 950, 900, 850 & 800) hPa have also been examined. The detected

sources and wind speeds at different heights were studied in conjunctions with different extreme smog events.

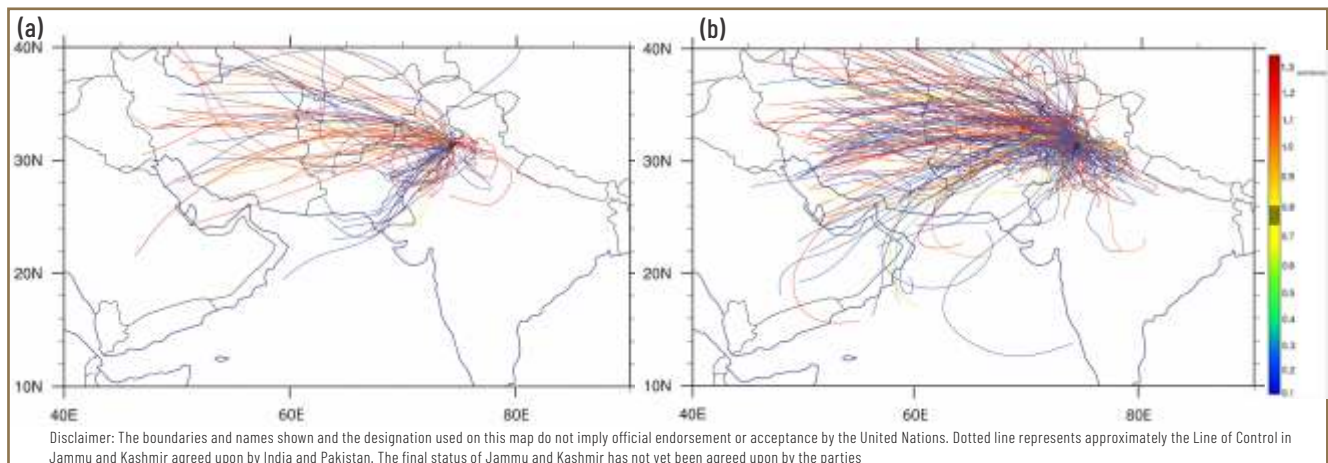
2.4.2 Seasonal dynamics with hysplit

In this study winter constitutes December, January, February and March, while post-monsoon constitutes October and November also shown by Hussain et al., 2005. Ali et al. (2014) studied the aerosol optical properties over Lahore (December 2009 to October 2011) and found increasing τ values over Lahore in winter. Their findings were also found consistent with Alam et al. (2010) and Alam et al. (2011) who also studied τ trends over Lahore using MODIS data for the period's 2001–2006 and 2002–2008 finding that high mean τ was obtained during the winter season. Figure 2.1 presents analysis of 5-day air-back trajectories for winter (DJFM), pre-monsoon (AMJ), monsoon (JAS) and post-monsoon (ON). The model simulations show seasonal variations in air parcel

trajectories originating from different locations. In winter, most of the air parcels were arriving from west and south-west, in pre-monsoon the westerly and south westerly air masses also became southerly, monsoon exhibited eastern transport of air masses along with westerly and southerly air masses while post-monsoon predominantly exhibited south-westerly air masses. This trajectory analysis also demonstrate the western disturbances originating from the Mediterranean Sea in winter, dust storms associated with the southerly air masses carrying along dust aerosols from the deserts of Thar and Cholistan in pre-monsoon, easterly and southerly monsoon currents originating from the Bay of Bengal, and the Arabian Sea in monsoon and dry season as a result of south westerly air-masses with no moisture in the post-monsoon. The seasonal variations in air masses depicted by model air parcel trajectories are also found to be in-line with the previous literature (Section 2.3), therefore these are used as baseline climatology to further build upon in the future time periods.



2.1. Five-day daily backward trajectories ending at Lahore from 2010 to 2014 with trajectory colors representing values of α measured at Lahore. The trajectories are shown season wise (a) winter (b) pre-monsoon (c) monsoon and (d) post-monsoon. The position of Lahore is represented by the black dots
Source: zafar et al., 2018

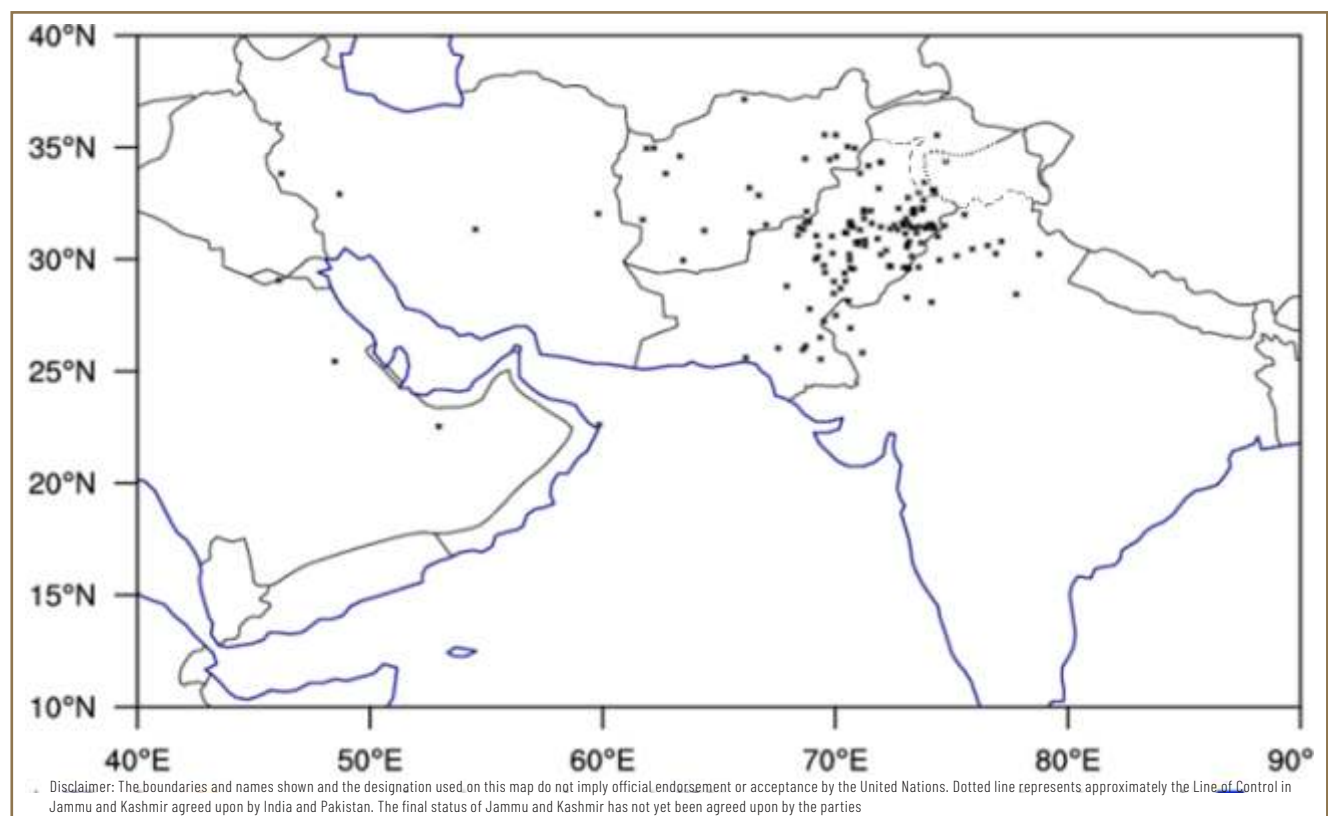


2.1.1. Five- day daily backward trajectories ending at Lahore from 2015 to 2017 with trajectory colors representing values of α measured at Lahore. The trajectories are shown season wise (a) Post–monsoon (b) Winter. Source: GCISC and adapted from United Nations World map, February 2020.

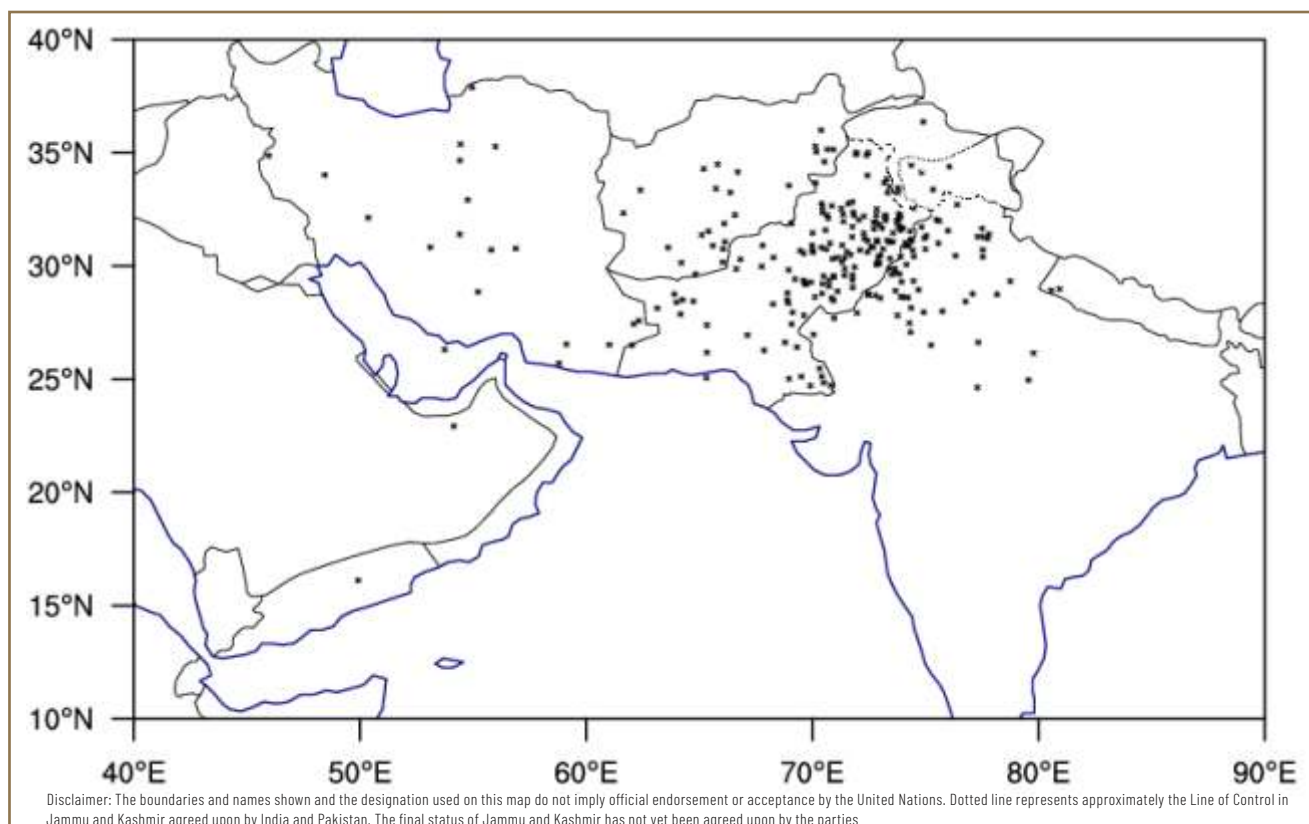
2.4.3 Assessment and mapping of regional point source locations

In order to understand smog conditions, point source locations were firstly identified based on HYSPLIT air parcel trajectories (period: 2008–2017). The methodology was

adopted from *Pace et al., 2006* which takes into consideration the interaction of an air parcel with the mixed layer to identify aerosol source locations. Air parcel heights along with the tropospheric boundary layer heights were obtained by HYSPLIT at the height of 2 000 m. The aerosol loading at the source location was assumed as the point where the height of



2.2. (a) Point source locations (Period: 2008–2017) for post-monsoon. Source: GCISC and FAO Pakistan



2.2. (b) Point source locations (Period: 2008–2017) for winter at 2000 m. Source: GCISC and adapted from United Nations World map, February 2020.

an air mass 'zair' gets lower or close to the height of the mixed layer 'zmxl', e.g. $(z_{air} - z_{mxl}) < 500\text{m}$ (entrainment condition). However, if the criteria was being satisfied at more than one point, that source location was chosen where the difference $z_{air} - z_{mxl}$ was smallest (sign included). Those cases in which the entrainment condition was never met during the 5- day travel time of any trajectory, the air mass was considered to be in 'permanence condition'. The point sources for anthropogenic aerosols were identified for winter and post- monsoon. Pan et al. (2015) performed a multi-model evaluation of polluted aerosols over South Asia and found that the aerosol vertical mixing was relatively uniform within the lowest 2 km and could extend up to an altitude around 6 km in the pre- monsoon season. Therefore, the model was configured to obtain 5- day air- back trajectories at the heights of 2 000 m by associating each trajectory with its corresponding t and α obtained from the sun photometer data. The sources were identified for the ten years period: 2008–2017 for post-monsoon and winter [Fig 2.2 a,b]. Looking at the source locations, the sources were identified

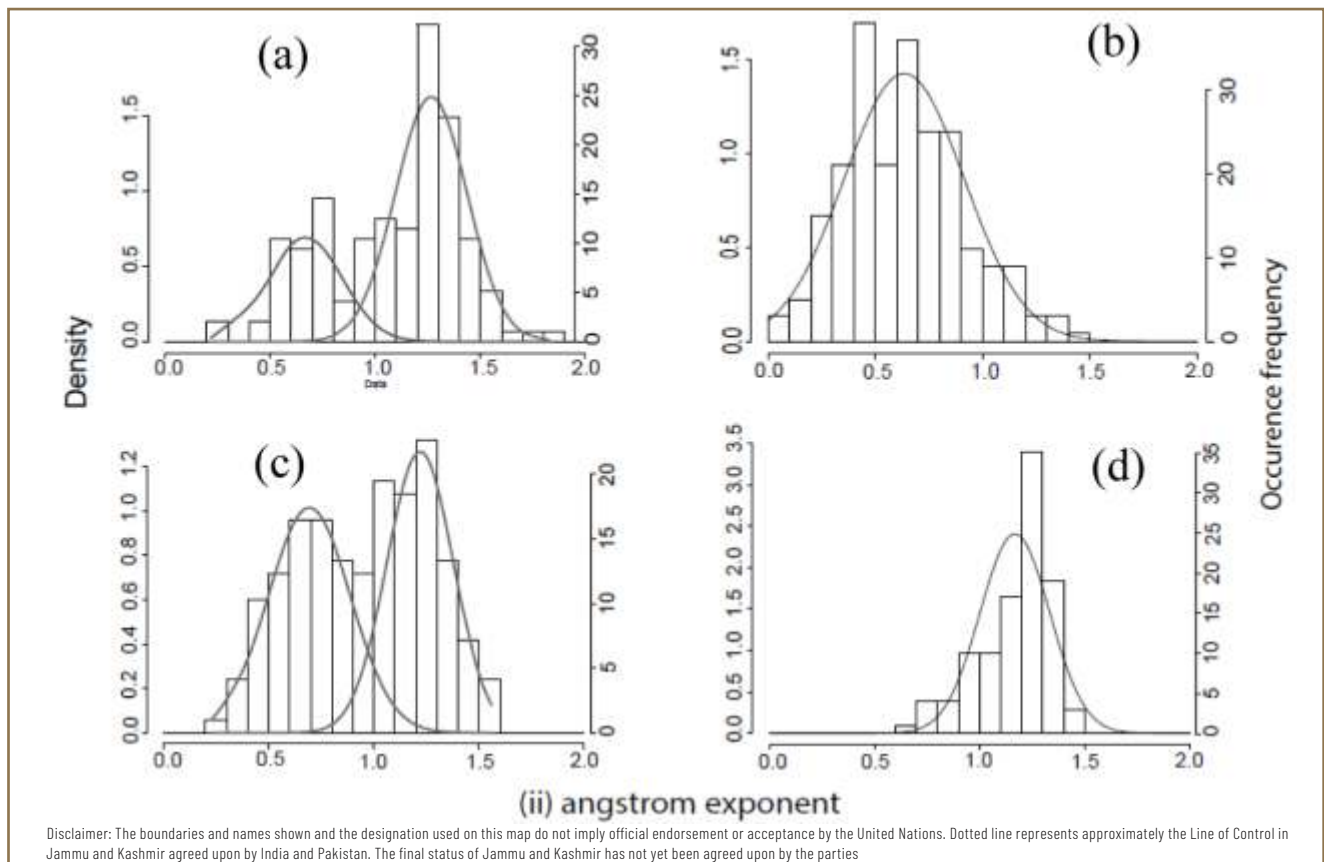
on a regional scale; throughout Pakistan, in north-eastern India, Afghanistan, Iran and only a few in Saudi Arabia. More sources were found in winter owing to the longer season length (i.e. four months in winter compared to the two months in post-monsoon).

2.4.4 Seasonal uni-modal and bi-modal distributions

Fig 2.3 shows that aerosols present in winter constituted two means (period: 2010–2014). The lower means (lower α) depict coarser aerosols while higher means (higher α) depict finer aerosols. The distribution of sources depicts that coarser aerosols that might be present over the region in winter constitute the mean range of α (0.6–0.7) while finer aerosols in range α (1.2–1.3). The distributions showed that winter was dominated by the finer particles, pre-monsoon with coarser particles (having a uni-modal distribution of coarser aerosols), monsoon with equally distributed coarser and finer particles (washed away with scattered rains and often depicted by cloudy conditions when studying with satellite) while post-monsoon dominated by finer aerosols (uni-modal

distribution of finer aerosols). In order to learn about the occurrence of smog sources in the current study, winter and post-monsoon seasons were selected, which were pre-dominated by the fine-mode aerosols with anthropogenic origin. Lahore was ultimately found to fall under mean α of 1.2-1.3, while coarser or dust aerosols with mean α of 0.6-0.7.

aerosols with $t < 0.2$ were characterized as a clean environment. It was found that Lahore exhibited virtually NO clean environment. From Fig. 2.4, it is evident that most of the detected aerosol sources in winter and post-monsoon were found to lie in the category of urban industrial/biomass burning 'bu' and then in the 'mixed' type category. , while the particles in pre-monsoon were lying in the desert dust (DD)



2.3. Gaussian distributions fitted to the aerosol sources found around Lahore from 2010 to 2014 for α showing the occurrence frequency of different aerosols in (a) winter (b) pre- monsoon (c) monsoon and (d) post- monsoon. (Source: Zafar et al., 2018)

2.4.5 Classification

An aerosol classification criteria developed by Zafar et al., 2018 to detect aerosol source locations around a northern Punjab site (Lahore) has been applied further. The criteria identify dust (i.e. dust), biomass burning/urban- industrial (i.e. bu) and mixed (i.e. mixed) type aerosols over the study region [Fig 2.4 a, b]. The properties of dust aerosols were defined by $t \geq 0.3$ and $\alpha \leq 0.75$, while the properties for anthropogenic aerosols 'bu' were defined by $t \geq 0.2$ and $\alpha \geq 1.15$. The aerosols which lie in between the two thresholds were put under the criteria for 'mixed' type of aerosols. The

category. The particles in monsoon were lying in all three categories depicting equal contribution of all types of aerosols during this season.

Therefore, based on the analysis, post-monsoon and winter have been considered to study smog conditions over Punjab. Previously, no such studies have been done regarding source detection of pollutants originating from any local or regional source locations, arriving the districts of Punjab or any other part of Pakistan. Also, this study is the first ever attempt in identifying the smog sources and smog aerosol types on a regional scale in light of certain threshold criteria for

characterizing an air parcel composition into DD, BU, mixed and maritime pollutants. Smog in the post-monsoon is also referred as 'smoky haze' as dry season constitutes dry (finer) particles, which when combined with smoke and other vehicular and industrial emissions turn into smog, hindering visibility. Smog in winter is also referred as 'smoky fog' because the lower temperatures condense the atmospheric gaseous water content in liquid droplets making fog, which traps incoming smoke and other pollutants, thus constituting smog.

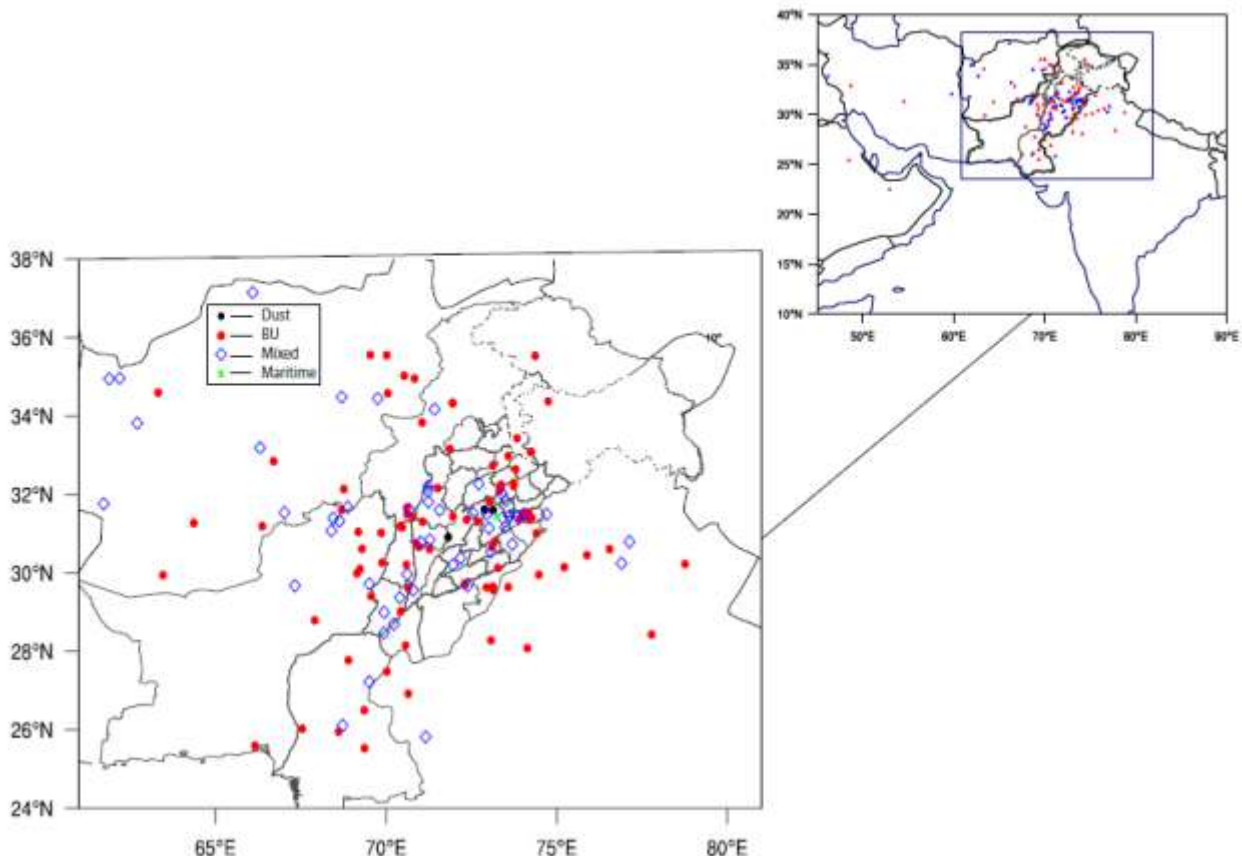
From the figure below, it can be seen clearly that 'bu' and 'mixed' aerosols are mostly concentrated within Punjab and around the eastern border of Punjab. All three types of sources are present throughout the study domain, however, mostly occurring sources are found within Punjab. The contributions from India, Afghanistan, and Iran were further assessed by finding out the total number of sources and their percentages in table 2.1 and 2.2.

2.4.6 Absolute and percentage distribution of point source regions

Of all types of aerosol sources found around Lahore during winter and post-monsoon, 65 % of the sources were detected within Pakistan, 17 % in India, 11 % in Afghanistan, 5 % in Iran and 1 % in Saudi Arabia 1 %. On a seasonal basis, 63 % of all types of regional sources were found in winter while 37 % in post-monsoon. Of all the sources detected in winter, 39 % were detected in Pakistan, 13 % in India, 6 % in Afghanistan, 4 %, in Iran, and no sources were detected from Saudi Arabia. In post-monsoon, 26 % of the sources were detected in Pakistan, 4 % in India, 5 % in Afghanistan, 1 % in Iran and 1 % in Saudi Arabia.

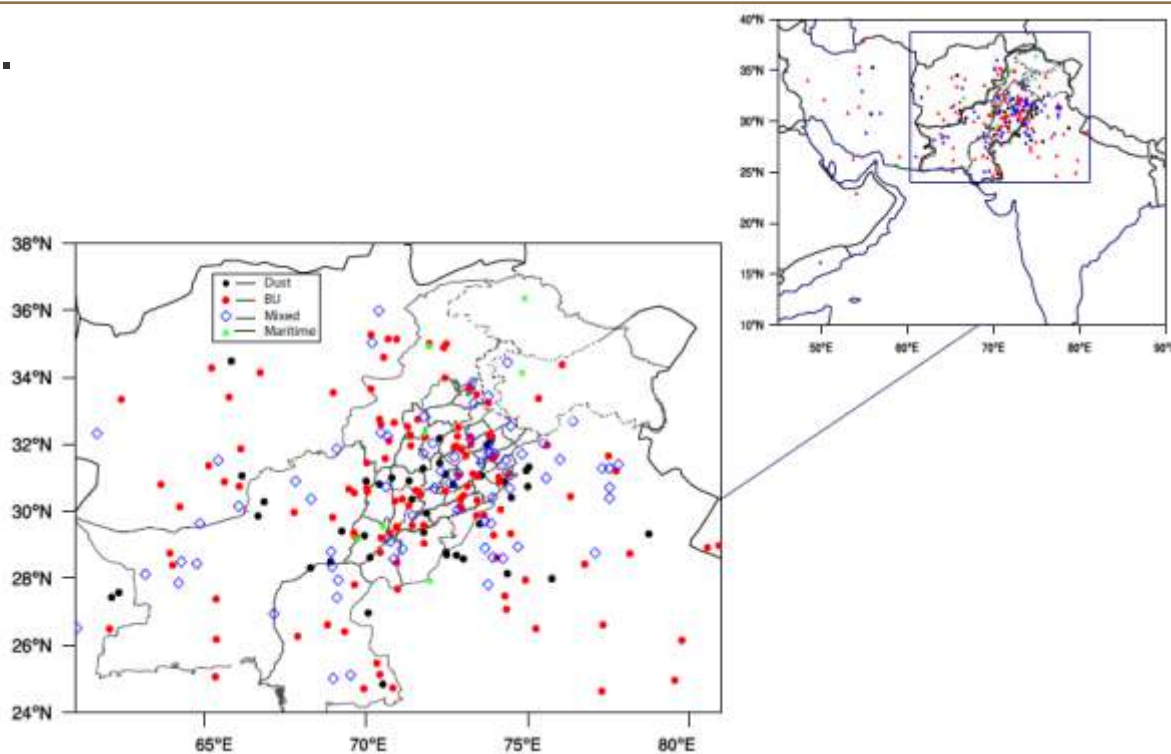
The overall detected sources were further categorized into coarse-mode, fine-mode and mixed type pollutants in both winter and post-monsoon. From all the sources detected in

a.



Disclaimer: The boundaries and names shown and the designation used on this map do not imply official endorsement or acceptance by the United Nations. Dotted line represents approximately the Line of Control in Jammu and Kashmir agreed upon by India and Pakistan. The final status of Jammu and Kashmir has not yet been agreed upon by the parties

b.



Disclaimer: The boundaries and names shown and the designation used on this map do not imply official endorsement or acceptance by the United Nations. Dotted line represents approximately the Line of Control in Jammu and Kashmir agreed upon by India and Pakistan. The final status of Jammu and Kashmir has not yet been agreed upon by the parties

2.4. Classification of point sources in to dust, biomass burning/urban—industrial, mixed and maritime pollutants (period: 2008–2017)(a) in post-monsoon (b) winter. Source: GCISC and adapted from United Nations World map, February 2020.

winter in Pakistan, it was found that 8% of the sources belonged to coarse-mode pollutants, 34% of them as fine-mode, 16 % as mixed-type while 2% as maritime. From India, it was found that 5% belonged to coarse-mode aerosols, 7% to fine-mode aerosols, 8% to mixed-type aerosols and 1% maritime aerosols. From Afghanistan, 1 % of the sources belonged to coarse-mode, 6% to fine-mode and 3% to mixed-type. From Iran, 2% belonged to coarse-mode, 3% to fine-mode and 2% to the mixed-type category. There is no significant contribution of fine-mode aerosols in winter from Saudi Arabia.

The sources detected in post-monsoon within Pakistan, 2% belonged to the coarse-mode category, 46% to the fine-mode category, 23% to mixed-mode category while 1% to the maritime category. From India, no sources were detected in post-monsoon in coarse-mode category, 9% were detected in the fine-mode category while 2% in the mixed-type category. From Afghanistan, 7% in fine-mode and 6% in mixed mode while both Iran and Saudi Arabia, had 1–2% contribution of fine-mode sources.

Overall 37% of all 'bu' pollutants in winter were detected within Pakistan with India being the second biggest source (at 13%). In post-monsoon, 23 % of sources were detected within Pakistan and 4–5 % in both India and Afghanistan. Iran and Saudi Arabia was found to have a minimal share.

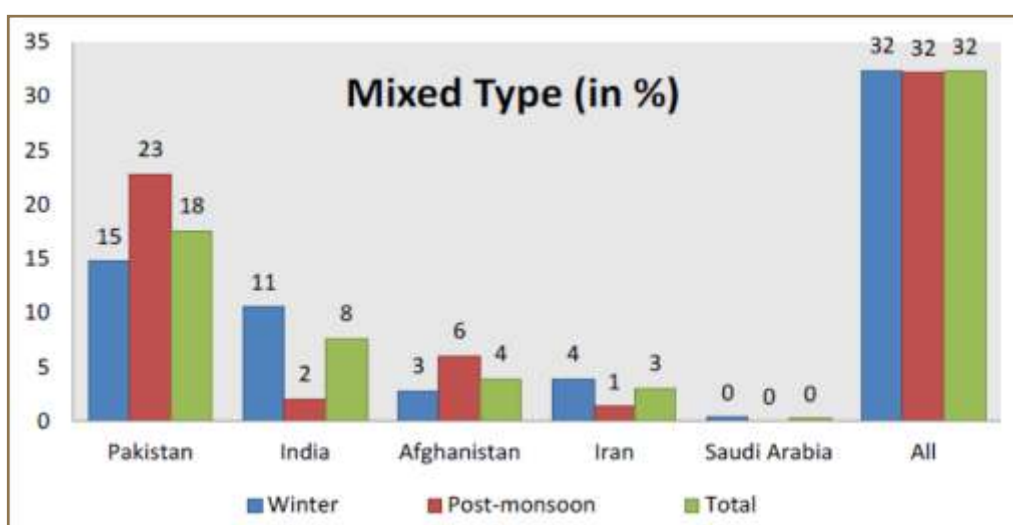
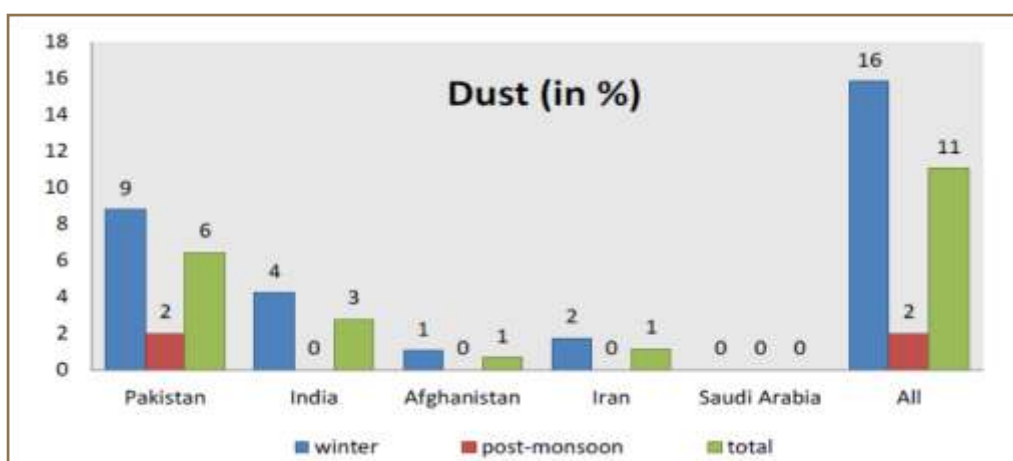
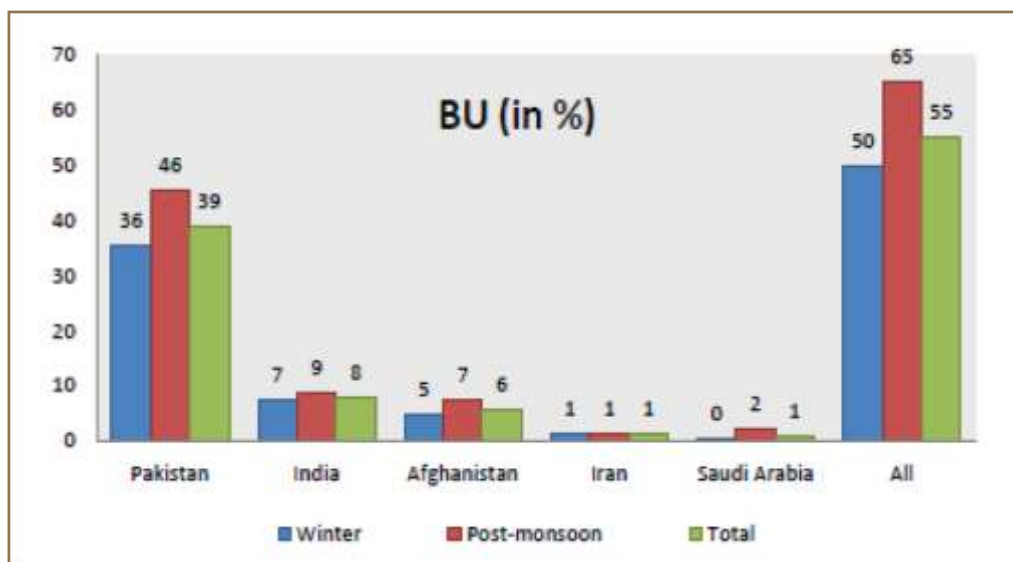
Looking at the following tables, overall 65% of both 'bu' and 'mixed' type pollutant sources were detected within Pakistan, making it a major share of sources. Therefore, any mitigation/adaptation measures eventually needed to eradicate the smog problem are needed to be addressed and implemented on an urgent basis within Punjab. Fig. 2.5 represents table 2 graphically.

2.1. Different types of aerosol sources (coarse mode/dust, fine mode/urban—industrial, mixed type, and background type)

	Pakistan	India	Afghanistan	Iran	Saudi Arabia	All
No. of Sources						
Winter	158	52	25	18	2	259
Post-monsoon	106	16	20	4	3	149
Total	264	68	45	22	5	408
% of total	65	17	11	5	1	100
Coarse—mode aerosols						
Winter	22	12	2	4	0	40
Post-monsoon	3	6	0	0	0	3
Total	25	12	2	4	0	43
Fine—mode aerosols						
Winter	89	18	15	7	1	120
Post-monsoon	68	13	11	2	3	97
Total	157	31	26	0	4	227
Mixed type aerosols						
Winter	42	20	7	6	1	76
Post-monsoon	34	3	9	2	0	48
Total	76	23	16	8	1	124
Marinetime aerosols						
Winter	5	2	1	1	0	9
Post-monsoon	1	0	0	0	0	1
Total	6	2	1	1	0	10

2.2. Percentage wise types of aerosol sources

	Pakistan	India	Afghanistan	Iran	Saudi Arabia	All
All detected source locations (%)						
Winter	39	13	6	4	0	63
Post-monsoon	26	4	5	1	1	37
Total	65	17	11	5	1	100
Coarse—mode aerosols						
Winter	8	5	1	2	0	15
Post-monsoon	2	0	0	0	0	2
Total	6	3	0	1	0	11
Fine—mode aerosols						
Winter	34	7	6	3	0	50
Post-monsoon	46	9	7	1	2	65
Total	38	8	6	2	1	56
Mixed type aerosols						
Winter	16	8	3	2	0	29
Post-monsoon	23	2	6	1	0	32
Total	19	6	4	2	0	30
Marinetime aerosols						
Winter	2	1	0	0	0	3
Post-monsoon	1	0	0	0	0	1
Total	1	0	0	0	0	2



2.5. Graphical representation of aerosol sources

2.5 Spatial source identification using MODIS deep blue imagery

2.5.1 Data and methodology

2.5.1.1 Aqua MODIS deep blue imagery

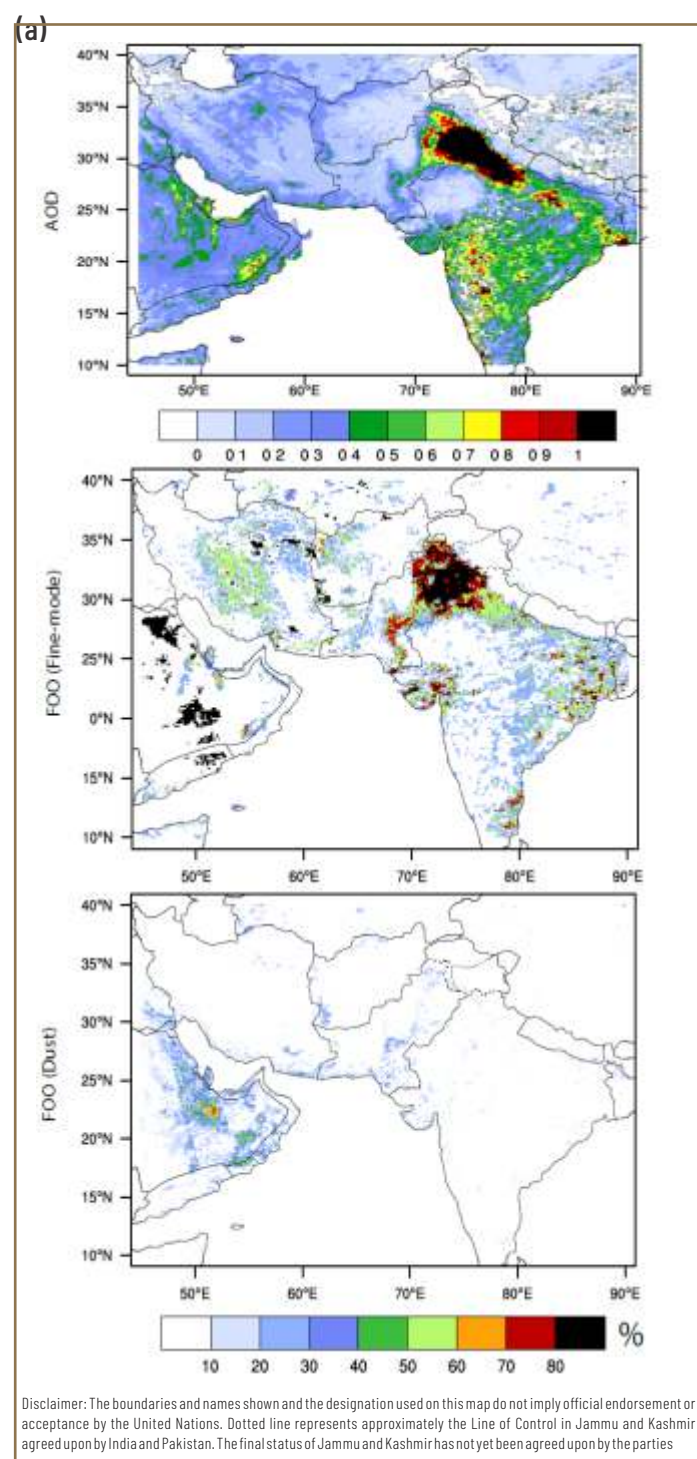
Daily images were obtained from aerosol product (MYD04_L2, Collection 6.1, Level 2.0, 10 x 10 km) from sensors such as Moderate Resolution Imaging Spectrometer (MODIS) (<http://modis-atmos.gsfc.nasa.gov/>) onboard Aqua satellite (reflectance at 550 nm), employed with the Deep Blue (DB) algorithm (Hsu *et al.*, 2004, 2006; Sayer *et al.*, 2013) which provides an aerial coverage of the aerosol optical parameters. The algorithm brightens the satellite reflectance in the presence of dust and enhances the spectral contrast. The algorithm also consists of a suite of aerosol models for dust, smoke and continental aerosols. The HDF-EOS to GeoTIFF Conversion Tool (HEG) of NASA (<https://newsroom.gsfc.nasa.gov/sdptoolkit/HEG/HEGHome.html>) allowed using the Aqua MODIS DB data by re-projecting it on a regular latitude-longitude grid with 0.1 spacing and stitching into daily files (Klein *et al.*, 2006). Linear interpolations were performed for all MODIS granules from 2008 to 2017.

2.5.2 Assessment of frequently occurring spatial source regions of smog

To further assess spatial source locations on seasonal basis (period: 2008–2017) of anthropogenic aerosols over the smog dominated region, different extreme events i.e. dense smog days, were selected. The criteria were selected as >1.0 , $\alpha \geq 1.15$ and >1.0 , $\alpha \leq 0.75$ to classify high loadings of 'dust' and 'bu' type aerosols on a spatial scale. Fig. 2.6 a, b shows the presence of 'bu' and 'dust' source locations for winter and post-monsoon. 'FOO' represents the frequency of occurrence of spatial source locations (in percentage).

Figure 2.6 depicts that in post-monsoon, more than 80% of the source regions are centered around northern Punjab expanding towards the central and southern regions (FOO (anthro)). The values (AOD) are attributed to the anthropogenic activity on-going in and around Punjab as no dust source regions were found (FOO (dust)). In winter, the aerosol loadings are again attributed to the presence of anthropogenic source locations (FOO (anthro)). During winter,

burning of coal, wood and brick kiln etc. are an on-going process which produce NO_x and CO emissions in the presence of other vehicular and industrial emissions. These activities can be seen taking place across the whole Indo-Gangetic plain and the eastern central states of India. This provides an indicator that rice stubble burning activities in the post-monsoon take place at locations different than the winter combustion activities.



(b)

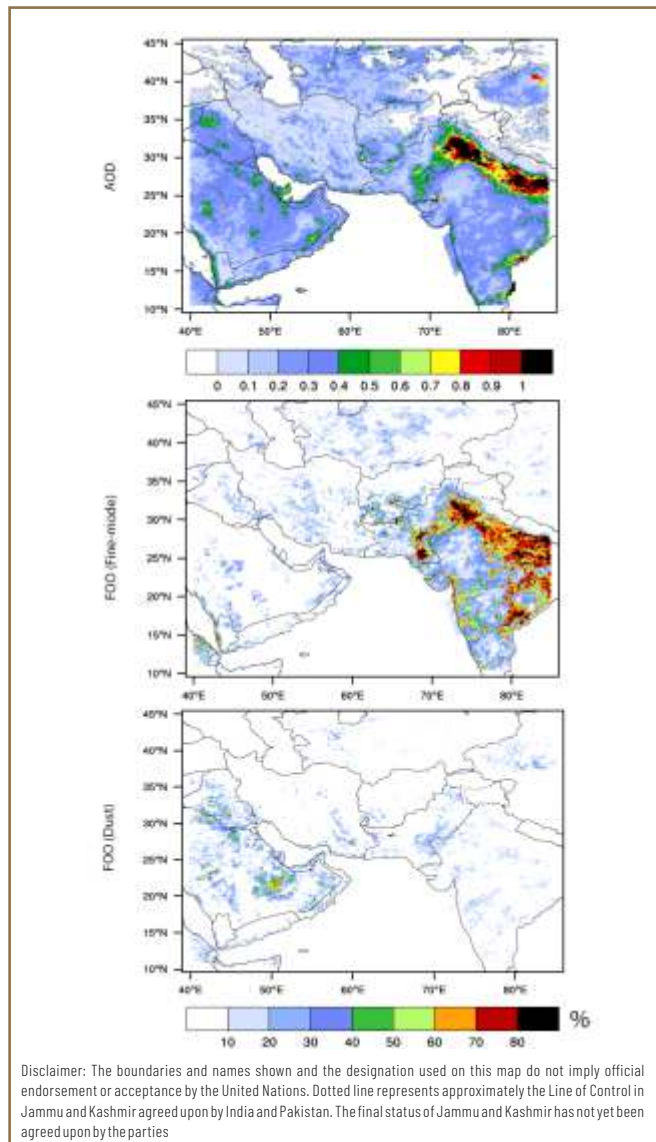
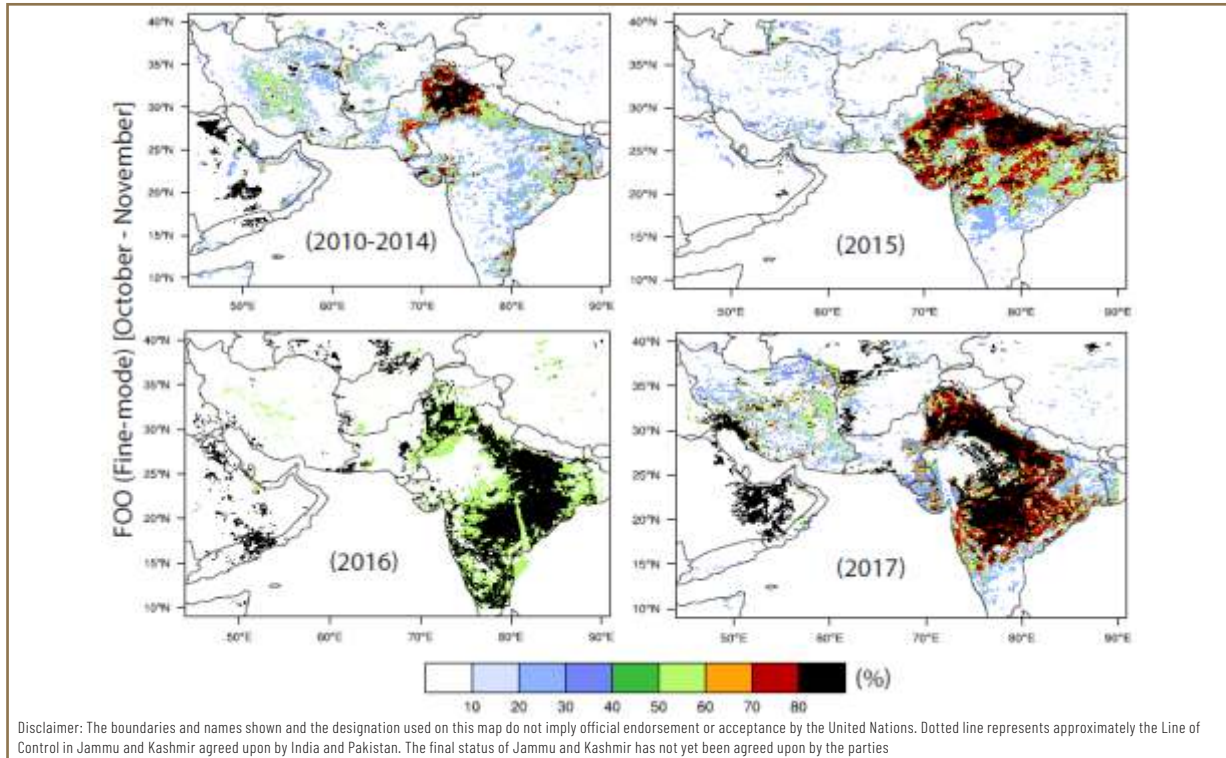


Figure 2.7 [a, b] indicates that the problem has indeed been intensified during the past three years in which the burning activities have spread both south of Punjab and west of Punjab. Also, the burning activities have intensified more across the Gangetic plains and across the eastern and southern states of India especially in the post-monsoon season. Looking at the percentage of sources, more than 80% are found in eastern Punjab with a lateral spread and across the Indian regions of burning activities.

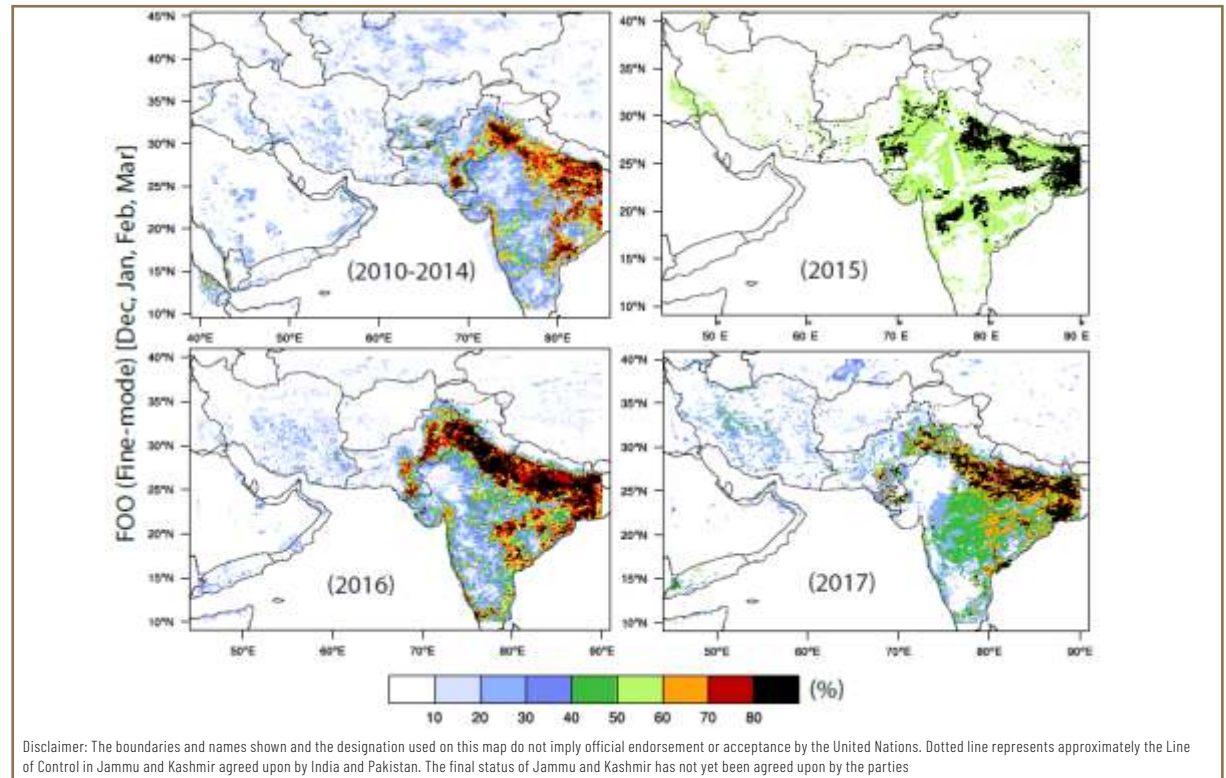
2.6. Seasonal spatial source locations (in %) of 'bu' and 'dust' aerosols. (period: 2008-2014). (a) post-monsoon (b) winter. For both seasons, top figures represent 'bu' values, middle figs represent FOO for 'bu' type pollutants and bottom figs as 'dust' type pollutants.

Source: GCISC and adapted from United Nations World map, February 2020.

(a)



(b)

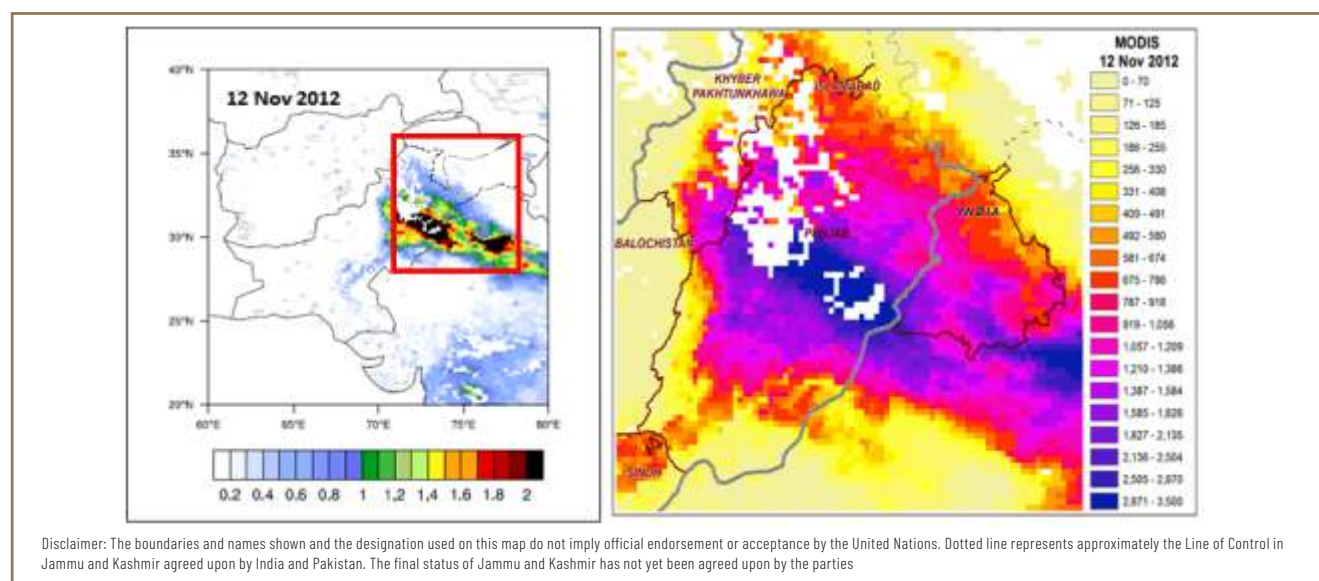
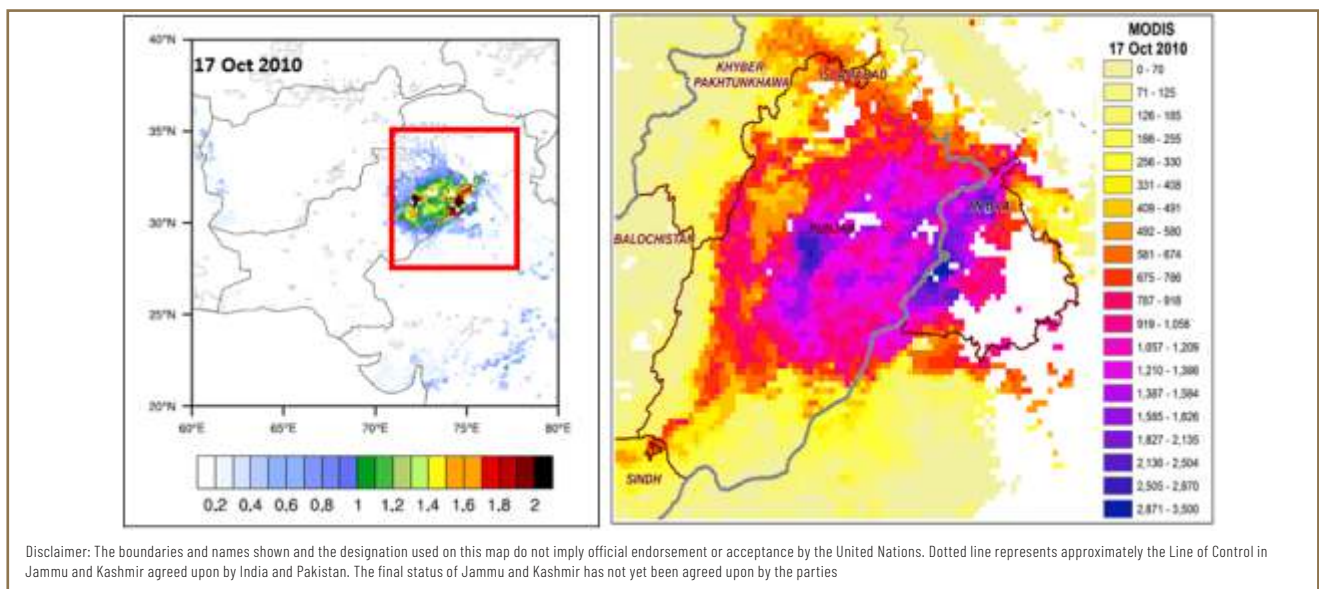


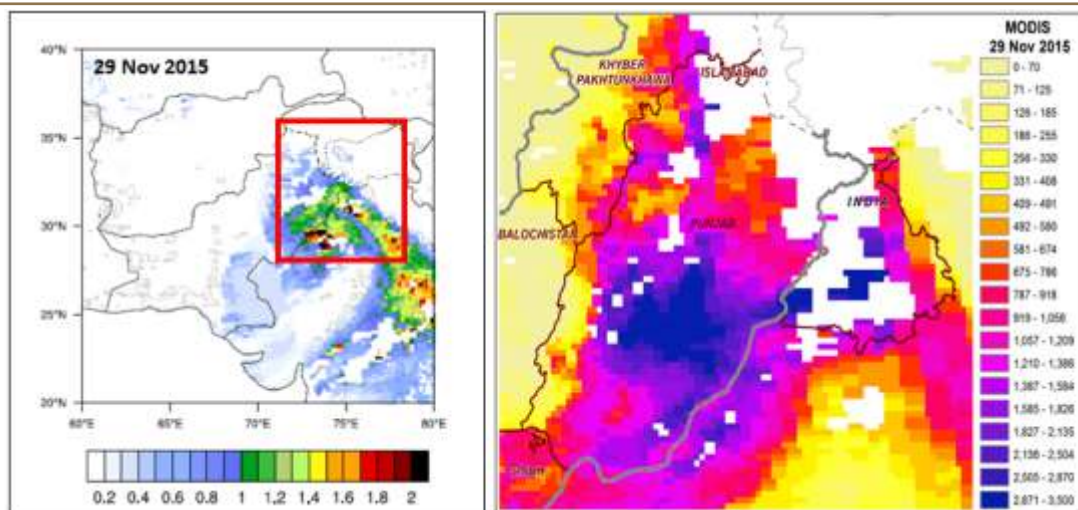
2.7. (a) Upper panel (post-monsoon) Left-Right (2010–2014)–2017, (b) Lower panel (winter) Left-Right (2010–2014)–2017.
Source: GCISC and adapted from United Nations World map, February 2020.

2.5.3 Assessment of smog affected regions (case to case basis)

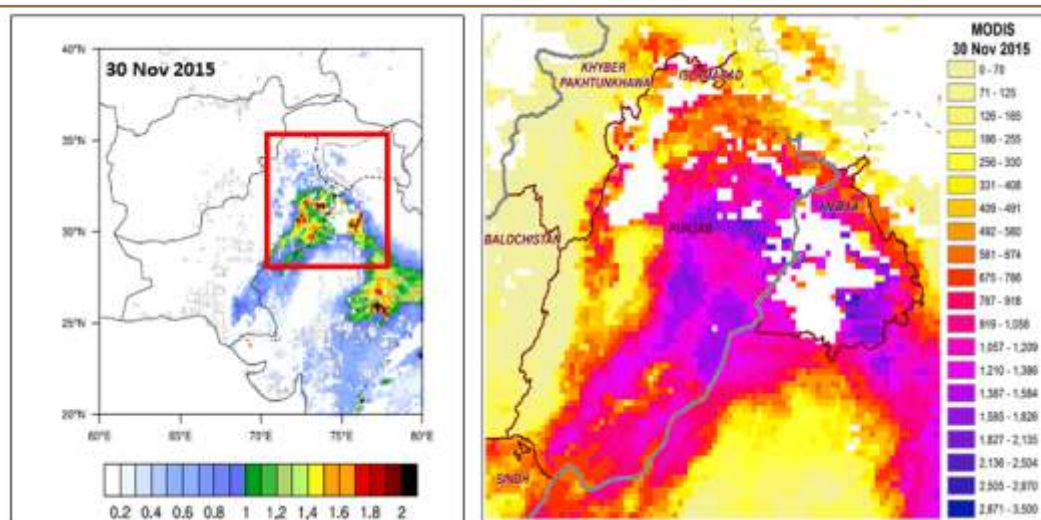
The individual cases of various extreme smoggy days were further investigated to find event- based analysis of anthropogenic aerosols. Below is the sequence of figures depicting individual events. The figures have been created by projecting values against the non- missing α values for anthropogenic aerosols. All events have been taken for > 1.0 and $\alpha \geq 1.15$ to detect the presence of 'bu' type pollutants.

The intense smog events have only been taken for the post-monsoon as this season brings along more smoky haze compared to winter. Events have been taken from 2008–2017. Individual events give an idea of the lateral spread of smog in Punjab and across the Gangetic plains including the eastern Indian states, depicting that burning activity have indeed been increased at both sides due to which the problem has increased and spread to the vast localities.

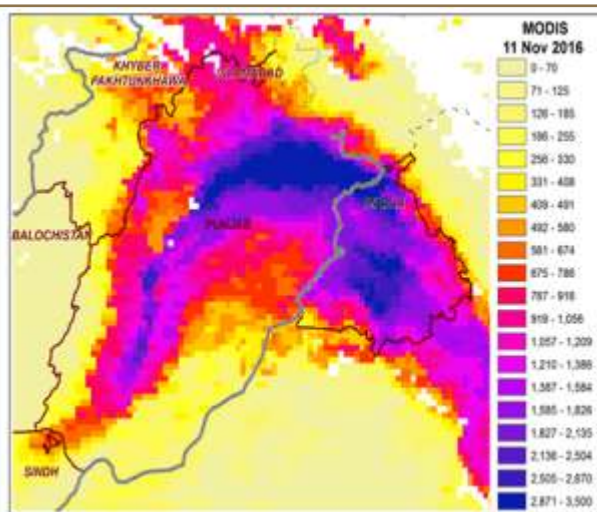
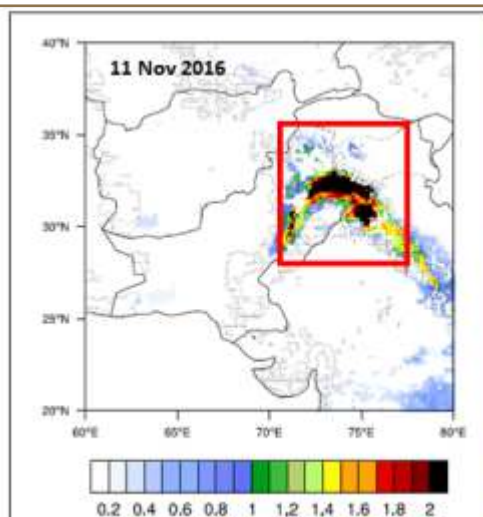




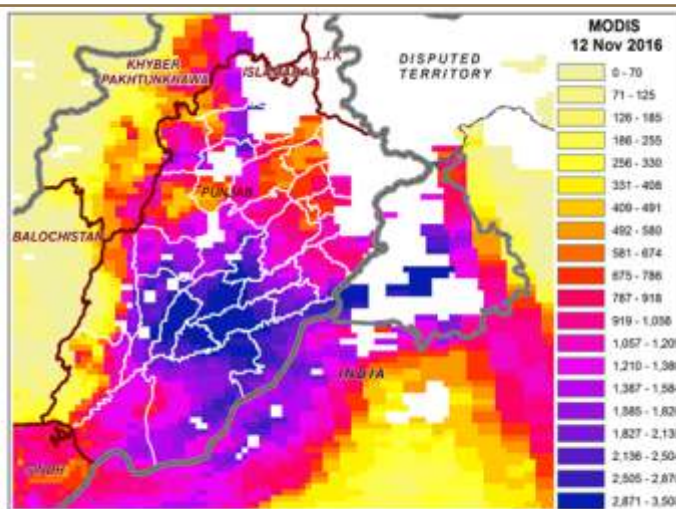
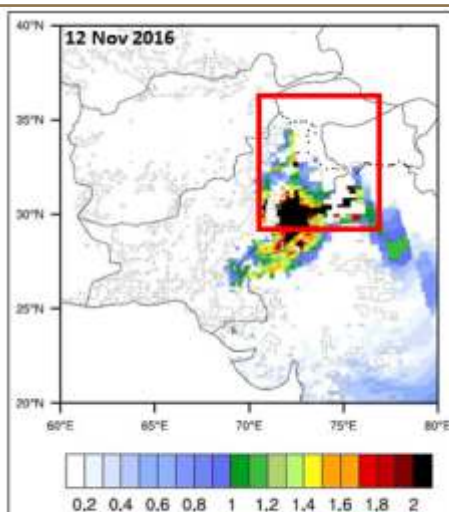
Disclaimer: The boundaries and names shown and the designation used on this map do not imply official endorsement or acceptance by the United Nations. Dotted line represents approximately the Line of Control in Jammu and Kashmir agreed upon by India and Pakistan. The final status of Jammu and Kashmir has not yet been agreed upon by the parties



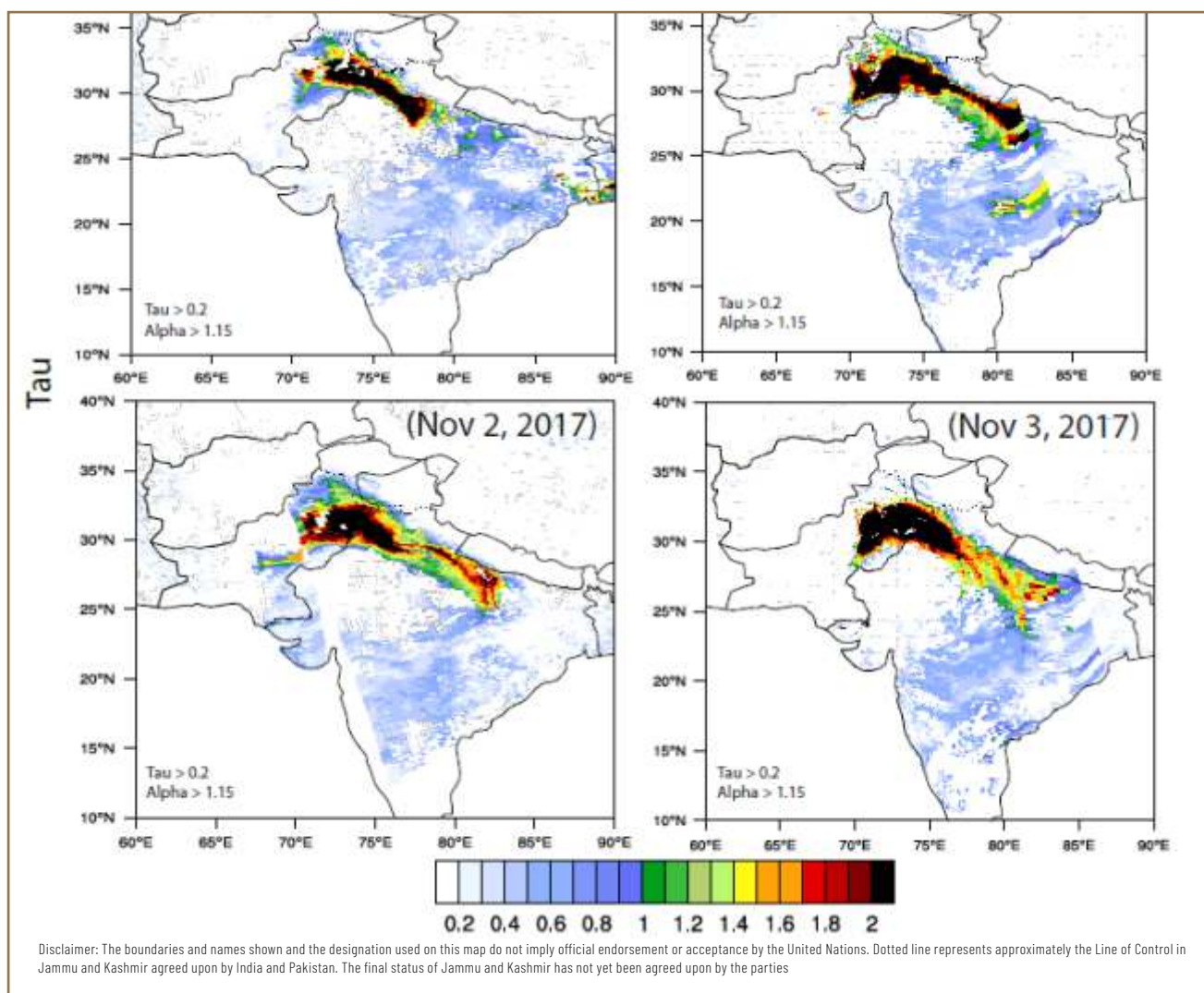
Disclaimer: The boundaries and names shown and the designation used on this map do not imply official endorsement or acceptance by the United Nations. Dotted line represents approximately the Line of Control in Jammu and Kashmir agreed upon by India and Pakistan. The final status of Jammu and Kashmir has not yet been agreed upon by the parties



Disclaimer: The boundaries and names shown and the designation used on this map do not imply official endorsement or acceptance by the United Nations. Dotted line represents approximately the Line of Control in Jammu and Kashmir agreed upon by India and Pakistan. The final status of Jammu and Kashmir has not yet been agreed upon by the parties



Disclaimer: The boundaries and names shown and the designation used on this map do not imply official endorsement or acceptance by the United Nations. Dotted line represents approximately the Line of Control in Jammu and Kashmir agreed upon by India and Pakistan. The final status of Jammu and Kashmir has not yet been agreed upon by the parties



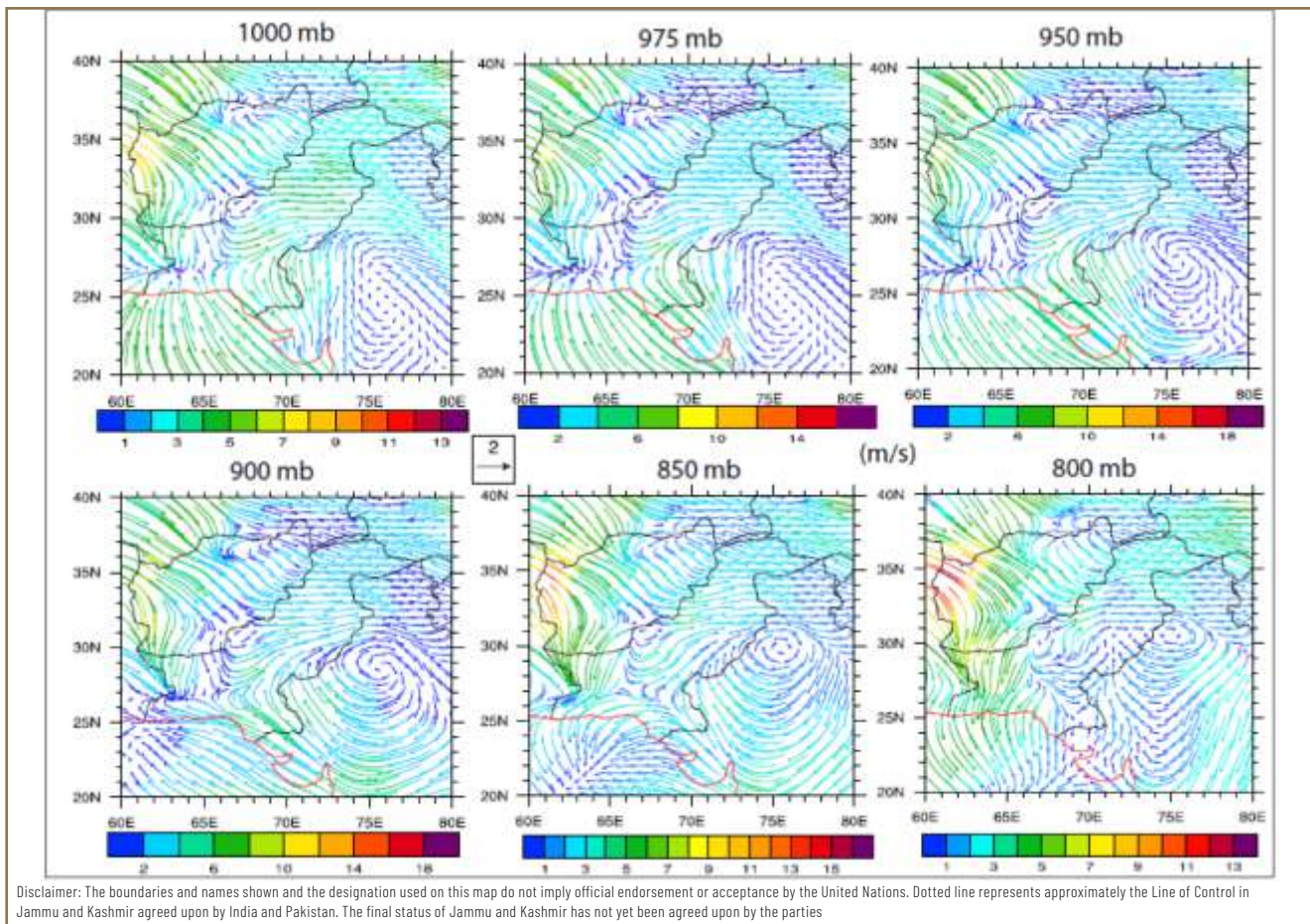
2.8. Different extreme smog events in the post-monsoon from 2010–2017. (R.H.S) aerosol optical depth (τ). (L.H.S) τ values have been plotted against anthropogenic α . Source: GCISC and adapted from United Nations World map, February 2020.

2.6 Seasonal dynamics and trends of smog (period: 2008–2017)

2.6.1 Dynamics in post-monsoon

The wind vectors in fig. 2.9 presents (magnitude of zonal and meridional winds) from surface (1000 hPa) to 2 km (800 hPa) in the month of October averaged from 2008–2017. The data shows a persistent high pressure over central and eastern India at 1000 hPa, which starts shifting to the north when seen at higher pressure levels. At 800–850 hPa the high pressure can be seen over east of Punjab with a meridional shift of 5° to the north (i.e. 26° N– 31° N). The presence of high pressure up to the high levels depicts high atmospheric stability which serves to inhibit any atmospheric movement

(and traps the pollutants in that region) that might be present at that time. High stability conditions from central India up to northern Punjab also seem to welcome high accumulations of pollutants into northern Punjab in the month of October which might not get clear even in November due to the absence of rains. From surface to 950 hPa, northwesterly winds can be seen blowing over Punjab entering into the Gangetic Plains. Winds become southerly at 900 hPa while easterly and southeasterly going up to 800 hPa entering from central India into central Punjab. Therefore, we might infer that the high-pressure center present over 800 hPa to the east of northern Punjab acts as a precursor of movement of pollutants outside of Punjab at surface levels and inside of Punjab at higher levels along the movement of winds. Colors and length of the wind vectors indicate the wind speeds.

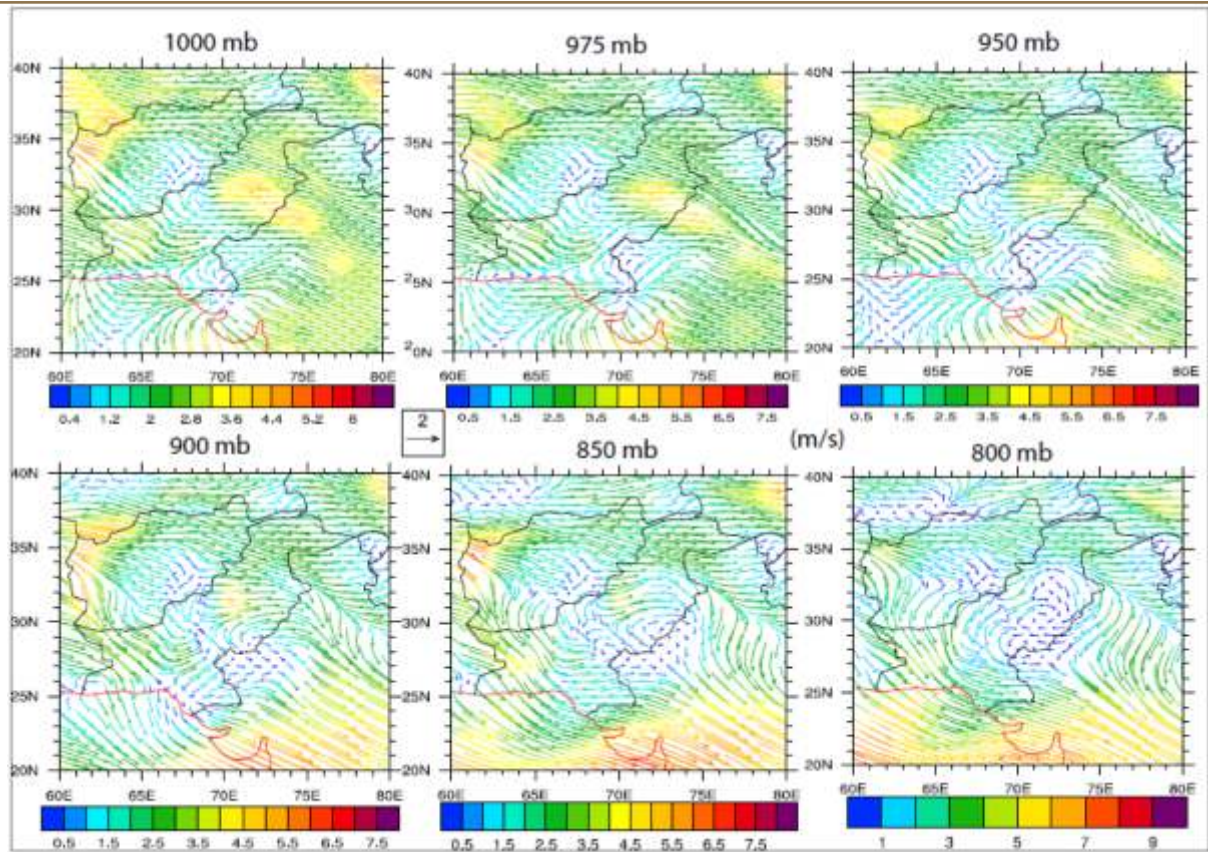


2.9. Wind speeds in October (period: 2008–2017) from 1000 hPa–800 hPa (upper left to lower right). Source: GCISC and adapted from United Nations World map, February 2020.

2.6.2 Dynamics in winter

The wind speeds in winter (fig. 2.10) were also assessed. A prominent high pressure was found centered over the southeast of the Sindh province of Pakistan in the month of January. Also, a seasonal shift in winds has been observed during the month of November and December (not shown here), with no significant cyclonic or anti-cyclonic activity. The high pressure signifies atmospheric stability conditions in this region, when assessed at higher levels, where stability conditions prevail, however, shift to the northeast with a 5° meridional shift (i.e. from 25° N – 30° N) and a 2° zonal shift (i.e. 70° E – 72° E), entering into the south-central Punjab of Pakistan. In January, we see that westerly winds prevail over the surface at 1000 hPa, however, when we go to the higher levels i.e. 950 hPa winds become more southerly. At 850 hPa, south and central Punjab experience persistence of a localized high-pressure center, which eventually engulfs most

of Punjab at 800 hPa. Presence of high pressure at higher levels seems to be an indicator of vertical mixing and transport of regional pollutants across the eastern boundaries into south Punjab, while outside of Punjab into the Gangetic plains at the surface levels. In winter, due to lower temperatures foggy conditions occasionally prevail which act as a precursor to trap any incoming pollutants causing hazardous health conditions. Any incoming rains are a result of western disturbances entering into Balochistan with positive vertical velocities (indicating cold air and subsistence) over the region and negative vertical velocities (indicating warm air and ascent) over most parts of Punjab. Such a system establishes as a result of atmospheric disturbances originating from the Mediterranean carrying along the moisture, at 200–300 hPa with triggers ascending and descending air masses at 500 hPa and the surface, creating atmospheric instability conditions.



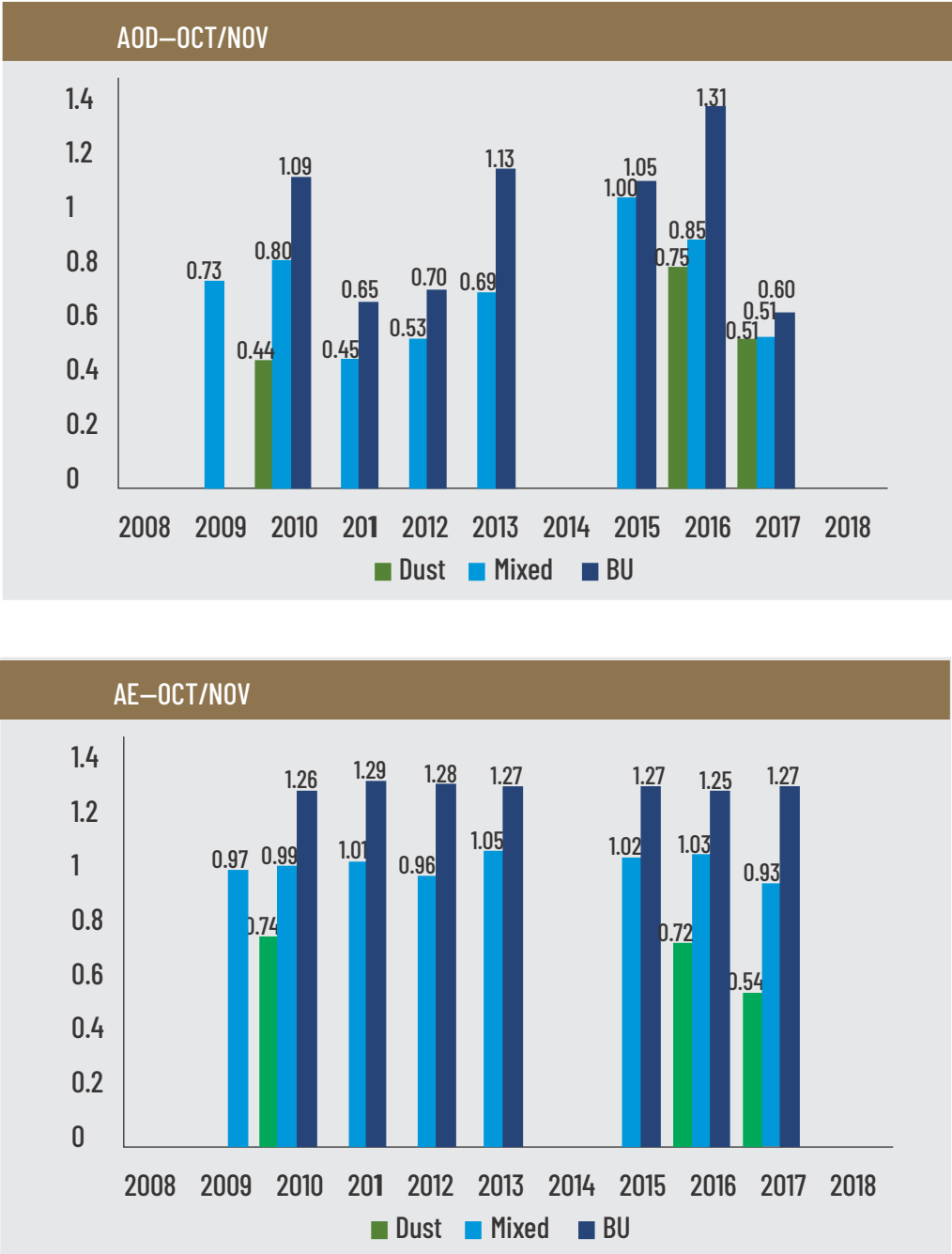
Disclaimer: The boundaries and names shown and the designation used on this map do not imply official endorsement or acceptance by the United Nations. Dotted line represents approximately the Line of Control in Jammu and Kashmir agreed upon by India and Pakistan. The final status of Jammu and Kashmir has not yet been agreed upon by the parties

2.10. Wind speeds in January (period: 2008–2017) from 1000 hPa–800 hPa (upper left to lower right). Source: GCISC and adapted from United Nations World map, February 2020.

2.6.3 Trends of smog in post-monsoon

The trends of all three types of identified aerosol detection points or sources were assessed on yearly basis (i.e. from 2008–2017) in order to capture the average annual variations

of smog over the region. The trend plots were obtained for both t and α for post-monsoon and winter. Looking at the yearly trends, in post-monsoon, 'bu' and 'mixed' type pollutants were found comparatively higher than 'dust' in the years 2010, 2013, 2015 and 2016 (the data was missing for years 2008 and 2014).



2.11. Upper Panel indicates trends of post monsoon values from 2008–2017, Lower Panel indicate trends of α values from 2008–2017.

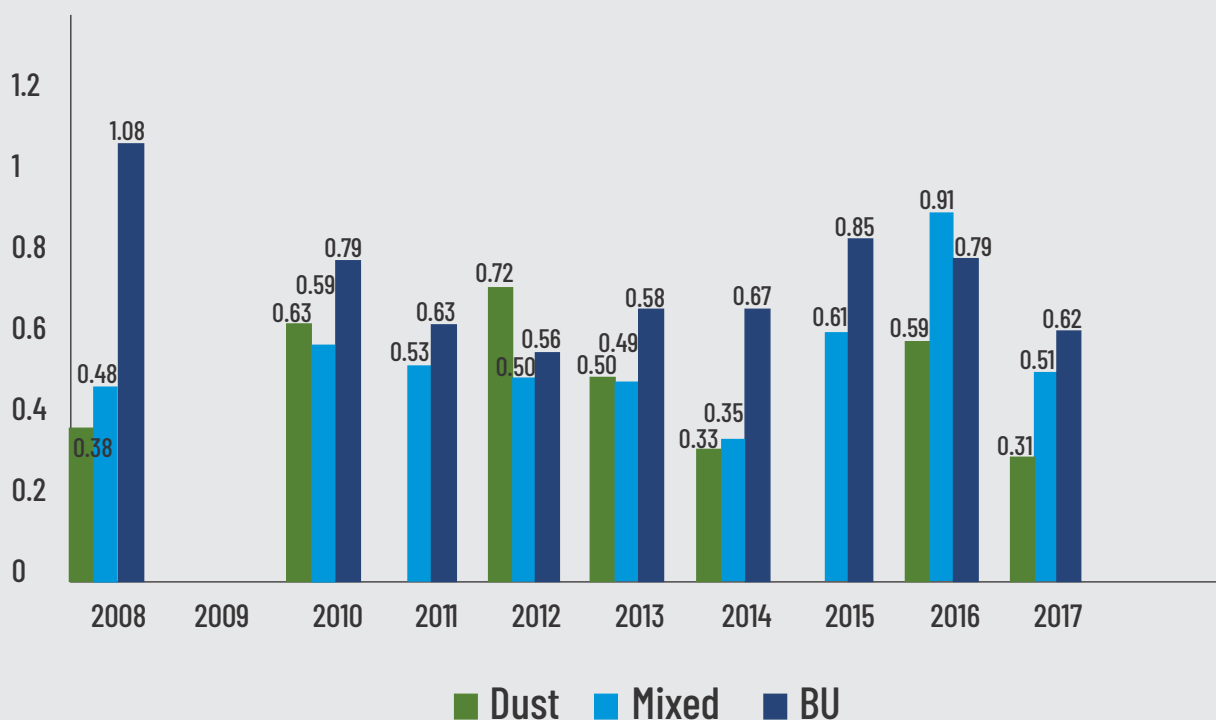
The highest loadings of 'bu' were found during 2016 while the highest loadings of 'mixed' were found during 2015. In 2017, there seems to be some policy intervention as the loadings were found much lower compared to the two previous years. Looking at the α trends, the size distribution remains the same throughout the years showing that nature of anthropogenic activities remained the same, however intensity of activities kept on changing (graph) with changing aerosol loadings of 'bu' and 'mixed' type pollutants from year to year.

2.6.4 Trends of smog in winter

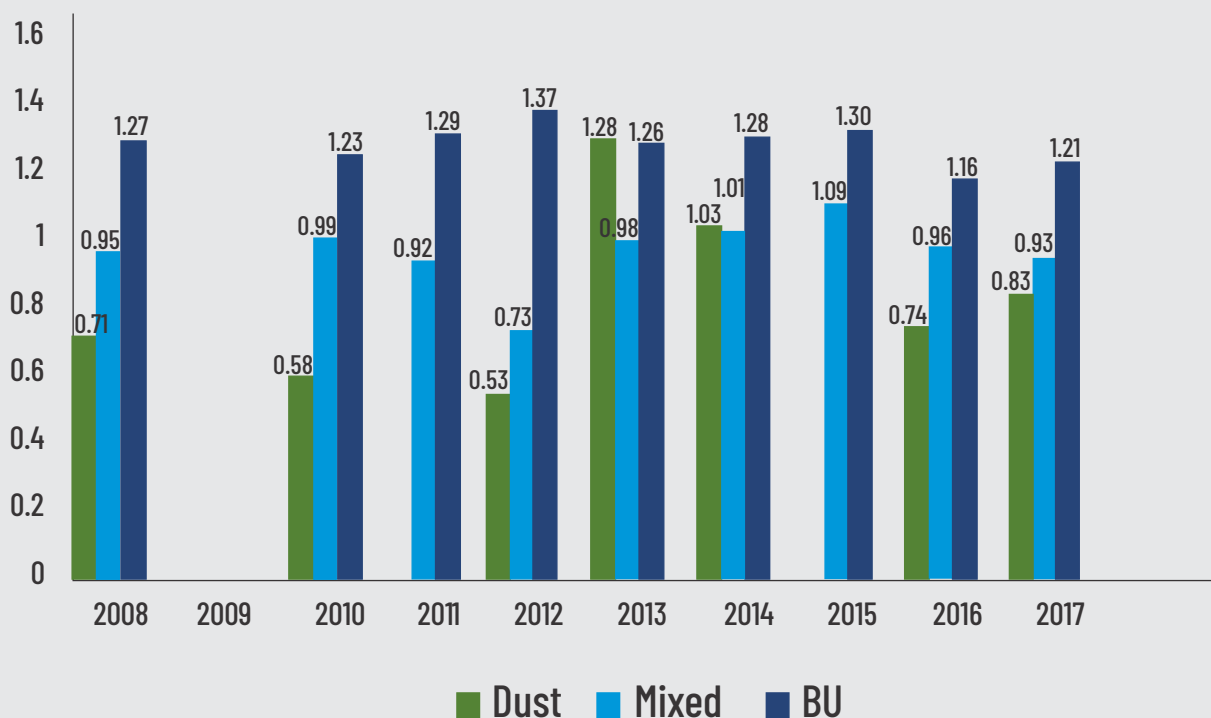
Looking at winter trends, high loadings of 'bu' type pollutants were found during the years 2010, 2014, 2015 and 2016 in which the highest was observed during the year 2015 followed

by 2016. Highest 'mixed' type pollutant loadings were observed during the year 2016 followed by 2015. Again, in the year 2017, the loadings were observed as lowered compared to the previous two years. High 'dust' loadings were observed in the years 2010 and 2012. S values were found uniform up to the year 2014, however, there was a significant increase in the aerosol loading during the 2015 and 2016. In 2017, aerosol loading was again found to be consistent with the previous years during both seasons. The α values indicated that almost uniform trends of fine- mode particles or pollutants prevailed throughout the years with slight fluctuations (increase) in 'bu' type particles i.e. more fine particles in 2012 and 2015. Winter trends also show that the nature of winter anthropogenic activities remained the same, however, the loadings of fine- mode and mixed particles kept changing from year to year.

AOD—DJFM



AOD—DJFM



2.12. Upper Panel indicates trends of winter values from 2008–2017. Lower Panel indicates trends of α values from 2008–2017.

2.7 Results and findings of climatological modelling

Most of the aerosol sources were detected within Pakistan. 'biomass/urban' and 'mixed-type' pollutants were found mostly originating from within Pakistan in the smog dominated zone, however, sources were also detected in neighboring regions such as India, Afghanistan, and Iran with Indian contributions mainly constituting fine mode 'biomass/urban' type pollutants. On a seasonal basis, winter was found to comprise more sources than post-monsoon due to the greater season length, however, more 'biomass/urban' type pollutant sources were found in the post-monsoon.

Trend analysis showed higher concentration during the recent years i.e. 2015–2017, which is also confirmed by the spatial source locations found by the satellite data. The satellite pictures of smog dominated area show that burning activities in winter take place in different locations than the post-monsoon even though the composition of pollutants show the uniform α with high t . In the high-pressure system, accumulation of pollutants is evident, therefore, if burning and combustion activities are controlled, the smog problem can be controlled.

SECTION III

REMOTE SENSING ANALYSIS AND NUMERICAL MODELING

Key messages

1 Though the assessment of regional point sources show majority of smog sources lying within Pakistan, the Remote Sensing analysis of fire events indicates more fire events occurring in Indian administered Punjab. It is therefore evident that Smog is a trans-boundary issue and requires regional cooperation.

SECTION III

Remote sensing analysis and numerical modeling

3.1 Data acquisition and their characteristics

Based on the available literature and review of available remote sensing-based data sources, total 6 types of data products were selected for mapping of smog, thermal anomalies, and air pollutants. Table 3.1 lists the sources from where the datasets were acquired. Owing to the complex nature of smog where it resembles a lot with fog (at least visually), direct detection and mapping of smog through satellite remote sensing was quite difficult and required a lot more data variables and complex data processing. Therefore, this research study explored the methods for indirect mapping of smog using the satellite images and data of a variety of pollutants, through establishing spatiotemporal relationships between the visually evident smog/fog and the relevant air pollutants.

3.1. Sources, format, temporal and spatial resolutions of data acquired.

Sr. No.	Data Type	Data Source	Data Format	Temporal Frequency	Spatial Resolution
1	Active fire	VIIRS/MODIS	Point	Daily	375m/1km
2	AOD	MODIS	NetCDF	Daily	1 degree
3	Ozone	OMI	NetCDF	Daily	0.25 degree
4	Optical and chemical characteristic of Aerosols	CALIPSO	NetCDF	Daily	500m
5	NO ₂	OMI	NetCDF	Daily	0.25 degree
6	SO ₂	OMI	NetCDF	Daily	0.25 degree

3.1.1 Aerosol optical depth

The presence of atmospheric aerosols performs a substantial role in the radiation of earth by means of radiative forcing along with chemical fluctuations. The aerosols produced by anthropogenic activities are complicatedly associated with the earth's self-regulating systems. The aerosols reflect the sunlight and their presence results in the overall cooling of the climate (Kaufman *et al.*, 2002). The calculation of the total effect requires precise information on aerosols distribution around the globe by means of satellite observations (Kaufman *et al.*, 1997). Aerosols can scatter and/or absorb the solar radiation coming to the earth, where Aerosol Optical Depth (AOD) is a description of light absence in the path from source to the observer. Hence, more aerosols tend to reduce the intensity of light reaching the surface which is abundantly evident in the smog period. Therefore, this study uses daily AOD from MODIS for the study period over the region.

3.1.2 Mapping of ozone

Ozone present in the lower troposphere (ground level) is a well-known secondary pollutant. It is a product of complex series of photochemical reactions including hydrocarbons such as volatile organic compounds (VOCs), and nitrogen oxides NO_x (NO, NO₂) in the presence of solar irradiation (Sillman, 1999). The chemical components required for Ozone formation originate from both anthropogenic activities (e.g., industry and vehicle emissions) and biogenic sources (e.g., forest, and soil). Unlike Ozone in the upper atmosphere (Stratosphere) where it occurs naturally and is responsible for the protection of earth by absorbing the Ultra Violet (UV) radiations.

The man-made Ozone has adverse health and ecosystem effects; it is a strong greenhouse gas that contributes directly to global warming with radioactive forcing (IPCC, 2007; Stevenson *et al.*, 2013; Monks, 2014; Sillman and Samson, 1995). The atmospheric lifetime of Ozone gas is short in polluted areas, whereas the concentrations of its precursor are relatively high. Their atmospheric residence time in the troposphere is around a week (Monks, 2014).

In this study, Ozone Total Column (OTC) daily measured by NASA Ozone Monitoring Instrument (OMI) was used. Total Column Ozone, or Column Amount Ozone, is the atmospheric density of Ozone in a vertical column of air. The Dobson Unit (DU) is a measure of total Ozone and is used for OMI and TOMS data. The Ozone monitoring instrument is a visual and ultraviolet spectrometer aboard the NASA Aura spacecraft. OMI can differentiate between aerosol types, such as dust, smoke, and sulfates, and can quantify the cloud pressure and coverage, which provides information to estimate the troposphere Ozone. The data ranges from the year 2008 to 2018 for the months of October to February. The Ozone gridded product was downloaded for global scale, and then study area was extracted in a GIS environment.

3.1.3 Mapping of SO₂ and NO₂

NO₂ being a strong pollutant has been listed as a target pollutant. It plays an acute role in the chemistry of the atmosphere (specifically troposphere) being mainly concerned for the formation and deposition of secondary air pollutants such as photochemical smog and acid rain (Seinfeld and Pandis, 2008).

NO₂ can absorb the visible radiation and ultimately contribute in reducing the atmospheric visibility. Having this property along with the increased amount of its presence in the atmosphere, NO₂ carries a threat to alter the world climate. The world's climate, environment, and human health are already at risk due to air pollution. Urban air pollution is formed because of a combination of Carbon monoxide (CO), Sulphur dioxide (SO₂), oxides of Nitrogen (NO_x), Ozone, and suspended particulate matter (SPM) along with volatile organic compounds.

As a result, the air pollution is continuously escalating in the metropolitan cities of Pakistan due to the rapid increase in industrialization, means of transportation and population growth. The main source of air pollutants such as sulphur dioxide, nitrogen oxides, and carbon monoxide along with the particulate matter is combustion processes in industrial sectors and vehicles. NO₂ in the atmosphere is discharged through the burning of biomass, microbial processes in soil and combusting process of fossil fuels. The fastest escalation has been observed in Asia annually, at a 4–6 % increase (Ghude *et al.*, 2009). Approximately 50% of NO_x is released from traffic and industries and 20 to 25% is released by the burning of biomass. In Pakistan, unlike global trends, anthropogenic activities play a major role in contribution to NO_x sources. Based on the new and modern satellite technology and knowledge, the dynamic global trends scenarios can be observed well in time (Bortoli *et al.*, 2007). Measurements of certain features or components are easily available since certain satellites became operational. This study uses the NO₂ and SO₂ data from the OMI sensor for the study period and area of interest.

3.1.4 Optical and chemical characteristics of aerosol

Cloud-Aerosol Lidar and Infrared Pathfinder Satellite Observations (CALIPSO) data were utilized to identify the vertical depth and types of aerosol season wise from 2008–2018 using Vertical Feature Mask (VFM). CALIPSO is spaceborne LIDAR which can detect the presence of the aerosols at small vertical intervals starting from near earth surface up to the top of the atmosphere. CALIPSO can estimate the possible nature of the detected aerosols along the vertical profile. This data termed as VFM is used in this study.

3.1.5 Active re-mapping

Fire plays a crucial role in the structure and distribution of an ecosystem. Fires are caused by several reasons, for instance, pasture renewal in agricultural processes. Generally, fires are mainly run by several climatic factors. They can be caused by short-term or long-term factors such as precipitation patterns, temperature variations, and drought conditions etc. Biomass burning can also be caused due to decaying forest residues and crop stubbles. The smoke from biomass burning consists of numerous chemicals including carbon dioxide, carbon monoxide, hydrocarbons, water vapours, nitrogen oxides, and many other compounds. The smoke concentrations during burning tend to be higher when carbon monoxide along with other compounds and materials is emitted from smoldering fires.

Because of incomplete combustion, carbon dioxide, carbon monoxide, methane and compounds of other elements such as Nitric oxide and Sulphur dioxide are also produced. The increased level of carbon monoxide can affect human health.

The emissions from these gases ultimately leave an impact on the atmosphere's chemical compositions and biogeochemical cycles (Andreae *et al.*, 2005). The process of burning takes place in three steps:

- a. Ignition
- b. Flaming
- c. Smouldering

Biomass burning serves a variety of purposes. It can help control weed, brush and garbage accumulation in crop fields and grazing lands. It clears brushland and forest for agricultural purposes. It also provides with nutrient regeneration in croplands. In addition, biomass burning also produces charcoal for industrial use along with energy production for domestic purposes. The number of major aerosols in the atmosphere includes sulphate (SO₄), nitrate (NO₃⁻), black carbon, ammonia (NH₄⁺) and organic carbon that are highly present in the eastern side of Pakistan. The lack of effective monitoring and measuring of air pollution is making Pakistan a vulnerable region as compared to the developed world (Shahid *et al.*, 2015).

This study also utilized the fire data from MODIS as recent studies have uncovered that employing MODIS active fire product enables us to identify burning crop residue, especially in the areas where traditional methods like normalized burn ratio were not sufficient (McCarty *et al.*, 2007; Anderson *et al.*, 2012). MODIS collects fire data twice on daily basis by two satellites terra, commenced in 1999 and Aqua commenced in 2002 at morning and evening respectively. NASA's active fire product MODIS (Moderate Resolution Imaging Spectroradiometer) (Justice *et al.*, 2002) was the first fire data set made from the latest generation of 1 km fire-capable sensors on-board terrestrial satellites. Since 2000, fire products of MODIS have been utilized to address concerns regarding biomass burning and its impact on earth's ecosystem (e.g. Chen, Velicogna, Famiglietti, & Randerson, 2013; Chuvieco, Giglio, & Justice, 2008; Ichoku & Kaufman, 2005; McCarty, Justice, & Korontzi, 2007; Mollicone, Eva, & Achard, 2006; Peterson, Hyer, & Wang, 2014; Vadrevu *et al.*, 2012; Wooster & Zhang, 2004) and multiple other applications (e.g. Kaiser *et al.*, 2012; Longo *et al.*, 2010; Reid *et al.*, 2009; Ressler *et al.*, 2009; Sofiev *et al.*, 2009; Wiedinmyer *et al.*, 2011). The fire products such as of MODIS and VIIRS are useful in terms of cultural analysis as well (e.g. Bromley, 2010; Koren, Remer, & Longo, 2007; Schroeder, Giglio, & Aravéquia, 2009). The MODIS active fire algorithm is based on algorithms formulated for AVHRR and TRMM VIRS (Giglio, Kendall, & Justice, 1999; Giglio, Kendall, & Mack, submitted for publication; Justice, Kendall, Dowty, & Scholes, 1996; Kaufman *et al.*, 1990). The algorithm detects thermal irregularities per pixel by utilizing multiple channels (Giglio *et al.*, 2003), followed by secondary emphasis which involves the application of the MODIS burned area algorithm (Roy, Lewis, & Justice, 2002).

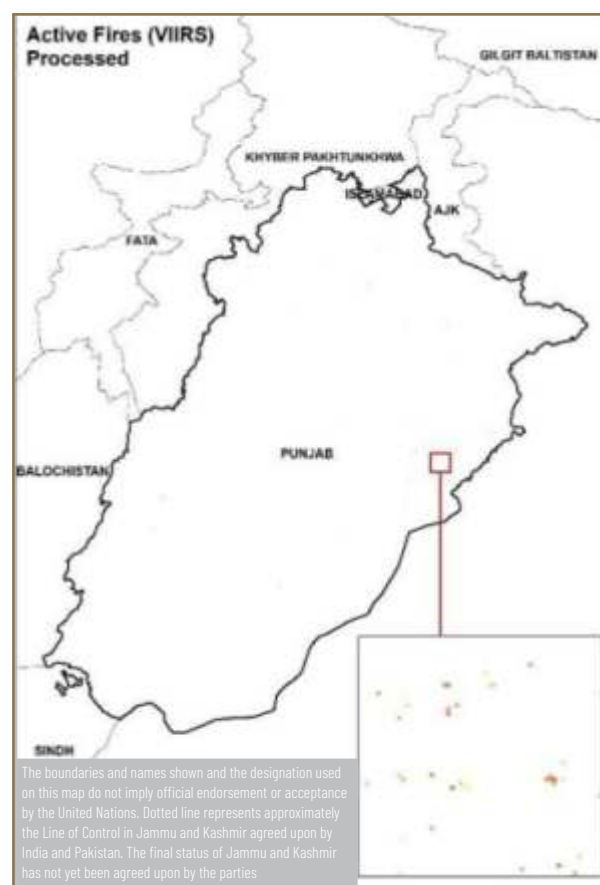
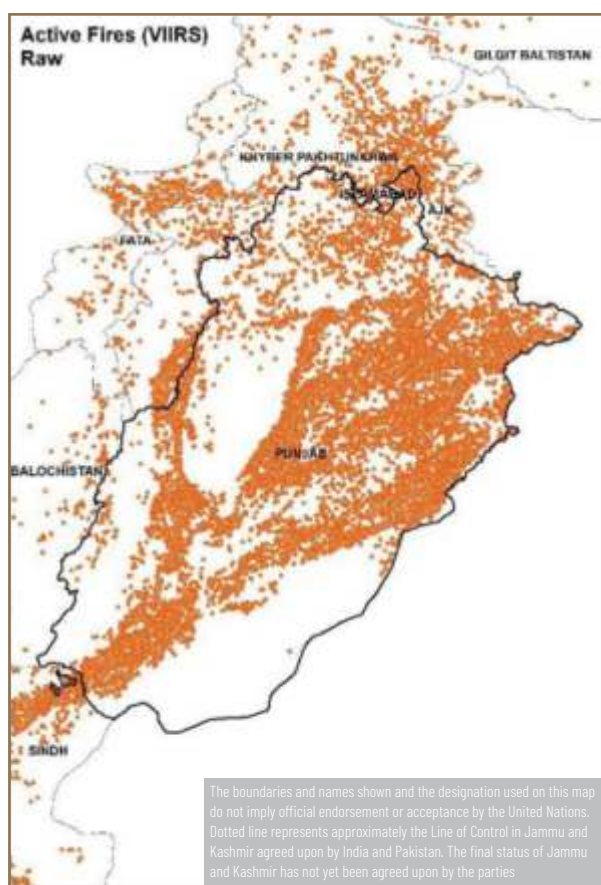
The fire products of MODIS contain Fire Radiative Power (FRP), along with the grid location of fire pixels with respect to a coordinate system, date and time of fire occurrence (Kaufman *et al.* 1996). FRP refers to fire intensity which is the assessable degree of radiant heat that is directly related to the rate of combustion and emission of smoke. (Ichoku and Kaufman, 2005; Wooster *et al.*, 2003; Wooster *et al.*, 2005). Many modifications and validations have been made in the derivation of FRP and fire by Wooster (2002), Wooster *et al.* (2005), Schroeder *et al.* (2010), Peterson *et al.* (2013), and Freeborn *et al.* (2014).

The quality of individual fire pixel is determined by means of confidence, it has three main classes:

- Low confidence fire
- Nominal confidence fire
- High confidence fire

Many studies have validated the accuracy of MODIS products by comparing it with an independent well-established source at a global level (Justice *et al.*, 2000). There are also numerous ground-based validation processes formulated by collaborating with fire groups internationally (Morissette, Justice, Pereira, Gregoire, & Frost, 2001, Schroeder *et al.*, 2014). The active fire data product of Visible Infrared Imaging Radiometer Suite (VIIRS) 375 m was also selected for mapping thermal anomalies/crop burning. This data product is provided by the Fire Information for Resource Management System (FIRMS), where the data is obtained through the VIIRS sensor aboard the joint NASA/NOAA Suomi National Polar-orbiting Partnership (Suomi-NPP) satellite. The 375 m data complements Moderate Resolution Imaging Spectroradiometer (MODIS) fire detection; they both show good agreement in hotspot detection, but the improved spatial resolution of the 375 m data provides a greater response over fires of relatively small areas and provides an improved mapping of large fire perimeters. The 375 m data also has improved night-time performance. Consequently, these data are well suited for use in support of fire management (e.g., near real-time alert systems), as well as other science applications requiring improved fire mapping (EOSDIS, 2017).

There is the potential for false positives detection of the fires. Therefore, only data with a confidence level greater than 95% is used in this study provided by NASA for each detection point of fire (Figure 3.1). It is important to mention that fire event discussed in the study does not include fires burning out between the passes of the satellite and very small or low energy fires. Therefore, it is to bear that results of the study will not overestimate the fire events and relative inferences are at the discretion of the reader.



3.1. Raw (left) and processed (right) active fires data (VIIRS) of Punjab, Pakistan for a sample time. Number fire events significantly reduced when a confidence level of 95% or above is selected. Source: Adapted from United Nations World map, February 2020.

3.1.6 Forward trajectories – transportation of air pollutants

Satellite-based remote sensing undoubtedly provides a unique opportunity to derive regional, global, and seasonal spatial patterns for aerosol loads and aerosol properties. The spatiotemporal processes involved can then be indirectly described and mapped through modeling techniques, e.g., by using the USA's National Oceanic and Atmospheric Administration (NOAA) HYSPLIT model (*Draxler and Rolph, 2003*). In order to understand the effects of aerosols on the earth's climate system and the human health, there must be a routinely monitoring system setup, both on a global scale and on regional or local scales, in particularly by analysing their spatial and temporal patterns.

To study the atmospheric transportation of chemical species both short term and long term, over the geographical location is performed by using the trajectory model. The spatial position of air parcels in the atmosphere makes it easy to identify the possible pathways, routes, and locations where pollutants can be transported.

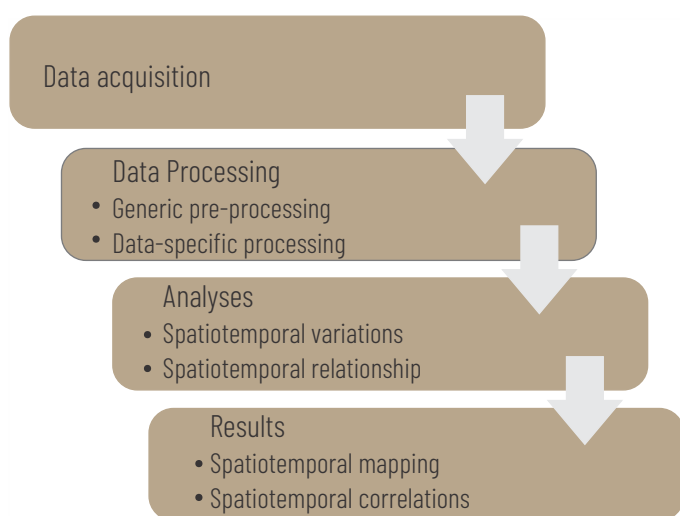
The aim of the analysis was to examine the transboundary fire smoke and within Pakistan in association with crop type overlay with hotspot analysis of all fire events.

3.2 Data processing

Keeping in view the objectives and scope of this study, a period of ten years was considered i.e. from October 2008 to February 2018. It should be noted that only month of October, November, December, January, and February was included. Preference was given to select the weekly data (around 20 – time steps between October and February) in the case where weekly data was not available, monthly data was used.

The overall methodology of this Remote Sensing analysis revolves around mapping thermal anomalies/crop burning and smog using satellite-based remote sensing data sources, and to determine the extent of the relationship, if any, between these two.

Figure 3.2 presents the general framework of this study, whereas further details are described in the following sections: The basic pre-processing of all the datasets was carried out, where almost all the pre-processing steps were applied to the data acquired. The second step involved data-specific processing as the data preparation requirements were different for each dataset.



3.2. General Methodology

1. Conversion to raster grids: Where data were not available natively in raster format, it was converted to raster data format, mainly using QGIS, Interactive Data Language (IDL) and/or other tools.
2. Re-projection: The data were re-projected to a common geographical reference system WGS-84.
3. Mosaic and subset: Data was mosaicked (where needed) and clipped to the boundaries of Pakistan and Indian administered Punjab.
4. Statistical operation: Weekly/Monthly/Seasonal averages of the data were computed, where applicable using daily data.

Later processed data was subjected to basic analyses for the spatiotemporal variations and relationships among different variables. The spatiotemporal variations in each data variable were examined as the first part of data analyses. Mapping of each data variable for each time a step was carried out, and the maps prepared were later examined visually to comprehend the spatiotemporal variations within each data variable. Apart from regular mapping, density

in ArcMap to identify the hotspots of fire instances. Moreover, the low and high values of the relevant data variables were also examined to see the temporal variations in each. Animated images illustrating the spatiotemporal variations in each data variable were also created.

The spatiotemporal relationships were examined using rigorous statistical machine learning algorithms applied to test the relationships between the AOD and other data variables. Different options were explored to carry out regression analysis to investigate the relationships between the dependent variable, for instance, smog, and the explanatory/predictor variables, for instance, active fire, AOD, CO, SO₂, and NO₂. The most common regression analysis, i.e. Ordinary Least Square (OLS) could not be applied since the dependent variable, in the case of the first framework, is discrete and binary in nature with only two data values, i.e. 0 (no smog/fog) and 1 (smog/fog). To account for this, it was necessary to apply a generalized linear modelling (Nakaya, 2015), where a linear regression model describes a linear relationship between a response and one or more predictive terms. Most of the times, however, a nonlinear relationship exists between the data where a nonlinear regression describes general nonlinear models. A special class of nonlinear models, called generalized linear models, uses linear methods. In generalized linear models, each set of values for the predictors, the response has a distribution that can be normal, binomial, Poisson, gamma, or inverse Gaussian. In the case of the current study, it was a binomial response which was recorded, the intention was to examine the relationship of 'presence' or 'absence' of smog delineated through satellite imagery. Different software programs were considered (the majority of them tested as well) for these analyses, e.g. R, and GWR4 tool. R and Interactive Data Language (IDL) was selected and used for the analyses as it provided an edge over other programs in terms of performance and reliability, and because it also supported generalized linear modelling for the binomial distribution.

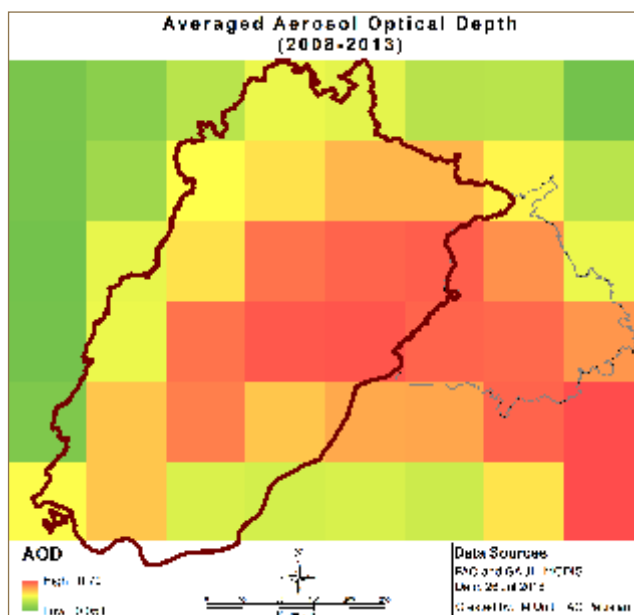
The data needed appropriate preparation to perform regression analysis in R and Minitab, which involved several sequential processing steps – the majority of these geoprocessing tasks were performed in ArcMap, ERDAS Imagine and IDL. The overall geoprocessing workflow, from processing the data for regression analysis to performing the actual correlation analyses, as illustrated in a later relevant section.

3.3 Results of remote sensing analysis

This section presents the results and discussion on the spatiotemporal analyses of the data variables. Each data variable is discussed individually in the following sub-sections.

3.3.1 Aerosol optical depth

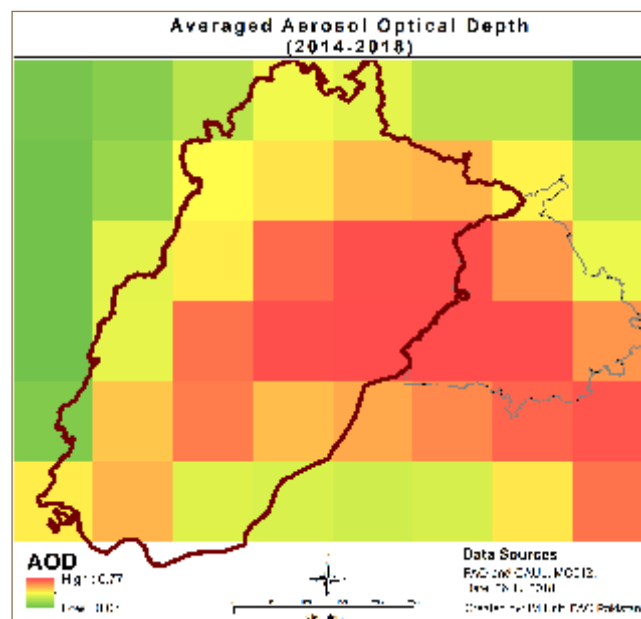
All data is scaled between 0 to 1 for improving the display showing an extremely clean environment or cloud free environment for values close to 0.0 and 1.0 refer to hazy atmospheric conditions. Every map of AOD is generated by taking the mean of a season, one season includes the months October, November, December, January, and February from each year from 2008 to 2018. Maps for all the ten years were produced in a similar way. The high level of aerosols is indicated by red color whereas lower levels are indicated by green color. The bigger polygon indicates boundaries of Punjab within Pakistan, while the smaller polygon indicates Punjab in Indian Territory.



Disclaimer: The boundaries and names shown and the designation used on this map do not imply official endorsement or acceptance by the United Nations. Dotted line represents approximately the Line of Control in Jammu and Kashmir agreed upon by India and Pakistan. The final status of Jammu and Kashmir has not yet been agreed upon by the parties

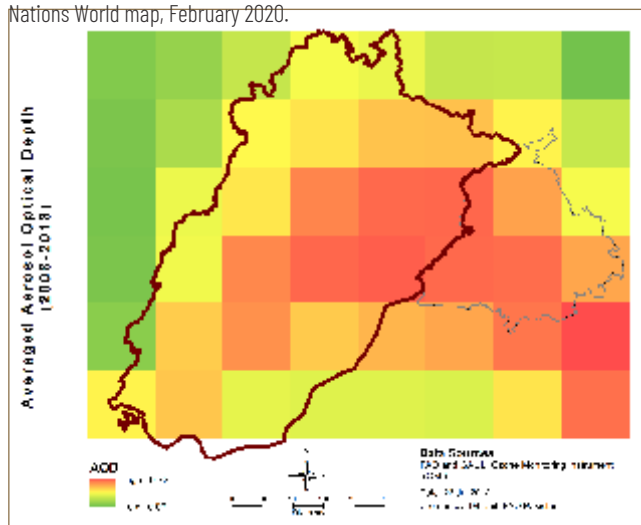
3.3. Seasonal average of AOD from 2008–2013.

Source: Adapted from United Nations World map, February 2020.



Disclaimer: The boundaries and names shown and the designation used on this map do not imply official endorsement or acceptance by the United Nations. Dotted line represents approximately the Line of Control in Jammu and Kashmir agreed upon by India and Pakistan. The final status of Jammu and Kashmir has not yet been agreed upon by the parties

3.4. Seasonal average of AOD from 2014–2018. Source: Adapted from United Nations World map, February 2020.



Disclaimer: The boundaries and names shown and the designation used on this map do not imply official endorsement or acceptance by the United Nations. Dotted line represents approximately the Line of Control in Jammu and Kashmir agreed upon by India and Pakistan. The final status of Jammu and Kashmir has not yet been agreed upon by the parties

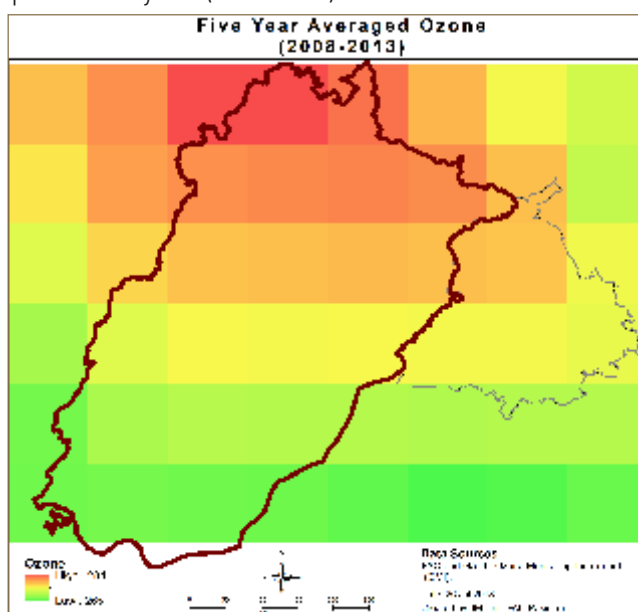
3.5. Seasonal average of AOD from 2008–2018. Source: Adapted from United Nations World map, February 2020.

High loading of the aerosol is observed annually over Pakistan (Appendix C). There is an increasing trend in the AOD from December to February. There are substantial spatiotemporal changes in the concentrations of AOD between 2008–2018 (Figure 3.5). Nonetheless, the Indian Punjab represents minimum variations and depicts high concentrations of AOD throughout the study period.

The AOD analyses also indicate the increase in air pollution as shown in figures 3.3 and 3.4. Almost all the images show Indian Punjab covered with high aerosol loading, whereas, Pakistani Punjab experienced high loading close to the Indian border. Overall, it is concluded that AOD has increased over the period of time in the study area with high loading on the Indian side.

3.3.2 Mapping of ozone

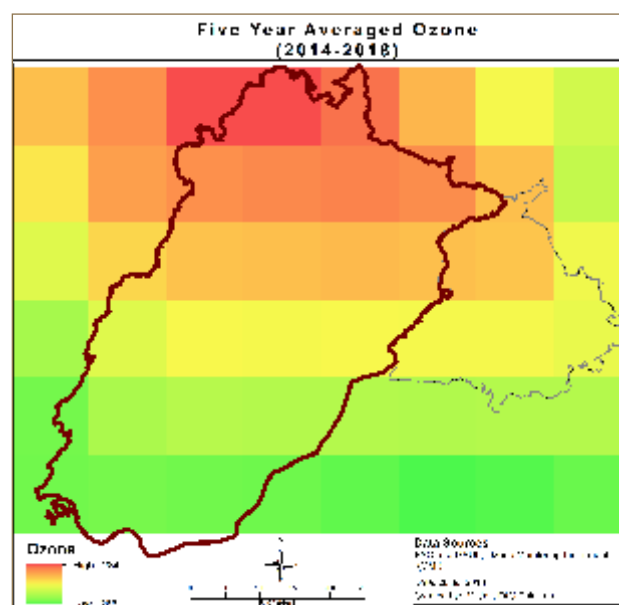
The results for the five-year averaged Ozone of 2008–2013 for the months of October to February are shown in figure 3.6. The highest value for ozone was approximately 284.85 DU and the lower value id approximately 265.66 DU. It should be noted that the concentration of ozone is higher in the northern part of Punjab (Pakistan) between 71°E to 74°E. Also, it is clear from figure 3.6 that the ozone concentration between 32°N and 34° N is much higher. The variation in ozone concentration in northern (high value) and southern (low value) parts of the study area can be attributed to the differences in temperatures which causes the inversion. The high value is 289.44 and low value is 270.53 DU. The spatial distribution of ozone concentration is similar as during 2008–2013. The southern part of the study area has a lower concentration of ozone. After analyzing the spatial and temporal distribution of O₃ in the study area, the overall averaged O₃ for the study period of 10 years (2008–2018) was also measured.



Disclaimer: The boundaries and names shown and the designation used on this map do not imply official endorsement or acceptance by the United Nations. Dotted line represents approximately the Line of Control in Jammu and Kashmir agreed upon by India and Pakistan. The final status of Jammu and Kashmir has not yet been agreed upon by the parties

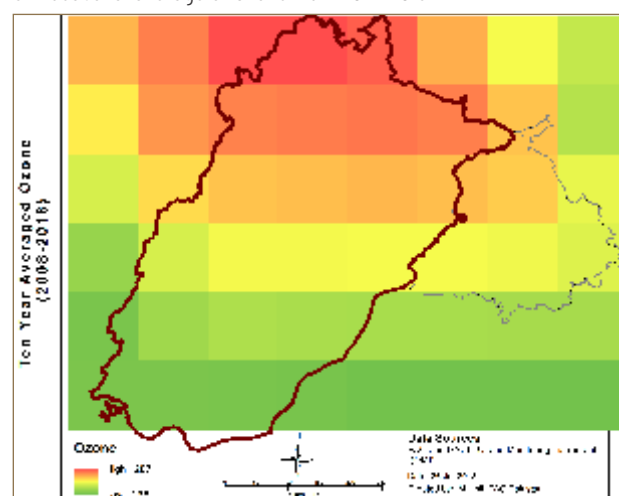
3.6. Seasonal average of Ozone from 2008–2013.

During the last 10 years, the O_3 concentration ranged between 287.1–268.04 DU, as shown in figure 3.8. The decadal analysis of O_3 concentration reveals that the northern region of Punjab was significantly influenced by higher O_3 and southern regions with lower concentration. Overall, annual spatial distribution of Ozone didn't show any significant spatial variation, where higher concentration was observed in the northern region and lower concentration in the southern region. Ozone concentration increased significantly during the study period.



Disclaimer: The boundaries and names shown and the designation used on this map do not imply official endorsement or acceptance by the United Nations. Dotted line represents approximately the Line of Control in Jammu and Kashmir agreed upon by India and Pakistan. The final status of Jammu and Kashmir has not yet been agreed upon by the parties.

3.7. Seasonal average of Ozone from 2014-2018.

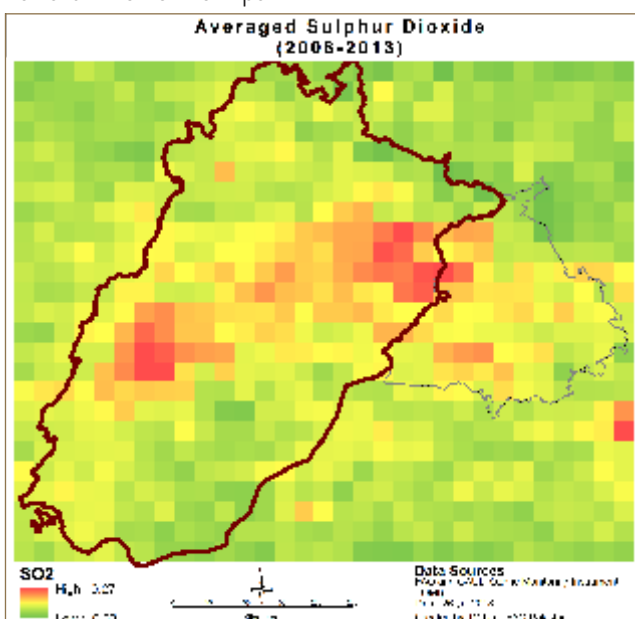


Disclaimer: The boundaries and names shown and the designation used on this map do not imply official endorsement or acceptance by the United Nations. Dotted line represents approximately the Line of Control in Jammu and Kashmir agreed upon by India and Pakistan. The final status of Jammu and Kashmir has not yet been agreed upon by the parties.

3.8. Seasonal average of Ozone from 2008–2018.

The highest value for sulphur dioxide (SO_2) was approximately 0.27. It should be noted that the concentration of Sulphur dioxide is higher in central and southern part of Punjab (Pakistan) between 71°E to 74°E . It is also clear from Figure 3.9 that the SO_2 concentration between 30°N and 32°N is very high. The variation in SO_2 concentration over the study area can be attributed to the total emission due to anthropogenic activities which may be vehicular emission in urban areas and crop burning in rural areas.

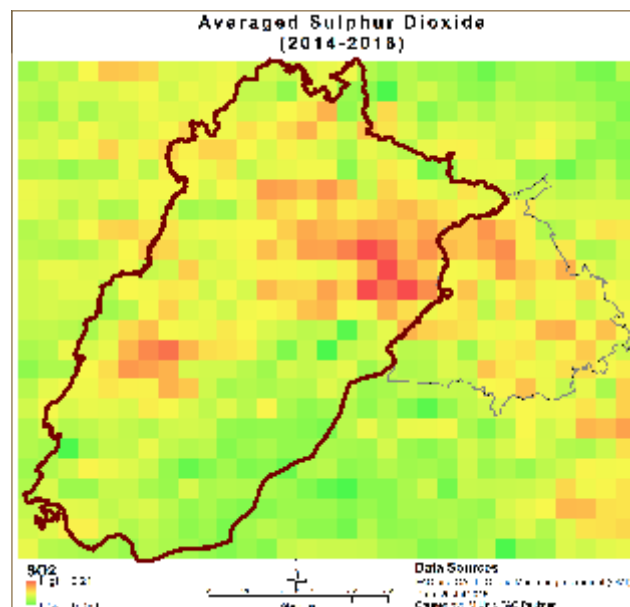
As reflected, there is a decrease in the concentration of SO_2 during 2014–2018 in the study area (Figure 3.10). The higher and lower value for SO_2 is 0.24 and -0.06 respectively. The spatial distribution of SO_2 was slightly different from the previous map. Most of the Sulphur dioxide was concentrated in the central and southern Punjab but has also moved a bit towards the northern parts.



Disclaimer: The boundaries and names shown and the designation used on this map do not imply official endorsement or acceptance by the United Nations. Dotted line represents approximately the Line of Control in Jammu and Kashmir agreed upon by India and Pakistan. The final status of Jammu and Kashmir has not yet been agreed upon by the parties

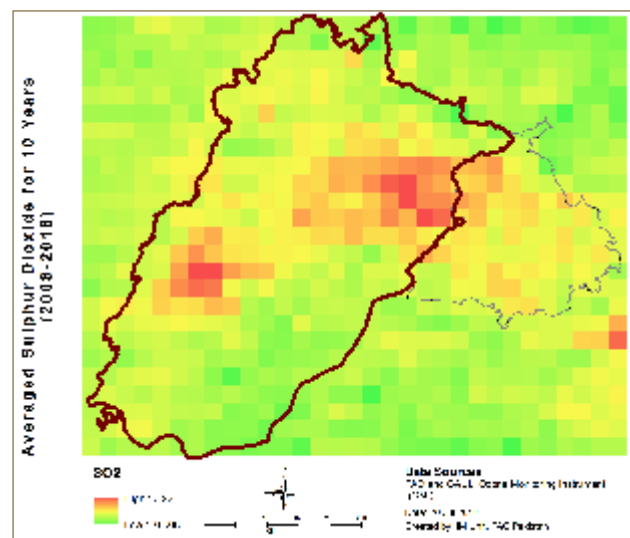
3.9. Seasonal average of SO₂ from 2008–2013.

After analyzing the spatial and temporal distribution of sulfur dioxide in the study area, the overall averaged SO_2 for the whole study period which is about 10 years, (2008–2018) was also measured. It was noted that during the last 10 years, the SO_2 concentration ranged between 0.23 and -0.01, shown in figure 3.11. The decadal analysis of Sulphur dioxide concentration reveals that the central region (Lahore) of Punjab were significantly influenced by higher SO_2 and undeveloped southern regions with lower concentration.



Disclaimer: The boundaries and names shown and the designation used on this map do not imply official endorsement or acceptance by the United Nations. Dotted line represents approximately the Line of Control in Jammu and Kashmir agreed upon by India and Pakistan. The final status of Jammu and Kashmir has not yet been agreed upon by the parties

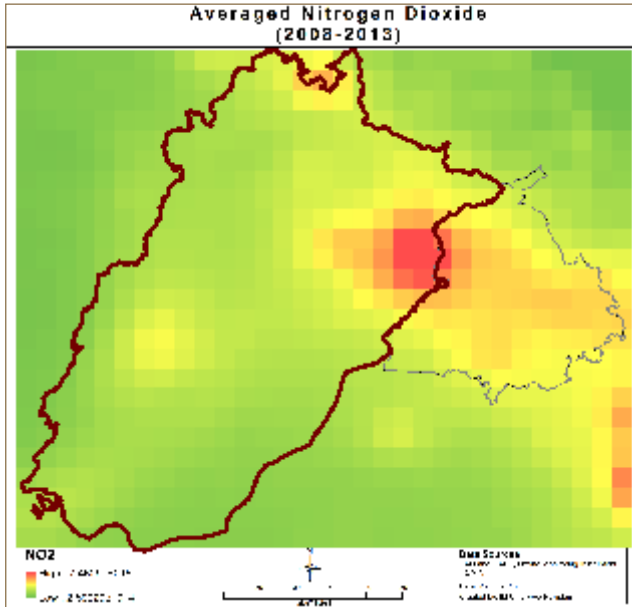
3.10. Seasonal average of SO₂ from 2014–2018.



Disclaimer: The boundaries and names shown and the designation used on this map do not imply official endorsement or acceptance by the United Nations. Dotted line represents approximately the Line of Control in Jammu and Kashmir agreed upon by India and Pakistan. The final status of Jammu and Kashmir has not yet been agreed upon by the parties

3.11. Seasonal average of SO₂ from 2008-2018.

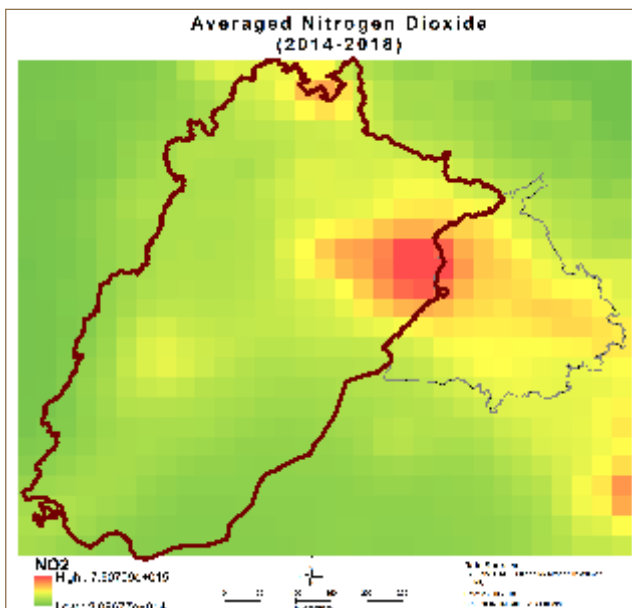
The NO₂ was highest in 2017 and 2018 which leads with a value of 8.33×10^{15} . The difference in values has been quite significant from 2008 to 2018 with constantly increasing amounts. Pakistan administered Punjab is dominated by intense concentrations of NO₂.



Disclaimer: The boundaries and names shown and the designation used on this map do not imply official endorsement or acceptance by the United Nations. Dotted line represents approximately the Line of Control in Jammu and Kashmir agreed upon by India and Pakistan. The final status of Jammu and Kashmir has not yet been agreed upon by the parties

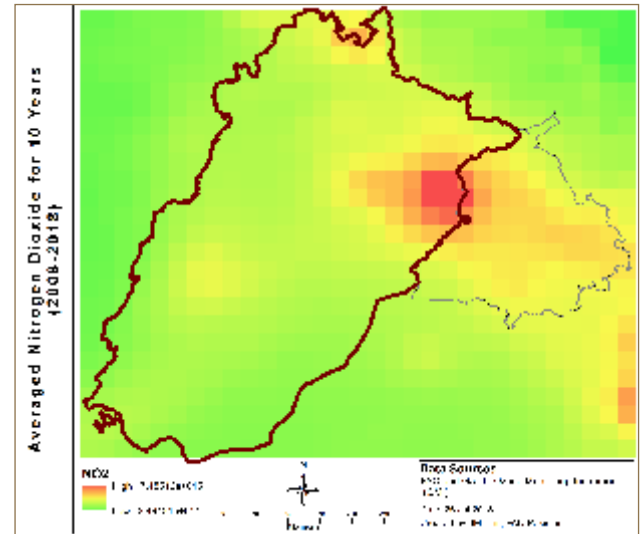
3.12. Seasonal average of NO₂ from 2008–2013.

Notable regions of high concentrations of NO₂ are found to be within Pakistani cities including Lahore. Figures 3.12 to 3.13, show significant variations in the presence and intensities of NO₂ over Pakistan administered Punjab. Increased NO₂ column concentrations were found in areas with potentially high industrial activities. The observed results of NO₂ are beyond the permissible limits by environmental departments because of its major impact on air quality of the region.



Disclaimer: The boundaries and names shown and the designation used on this map do not imply official endorsement or acceptance by the United Nations. Dotted line represents approximately the Line of Control in Jammu and Kashmir agreed upon by India and Pakistan. The final status of Jammu and Kashmir has not yet been agreed upon by the parties

3.13. Seasonal average of NO₂ from 2014–2018.



Disclaimer: The boundaries and names shown and the designation used on this map do not imply official endorsement or acceptance by the United Nations. Dotted line represents approximately the Line of Control in Jammu and Kashmir agreed upon by India and Pakistan. The final status of Jammu and Kashmir has not yet been agreed upon by the parties

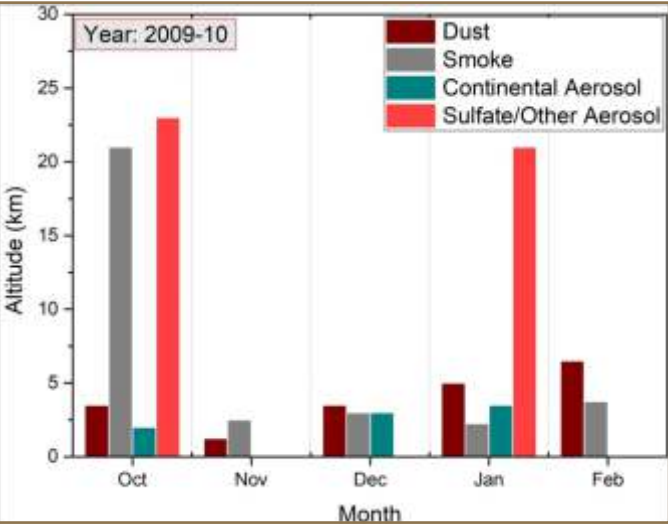
3.14. Seasonal average of NO₂ from 2008–2018.

3.3.5 Optical and chemical nature of aerosol types

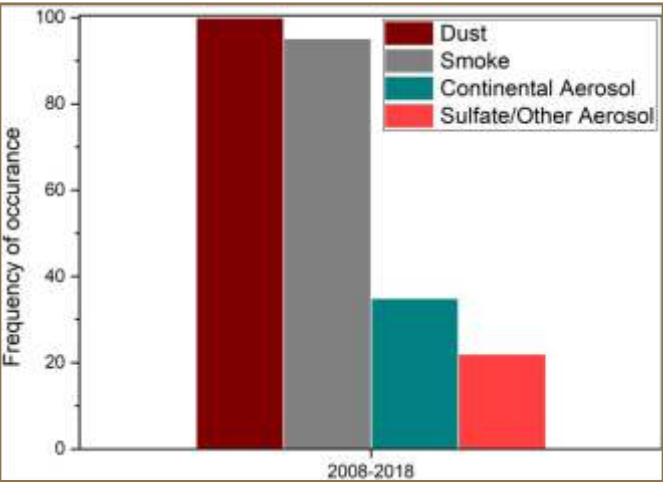
CALIPSO data over Pakistan were utilized to identify the vertical depth and types of aerosol in each season from 2008–2018. The type of aerosols which were identified over the study area were dust, smoke, continental aerosols, sulfate, and other aerosols. The frequency analysis of yearly, and overall frequency from 2008–2018 was performed for the study area.

For instance, for the year 2009–10, the most dominant parameter was sulfate/other aerosol at a higher altitude during the months of October and January. The interesting aspect is the presence of smoke at a higher altitude during the month of October. While all other types which include dust, continental aerosol, and smoke (except for the month of October) remained at lower altitudes (Figure 3.15). Other years also followed nearly a similar pattern for temporal and vertical spatial distribution. The monthly data of CALIPSO during the years 2008–18 for months of October–February are shown in figure 3.16. The most prominent parameters were smoke and Sulfate/other aerosols. Continental aerosols were identified at lower altitude during the month of December while Sulfate/other aerosol were found at a higher altitude during the month of October.

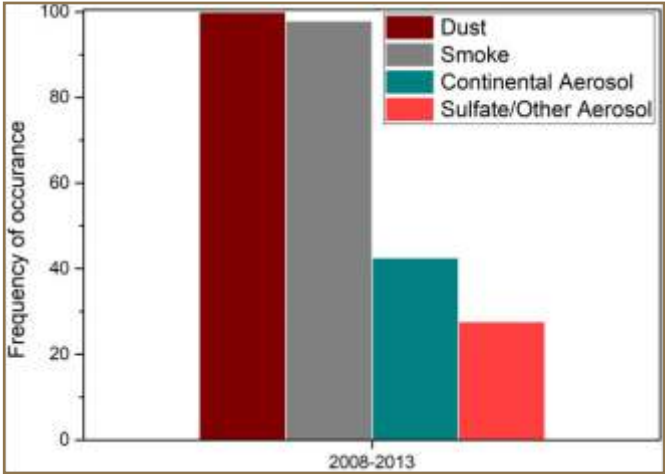
The frequency of occurrence for each parameter during the year 2008-13 (5-year) is displayed in figure 3.17. Dust events were highest among all, with smoke at second position while continental and sulfate/other aerosol remain at 3rd and 4th positions, respectively. The figure reveals that dust was most frequent in the area under study. Smoke remained close to dust, while sulphate/other aerosol and continental aerosol are less frequent in the region during 2008-18. The occurrence of dust events again topped the list ahead of smog. The remaining two parameters occurred less frequently (Fig 3.17).



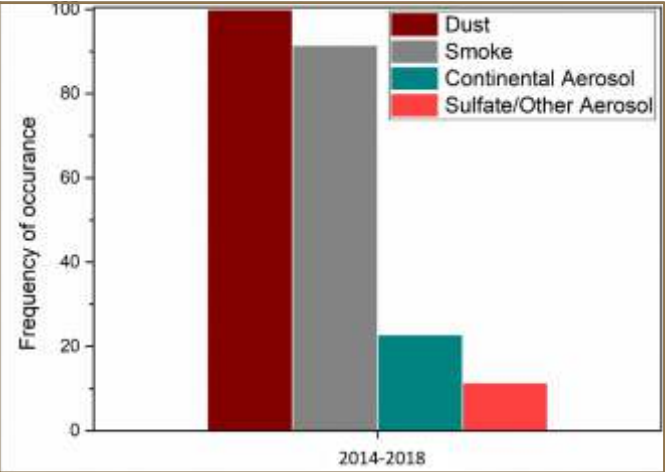
3.15. CALIPSO derived aerosol types and altitude for the year



3.16. CALIPSO derived aerosol types and altitude from 2008-18.



3.17. CALIPSO derived aerosol types and altitude from 2008-2013.



3.18. CALIPSO derived aerosol types and altitude from 2014-2018.

3.3.6 Fire mapping

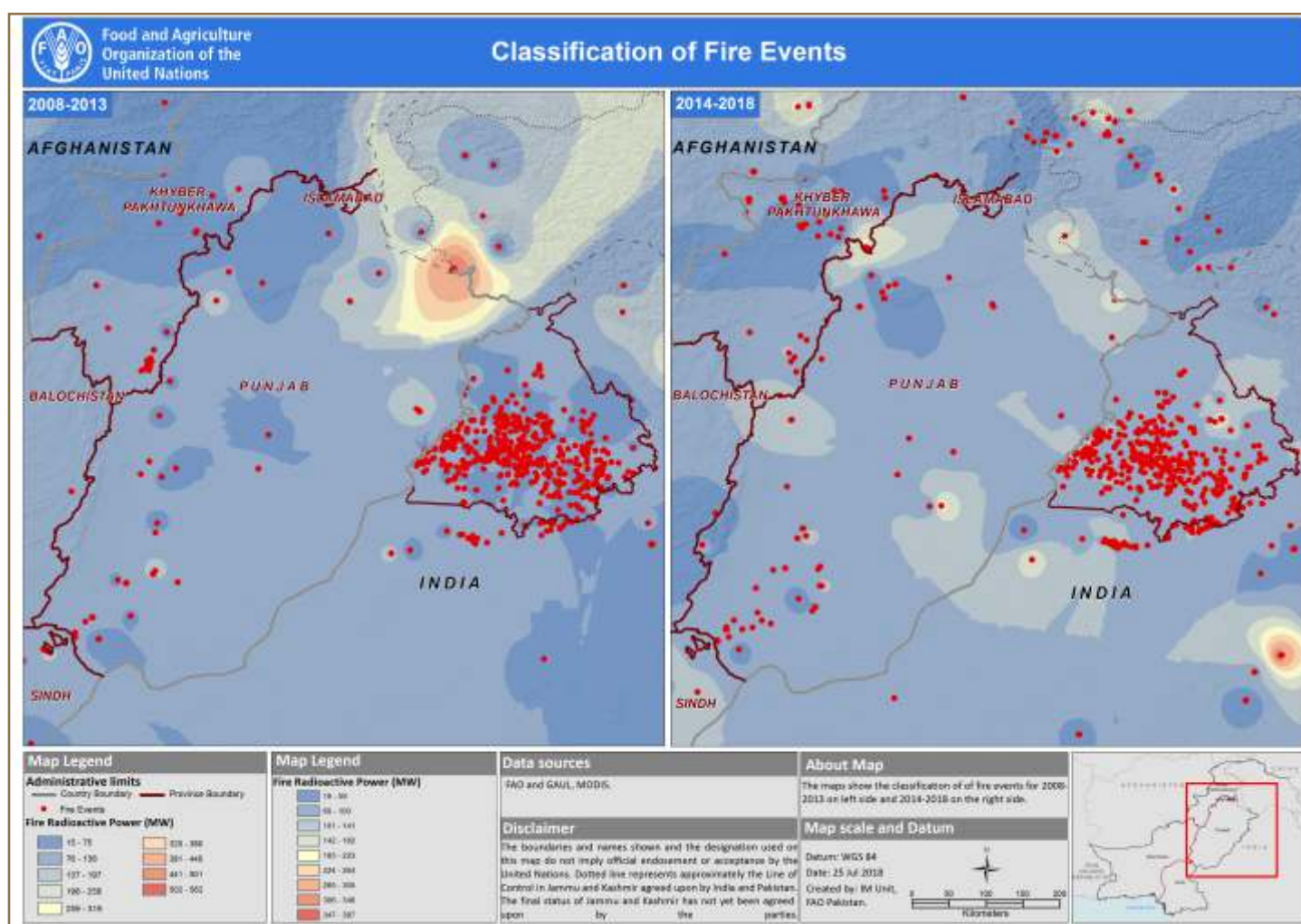
Daily MODIS data were used to identify the active fire areas by using temperature and FRP (fire radiative power) in megawatts (MW). The fire data for a confidence level of 95% and above, has been used for this study. FRP aided in quantifying burned biomass and the amount of radiant energy released per unit of time by burning vegetation. The point data of fire were interpolated to estimate the effect of fire in the study area. It is evident from detection of seasonal fire events (shown in Appendix G) that there is a considerable spatiotemporal variation in locations and intensities of the fire events. Many fire events occurred inside the Indian administered Punjab as

compared to the Pakistani administered Punjab where fire events were relatively less intense FRP occurred. Further, two sets of five yearly seasons i.e. from 2008 to 2013 and 2014 to 2018, were made to further classify the number of events other than yearly seasons. These sets also verified that the maximum numbers of fire events occurred in the Indian administered Punjab. Figure 3.19 shows a total number of fire events from October 2008 to February 2013 and from October 2014 to February 2018, which also verifies that Indian administered Punjab showed an increased number of fire events as compared to Pakistan administered Punjab. These observations and analyses demonstrate the importance of aerosols and their transboundary impacts (Figure 3.19). Unique day fire event frequency analyses were performed on

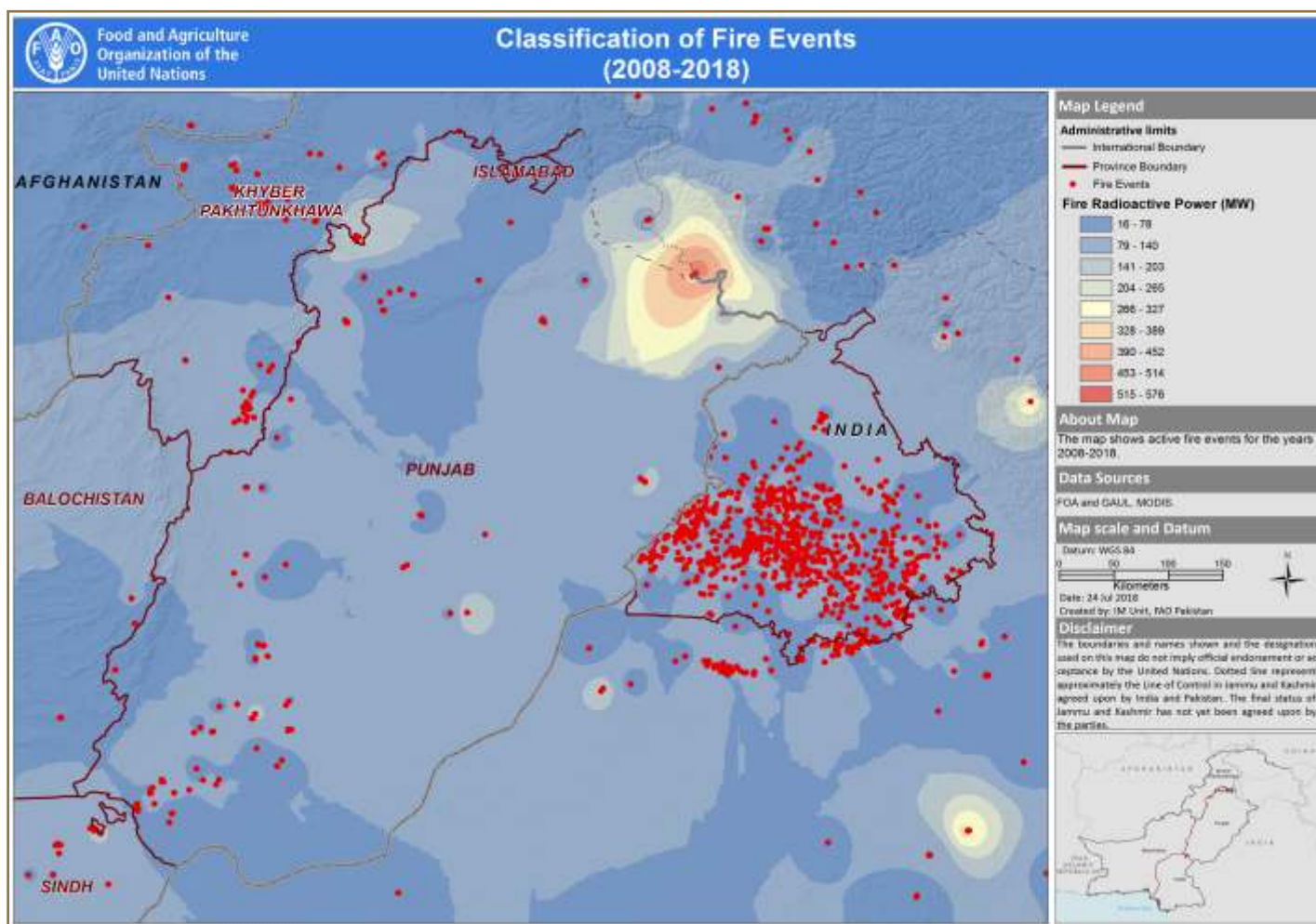
monthly basis from 2008–2018. Figure 3.21 reveals that during the month of November, most of the fire events occurred 593, while in January only 36 unique fire events were identified. During the month of October, February and December 389 123 and 74 unique fire events were measured, respectively.

3.3.7 Hotspot analyses to identify areas of crop residue burning

Fire data sets were acquired from MODIS active fire detections standard product (MCD14ML), distributed by NASA FIRMS for the season (ONDJF) from 2008 to 2018. Every point of the data represents the midpoint of 1 km pixel indicating single or multiple active fires when satellites scanned the

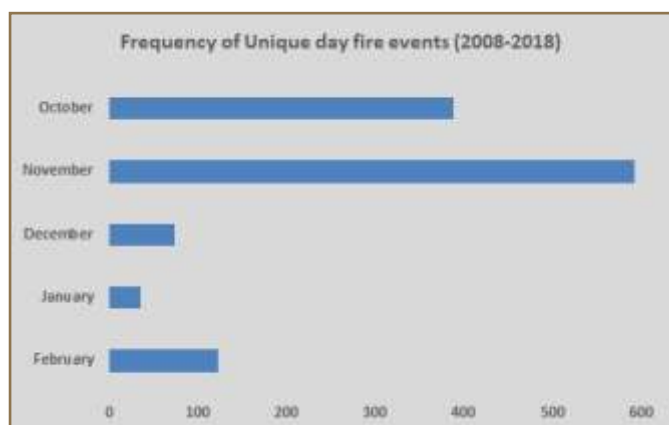


3.19. Classification of fire events from October 2008 to February 2013 (left) and from October 2014 to February 2018 (right). Source: Adapted from United Nations World map, February 2020.



3.20. Active fire status from October 2008 to February 2018. Source: Adapted from United Nations World map, February 2020.

area. Every detected fire consists of a confidence value ranging from 0 to 100%, where 0 and 100 are the lowest and highest confidence values, respectively (Giglio, 2013). Detected active fires with a confidence level of 95% and above were



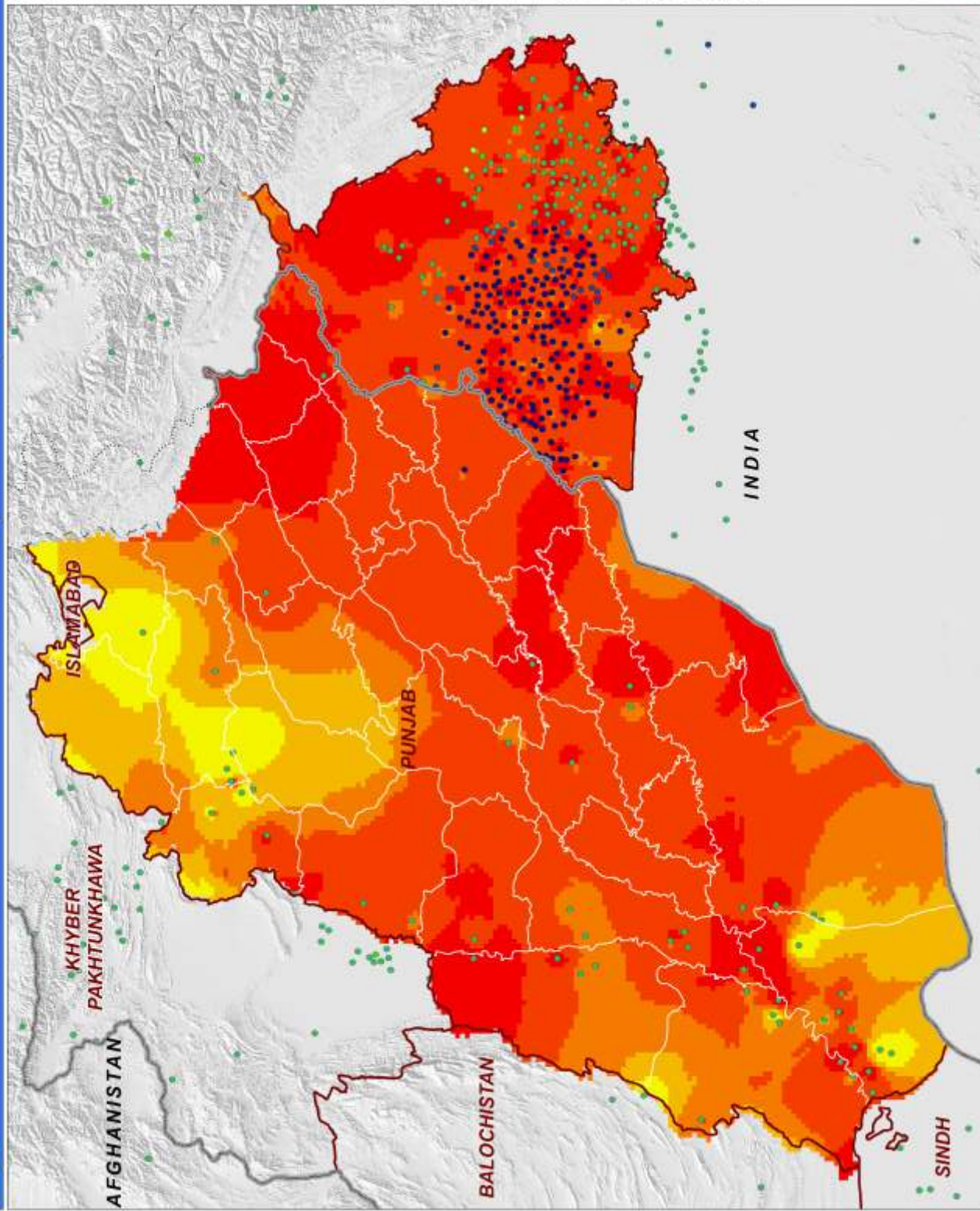
3.21. Unique day fire events frequency from 2008-2018.

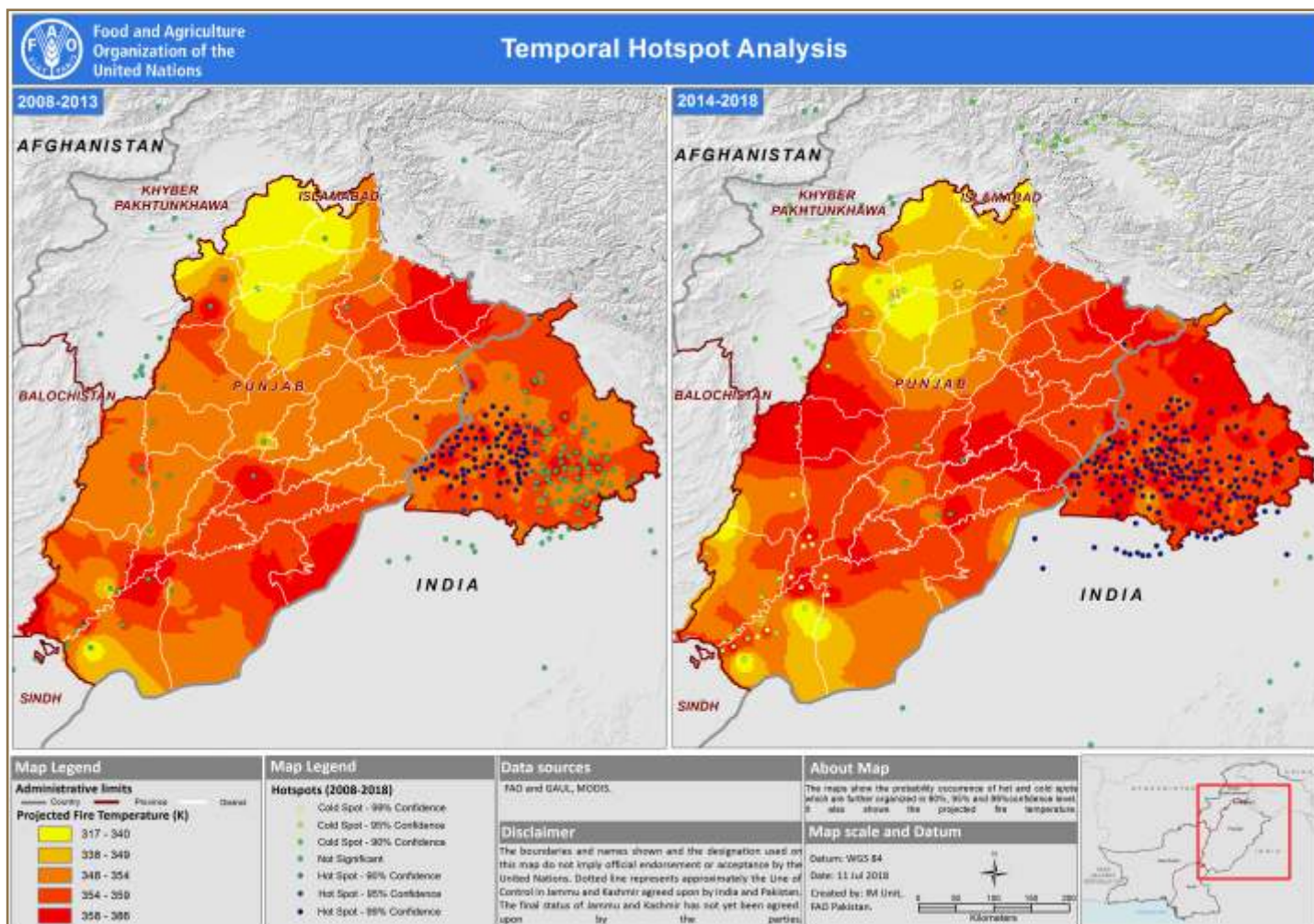
selected to minimize the occurrence of false alarms (Giglio, 2013). This criterion resulted in total 3 578 active fire occurrences during the studied period. Further, two types of approaches were incorporated for data analysis:

1. Temporal: it dealt with variables that changed over time such as temperature.
2. Spatial: it dealt with all variables except climate that was having a spatial component.

In the temporal fire occurrences, patterns were analyzed on weekly, monthly, seasonally and yearly basis, months from October to February were termed as the dry season (Restrepo et al., 2014). For detecting the spatial patterns of the active fires, hotspot analysis was used which enabled to determine whether the fire occurrence was random, or these were spatially scattered clusters.

Temporal Hotspot Analysis (2008-2018)





3.23. Five-year Hotspot analysis for 2008–2013 (left) and 2014–2018 (right). Source: Adapted from United Nations World map, February 2020.

The data point clusters are identified by the hotspot technique itself. Hotspots were identified by using the spatial analyst tool Optimized Hotspot Analysis. The input data was given in the form of point, the tool performed the process of clustering based on hotspot occurrence per fishnet (grid), which was derived automatically in the process. The spatial tool then classified the clusters statistically, the high-value clusters are categorized as hotspots and lower values are categorized as cold spots. Based on probability occurrence, hot and cold spots were further organized in 90%, 95% and 99% confidence levels (Figures 3.22 and 3.23).

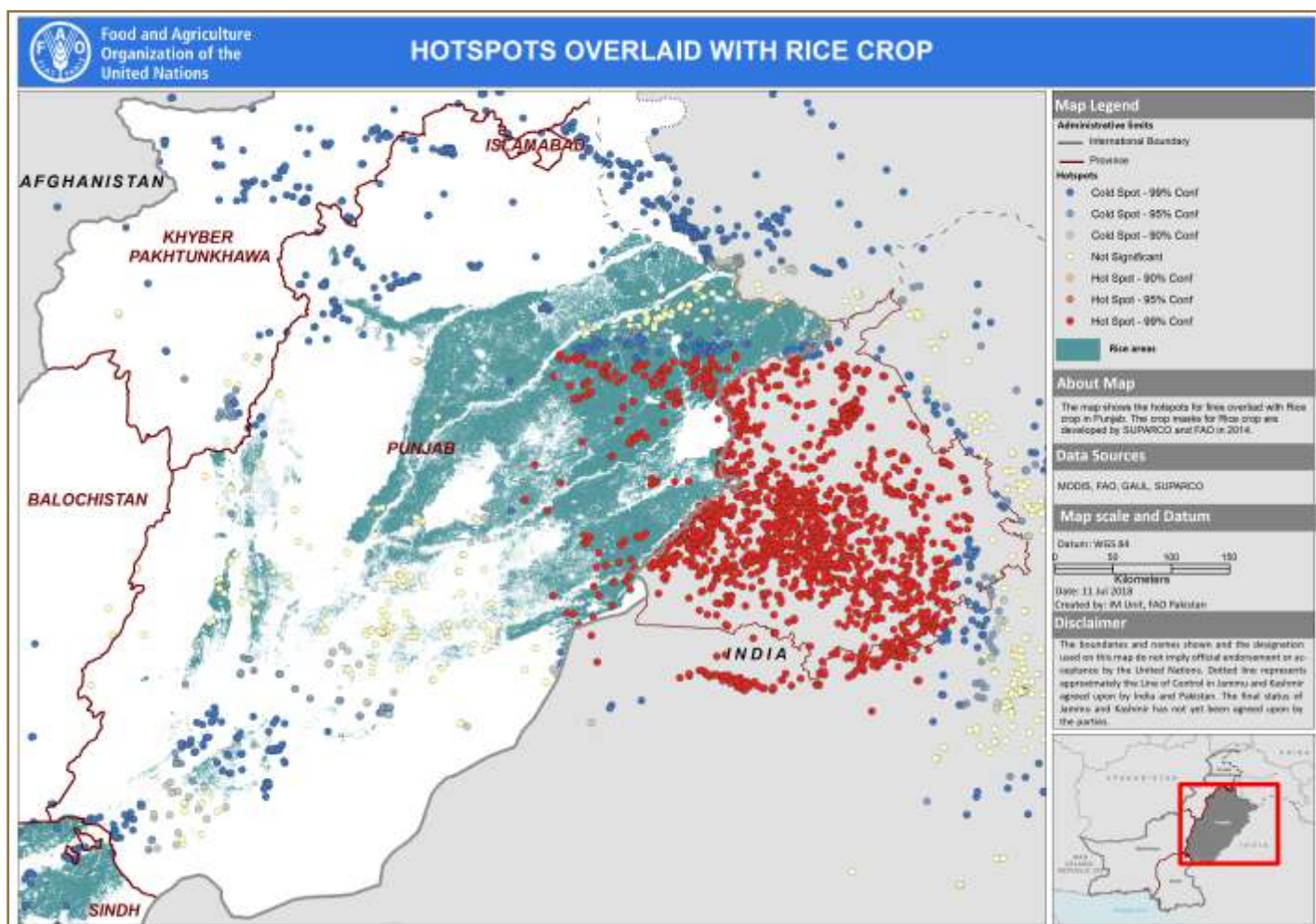
3.3.8 Fire events overlaid on rice crop

Paddy crops residue burning in the Punjab region are a major source of the smoke. The growing seasons in the study area are from May to September and from November to April. Farmers usually start sowing crops and set the fire before plantation to clear the fields (K. Vijayakumar et al., 2016).

Hotspot analysis using the fire events in the study area was performed and the results were overlaid on crop masks of rice (Fig 3.24).

The results revealed the hotspot & rice crop with 95% confidence in the eastern region of India and some parts of central Punjab (Pakistan). The Pakistani region includes districts of Okara, Bahawalpur, and Kasur with major hotspots. Some cold spots and non-significant events are covered in the Pakistan administered Punjab.

The results for the rice crop with hotspot analysis are shown in figure 3.24. It was evident that the hotspot with 99% confidence, resides in the Indian administered Punjab while some hotspots were present in few districts of Pakistani administered Punjab. The most affected districts include Sheikhupura, Hafizabad, Narowal, Nankana Sahib and Okara.



3.24. Hotspot analysis and rice crop. Source: Adapted from United Nations World map, February 2020.

Most of the cold spots and non-significant locations were in Pakistani administered Punjab. The number of fire events contributed by rice crop residue burning was concentrated in the Indian side.

3.3.9 Forward trajectory analysis

A 24-hour trajectory analyses based on the NOAA HYSPLIT model was performed in the study area to understand the transportation path of fire smoke. The meteorological input for the trajectory model was the GDAS (Global Data Assimilation) dataset (reprocessed from NCEP by Air Resources Laboratory). All the trajectories were drawn at 300 m altitudes for every top ten fire events (2008–2018). The years 2016 and 2017 were focused due to worse smog conditions in the study area. Top ten fire events trajectories for the year 2008 to 2018 are illustrated in figure 3.25.

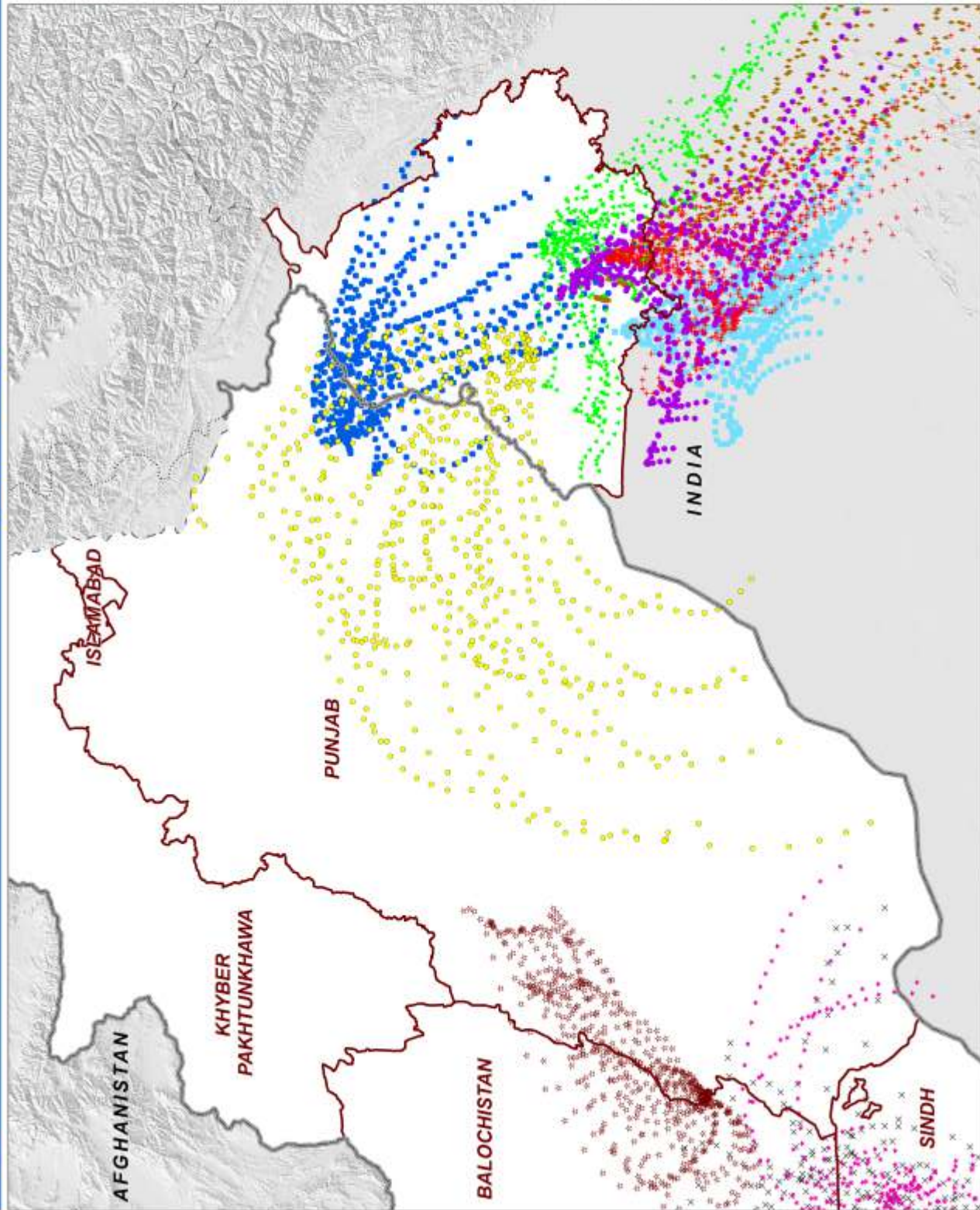
The figure reveals that the air masses with fire smoke reaches from India to Pakistan, Pakistan to India and within Pakistan. Out of 10 fire events, four events occurred during the years 2016 and 2017. Trajectories of each plume were monitored to note, whether plume is transported from India to Pakistan, transported from Pakistan to India, remained within Pakistan or remained within India. Based on the results it was suggested that Pakistan may suffer from local as well as trans-boundary smog events. The plumes (fire smoke) direction was not uniform, as it starts from the origin and transported in all directions in the study area. Majority of the air masses were found in the Indian administered Punjab while in Pakistan (Punjab), only two major events were found.

As the air moves towards the north, away from the equator at high elevations, the Coriolis force affects by dominating the south and south-westerly winds.



Food and Agriculture
Organization of the
United Nations

Top 10 Fire Event Trajectories (2008-2018)



Map Legend

Administrative limits
— International Boundary
— Province Boundary

Top 10 Fire Events

26 Oct 2016
03 Nov 2013
05 Nov 2008
11 Nov 2016
13 Nov 2016
16 Nov 2015
13 Feb 2017
05 Feb 2012
18 Oct 2013
14 Oct 2008

About Map

The map shows the trajectories of top 10 fire events occurred in the years 2008-2018.

Data Sources

FOA and GAUL, NOAA, HYSPLIT, GDAS, and NCEP.

Map scale and Datum

Datum: WGS 84

0 50 100 150
Kilometers
N

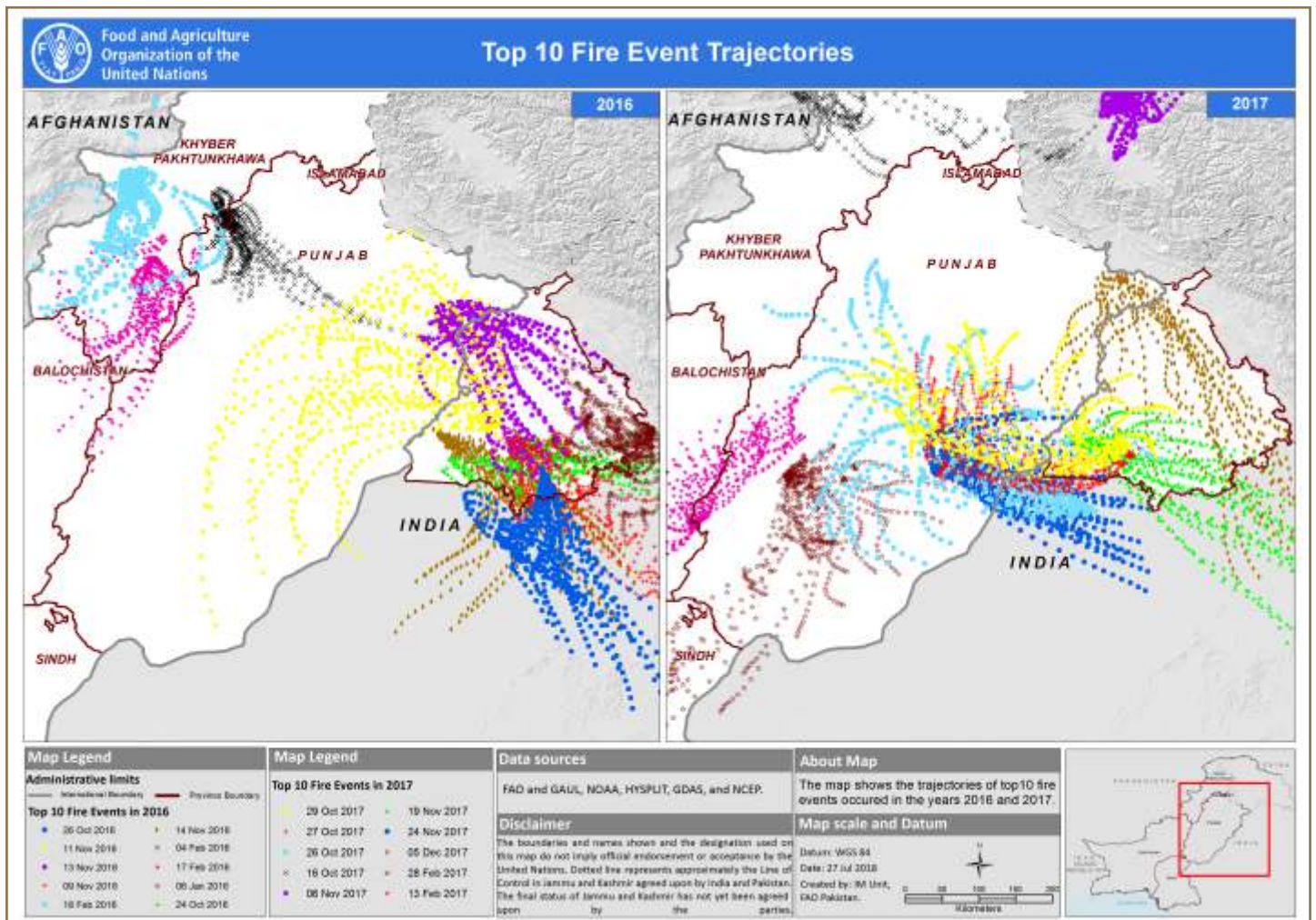
Date: 31 Jul 2018

Created by: IM Unit, FAO Pakistan

Disclaimer

The boundaries and names shown and the designation used on this map do not imply official endorsement or acceptance by the United Nations. Dotted line represents approximately the Line of Control in Jammu and Kashmir agreed upon by India and Pakistan. The final status of Jammu and Kashmir has not yet been agreed upon by the parties.





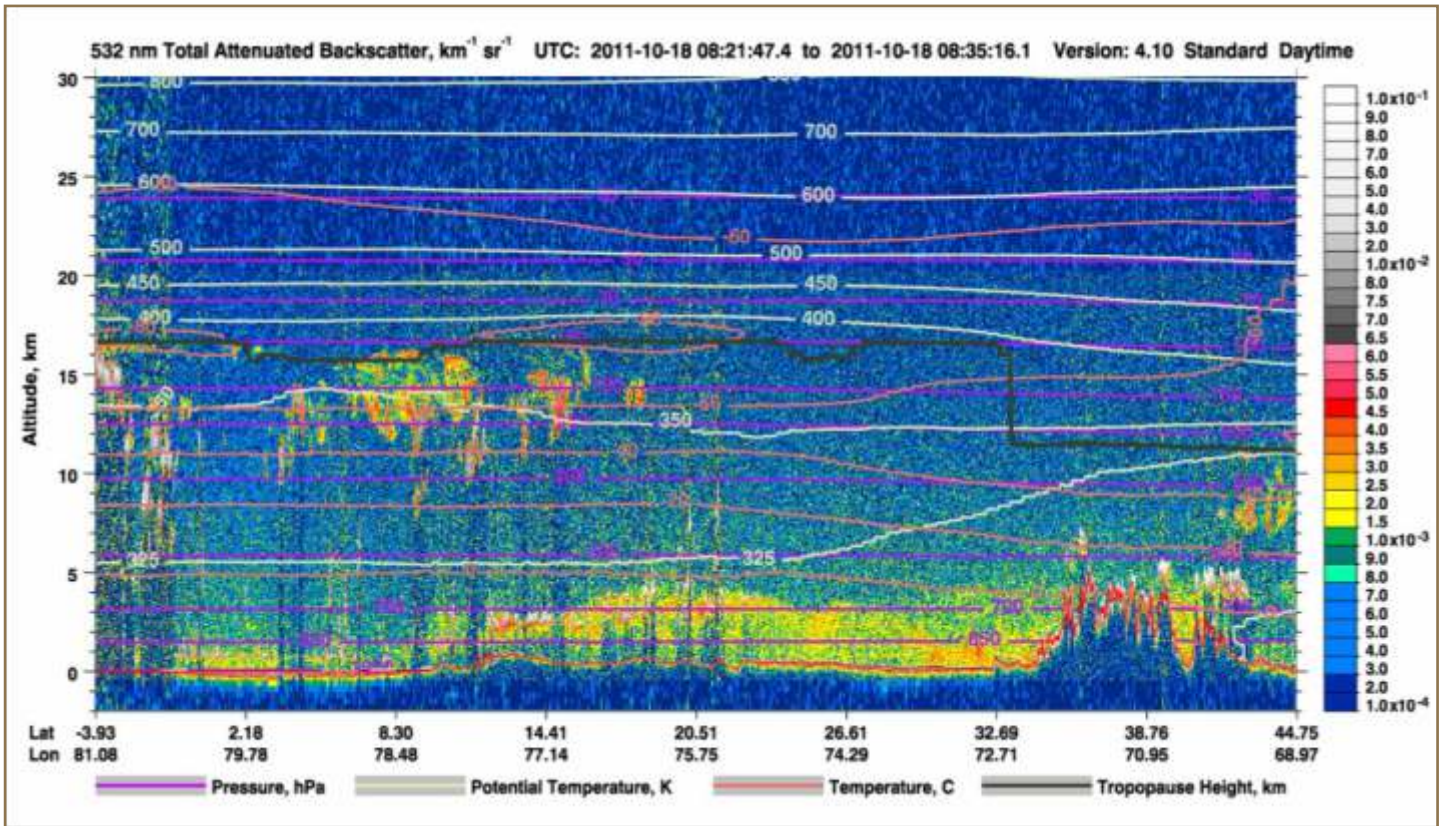
3.26. Top 10 Fire Events Trajectories 2016 and 2017. Source: Adapted from United Nations World map, February 2020.

Major fire events along with HYSPLIT trajectories for the year 2016 are illustrated in figure 3.26, where the major fire events reside in the Indian region while some of the events were within Pakistan. One event directed from India to Pakistan in the eastern region covered a wide area facilitating in the dilution of the pollutants. Trajectories for top ten fire events for the year 2017 are shown in figure 3.26. It is evident that the entry and residence of smoke in Pakistan were more than in India. The direction of major fire smoke remains inside Pakistan, except one. The distribution of air masses influences the flow and direction of the pollutants and their movement over the region.

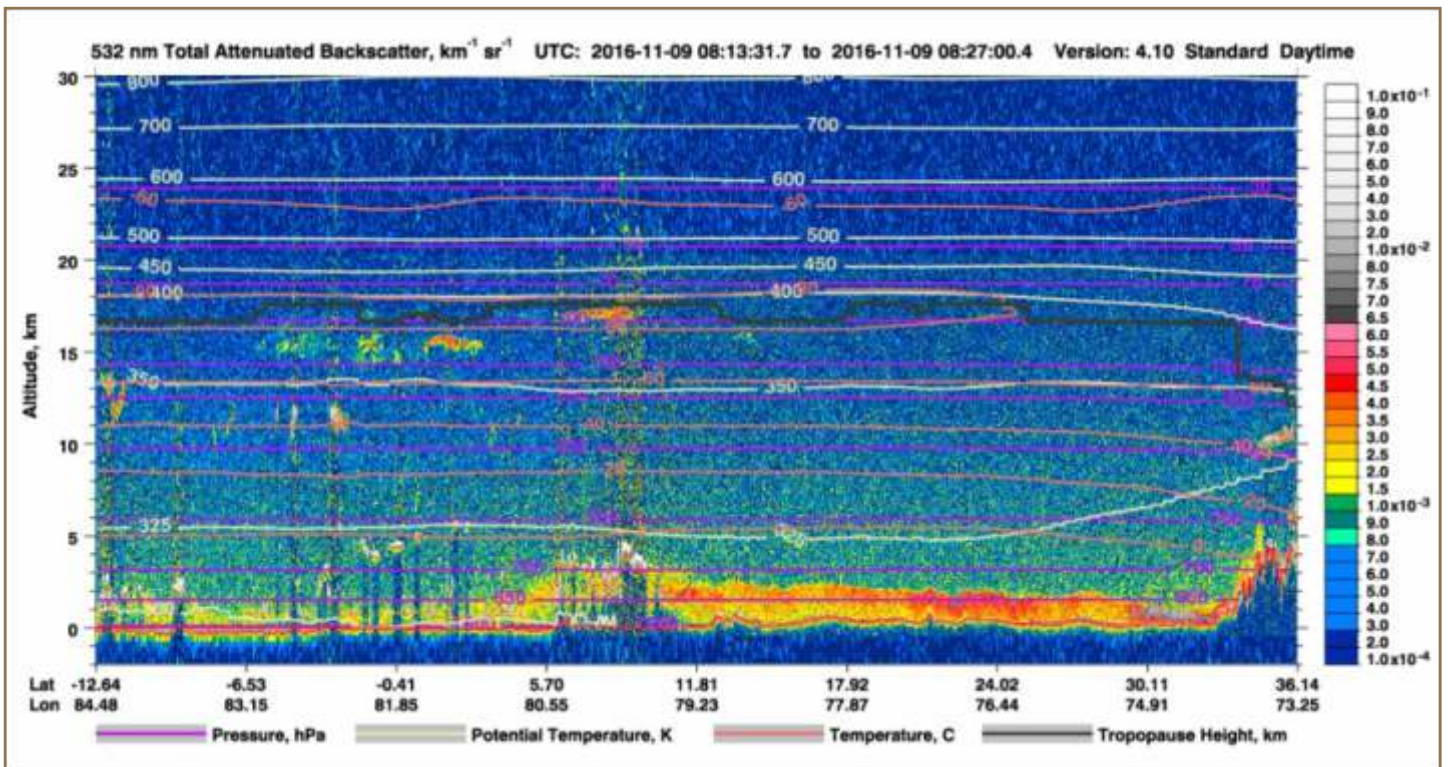
3.3.10. Vertical extent of air pollution

The study area has been monitored to identify air pollutants and their types. The blue color in the figures 3.27 and 3.28 indicates no or very low air pollution, whereas white depicts a high level of air pollution. The vertical axis in the figures indicates height in kilometers corresponding to each color, which indicates the extinction of light due to the presence of aerosols in the air.

Aerosol seasonal variations are forced by both, emissions along with meteorological conditions of any area. There exists variation in presence of aerosols with respect to altitude but overall, air pollution remained very close to the earth's surface i.e. within 1 to 2 km of height. Moreover, the transportation of these aerosols will leave an impact on the population of the study area. Apart from pure meteorological factors, transport of these aerosols can also take place under the thermal turbulence due to the burning of biomass.



3.27. Vertical extent of air pollution on 18 October 2011.



3.28. Vertical extent of air pollution on 9 November 2016.

3.3.11. Numerical modeling

A regression model was developed for the estimation of SMOG using the NO₂, Fire Count, Brightness and FRP. MODIS AOD is used as surrogate to SMPG in this model development. Different types of transformations (i.e. logarithmic, square root and inverse) were used to normalize the datasets. The normality of the data sets was determined through the Anderson-Darling test, followed by a Pearson correlation using Minitab Statistical Software.

To make sure that the proposed model should be reliable, three different approaches were used. First, a manual method, named as general regression model (GRM), second and third were automated approaches named as stepwise regression model (SRM) and best subset Regression model (BRM), respectively. To develop a GRM, independent and dependent variables with maximum correlation coefficients (r) and a p-value of less than 0.01 were grouped together as potential candidates for multiple linear regressions. Each group of variables was subjected to multiple linear regression and a further selection of variables from each group was undertaken based on their p-values, T statistics, and coefficients of determination (R²). Independent variables with significantly larger p-values and smaller T statistics were omitted one by one, and the regression was repeated until a threshold p-value of 0.01 was reached for all the remaining variables. Each statistical set satisfying the above-mentioned criteria was further subjected to two more modeling approaches, namely, SRM and BRM. This helped to examine the principal factors affecting the estimation of SMOG using different variables. BRM is based on “add” and “drop” approaches, where the “add” approach allows only those independent variables that can improve model fitting to enter the regression one by one, based on their p-value of correlation. A variable is retained in the regression equation until the p-value of its correlation is less than the threshold value (i.e., 0.01). The Inclusion of another variable can reduce the significance of the previously added variable, and hence, it will be removed from the regression equation. The “drop” approach contrasts the “add” approach. A combination of both approaches was used in this study for a threshold p-value of 0.01. The resultant model is called the Final Regression Model (FRM) and was subjected to further validation. The selection of the FRM was accomplished by considering measures of collinearity among predictors, namely, the Variance Inflation Factor (VIF) and adjusted R² (adj. R²), such that the FRM contains predictors with a minimum VIF only.

The FRM had five variables (Table 3.2). One independent variable i.e. Log of MODIS retrieved AOD (AOD_log), against which dependent variables, the inverse of NO₂ (1/NO₂), log of number fire events (Fcount_log), the square root of brightness detected by satellite during fire events (Bright_sqrt) and the inverse of fire radiative power (1/FRP) were taken. The proposed model successfully explained 87.0 % (R²) of the variance in the AOD with an adjusted R² value of 78.60 %.

3.2. Numerical modeling results for the FRM for prediction of SMOG.

Predictor	coefficient	standard error coefficient	T Statistics	P value	Variance Inflation Factor (VIF)
Constant	114.85	56.09	2.05	0.009	
1/NO ₂	-2.89E+14	1.37 459E+14	-2.11	0.004	1.161
Fcount_log	-0.032	0.016	-1.89	0.008	1.096
brght_sqrt	-4.047	2.000	-2.02	0.002	1.763
1/FRP	-13 526	6 531	-2.07	0.007	1.688

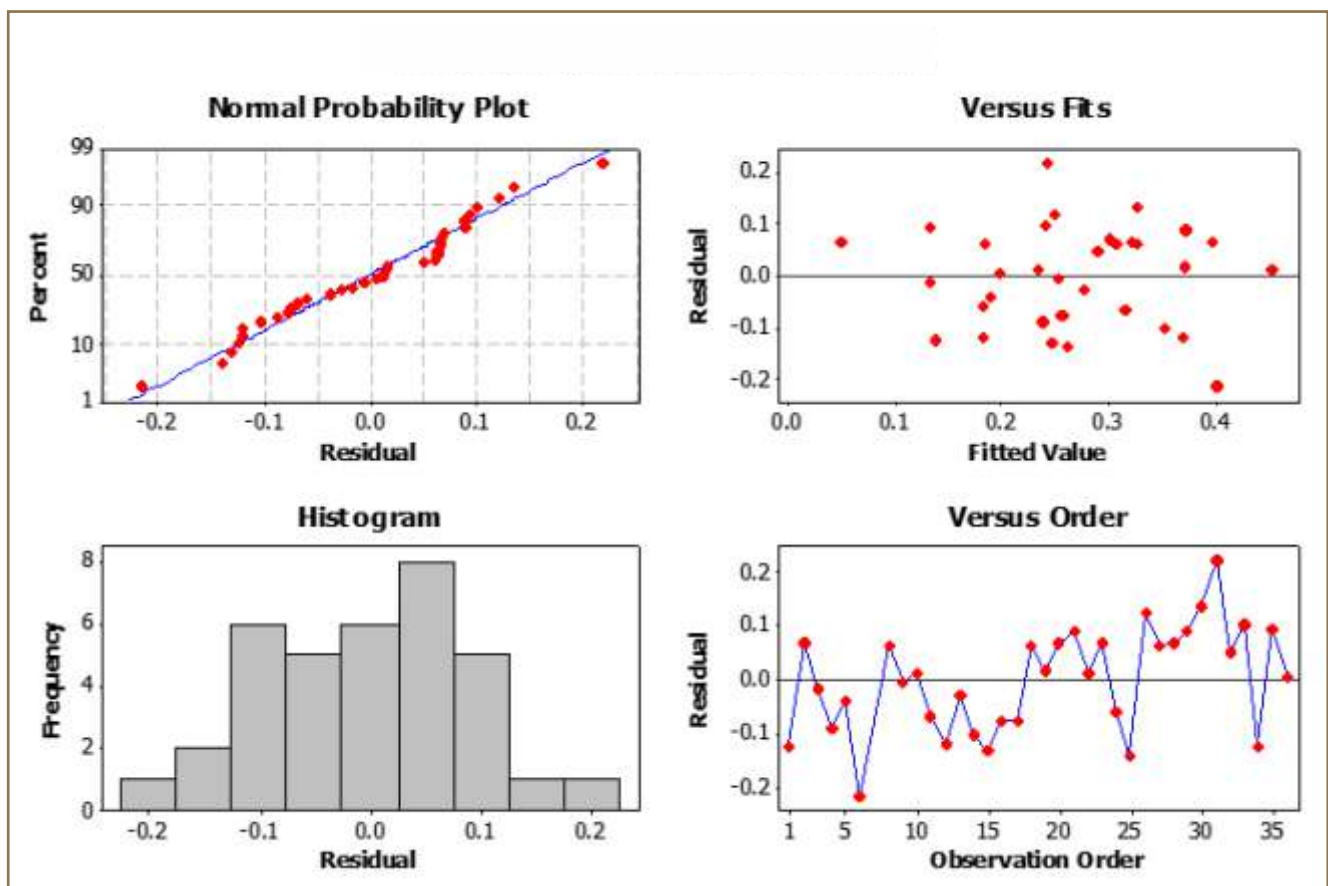
The final form of the equation can be written as follows (Eq. 1) for the prediction of AOD;

$$\text{AOD_log} = a + b (\text{NO}_2\text{-1_A}) + c (\text{Fcount_log}) + d (\text{Bright_sqrt}) + e (1\text{-FRP}) \quad (3.1)$$

Where a is the regression constant and b–e are regression coefficients, as shown in table 3.2. Overall, for the FRM, the coefficient of determination (R²) was 0.87. It should be noted that all the independent variables showed significant p-values in the FRM. From table 3.2, each variable can be interpreted in terms of its coefficient value. Such as it can be said that AOD_log is expected to decrease by a factor of 2.89 1 014 for any increase in NO₂ when all other variables are held constant. Similarly, it can be said that AOD_log is expected to decrease by a factor of 0.032, 4.047 and 13 526 for an increase in Fire counts, fire brightness, and FRP. Another factor which supports the best performance of Eq. 1 is the VIF (table 3.2). VIF indicates the extent to which multicollinearity (correlation among predictors) is present in a regression analysis. Multicollinearity is problematic because it can increase the variance of the regression coefficients (such as given in table 3.2), making them unstable and difficult to interpret. It also measures how much the variance of the estimated regression coefficients are inflated as compared to when the predictor variables are not linearly related.

A VIF value of 1, between 1 and 5, between 5 and 10 and greater than 10 represents that the predictors are not correlated, moderately correlated, highly correlated and severely correlated, respectively. In our model (Eq. 3.1) for the prediction AOD_{log}, there is no multicollinearity in the variables and all can significantly estimate the AOD_{log}. The VIF in this study has been ranged between 1.096 to 1.763 indicating that VIF is not a problem in this model. Compatibility and strength of the proposed model are also evident from the following graphs.

Studies have suggested that for a reliable model Normal Probability Plot should be along the diagonal, Residual versus Fitted Values should be spread majorly across the plot region, Histogram should predominantly follow the normal distribution and magnitude of the residuals should be minimum which in this case is between ± 0.2 . Therefore, the model has the strength of predicting the SMOG with negligible error. Model confidently suggests that SMOG events during the study period have occurred due to extensive fire events in Punjab (Pakistan and Indian).



3.29. Residual plot for the numerical model

SECTION IV

SECTORAL EMISSION INVENTORY OF AIR POLLUTANTS IN PUNJAB

Key messages

1 Sectoral emission inventory of Punjab shows that the major portion of total air pollutant emissions are coming from the transport sector which holds 43% share, followed by Industrial sector which has 25% share and agriculture with 20% share.

2 The contribution of Agriculture sector (crop residue burning) is significant to the seasonal smog phenomenon in Punjab, although it is the third sector by emissions following transport and industrial sector.

SECTION IV

Sectoral emission inventory of air pollutants in Punjab

4.1 Fuel combustion – power, industry, and transport

4.1.1 Fuel combustion

In order to meet the objective of estimating major air pollutant emissions in Punjab, district-wise disaggregated fossil fuel consumption activity data for three energy sectors (power, industry, and transport) was required. The data was needed for the period 2008 to 2017 (10 years). However, due to the unavailability of district-wise fossil fuel consumption activity data in Punjab, activity data on total oil, gas, and coal consumption in all the three sectors in whole Punjab for selected time series has been utilized as it was available from the national statistics – Pakistan Energy Year Book (PEYB), published by Hydrocarbon Development Institute of Pakistan (HDIP) yearly.

In the case of transport sector (road transport) in Punjab, data on oil consumption for both the fuels (diesel and gasoline) was required as emission factors, this data was available for both fuels. However, for the reason, that of unavailability of fuel wise data, an average of both emission factors was taken and used to multiply with total oil consumption in Punjab's road transport to estimate air pollutant emissions. The data on natural gas consumption as Compressed Natural Gas (CNG) in the transport sector is separately available and taken from PEYB for the years 2008–2017. For power and industry sectors, total oil consumption is used as available.

Furthermore, province-wise coal consumption data in the power and industry sector of Punjab was not available from PEYB. The number available is for whole Pakistan. For that reason, the coal consumption data in Punjab is estimated from national level data. As coal is mainly used as fuel in cement and brick kiln industries, a total number of brick kilns and cement plants in Punjab were investigated and compared to a total number of these in Pakistan and then multiplied that fraction with a total consumption of coal by sector to get the sector-province wise coal consumption in Punjab.

4.1.2 Selection of methodology and emission factors

The methodology for calculating air pollutant emissions from fossil fuel combustion is well recognized by the Intergovernmental Panel on Climate Change (IPCC). The IPCC established methodology has been used for the emissions estimation of air pollutants from various sectors.

The methodological approaches by the IPCC are classified into three different tiers depending upon the quantity of information available or required, and degree of analytical complexity.

In this study, Tier 1 approach of IPCC methodology is employed for estimating five emissions of five major air pollutants types (NO_x , CO, NMVOCs, SO_x , & $\text{PM}_{2.5}$) from power, industry and transport sectors (IPCC, 2006; IPCC, 1997; Houghton, 1997). Tier 1 uses the country-specific activity data and the default emission factors established by the IPCC. The purpose of using Tier 1 method lies in the limitation of country-specific data availability of fuel and technology. Tier 1 methodology is intended to be the least complex and ignores some dependent factor such as combustion, control technology, fuel type, operating conditions, equipment's age, and maintenance. On the other hand, Tier 2 employs country-specific emission factors instead of Tier 1 defaults and required highly stratified activity data to correspond with country-specific emission factors for a specific region. Similarly, Tier 3 method uses detailed emission models to address national circumstances. In general, these methods provide greater certainty in estimates as compared to lower tiers though at the cost of detailed information and measurement complexity. Consequently, Tier 2 and Tier 3 methodologies at present cannot be used for these estimates due to unavailability of country or region defined emission factors, absence of air pollutant inventories and models measurement systems as per national conditions repeated over time, and driven by high-resolution activity data and disaggregated at the subnational level (IPCC, 2006; IPCC, 1997; Houghton, 1997).

In general:

- For the power industry, emissions of NO_x > CO > NMVOCs have been investigated
- For the manufacturing industry, emissions of NO_x > CO > NMVOCs have been investigated
- For the transport sector, emissions of CO > NO_x > NMVOCs have been investigated

4.1.3 Crop residue burning – rice

Activity data needs and availability

Crop residue burning contributes significantly towards the emissions of air pollutants mainly – NO_x and CO and is a common practice in the developing countries. In Southeast Asia, rice straw burning is the most common practice which constitutes 31% of agriculture waste. Crop residue burning is a global phenomenon and about 40% of the residues produced in developing countries are burned in-field, however, the percentage for developed nations is lower. It has been estimated that approximately 425 TG dry matter agriculture waste is burned in fields in the developing world which is about one-tenth as much is burned in the developed countries (IPCC, 1997).

In Pakistan as well as in India, large quantities of crop residues including cereal straws, rice stubbles, woody stalk, and sugarcane tops are generated every year, and to clear

the field for the next cropping cycle, in-situ burning of residue is the widely adapted disposal method (Jain *et al.*, 2014). The study was designed to estimate the air pollutant emissions of NO_x and CO from burning of rice residue in Punjab particularly in eleven districts of the study area. The area under study covered the following eleven districts as well as the whole of Punjab.

1. Gujranwala
2. Gujrat
3. Hafizabad
4. Mandi Bahaudin
5. Narowal
6. Sialkot
7. Kasur
8. Lahore
9. Nankana Sahib
10. Sheikhupura
11. Faisalabad

4.1. District wise rice production (000 tonnes) of Punjab (2008–2017)

Districts	2008	2009	2010	2011	2012	2013	2014	2015	2016	2017
Gujranwala	487.2	494.9	501.1	507.30	545.4	578.36	493.9	472	480	496
Gujrat	82.3	109.3	86.45	63.6	55.5	63.3	63.3	71	52	14
Hazabad	223.3	245.9	254.3	262.7	251.6	271.89	271.3	237	279	363
Mandibahaudin	160.1	163.1	150.85	138.6	148.8	157.15	158.6	127	115	91
Narowal	154.6	143	150.35	157.7	146.1	149.12	134	123	115	99
Sialkot	350.8	341	326.6	312.2	290.4	302.29	261	248	238	218
Kasur	144.1	179.8	163.25	146.7	146.8	160.22	152.7	164	143	101
Lahore	62.9	83.4	71.4	59.4	55.9	59.2	64.9	79	66	40
Nankana Sahib	179.6	210.6	191.65	172.7	175	186.42	208.3	222	216	204
Sheikhupura	299.9	310	324	338	368	382.15	351.7	357	333	285
Faisalabad	42.8	61.8	54.35	46.9	46.1	50.37	52.7	58	53	43
Total	2187.6	2342.8	2274.3	2205.8	2229.6	2360.5	2212.4	2158	2090	1954

4.1.4 Selection of methodology and emission factors

The methodology for calculating air pollutant emissions from crop residue burning is well recognized by the Intergovernmental Panel on Climate Change (IPCC). The IPCC established methodology has been used for the emissions estimation of following air pollutants – CO and NO_x resulting from burning of rice residue in the fields. The methodological approaches by the IPCC are classified into three different tiers depending upon the quantity of information available or required and degree of analytical complexity (IPCC, 2006; IPCC, 1997; Houghton, 1997).

District wise crop production data of rice were obtained from Bureau of Statistics Punjab (2011–2016), Pakistan Bureau of Statistics (2008–09), and 2017 Statistical Pocket Book of Punjab (BOS, 2017; BOS, 2016; BOS, 2013; BOS, 2012; BOS, 2011). The production data for the years 2010 and 2017 was interpolated and extrapolated respectively owing to the lack of reported statistics for these years. The production data of crop for the given timeline (2008–2017) are presented in Table 6 4.1 respectively. The ratio of residue to crop yield, a fraction of residue burned, and dry matter content of residue was taken from the FAO survey results. The fraction oxidized in burning and carbon content of the residue was taken from default values of IPCC.

4.2 RESULTS

4.2.1 Sectoral (power, industrial, and transport sectors) overview

Punjab province, being the most populous and economic centre has a major share in the consumption of all energy products with 62% of electricity, 63% of POL products, 62% of liquefied petroleum products and 38% of Natural gas. Petroleum demand of the power sector in Punjab is about 36% of the total demand in the province, which comprises 57% of the total power sector's demand in the country (Policy Paper, 2017).

The energy mix of the country comprises of thermal, hydel and nuclear power plants, in which 67.82% of the electricity is generated through oil and gas burning in thermal plants, hydel power plants generate 28.40%, while 3.78% comes from nuclear and renewable sources. The total installed capacity of grid power supply is 23 644 MW as per indicated

by the reported data (Abas *et al.*, 2017). Fuel consumption breaks down in power plants indicate oil and natural gas constitute 29% and 35.20% of share respectively, while coal utilization is negligible 0.10% of the total fuel mix (HDIP, 2013). The fuel consumption data in Punjab for the year 2017 indicates consumption of 145 088.11 TJ of natural gas and 192 014.55 TJ of oil in power sector. Owing to heavy reliance on thermal power plants, the power sector is one of the major contributors to air pollutant emissions. The table 6 below presents the total number of thermal power plants located in the 11 – districts (study area) of Punjab along with the type of fuel used and installed capacity (HDIP, 2017). The total number of thermal power plants in Punjab are 26, out of which 15 exist in the study area districts. These thermal power plants represent 58% of the total thermal power plants located in Punjab.

The manufacturing industry in Pakistan is the third largest sector of the economy and accounts for 13.56% of the GDP. Manufacturing industry constitutes share in fossil fuel consumption after the power sector (MoF, 2018). The analysis of the sectoral share of fuel consumption in Punjab indicates that the highest share in consumption of gas remained in power sector (27.5 %) followed by industry which stands at 22.6 % and 9.5% (54 312.93 TJ) of the total oil in the year 2017. While the manufacturing industry is the major consumer of coal usually in brick kilns and cement facilities.

Industrial facilities, particularly those consuming fossil fuel (cement, brick kiln, fertilizer, and general industries which may include paper, food, beverages, tobacco, glass, leather, textile etc.) in Punjab, are significant sources of air pollutant emissions. Hence, emissions from large-scale manufacturing facilities as cement, fertilizer, brick kilns and other industries are of great concern as a major contributor to air pollution. As per the census of manufacturing industries, there are 6 417 manufacturing industrial units in Pakistan and most of them are located in industrial clusters of Punjab and Sindh having 56% and 28%, share in total respectively. The remaining 16% of industries lies in KPK, Baluchistan, and Islamabad.

Furthermore, the total number of manufacturing industries in study area districts as per census is 2 486 which is 69% of total manufacturing industries in Punjab (PBS, 2013).

The total number of brick kilns in Punjab as per census is 10 347 while in study area districts the number is 3 690 which considers 36% share in total. A total number of manufacturing industries including brick kiln in Punjab are 13 937, while in study area districts the number is 6 176 which is 44% of total manufacturing industries in Punjab (PBC, 2016).

The cement industry plays a vital role in the country's economy with 19 cement units in north and 5 in the south region, it has a significant share in the country's GDP. The annual production capacity of cement industry stood 44.8 million tons in the year 2013. The production capacity has increased two-fold over the last decade to 45.6 MT per annum (Ali et al., 2015).

Top five cement manufacturers (Lucky, Bestway, D.G. Khan, Fauji & Maple Leaf) comprised 58% of total installed capacity and has a market share of over 55%, all the cement units are located in Punjab (JCR—VIS 2016a). The fuel consumption statistics show that coal constitutes a major share in the cement manufacturing process and accounts for 131 273.37 TJ in FY2017 in Punjab (HDIP, 2017).

4.2. List of Thermal Plants Located in 11-districts of Punjab Province

	Name	Location	Fuel used	Capacity (MW)
1	Atlas Power	Shekhupura, Punjab	Furnace Oil	219
2	CCPP Nandipur	Gujranwala, Punjab	Furnace oil+Gas	425
3	GTPS Faisalabad	Faisalabad, Punjab	Gas	244
4	Halmore Power	Shekhupura, Punjab	Gas	225
5	Japan Power	Raiwind, Punjab	Furnace Oil	135
6	Kohinoor Energy	Lahore, Punjab	Furnace Oil	131
7	Liberty Power Tech	Faisalabad, Punjab	Furnace Oil	202
8	Nishat Chunian Power	Kasur, Punjab	Furnace Oil	200
9	Nishat Power	Lahore, Punjab	Furnace Oil	200
10	Orient Power	Kasur, Punjab	Natural Gas	229
11	Quaid—e—Azam Thermal Power Plant	Lahore, Punjab	Natural Gas	1180
12	Saba Power	Shekhupura, Punjab	Furnace Oil	125
13	Southern Electric	Raiwind, Punjab	Furnace Oil	136
14	SPS Faisalabad	Faisalabad, Punjab	Furnace Oil+Gas	132
15	Sapphire Electric	Shekhupura, Punjab	Gas	102

Brick kilns are another stationary source of air pollutants, use of low-grade coal and other fuel mixes like old rubber tires, lignite coal, rice husk agricultural residues, plastics, and different industrial waste ultimately causing air pollutant emission and black dense smoke. Brick kilns industry being the major users of coal after the cement sector consumed 41% (2 million) of the total coal consumed and 1.6 TG per annum (SAARC, 2012). In Pakistan, 59 billion bricks are produced yearly and there are around 18 000 units of brick kiln in the country out of which 10 347 are located in Punjab (PBC, 2016).

Fertilizer production in Pakistan stands at 5.4 TG in 2012, which includes all type of fertilizer produced i.e. urea, super [phosphate, ammonium nitrate, and nitro phosphate] (MoF, 2016). Natural gas is the key fuel used as feedstock and fuel in the fertilizer manufacturing. The consumption of gas was 141 120.37 TJ for the year 2017. Fertilizer demand met through local as well as foreign production, with domestic production accounting for 7.6 million tons while 1.8 million tones were imported during FY15 (JCR-VIS 2016b).

Road transport has played a substantial role in the country's economy accounting for almost 13.27% in the GDP, 17% of Gross Capital Formation, 6% of employment and 15% of the Federal Public Sector Development Programme (PSDP). The road network carries over 96% of inland freight (273 MT per year) and 92% of passenger freight and has been growing at an average rate of 14.1% during 1985–2005 (MoF, 2017). On the other hand, railway freight traffic has declined by 48% during this period, consequently, all the growth was handled by road sector (ADB, 2006). Due to the dependence of transport sector on carbon-intensive fuel, this sector accounts for its highest contribution in air pollutant emissions out of which 67% are attributed to gas and diesel oil (Sanchez-Triana et al., 2014). The transport sector is one of the major commercial energy consumers of the country accounts for 38% of the total energy consumption (48MTOE). 90% of the fuel used in this sector is oil – (diesel and gasoline) representing 57% share of the total petroleum products, while compressed natural gas (CNG) and electricity meet the remaining requirement of 22%. The natural gas consumption, especially in the form of CNG in road sector, has experienced a significant increase of 84% from 1998 to 2007, although its share in total consumption of gas has increased from 0.6% to 9% in the last ten years (Sanchez-Triana et al., 2014; HDIP 2013).

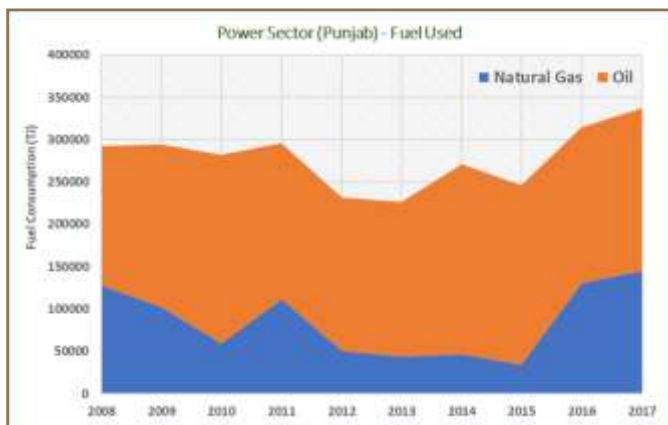
The fuel consumption data of transport sector shows a tremendous increase with 15 351.14 TJ of natural gas and 369 935.52 TJ of oil in 2017, while the consumption data of 2008 stands at 42 088.66 TJ of natural gas and 204 381.5 TJ of oil-based fuel (HDIP, 2017; HDIP, 2008). As per Punjab Statistical Pocket Book, in 2015, a total number of registered vehicles in Punjab were 14 532 353 while in study area districts the number is 7 428 114 which comes out to be 51% of total road vehicles in Punjab (PSPB, 2017).

Air pollutants depend upon several factors including the type of fuel used, vehicle type and size age and accumulated mileage of the vehicle, weather condition and maintenance of vehicles. The amount of emission is directly linked to the amount and type of fuel consumed. The number of vehicles increased from 2.71 million to 11.77 million during the last 20 years. Road transport is dominated by two-wheelers and cars with 82% of the total share (Mir et al., 2017). Total fossil fuel consumption of the transport sector from all fuel types as petrol, diesel, fuel oil, kerosene, liquefied petroleum gas (LPG), is estimated to be 10.06 Mtoe for the year 2012. The breakdown statistics of fuels represent 50% of diesel, 23% gasoline, 22% CNG and 5% of LPG, kerosene, and fuel oil (HDIP, 2012).

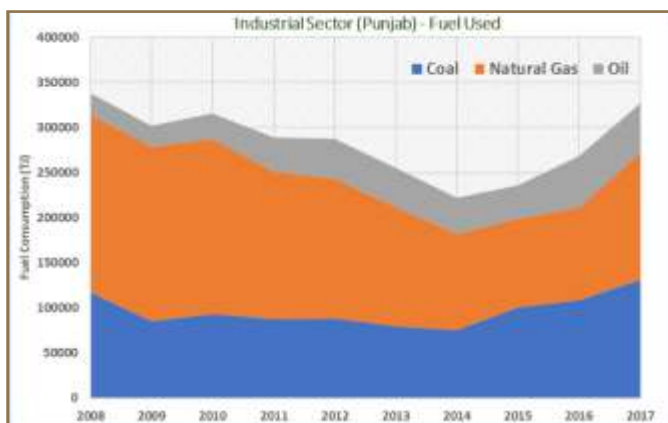
4.2.2 Sectoral (power, industrial, and transport sectors) fuel used

The fuel consumption trend over the years (2008–2017) in power, industrial and transport sector illustrates that the transport sector has remained the biggest oil consumer followed by power sector (Figure 4.1–4.3) (HDIP, 2008–2017). Also, the sector-wise share indicates that for the power sector the irregular trend can be seen over the ten years (Figure 4.1).

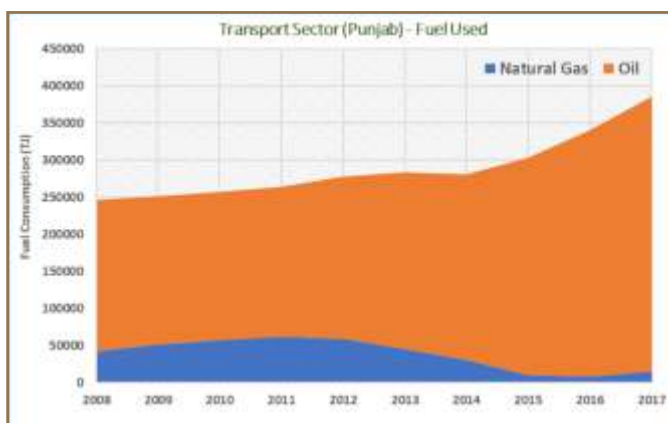
The industrial sector of Punjab consumed coal, natural gas, and oil for energy generation. The graph (Figure 4.2) indicate that the natural gas sector has shown a tremendous decrease in the last ten years in Punjab and make up the largest fuel consumed by the industrial sector followed by coal. The fuel consumption statistics show 117 729.61 TJ of coal consumption, 196 197.20 TJ of natural gas and 24 387.09 TJ of oil for the year 2008 which increased tremendously over the



4.1. Fuel consumption trend of power sector – Punjab (2008–2017)



4.2. Fuel consumption trend of industrial sector – Punjab



4.3. Fuel consumption trend of transport sector – Punjab

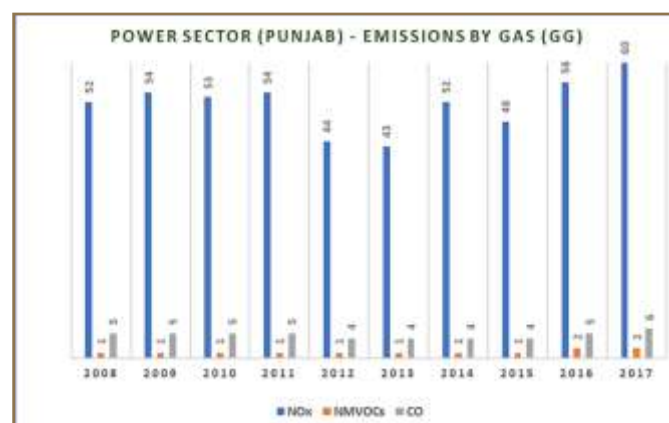
years and reached up to 131 273.37 TJ of coal, 141 120.37 TJ of natural gas, while oil consumption reached to 54 312.93 TJ in the year 2017. The trend also illustrates the minimal share of oil-based fuel in the industrial sector. The dramatic change in natural gas consumption can be viewed in the context of a decrease in gas supply owing to gas load shedding in the year 2011 to 2014, and the consumption increases onward with the imports of liquefied natural gas (LNG).

The consumption of transport fuel has increased gradually over the last ten years (2008–2017). Figure 4.3 illustrates the fuel consumption trend of the transport sector in Punjab indicating the sector which has been dominated by oil over the past ten years. Gas consumption as transport fuel increased significantly from 2008 to 2013 by virtue of friendly government policies. Owing to the gas shortage problem and shutting down of CNG stations after 2012 resulted in the fall of gas consumption trend.

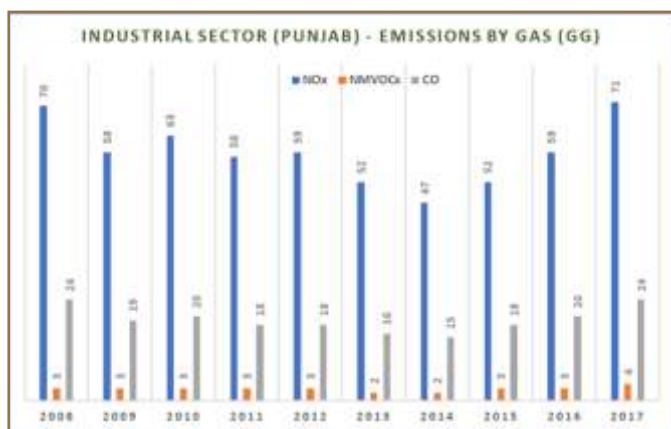
4.2.3 Disaggregation of emissions by gas (NO_x , NMVOCs, and CO)

The increased use of fossil fuel with the advent of industrial revolution and urbanization, the concentration of air pollutant emissions (NO_x , SO_x , CO, NMVOCs, $\text{PM}_{2.5}$) is rapidly growing. Punjab, being the most populated province and the economic hub of the country, is a major consumer of all energy products.

Owing to heavy reliance on oil and gas based thermal power plants, the power sector of Punjab emits a significant amount of air pollutant including NO_x , NMVOCs, CO. The graph (Figure 4.4) shows the estimated contribution of the power sector in air pollutant emissions, which clearly demonstrate the significant increase and higher share of NO_x emissions from power plants of Punjab (2008–2017). Due to the decrease in consumption of fuels from 2012–2013, the graph shows a decrease in NO_x emissions for the corresponding years. CO and NMVOCs emissions from the power sector remain almost flat over the past ten years. The estimated emissions solely from the power sector are 60 GG, 2GG and 6 GG of NO_x , NMVOCs and CO, respectively in 2017.



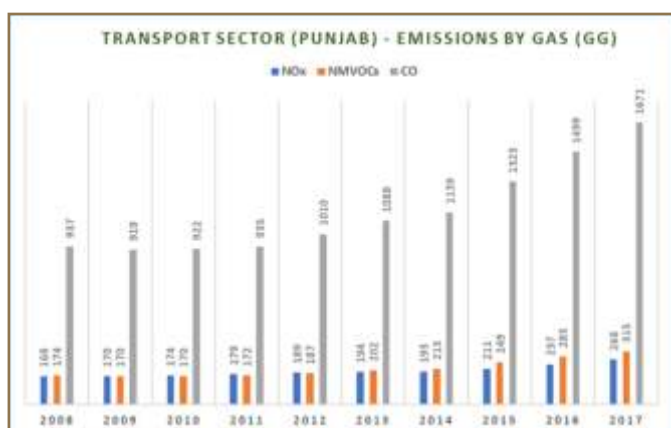
4.4. Power sector emissions (NO_x , NMVOCs, CO) during 2008–2017 Punjab



4.5. Industrial sector emissions (NO_x, NMVOCs, CO) during 2008-2017 – Punjab

The trend demonstrates the highest share of NO_x emissions from the industrial sector, and it corresponds to the fuel consumption trend over the years (Figure 4.5). CO makes up the second highest share of total emissions from the industrial sector, and the CO emissions increased gradually from 2014. In 2017, NO_x emissions from the industrial sector are estimated at 71 GG, CO at 24 GG and tiny share of NMVOCs (4 GG).

Road transport released approximately 1 671 GG of CO which is 74% of the total emissions from the transport sector in 2017, whereas NO_x and NMVOCs were 268 GG, and 315 GG respectively. The emission trend for the years 2008-2017 shows that share of CO emissions is increasing significantly over the last seven years owing to an increase in fuel consumption by the transport sector (Figure 4.6). The trend depicts the highest share of this sector in total air pollutants.



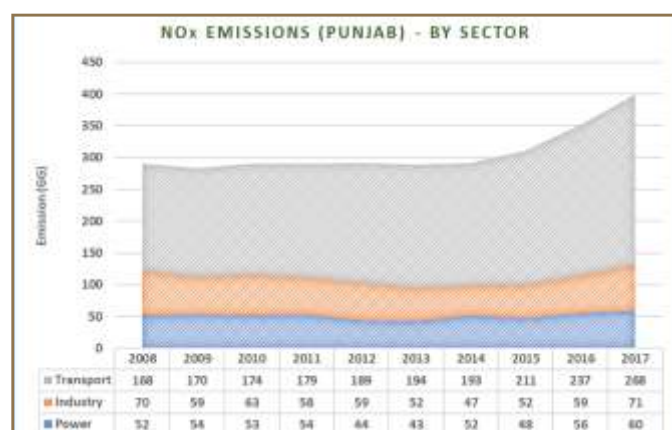
4.6. Transport sector emissions (NO_x, NMVOCs, CO) during 2008-2017 – Punjab

4.2.4 Disaggregation of emissions by sector (NO_x, NMVOCs, and CO)

The sectoral distribution and average share (10 years) of emissions of ozone precursors (NO_x, NMVOCs and CO) in Punjab are shown in figure 4.7, 4.8, 4.9, 4.10, 4.11, and 4.12 respectively. The graphs indicate the largest share of the transport sector in these pollutant emissions with an average share of 64% in NO_x and 98% share in CO and NMVOCs in total emissions from all three sectors. Power and industry contribute 17%, and 19% respectively in the NO_x emissions and holds an insignificant share of NMVOCs and CO emissions as compared to the transport sector.

In 2017, the total NO_x emissions from all the three sectors were about 399 GG, CO 1,701 GG and NMVOCs were 321 GG, this trend highlights the gradual increase in emissions over the past ten years.

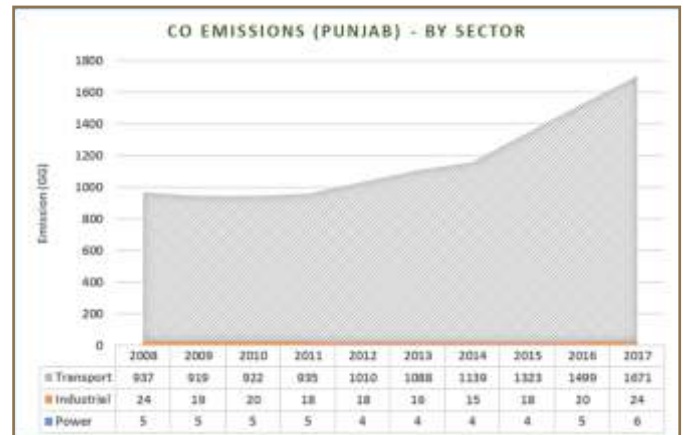
CO emissions are highest from the transport sector accounting for about 98% of the emission followed by the industrial sector. The significant increase in CO emissions from the transport sector in Punjab is owing to the increase in the number of vehicles in the region in the past ten years.



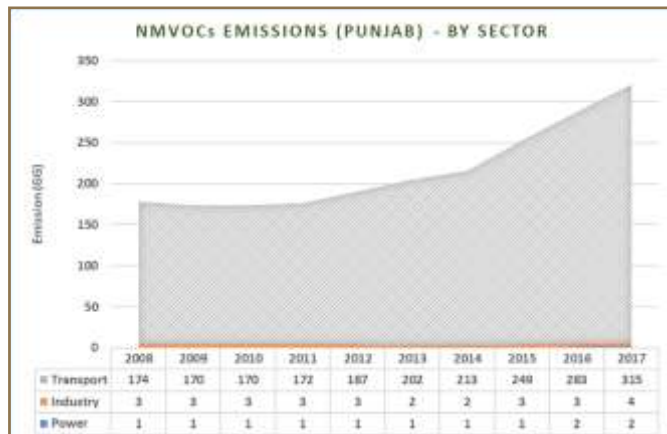
4.7. Transport sector emissions (NO_x, NMVOCs, CO) during 2008-2017 – Punjab



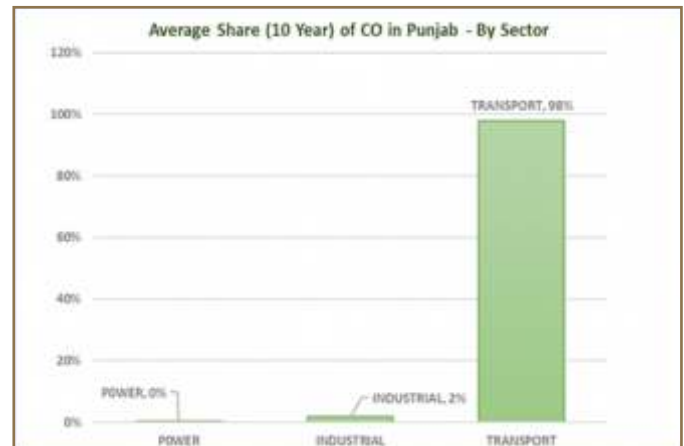
4.8. Average share (10 years) of NO_x in Punjab by sector



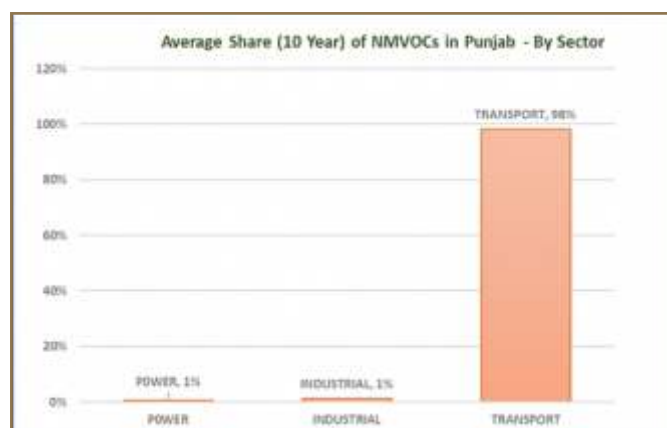
4.11. CO Emissions in Punjab — By sector



4.9. NMVOCs, emissions Punjab — By sector



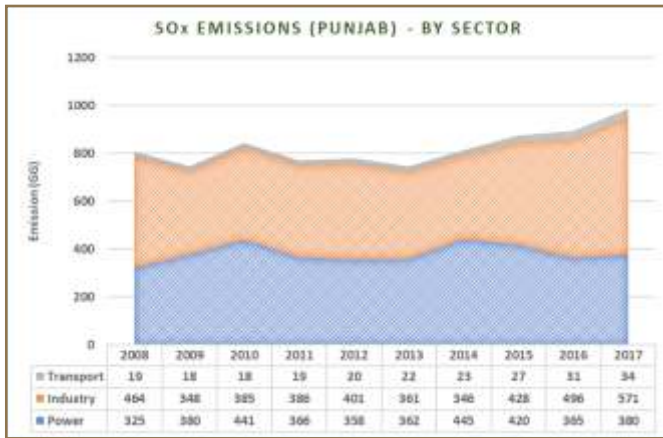
4.12. Average share (10 years) of CO in Punjab by sector



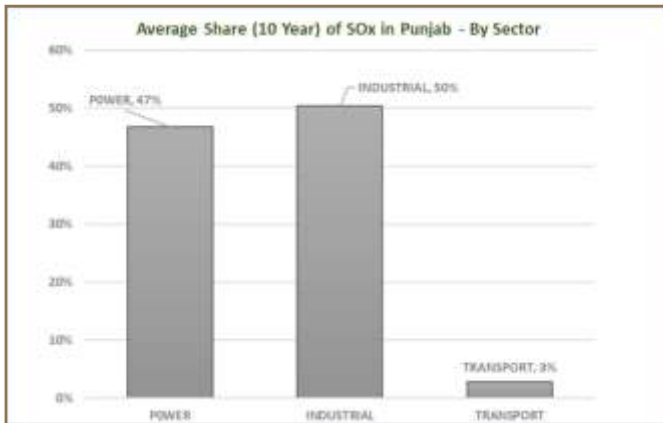
4.10. Average share (10 years) of NMVOCs in Punjab by sector

4.2.5 Sector wise emissions of SO_x

The SO_x emissions from three sectors (Power, Industry, and Transport) in Punjab has increased tremendously over the last ten years for all major sectors. This increase is attributed to the increase in fuel consumption. 80% of total SO_x emission and three-quarter of this is arising from coal, which contains high sulphur content. In 2017, the total SO_x emission in Punjab from the power sector was 380 Gg, the industrial sector emitted 571 GG, while the transport sector accounted for 34 GG (Figure 4.13). As shown in the figure 4.14, an average share of industrial sector in SO_x emission is the highest 50%, followed by the power which accounts for 47% of the total SO_x emissions in Punjab from three sectors.



4.13. SO_x Emissions in Punjab by sector



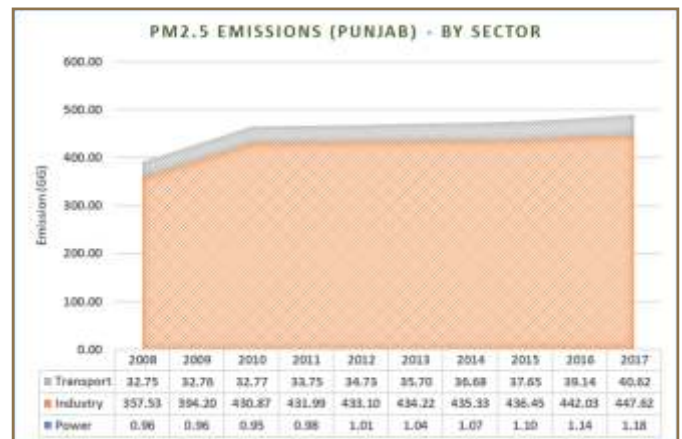
4.14. Average share (10 years) of SO_x Emissions in Punjab by sector

4.2.6 By sector emissions of PM_{2.5}

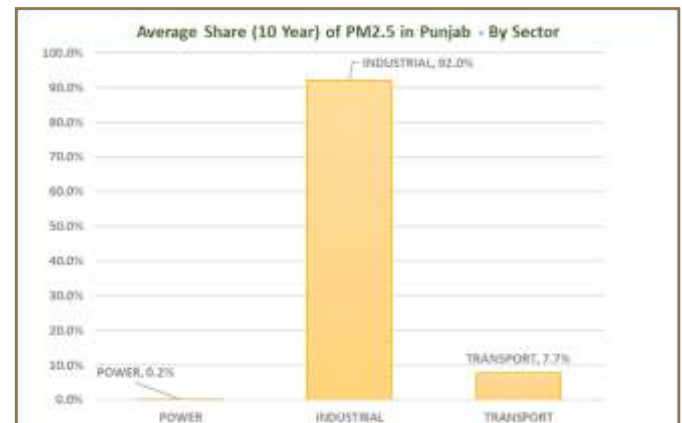
Emissions (in Gg) and ambient concentration (in $\mu\text{g per m}^3$) of PM_{2.5} over Punjab has been assessed through GAINS model based on *Mir et al. (2016)*.

In this study, air quality scenarios were analyzed using two models i.e. Pak-IEM and GAINS. Pak-IEM is an energy model for projection of energy demands in a country while GAINS is an environment model for projections of air pollutant and GHG emissions. The model gave projections of PM_{2.5} till 2030 with five years' interval having the base year 2007. The model takes into account the whole Pakistan as well as regions and all sectors. Since our study is focused on Punjab province and for four sectors, therefore the model is set again to run for the Punjab region. The estimates of PM_{2.5} from 2007 to 2030 with five years' interval were then interpolated to get the desired yearly time series from 2008 to 2017.

Figure 4.15 indicates by sector quantification of PM_{2.5} emissions in Punjab for the time series 2008–2017. On the other hand, Figure 4.16 shows the average 10 years share of PM_{2.5} emissions in Punjab. It is obvious from the chart the significant sector contributing to PM_{2.5} emissions in Punjab is industrial which hold 92% contribution.

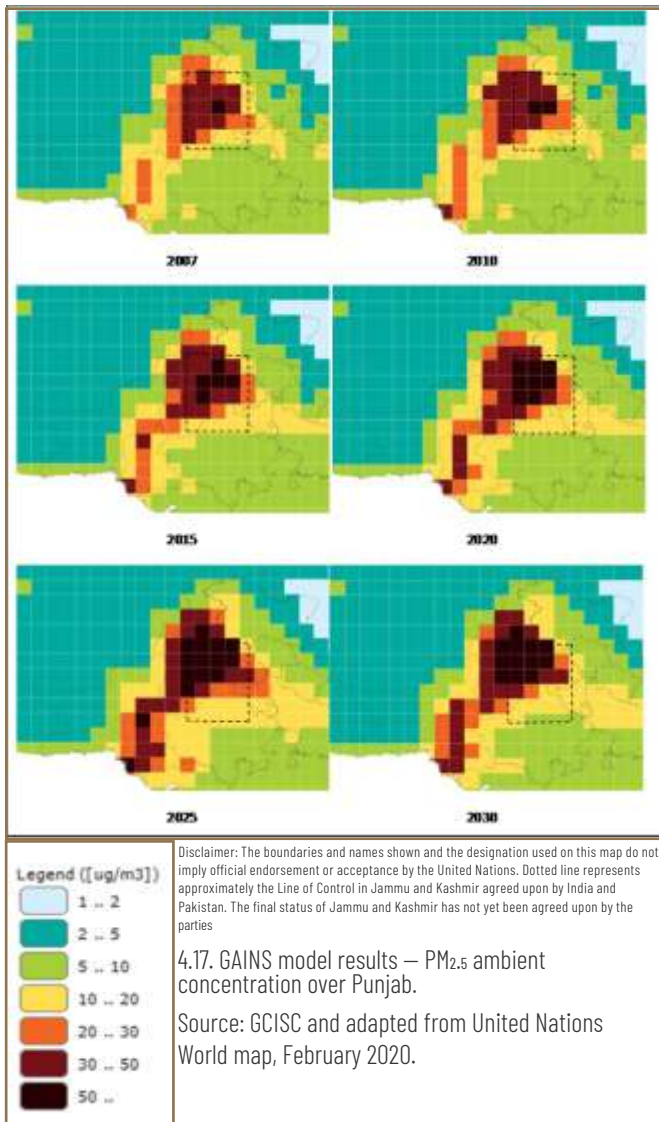


4.15. PM_{2.5} emissions in Punjab — By sector



4.16. Average share (10 years) of PM_{2.5} in Punjab by sector

Figure 4.17 shows the modelled results of ambient PM_{2.5} concentrations over Pakistan from 2007 to 2030 with five years' interval. It is clear from the maps that the PM_{2.5} concentrations are getting intense over time particularly on the rice-wheat belt districts of Punjab which are under consideration in this study. The concentration of PM_{2.5} above 50 $\mu\text{g per m}^3$ is shown in almost all study districts and it is projected to increase 8 times in 2020 and 12 times in 2030 with respect to the base year 2007.

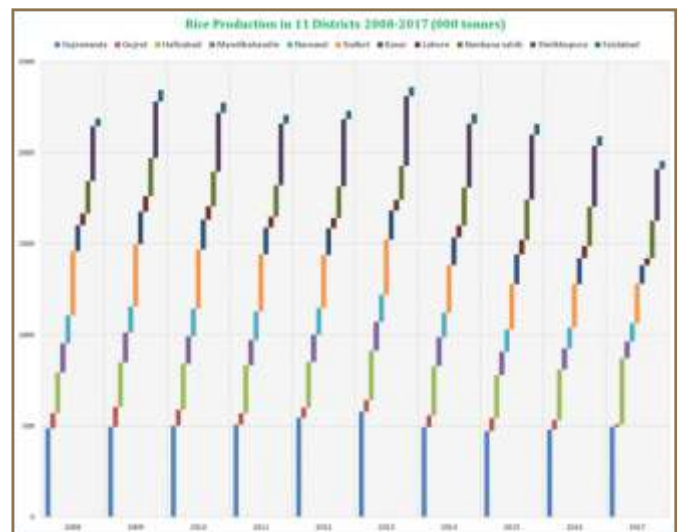


4.2.7 Emissions from crop residue burning sector

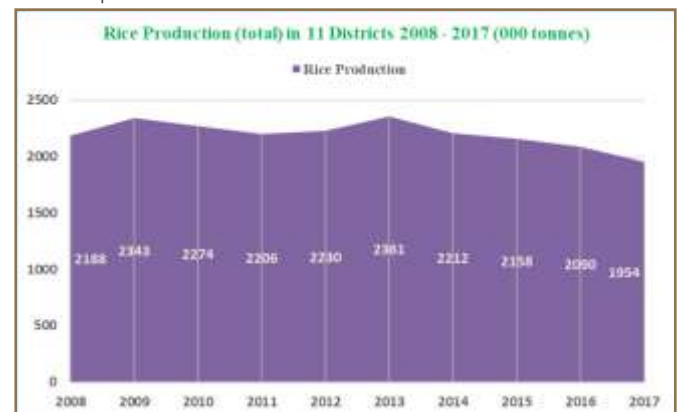
Open field burning of rice stubble results in the emission of many harmful air pollutants, like carbon monoxide, NO_x , SO_x , along with particulate matter and hydrocarbons. Emissions generated from crop residue burning of rice are presented in the figures indicate large variations across 11-districts of Punjab depending upon the crop productivity. In the present estimates, total rice production of 1 954 thousand tonnes led to the total emissions of 66.248 GG of CO and 2.633 GG of NO_x for the year 2017 in 11-districts of Punjab. Figure 4.18 and 4.19 provides details of total rice contribution and by each district in Punjab pool over the last ten years. Rice production statistics depicted in the figures indicates highest production for the year 2013 (2 361 thousand tonnes) with Gujranwala ranking first with 578.4 thousand tonnes of production, followed by Sheikhupura with the production of 382.2 thousand tonnes.

CO and NO_x emissions from rice residue burning in 11-districts are presented in figure 4.20, the total emissions from all districts stand at 66.25 GG of CO and 2.63 GG of NO_x for the year 2017. It can also be depicted here based on rice production graph by districts that the maximum share in 2017 emissions is of rice residue burning in Gujranwala, Sheikhupura, Hafizabad, and Sialkot, with Gujranwala contributing maximum from rice burning.

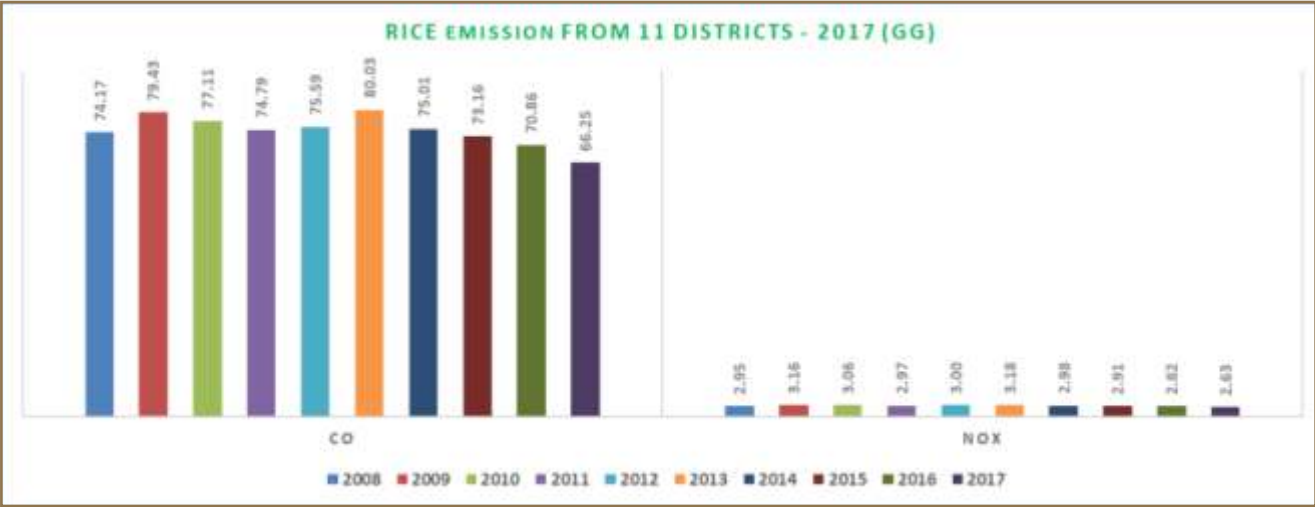
The total production of rice increases substantially from 3 277 thousand tonnes in 2012 to 3 648 thousand tonnes in 2015 (Figure 4.21). During the same period, the area under rice crop increased from 1.71 million hectares in 2012 to 1.87 million hectares in 2015. On an average, the study area (11 districts) share in the total production of rice in Punjab stands at about 64%.



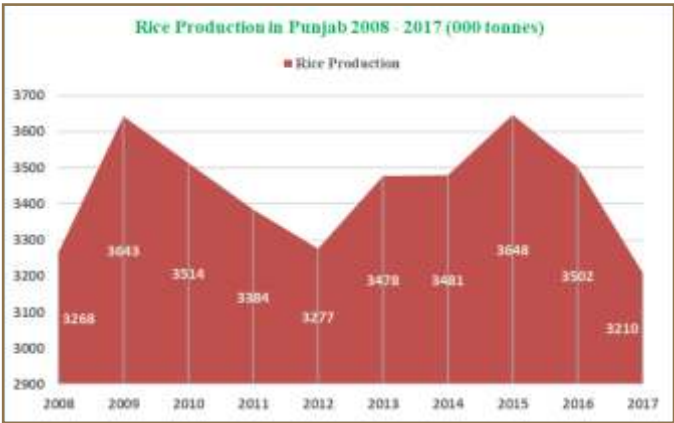
4.18. Rice production in 11 districts from 2008–2017



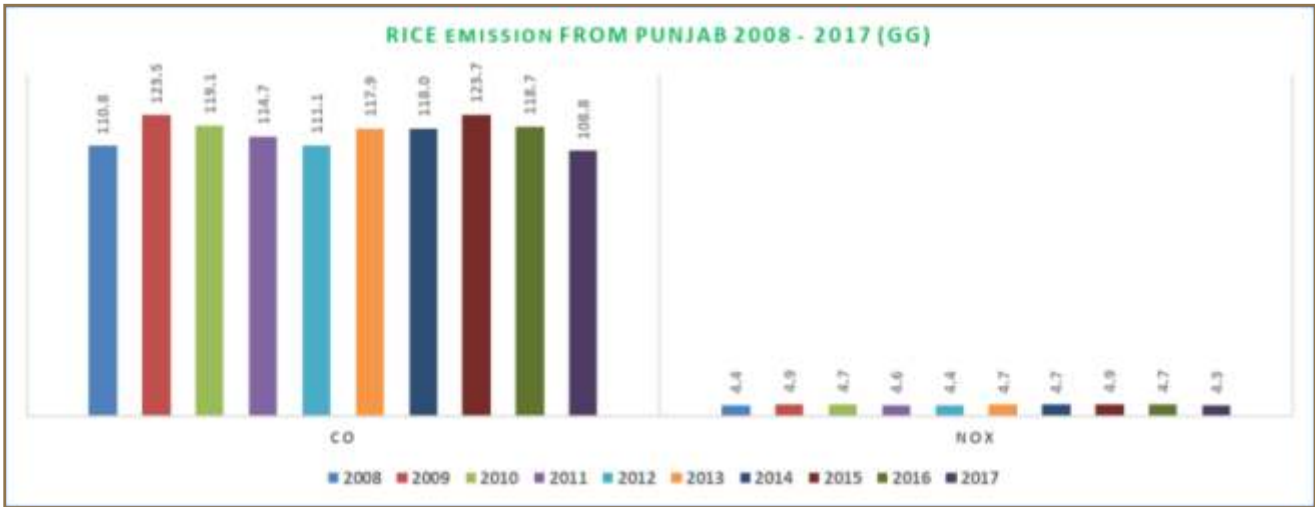
4.19. Total rice production of all 11 districts in Punjab



4.20. Emissions from rice residue burning in 11-districts



4.21. Rice Production (total) in Punjab from 2008–2017



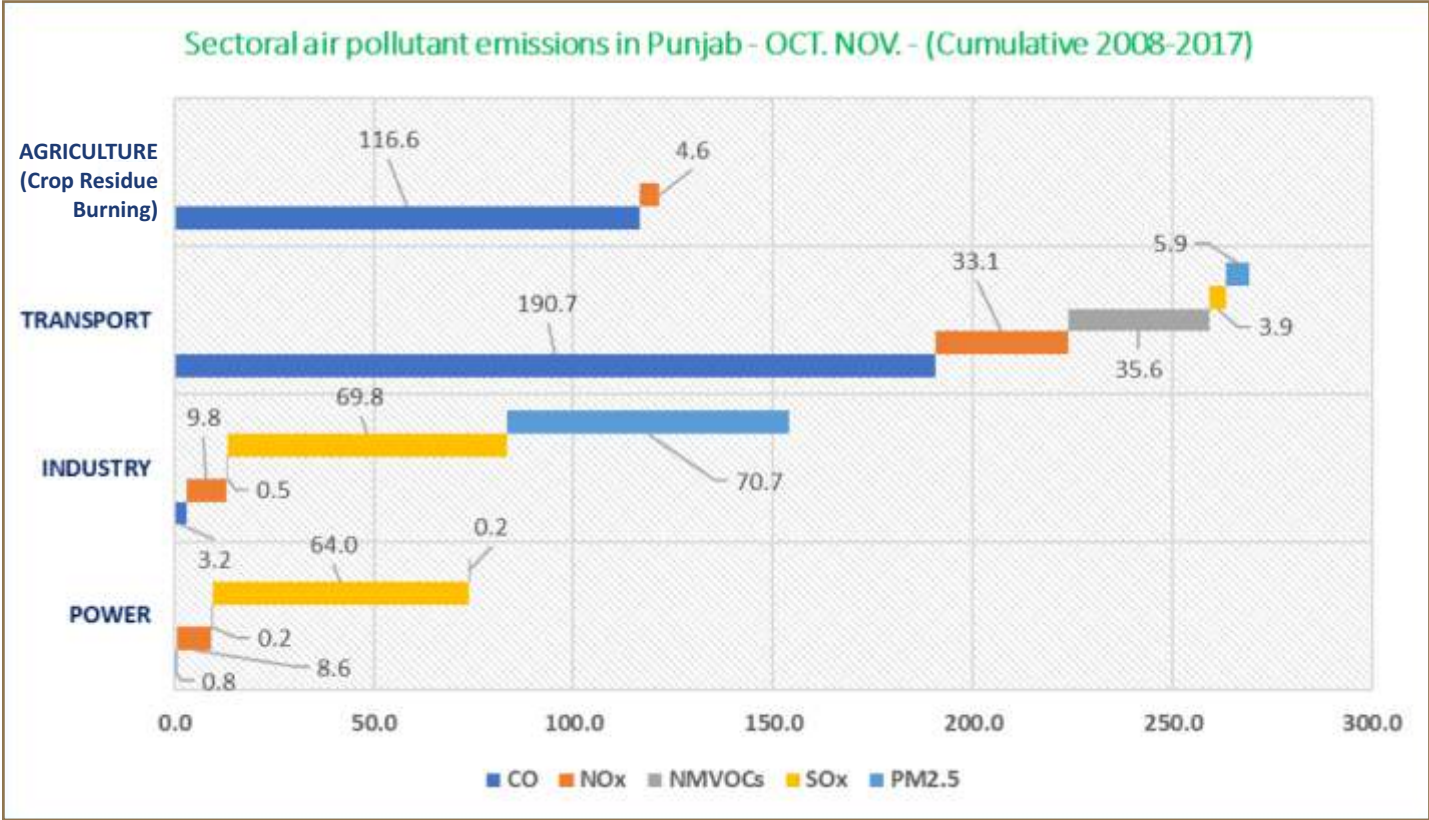
4.22. Emissions (total) from rice residue burning in Punjab from 2008–2017

CO and NO_x emissions from all over Punjab for the years 2008–2017 are presented in figure 22 signifying a subsequent increase in the emissions from 2014 to 2017 accounting 96% of CO and 4% of NO_x. It has been estimated that for the year 2017, the emissions of CO and NO_x was 108.83 GG and 4.325 GG respectively from the field burning of rice straw in Punjab. While the estimated emissions from districts under study are 66.25 GG of CO and 2.63 GG of NO_x, accordingly contributing 61% share of total air pollutant emissions from Punjab.

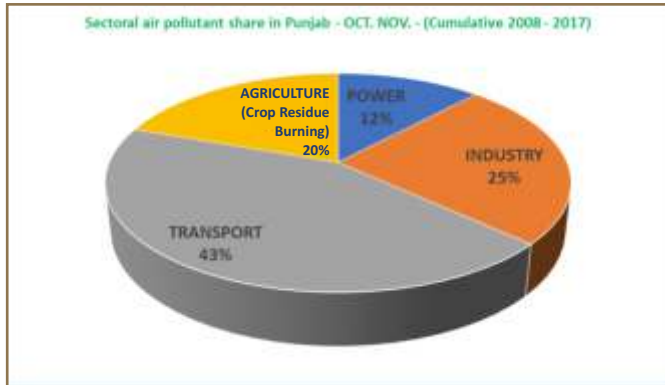
4.3 CONCLUSIONS & RECOMMENDATIONS

Since the burning activity of rice residue occurs in October and November every year, the resultant air pollutant emissions from this burning activity would also be occurring only in these two months. On the other hand, power, industry, and transport runs all over the year, the resultant air pollutant emissions from these sectors would also be occurring during the twelve months. Assuming that energy sector activities operate uniformly in a year, the total emissions are disaggregated into per month emissions. This gives a eelialistic comparison of sectoral air pollutant emissions and share in Punjab as shown in Figure 4.23 and Figure 4.24.

The major portion of total air pollutant emissions are coming from the transport sector (269 GG) and it holds 43% share in all sectors (power, industry, transport, and crop residue burning – CRB). The second key sector responsible for air pollutant emissions in Punjab is industry whose share is 25% and amounts 154 GG. The sector at number three is agriculture (rice residue burning). It accounts for 20% (121 GG) of total air pollutant emissions with respect to other sectors. The emissions from residue burning of other crops have not been estimated due to the fact that since smog usually happens in October and November and these two months only involves burning of rice residue. The last sector is a power which amounts 74 GG and contributes 12% in total emissions. Collectively, it is clear from the figures that the main sectors responsible for air pollutant emissions in Punjab are power, industry, and transport which together hold 80% contribution in air pollutant emissions and aids in the formation of photochemical smog in Punjab. Though the emission contribution of the burning of rice residue is minimal as compared to other sectors but may support significantly the seasonal smog phenomenon in Punjab.



4.23. Sectoral emissions in Punjab (cumulative)



4.24. Sectoral emissions shares in Punjab

Based on the conclusion, the following are some of the key sectoral recommendations with regard to the reduction of air pollutant emissions from fuel combustion process and crop residue burning:

1. SO_x emissions from combustion processes in power stations and industry could be controlled by implementing following five distinguished technical measures (*Cofala and Syri, 1998a*).

- Changes in the energy system leading to lower consumption of sulfur containing fuels (by energy conservation or fuel substitution).
- The use of low-sulfur fuels, including fuel desulfurization.
- In-furnace control of SO emissions (e.g., through limestone injection or with several types of fluidized bed combustion).
- Conventional wet flue gas desulfurization processes.
- Advanced, high-efficiency methods for capturing sulfur from the flue gas.

2. For NO_x emissions control in power and industry sector, the following two broad groups of technical emission control options are well-known (*Cofala and Syri, 1998b*):

- In-furnace control of NO_x emissions for stationary sources, i.e., the so-called combustion modifications (CM) or primary NO_x reduction measures.
- Secondary measures depending on the treatment of flue gases (selective catalytic reduction (SCR), selective non-catalytic reduction (SNCR)).

3. In the case of controlling VOCs and CO emission in power and industry sector, there is a number of ways in which the combustion efficiency could be increased and emissions reduced. Some of them include the following options (*Klimont et al., 2000*):

- Replacing old with the new boilers can significantly reduce VOC and CO emissions.
- Improving the performance of old boilers which include external furnaces, ceramic inserts, and pellet burners.
- Utilization of oxidation catalysts which the most cost-effective way to eliminate or reduce VOC and CO.

4. Furthermore, for reducing particulate matter (PM_{2.5}) emissions from large boilers in power stations and industry, there are following seven end-of-pipe options available (*Klimont et al., 2002*).

- Cyclones
- Wet scrubbers
- Electrostatic precipitators (three stages, i.e., one field, two fields, and more than two fields)
- Wet electrostatic precipitators
- Fabric filters
- Regular maintenance of oil-fired industrial boilers
- Two stages (low and high efficiency) of fugitive emissions control measures

5. For controlling air pollutant (NO_x, CO, VOCs, PM_{2.5} and SO_x) emissions from road transport, options available are divided into the following categories (*Klimont et al., 2002; Cofala and Syri, 1998a; Cofala and Syri, 1998b; Klimont et al., 2000*):

- Changes in engine design, which result in better control of the combustion processes in the engine.
- Changes in fuel quality, e.g., decrease in sulfur content. Changes in fuel specifications may provide engine manufacturers with the greater flexibility to use new emission reduction technologies.

c) Flue gas post-combustion treatment, using various types of trap concepts and catalysts to convert or capture emissions before they leave the exhaust pipe.

d) Better inspection and maintenance. Examples are in-use compliance testing, in-service inspection, and maintenance, onboard diagnostic systems.

6. For reducing crop residue burning, following control measures could be taken into account (*Sarkar et al., 2018; Zhang et al., 2017*)

a) Awareness must be created amongst the farming communities about the negative impacts of crop biomass burning and importance of crop residues incorporation in the soil for maintaining sustainable agricultural productivity.

b) With the development of recent technologies, rice residues can be processed and managed using better practices. Management options for rice residues can be classified as in-field and off-field management. Some of the off-field options include using rice straw for livestock feed, mushroom production, anaerobic digestion (biogas production) and mulching.

c) Support to be provided by the government to help farmers to purchase machines that can harvest with less residues, to adopt relevant climate smart practices to help increase yields and to use residues as fertilizer, animal feed supply, biogas production, or sell for use in different industries instead of being burnt.

d) Avoid usage of combine harvesters and promote no till and zero till methods of cultivation.

e) Manual harvesting of crops is a much better option than mechanical harvesting as the fields are ploughed easily, so everything is mixed up and acts as a fertilizer. However, as this is labor-intensive, there are some locally developed machines that can harvest crops from the roots. But they are expensive, so government subsidies can help farmers in this regard.

f) Educating farmers to make them aware of the monetizing opportunities from selling the residue products.

g) Responsibilities of local and central governments should be defined to improve coordination and cooperation between departments; to carry out various forms of information and education; to monitor fire spots by meteorological and environmental satellite; and to strengthen the inspection of illegal activities, etc.

h) To curb smoke from stubble burning in the post-monsoon, such technologies as Turbo Happy Seeder machines could be introduced to farmers (a tractor-mounted machine that cut and lifts standing stubble and drills wheat seeds into the bare soil without burning).

i) There is a need for crop residue-based renewable energy planning. A number of such initiatives are being undertaken in the neighboring countries to utilize the potential of crop residues for bio-energy generation .

7. An urgent need is the collection of high-quality data in various districts of Punjab, especially those which cover the rice belt, on a regular basis. It is suggested that air-quality monitoring stations may be installed throughout Punjab province, and air samples of winter smog and post-monsoon smoky haze should be taken. More evidence needs to be collected regarding sources and transport pathways of emissions of fine mode aerosols affecting northern Punjab.

8. The data can help create awareness and provide information necessary for crafting targeted solutions. For example, if it is established that winter smog contains vehicular and industrial pollutants rather than smoke particles, the remedy would be to improve fuel quality, install catalytic converters (which render NO_x emissions inert), and regulate point sources of emissions.

9. Promotion of such practices such as water sprinkling and vacuum cleaning of roads, restrictions (e.g., through a ruling by law courts) on field fires to burn crop remnants, provision of public health education, especially for school going children, or the creation of artificial rain depending upon the feasibility.

10. Establishment of early-warning systems for potentially severe smog incidents and smog monitoring network is also recommended.

11. Long run recommendations include investment in public transport to reduce aggregate fuel consumption, shift to cleaner fuels and renewable energy, and smart urban design, with indigenous species of plants and on a human-centric approach.

12. Finally, since smog is a regional problem, which also affects neighboring countries (e.g., India, Iran, and Afghanistan), there may be a case for inter-country collaboration on data and information exchange as well as collaborative strategies. Cumulative measures and joint efforts can help eradicate a problem that respects no boundaries.

REFERENCES

- Abas, N., Kalair, A., Khan, N. & Kalair, A.R. 2017. Review of GHG emissions in Pakistan compared to SAARC countries
- ADB. 2006. Country Synthesis Report on Urban Air Quality Management Pakistan, Asian Development Bank and the Clean Air Initiative for Asian Cities (CAI—Asia) Center, Mongolia
- Acharya, P. & Sreeekesh, S. 2013. Seasonal variability in aerosol optical depth over India: A spatio—temporal analysis using the MODIS aerosol product. *International Journal of Remote Sensing*. <https://doi.org/10.1080/01431161.2013.782114>
- Ackerman, A.S., Toon, O.B., Stevens, D.E., Heymsfield, A.J., Ramanathan, V. & Welton, E.J. 2000. Reduction of tropical cloudiness by soot. *Science*. <https://doi.org/10.1126/science.288.5468.1042>
- Alam, K., Iqbal, M.J., Blaschke, T., Qureshi, S. & Khan, G. 2010. Monitoring spatio—temporal variations in aerosols and aerosol—cloud interactions over Pakistan using MODIS data. *Advances in Space Research*. <https://doi.org/10.1016/j.asr.2010.06.025>
- Alam, K., Qureshi, S. & Blaschke, T. 2011. Monitoring spatio—temporal aerosol patterns over Pakistan based on MODIS, TOMS and MISR satellite data and a HYSPLIT model. *Atmospheric Environment*. <https://doi.org/10.1016/j.atmosenv.2011.05.055>
- Alam, K., Trautmann, T. & Blaschke, T. 2011. Aerosol optical properties and radiative forcing over mega—city Karachi. *Atmospheric Research*. <https://doi.org/10.1016/j.atmosres.2011.05.007>
- Alam, K., Trautmann, T., Blaschke, T. & Majid, H. 2012. Aerosol optical and radiative properties during summer and winter seasons over Lahore and Karachi. *Atmospheric Environment*. <https://doi.org/10.1016/j.atmosenv.2011.12.027>
- Ali, M., Tariq, S., Mahmood, K., Daud, A., Batool, A. & Zia—Ul—Haq. 2014. A study of aerosol properties over Lahore (Pakistan) by using AERONET data. *Asia—Pacific Journal of Atmospheric Sciences*. <https://doi.org/10.1007/s13143-014-0004-y>
- Amatulli, G., Pérez—Cabello, F., & de la Riva, J. 2007. "Mapping lightning/human—caused wildfires occurrence under ignition point location uncertainty," *Ecological Modelling*. <https://doi.org/10.1016/j.ecolmodel.2006.08.001>
- Andreae, M. O. 1991. Biomass burning: Its history, use, and distribution and its impact on environmental quality and global climate. In *Global Biomass Burning: Atmospheric, Climatic and Biospheric Implications*, pp. 3—21. MIT Press, Cambridge, Mass.
- Andreae, M.O., Jones, C.D. & Cox, P.M. 2005. Strong present—day aerosol cooling implies a hot future
- Ångström, A. & Angstrom, A. 1929. On the Atmospheric Transmission of Sun Radiation and on Dust in the Air. *Geografiska Annaler*. <https://doi.org/10.2307/519399>
- Amann, M., Bertok, I., Borken, J., Chambers, A., Cofala, J., Dentener, F., Heyes, C., Hoglund, L., Klimont, Z., Purohit, P., Rafaj, P., Schöpp, W., Texeira, E., Toth, G., Wagner, F., & Winiwarter W. 2008. GAINS Asia. A tool to combat air pollution and climate change simultaneously. *Methodology*
- Armenteras, D., Gibbes, C., Vivacqua, C.A., Espinosa, J.S., Duleba, W., Goncalves, F. & Castro, C. 2016. Interactions between climate, land use and vegetation fire occurrences in El Salvador Atmosphere. <https://doi.org/10.3390/atmos7020026>
- Badarinath, K.V.S., Kharol, S.K., Sharma, A.R. & Roy, P.S. 2009. Fog Over Indo—Gangetic Plains—A Study Using Multisatellite Data and Ground Observations. *IEEE Journal of Selected Topics in Applied Earth Observations and Remote Sensing*. <https://doi.org/10.1109/JSTARS.2009.2019830>
- Begum, B.A., Biswas, S.K., Markwitz, A. & Hopke, P.K. 2010. Identification of sources of fine and coarse particulate matter in Dhaka, Bangladesh. *Aerosol and Air Quality Research*. <https://doi.org/10.4209/aaqr.2009.12.0082>
- Bibi, H., Alam, K., Chishtie, F., Bibi, S., Shahid, I. & Blaschke, T. 2015. Intercomparison of MODIS, MISR, OMI, and CALIPSO aerosol optical depth retrievals for four locations on the Indo—Gangetic plains and validation against AERONET data. *Atmospheric Environment*. <https://doi.org/10.1016/j.atmosenv.2015.04.013>
- Biswas, K.F., Ghauri, B.M. & Husain, L. 2008. Gaseous and aerosol pollutants during fog and clear episodes in South Asian urban atmosphere. *Atmospheric Environment*. <https://doi.org/10.1016/j.atmosenv.2008.04.056>
- Biswas, S., Hu, S., Verma, V., Herner, J.D., Robertson, W.H., Ayala, A. & Sioutas, C. 2008. Physical properties of particulate matter (PM) from late model heavy—duty diesel vehicles operating with advanced PM and NOx emission control technologies. *Atmospheric Environment*. <https://doi.org/10.1016/j.atmosenv.2008.03.007>
- Bromley, L. 2010. Relating violence to MODIS fire detections in Darfur, Sudan. *International Journal of Remote Sensing*. <https://doi.org/10.1080/01431160902953909>
- Bond, T.C., Doherty, S.J., Fahey, D.W., Forster, P.M., Berntsen, T., Deangelo, B.J., Flanner, M.G., Ghan, S., Kärcher, B., Koch, D., Kinne, S., Kondo, Y., Quinn, P.K., Sarofim, M.C., Schultz, M.G., Schulz, M., Venkataraman, C., Zhang, H., Zhang, S., Bellouin, N., Guttikunda, S.K., Hopke, P.K., Jacobson, M.Z., Kaiser, J.W.,

Klimont, Z., Lohmann, U., Schwarz, J.P., Shindell, D., Storelvmo, T., Warren, S.G. & Zender, C.S. 2013. Bounding the role of black carbon in the climate system: A scientific assessment. *Journal of Geophysical Research Atmospheres*. <https://doi.org/10.1002/jgrd.50171>

BOS. 2011. Final Estimates of Major Kharif Crops in the Punjab, Bureau of Statistics, Government of the Punjab Lahore.

BOS. 2012. Final Estimates of Major Kharif Crops in the Punjab, Bureau of Statistics, Government of the Punjab Lahore.

BOS. 2013. Final Estimates of Major Kharif Crops in the Punjab, Bureau of Statistics, Government of the Punjab Lahore.

BOS. 2016. Statistical Pocket Book of the Punjab, Bureau of Statistics. Government of the Punjab Lahore.

BOS. 2017. Statistical Pocket Book of the Punjab, Bureau of Statistics. Government of the Punjab Lahore.

Boucher, O. & Haywood, J. 2001. On summing the components of radiative forcing of climate change. *Climate Dynamics*. <https://doi.org/10.1007/s003820100185>

Boucher, O. & Tanre, D. 2000. Estimation of the aerosol perturbation to the Earth's radiative budget over oceans using POLDER satellite aerosol retrievals. *Geophysical Research Letters*. <https://doi.org/10.1029/1999GL010963>

Chelani, A.B. 2015. Study of Temporal Variations in Aerosol Optical Depth over Central India. *International Journal of Environmental Protection*. <https://doi.org/10.5963/ijep0501004>

Chen, Y., Velicogna, I., Famiglietti, J.S. & Randerson, J.T. 2013. Satellite observations of terrestrial water storage provide early warning information about drought and fire season severity in the Amazon. *Journal of Geophysical Research: Biogeosciences*. <https://doi.org/10.1002/jgrg.20046>

Chuvieco, E., Giglio, L. & Justice, C. 2008. Global characterization of fire activity: Toward defining fire regimes from Earth observation data. *Global Change Biology*. <https://doi.org/10.1111/j.1365-2486.2008.01585.x>

Carslaw, K.S., Lee, L.A., Reddington, C.L., Pringle, K.J., Rap, A., Forster, P.M., Mann, G.W., Spracklen, D. V., Woodhouse, M.T., Regayre, L.A. & Pierce, J.R. 2013. Large contribution of natural aerosols to uncertainty in indirect forcing. *Nature*. <https://doi.org/10.1038/nature12674>

Chand, D., Wood, R., Anderson, T.L., Satheesh, S.K. & Charlson, R.J. 2009. Satellite-derived direct radiative effect of aerosols dependent on cloud cover. *Nature Geoscience*. <https://doi.org/10.1038/ngeo437>

Charlson, R.J., Schwartz, S.E., Hales, J.M., Cess, R.D.,

Coakley, J.A., Hansen, J.E. & Hofmann, D.J. 1992. Climate forcing by anthropogenic aerosols. *Science*. <https://doi.org/10.1126/science.255.5043.423>

Chylek, P., Lohmann, U., Dubey, M., Mishchenko, M., Kahn, R. & Ohmura, A. 2007. Limits on climate sensitivity derived from recent satellite and surface observations. *Journal of Geophysical Research Atmospheres*. <https://doi.org/10.1029/2007JD008740>

Cofala, J. & Syri, S. 1998a. Sulfur emissions, abatement technologies and related costs for Europe in the RAINS model database. *Methodology*.

Cofala, J. & Syri, S. 1998b. Nitrogen Oxides emissions, abatement technologies and related costs for Europe in the RAINS model database. *Methodology*.

Crutzen, P.J. & Andreae, M.O. 1990. Biomass Burning in the Tropics: Impact on Atmospheric Chemistry and Bio geochemical Cycles. *Science*. <https://doi.org/10.1126/science.250.4988.1669>

Csiszar, I.A., Morissette, J.T. & Giglio, L. 2006. Validation of active fire detection from moderate-resolution satellite sensors: The MODIS example in Northern Eurasia. *IEEE Transactions on Geoscience and Remote Sensing*. <https://doi.org/10.1109/TGRS.2006.875941>

Deaconu, L.T., Waquet, F., Josset, D., Ferlay, N., Peers, F., Thieuleux, F., Ducos, F., Pascal, N., Tanré, D., Pelon, J. & Goloub, P. 2017. Consistency of aerosols above clouds

characterization from A-Train active and passive measurements. *Atmospheric Measurement Techniques*. <https://doi.org/10.5194/amt-10-3499-2017>

Dey, S. & Di Girolamo, L. 2011. A decade of change in aerosol properties over the Indian subcontinent. *Geophysical Research Letters*. <https://doi.org/10.1029/2011GL048153>

Dey, S., Tripathi, S.N., Singh, R.P. & Holben, B.N. 2004. Influence of dust storms on the aerosol optical properties over the Indo-Gangetic basin. *Journal of Geophysical Research D: Atmospheres*. <https://doi.org/10.1029/2004JD004924>

Draxler, R.R. & Hess, G.D. 1998. An overview of the HYSPLIT_4 modelling system for trajectories, dispersion and deposition
Draxler, R.R. & Rolph, G.D. 2003. HYSPLIT (HYbrid Single-Particle Lagrangian Integrated Trajectory). NOAA Air Resources Laboratory, College Park, MD.

Dubovik, O., Holben, B., Eck, T.F., Smirnov, A., Kaufman, Y.J., King, M.D., Tanré, D. & Slutsker, I. 2002. Variability of absorption and optical properties of key aerosol types observed in worldwide locations. *Journal of the Atmospheric Sciences*.

[https://doi.org/10.1175/1520-0469\(2002\)059<0590:voaaop>2.0.co;2](https://doi.org/10.1175/1520-0469(2002)059<0590:voaaop>2.0.co;2)

EOSDIS. 2016. Fire Information for Resource Management System (FIRMS), VIIRS Active Fire locations 375m FIRMS V001 NRT.

Schroeder, W., & Giglio, L. In: NASA VIIRS Land Science Investigator Processing System (SIPS), <https://earthdata.nasa.gov/>. October 2, 2017. <https://doi.org/10.5067/FIRMS/VIIRS/VNP14IMGT.NRT.001>

EOSDIS. 2017. Fire Information for Resource Management System (FIRMS), VIIRS I-Band 375 m Active Fire Data Earthdata. Retrieved on October 3, 2017, from <https://earthdata.nasa.gov/earth-observation-data/near-real-time/firms/viirs-i-band-active-fire-data>

ESoP. 2013. Economic survey of Pakistan 2012-2013. Ministry of Finance, Pakistan. http://www.finance.gov.pk/survey_1213.html

EPA. US Environmental Protection Agency's Agricultural Center, 2012e.AgriculturalBurning. Accessed on August 22, 2015. <http://www.epa.gov/agriculture/tburn.html>

FAOSTAT. 2015. Land Use Indicators, Agriculture Data.

Accessed on August 22, 2015. <http://faostat3.fao.org/browse/E/EL>

Fleming, Z.L., Monks, P.S. & Manning, A.J. 2012. Review: Untangling the influence of air-mass history in interpreting observed atmospheric composition. <https://doi.org/10.1016/j.atmosres.2011.09.009>.

Freeborn, P.H., Wooster, M.J., Roy, D.P. & Cochrane, M.A. 2014. Quantification of MODIS fire radiative power (FRP) measurement uncertainty for use in satellite-based active fire characterization and biomass burning estimation. *Geophysical Research Letters*. <https://doi.org/10.1002/2013GL059086>

Gao, Y., Kaufman, Y.J., Tanré, D., Kolber, D. & Falkowski, P.G. 2001. Seasonal distributions of Aeolian iron fluxes to the global ocean. *Geophysical Research Letters*. <https://doi.org/10.1029/2000GL011926>

Giglio, L. & Justice, C.O. 2003. Effect of wavelength selection on characterization of fire size and temperature. *International Journal of Remote Sensing*. <https://doi.org/10.1080/0143116031000117056>

Giglio, L., Kendall, J.D. & Justice, C.O. 1999. Evaluation of global fire detection algorithms using simulated avhrr infrared data. *International Journal of Remote Sensing*. <https://doi.org/10.1080/014311699212290>

Giglio, L., Kendall, J.D. & Mack, R. 2003. A multi-year active fire dataset for the tropics derived from the TRMM VIRS. *International Journal of Remote Sensing*.

<https://doi.org/10.1080/0143116031000070283>

Giglio, L., Descloitres, J., Justice, C.O. & Kaufman, Y.J. 2003. An enhanced contextual fire detection algorithm for MODIS. *Remote Sensing of Environment*. [https://doi.org/10.1016/S0034-4257\(03\)00184-6](https://doi.org/10.1016/S0034-4257(03)00184-6)

Gonzalez-Olabarria, J.R., Brotons, L., Gritten, D., Tudela, A. & Teres, J.A. 2012. Identifying location and causality of fire ignition hotspots in a Mediterranean region. *International Journal of Wildland Fire*. <https://doi.org/10.1071/WF11039>

Güls, I. & Bendix, J. 2007. Fog detection and fog mapping using low cost Meteosat-WEFAX transmission. *Meteorological Applications*. <https://doi.org/10.1002/met.5060030208>

HDIP. 2008-2017. Pakistan Energy Yearbook 2008-2017. Hydrocarbon Development Institute of Pakistan (HDIP), Ministry of Petroleum and Natural Resources, Government of Pakistan, Islamabad.

Hantson, S., Padilla, M., Corti, D. & Chuvieco, E. 2013. Strengths and weaknesses of MODIS hotspots to characterize global fire occurrence. *Remote Sensing of Environment*. <https://doi.org/10.1016/j.rse.2012.12.004>

Hansen, J., Sato, M. & Ruedy, R. 1997. Radiative forcing and climate response. *Journal of Geophysical Research Atmospheres*. <https://doi.org/10.1029/96JD03436>

Hantson, S., Padilla, M., Corti, D. & Chuvieco, E. 2013. Strengths and weaknesses of MODIS hotspots to characterize global fire occurrence. *Remote Sensing of Environment*. <https://doi.org/10.1016/j.rse.2012.12.004>

Haywood, J. & Boucher, O. 2000. Estimates of the direct and indirect radiative forcing due to tropospheric aerosols: A review

Hiloidhari, M., Das, D. & Baruah, D.C. 2014. Bioenergy potential from crop residue biomass in India

Holben, B.N., Eck, T.F., Slutsker, I., Tanré, D., Buis, J.P., Setzer, A., Vermote, E., Reagan, J.A., Kaufman, Y.J., Nakajima, T., Lavenu, F., Jankowiak, I. & Smirnov, A. 1998. AERONET – A federated instrument network and data archive for aerosol characterization. *Remote Sensing of Environment*. [https://doi.org/10.1016/S0034-4257\(98\)00031-5](https://doi.org/10.1016/S0034-4257(98)00031-5)

Houghton, J.T., Meira, Filho L.G., Lim, B., Treanton, K., Mamaty, I., Bonduki, Y., Griggs, D.J., Callander, B.A. 1997. (eds) Revised 1996 IPCC Guidelines for National Greenhouse Gas Inventories. Intergovernmental Panel on Climate Change (IPCC), Meteorological Office

BracknellHsu, N.C., Tsay, S.C., King, M.D. & Herman, J.R. 2004. Aerosol properties over bright-reflecting source regions. *IEEE Transactions on*

Geoscience and Remote Sensing. <https://doi.org/10.1109/TGRS.2004.824067>

Ichoku, C. & Kaufman, Y.J. 2005. A method to derive smoke emission rates from MODIS fire radiative energy measurements. IEEE Transactions on Geoscience and Remote Sensing. Paper presented at, 2005.

IPCC. 1996. Revised 1996 IPCC Guidelines for National Greenhouse Gas Inventories; reference manual, Intergovernmental Panel on Climate Change (IPCC). Oceania, p.

IPCC. 2006. Guidelines for national greenhouse gas inventories. In: Eggleston, H.S., Buendia, L., Miwa, K., Ngara, T., Tanabe, K. (Eds.), Prepared by the National Greenhouse Gas Inventories Programme, IGES, Japan. Agriregionieuropa.

IPCC Working Group I, I., Stocker, T.F., Qin, D., Plattner, G.—K., Tignor, M., Allen, S.K., Boschung, J., Nauels, A., Xia, Y., Bex, V. & Midgley, P.M. 2013. IPCC, 2013: Climate Change 2013: The Physical Science Basis. Contribution of Working Group I to the Fifth Assessment Report of the Intergovernmental Panel on Climate Change. IPCC.

IPCC. 2007. Climate Change 2007: Synthesis Report. Contribution of working groups I, II and III to the fourth assessment. Report of the Intergovernmental Panel on Climate Change, p.

Jain, N., Bhatia, A. & Pathak, H. 2014. Emission of air pollutants from crop residue burning in India. Aerosol and Air Quality Research. <https://doi.org/10.4209/aaqr.2013.01.0031>

JCR—VIS. 2016a. Sector Update—Cement Industry, JCR—VIS Credit Rating Co. Ltd., Karachi.

JCR—VIS. 2016b. Sector Update—Fertilizer Industry, JCR—VIS Credit Rating Co. Ltd., Karachi.

Jethva, H., Torres, O., Remer, L.A. & Bhartia, P.K. 2013. A color ratio method for simultaneous retrieval of aerosol and cloud optical thickness of above—cloud absorbing aerosols from passive sensors: Application to MODIS measurements. IEEE Transactions on Geoscience and Remote Sensing. <https://doi.org/10.1109/TGRS.2012.2230008>

Jethva, H., Torres, O., Remer, L., Redemann, J., Livingston, J., Dunagan, S., Shinozuka, Y., Kacenelenbogen, M., Rosenheimer, S. & Spurr, R. 2016. Validating MODIS above—cloud aerosol optical depth retrieved from “color ratio” algorithm using direct measurements made by NASA’s airborne AATS and 4STAR sensors. Atmospheric Measurement Techniques. <https://doi.org/10.5194/amt-9-5053-2016>

Justice, C.O., Townshend, J.R.G., Vermote, E.F., Masuoka, E., Wolfe, R.E., Saleous, N., Roy, D.P. & Morisette, J.T. 2002. An overview of MODIS Land data processing and product

status. Remote Sensing of Environment. [https://doi.org/10.1016/S0034-4257\(02\)00084-6](https://doi.org/10.1016/S0034-4257(02)00084-6)

Justice, C. O., Wolfe, R. E., El Saleous, N., Descloitres, J., Vermote, E., Roy, D., Owens, J., & Masuoka, E. 2000. The availability and status of MODIS land products. The Earth Observer

Justice, C.O., Kendall, J.D., Dowty, P.R. & Scholes, R.J. 1996. Satellite remote sensing of fires during the SAFARI campaign using NOAA advanced very high resolution radiometer data. Journal of Geophysical Research Atmospheres. <https://doi.org/10.1029/95jd00623>

Kahn, R.A., Chen, Y., Nelson, D.L., Leung, F.Y., Li, Q., Diner, D.J. & Logan, J.A. 2008. Wildfire smoke injection heights: Two perspectives from space. Geophysical Research Letters. <https://doi.org/10.1029/2007GL032165>

Kahn, R.A., Li, W.H., Moroney, C., Diner, D.J., Martonchik, J. V. & Fishbein, E. 2007. Aerosol source plume physical characteristics from space—based multiangle imaging. Journal of Geophysical Research Atmospheres. <https://doi.org/10.1029/2006JD007647>

Kaiser, J.W., Heil, A., Andreae, M.O., Benedetti, A., Chubarova, N., Jones, L., Morcrette, J.J., Razinger, M., Schultz, M.G., Suttie, & Van Der Werf, G.R. 2012. Biomass burning emissions estimated with a global fire assimilation system based on observed fire radiative power

Kalabokidis, K.D., Koutsias, N., Konstantinidis, P. & Vasilakos, C. 2007. Multivariate analysis of landscape wildfire dynamics in a Mediterranean ecosystem of Greece. Area. <https://doi.org/10.1111/j.1475-4762.2007.00756.x>

Kaufman, Y. J., Setzer, A., Justice, C. Tucker, C. J., Pereira, C., & Fung, I. 1990. Remote sensing of biomass burning in the tropics. In J. G. Goldammer (Ed.), Fire and the tropical biota: ecosystem processes and global challenges. pp. 371–399.

Kaufman, Y.J., Remer, L.A., Ottmar, R.D., Ward, D.E., Li, R.—R., & Kleidman, R. 1996. Relationship between remotely sensed re intensity and rate of emission of smoke: SCAR—C experiment. In: Levin, J. (Ed.), Global Biomass Burning. pp. 685–696

Kaufman, Y.J., Tanré, D., Gordon, H.R., Nakajima, T., Lenoble, J., Frouin, R., Grassl, H., Herman, B.M., King, M.D. & Teillet, P.M. 1997. Passive remote sensing of tropospheric aerosol and atmospheric correction for the aerosol effect. Journal of Geophysical Research Atmospheres. <https://doi.org/10.1029/97jd01496>

Kaufman, Y.J., Tanré, D. & Boucher, O. 2002. A satellite view

of aerosols in the climate system. *Nature*. <https://doi.org/10.1038/nature01091>

Khattak, P., Khokhar, M.F. & Yasmin, N. 2014. Spatio-temporal analyses of atmospheric sulfur dioxide column densities over Pakistan by using SCIAMACHY data. *Aerosol and Air Quality Research*. <https://doi.org/10.4209/aaqr.2013.12.0357>

Kaskaoutis, D.G., Kumar, S., Sharma, D., Singh, R.P., Kharol, S.K., Sharma, M., Singh, A.K., Singh, S., Singh, A. & Singh, D. 2014. Effects of crop residue burning on aerosol properties, plume characteristics, and long-range transport over northern India. *Journal of Geophysical Research*. <https://doi.org/10.1002/2013JD021357>

Kishcha, P., Starobinets, B., Kalashnikova, O. & Alpert, P. 2011. Aerosol optical thickness trends and population growth in the Indian subcontinent. *International Journal of Remote Sensing*. <https://doi.org/10.1080/01431161.2010.550333>

Khokhar, M.F., Yasmin, N., Chishtie, F. & Shahid, I. 2016. Temporal variability and characterization of aerosols across the Pakistan region during the winter fog periods. *Atmosphere*. <https://doi.org/10.3390/atmos7050067>

Klein, L., Milburn, R., Praderas, C. & Taaheri, A. 2006. Tool for conversion of earth observing system data products to GIS compatible formats and for the provision of post-processing functionality. *Earth Science Satellite Remote Sensing: Data, Computational Processing, and Tools*. Paper presented at, 2006.

Klimont, Z., Amann, M., & Cofala, J. 2000. Estimating Costs for Controlling Emissions of Volatile Organic Compounds (VOC) from Stationary Sources in Europe. *IIASA Interim Report IR-00-051*.

Klimont, Z., Cofala, J., Bertok, I., Amann, M., Heyes, C. & Gyarmas, F. 2002. Modeling particulate emissions in Europe. A framework to estimate reduction potential and control costs. *IIASA Interim Report IR-02-076*.

Koren, I., Remer, L.A. & Longo, K. 2007. Reversal of trend of biomass burning in the Amazon. *Geophysical Research Letters*. <https://doi.org/10.1029/2007GL031530>

Korontzi, S., McCarty, J., Loboda, T., Kumar, S. & Justice, C. 2006. Global distribution of agricultural fires in croplands from 3 years of Moderate Resolution Imaging Spectroradiometer (MODIS) data. *Global Biogeochemical Cycles*. <https://doi.org/10.1029/2005GB002529>

Koppmann, R., von Czapiewski, K. & Reid, J.S. 2005. A review of biomass burning emissions, part I: gaseous emissions of carbon monoxide, methane, volatile organic compounds, and nitrogen containing compounds. *Atmospheric Chemistry and*

Physics Discussions.

<https://doi.org/10.5194/acpd-5-10455-2005>

Koutsias, N., Allgöwer, B., Kalabokidis, K., Mallinis, G., Balatsos, P. & Goldammer, J.G. 2016. Fire occurrence zoning from local to global scale in the European Mediterranean basin: Implications for multi-scale fire management and policy. *IForest*. <https://doi.org/10.3832/for1513-008>

Koutsias, N., Kalabokidis, K.D. & Allgöwer, B. 2004. Fire occurrence patterns at landscape level: Beyond positional accuracy of ignition points with kernel density estimation methods. *Natural Resource Modeling*. <https://doi.org/10.1111/j.1939-7445.2004.tb00141.x>

Lawrence, M.G. & Lelieveld, J. 2010. Atmospheric pollutant outflow from southern Asia: A review

Leon, J.F., Chazette, P., Dulac, F., Pelon, J., Flamant, C., Bonazzola, M., Foret, G., Alfaro, S.C., Cachier, H., Cautenet, S., Hamonou, E., Gaudichet, A., Gomes, L., Rajot, J.L., Lavenu, F., Inamdar, S.R., Sarode, P.R. & Kadadevarmath, J.S. 2001. Large-scale advection of continental aerosols during INDOEX. *Journal of Geophysical Research Atmospheres*. <https://doi.org/10.1029/2001JD900023>

Lentile, L.B., Holden, Z.A., Smith, A.M.S., Falkowski, M.J., Hudak, A.T., Morgan, P., Lewis, S.A., Gessler, P.E. & Benson, N.C. 2006. Remote sensing techniques to assess active fire characteristics and post-fire effects

Levine, N. 2016. CrimeStat: A Spatial Statistical Program for the Analysis of Crime Incidents. *Encyclopedia of GIS*, p.

Li, J. & Heap, A.D. 2008. A Review of Spatial Interpolation Methods for Environmental Scientists. *Australian Geological Survey Organisation*. https://doi.org/http://www.ga.gov.au/image_cache/GA12526.pdf

Lin, T.H., Hsu, N.C., Tsay, S.C. & Huang, S.J. 2011. Asian dust weather categorization with satellite and surface observations. *International Journal of Remote Sensing*. <https://doi.org/10.1080/01431160903439932>

Liu, Z., Vaughan, M., Winker, D., Kittaka, C., Getzewich, B., Kuehn, R., Omar, A., Powell, K., Trepte, C. & Hostetler, C. 2009. The CALIPSO lidar cloud and aerosol discrimination: Version 2 algorithm and initial assessment of performance. *Journal of Atmospheric and Oceanic Technology*. <https://doi.org/10.1175/2009JTECHA1229.1>

Longo, K.M., Freitas, S.R., Andreae, M.O., Setzer, A., Prins, E. & Artaxo, P. 2010. The coupled aerosol and tracer transport model to the brazilian developments on the regional atmospheric modeling system (catt-brams)—part 2: Model sensitivity to the biomass burning inventories. *Atmospheric*

Chemistry and Physics.

<https://doi.org/10.5194/acp-10-5785-2010>

Ma, Z., Hu, X., Huang, L., Bi, J. & Liu, Y. 2014. Estimating ground-level PM_{2.5} in China using satellite remote sensing. *Environmental Science and Technology*. <https://doi.org/10.1021/es5009399>

Mao, K.B., Ma, Y., Xia, L., Chen, W.Y., Shen, X.Y., He, T.J. & Xu, T.R. 2014. Global aerosol change in the last decade: An analysis based on MODIS data. *Atmospheric Environment*. <https://doi.org/10.1016/j.atmosenv.2014.04.053>

Mehta, M. 2015. A study of aerosol optical depth variations over the Indian region using thirteen years (2001–2013) of MODIS and MISR Level 3 data. *Atmospheric Environment*. <https://doi.org/10.1016/j.atmosenv.2015.03.021>

Mehta, M., Singh, R., Singh, A., Singh, N. & Anshumali. 2016. Recent global aerosol optical depth variations and trends – A comparative study using MODIS and MISR level 3 datasets. *Remote Sensing of Environment*. <https://doi.org/10.1016/j.rse.2016.04.004>

Meyer, K., Platnick, S. & Zhang, Z. 2015. Simultaneously inferring above-cloud absorbing aerosol optical thickness and underlying liquid phase cloud optical and microphysical properties using MODIS. *Journal of Geophysical Research*. <https://doi.org/10.1002/2015JD023128>

Mccarty, J. L., Pouliot, G., Raffuse, S. M., & Ruminski, M. 2015. Using Satellite Data to Quantify Cropland Burning and Related Emissions in the Contiguous United States: Lessons Learned. *Biomass*. Retrieved from https://www3.epa.gov/ttnchie1/conference/ei20/session2/j_mccarty.pdf

McCarty, J.L., Justice, C.O. & Korontzi, S. 2007. Agricultural burning in the Southeastern United States detected by MODIS. *Remote Sensing of Environment*. <https://doi.org/10.1016/j.rse.2006.03.020>

McCarty, J.L., Ellicott, E.A., Romanenkov, V., Rukhovitch, D. & Koroleva, P. 2012. Multi-year black carbon emissions from cropland burning in the Russian Federation. *Atmospheric Environment*. <https://doi.org/10.1016/j.atmosenv.2012.08.053>

Miller, A.J. 1984. Selection of Subsets of Regression Variables. *Journal of the Royal Statistical Society. Series A (General)*. <https://doi.org/10.2307/2981576>

Miller, R.L. & Tegen, I. 1998. Climate response to soil dust aerosols. *Journal of Climate*. [https://doi.org/10.1175/1520-0442\(1998\)011<3247:CRTSDA>2.0.CO;2](https://doi.org/10.1175/1520-0442(1998)011<3247:CRTSDA>2.0.CO;2)

MoF. 2016. Pakistan Economic Survey (2015–16). Ministry of Finance (MoF), Government of Pakistan, Islamabad.

Mir, K.A., Purohit, P. & Mehmood, S. 2017. Sectoral

assessment of greenhouse gas emissions in Pakistan. *Environmental Science and Pollution Research*. <https://doi.org/10.1007/s11356-017-0354-y>

Mir, K.A., Purohit, P., Goldstein, G.A. & Balasubramanian, R. 2016. Analysis of baseline and alternative air quality scenarios for Pakistan: an integrated approach. *Environmental Science and Pollution Research*. <https://doi.org/10.1007/s11356-016-7358-x>

Mishchenko, M.I., Geogdzhayev, I. V., Rossow, W.B., Cairns, B., Carlson, B.E., Lacis, A.A., Liu, L. & Travis, L.D. 2007. Long-term satellite record reveals likely recent aerosol trend. *Science*. <https://doi.org/10.1126/science.1136709>

Mollicone, D., Eva, H.D. & Achard, F. 2006. Ecology: Human role in Russian wild fires. *Nature*. <https://doi.org/10.1038/440436a>

Monfreda, C., Ramankutty, N., Foley, J.A. & Evan, A.T. 2008. Farming the planet: 1. Geographic distribution of global agricultural lands in the year 2000. *Global Biogeochemical Cycles*.

Monks, P.S. 2014. European pollution: investigate smog to inform policy. *Nature*.

Morisette, J., Justice, C., Pereira, J. M., Gregoire, J., & Frost. 2008. Report from the GOFc-fire: satellite product validation workshop. NASA's Earth Observer. <http://publications.jrc.ec.europa.eu/repository/handle/JRC22445>

Myhre, G., Samset, B.H., Schulz, M., Balkanski, Y., Bauer, S., Bernsten, T.K., Bian, H., Bellouin, N., Chin, M., Diehl, T., Easter, R.C., Feichter, J., Ghan, S.J., Hauglustaine, D., Iversen, T., Kinne, S., Kirkevåg, A., Lamarque, J.F., Lin, G., Liu, X., Lund, M.T., Luo, G., Ma, X., Van Noije, T., Penner, J.E., Rasch, P.J., Ruiz, A., Seland, Skeie, R.B., Stier, P., Takemura, T., Tsigaridis, K., Wang, P., Wang, Z., Xu, L., Yu, H., Yu, F., Yoon, J.H., Zhang, K., Zhang, H. & Zhou, C. 2013. Radiative forcing of the direct aerosol effect from AeroCom Phase II simulations. *Atmospheric Chemistry and Physics*. <https://doi.org/10.5194/acp-13-1853-2013>

Nakaya, T. 2015. Geographically weighted generalised linear modeling. *Geocomputation: A Practical Primer*.

NASA. 2017. Active Fires (1 month – Terra/MODIS) | NASA. Retrieved from https://neo.sci.gsfc.nasa.gov/view.php?datasetId=MOD14A1_M_FIRE

Soares Neto, T.G., Carvalho, J.A., Veras, C.A.G., Alvarado, E.C., Gielow, R., Lincoln, E.N., Christian, T.J., Yokelson, R.J. & Santos, C. 2009. Biomass consumption and CO₂, CO and main

hydrocarbon gas emissions in an Amazonian forest clearing fire. *Atmospheric Environment*. <https://doi.org/10.1016/j.atmosenv.2008.07.063>

Ogunjobi, K.O., Kim, Y.J. & He, Z. 2003. Aerosol optical properties during Asian dust storm episodes in South Korea. *Theoretical and Applied Climatology*. <https://doi.org/10.1007/s00704-003-0006-7>

Omar, A.H., Winker, D.M., Kittaka, C., Vaughan, M.A., Liu, Z., Hu, Y., Trepte, C.R., Rogers, R.R., Ferrare, R.A., Lee, K.P., Kuehn, R.E. & Hostetler, C.A. 2009. The CALIPSO automated aerosol classification and lidar ratio selection algorithm. *Journal of Atmospheric and Oceanic Technology*. <https://doi.org/10.1175/2009JTECHA1231.1>

Pace, G., di Sarra, A., Meloni, D., Piacentino, S. & Chamard, P. 2006. Aerosol optical properties at Lampedusa (Central Mediterranean). 1. Influence of transport and identification of different aerosol types. *Atmospheric Chemistry and Physics*. <https://doi.org/10.5194/acp-6-697-2006>

Pan, X., Chin, M., Gautam, R., Bian, H., Kim, D., Colarco, P.R., Diehl, T.L., Takemura, T., Pozzoli, L., Tsigaridis, K., Bauer, S. & Bellouin, N. 2015. A multi-model evaluation of aerosols over South Asia: Common problems and possible causes. *Atmospheric Chemistry and Physics*. <https://doi.org/10.5194/acp-15-5903-2015>

Pausas, J.G. & Keeley, J.E. 2009. A Burning Story: The Role of Fire in the History of Life. *Bio Science*. <https://doi.org/10.1525/bio.2009.59.7.10>

PBC. 2016. Punjab Brick Kiln Census, Labor and Human Resource Department, Government of Punjab, Lahore.

PBS. 2013. Census of Manufacturing Industries (2005–06) –District Wise Report, Pakistan Bureau of Statistics, Government of Pakistan, Islamabad.

Peers, F., et al. 2015. Absorption of aerosols above clouds from POLDER/PARASOL measurements and estimation of their direct radiative effect. *Atmos. Chem. Phys.* 15, 4179–4196

Penner, J.E., Andreae, M., Annegarn, H., Barrie, L., Feichter, J., Hegg, D., Jayaraman, A., Leaitch, R., Murphy, D., Nganga, J., Pitari, G., Ackerman, A., Adams, P., Austin, P., Boers, R., Boucher, O., Chin, M., Chuang, C., Collins, B., Cooke, W., Demott, P., Feng, Y., Fischer, H., Fung, I., Ghan, S., Ginoux, P., Gong, S., Guenther, A., Herzog, M., Higurashi, A., Kaufman, Y., Kettle, A., Kiehl, J., Koch, D., Lammel, G., Land, C., Lohmann, U., Madronich, S., Mancini, E., Mishchenko, M., Nakajima, T., Quinn, P., Rasch, P., Roberts, D.L., Savoie, D., Schwartz, S., Seinfeld, J., Soden, B., Tanré, D., Taylor, K., Tegen, I., Tie, X., Vali, G., Dingenen, R. Van & Weele, M. Van. 2001. Aerosols, their Direct and Indirect Effects. *Climate Change 2001: The Scientific*

Basis. Contribution of Working Group I to the Third Assessment Report of the Intergovernmental Panel on Climate Change, p.

Peterson, D., Hyer, E. & Wang, J. 2014. Quantifying the potential for high-altitude smoke injection in the north american boreal forest using the standard MODIS fire products and subpixel-based methods. *Journal of Geophysical Research*. <https://doi.org/10.1002/2013JD021067>

Peterson, D., Wang, J., Ichoku, C., Hyer, E. & Ambrosia, V. 2013. A sub-pixel-based calculation of fire radiative power from MODIS observations: 1. Algorithm development and initial assessment. *Remote Sensing of Environment*. <https://doi.org/10.1016/j.rse.2012.10.036>

Podur, J., Martell, D.L. & Csillag, F. 2003. Spatial patterns of lightning-caused forest fires in Ontario, 1976–1998. *Ecological Modelling*. [https://doi.org/10.1016/S0304-3800\(02\)00386-1](https://doi.org/10.1016/S0304-3800(02)00386-1)

Policy Paper. 2017. Demand–Supply Gap Analysis and Potential Energy Resources of Punjab, Punjab Economic Research Institute Lahore.

PSPB. 2017. Statistical Pocket Book of the Punjab, Bureau of Statistics. Government of the Punjab, Lahore.

Ramankutty, N., Evan, A.T., Monfreda, C. & Foley, J.A. 2008. Farming the planet: 1. Geographic distribution of global agricultural lands in the year 2000. *Global Biogeochemical Cycles*. <https://doi.org/10.1029/2007GB002952>

Ramachandran, S., Kedia, S. & Sheel, V. 2015. Spatiotemporal characteristics of aerosols in India: Observations and model simulations. *Atmospheric Environment*. <https://doi.org/10.1016/j.atmosenv.2015.06.015>

Ramachandran, S., Kedia, S. & Srivastava, R. 2012. Aerosol optical depth trends over different regions of India. *Atmospheric Environment*. <https://doi.org/10.1016/j.atmosenv.2011.11.017>

Ramanathan, V., Crutzen, P.J., Kiehl, J.T. & Rosenfeld, D. 2001.

Atmosphere: Aerosols, climate, and the hydrological cycle
Reid, J.S., Eck, T.F., Christopher, S.A., Koppmann, R., Dubovik, O., Eleuterio, D.P., Holben, B.N., Reid, E.A. & Zhang, J. 2004. A review of biomass burning emissions part III: intensive optical properties of biomass burning particles. *Atmospheric Chemistry and Physics Discussions*. <https://doi.org/10.5194/acpd-4-5201-2004>

Reid, J.S., Westphal, D.L., Curtis, C.A., Richardson, K.A., Hyer, J., Prins, E.M., Schmidt, C.C., Hoffman, J.P., Zhang, J., Wang, J., Christopher, S.A. & Eleuterio, D.P. 2009. Global Monitoring and Forecasting of Biomass–Burning Smoke: Description of

and Lessons from the Fire Locating and Modeling of Burning Emissions (FLAMBE) Program. *IEEE Journal of Selected Topics in Applied Earth Observations and Remote Sensing*. <https://doi.org/10.1109/JSTARS.2009.2027443>

Remer, L.A., Kaufman, Y.J., Tanré, D., Mattoo, S., Chu, D.A., Martins, J. V., Li, R.R., Ichoku, C., Levy, R.C., Kleidman, R.G., Eck, F., Vermote, E. & Holben, B.N. 2005. The MODIS aerosol algorithm, products, and validation. *Journal of the Atmospheric Sciences*. <https://doi.org/10.1175/JAS3385.1>

Roy, D.P., Lewis, P.E. & Justice, C.O. 2002. Burned area mapping using multi-temporal moderate spatial resolution data—a bi-directional reflectance model-based expectation approach. *Remote Sensing of Environment*. [https://doi.org/10.1016/S0034-4257\(02\)00077-9](https://doi.org/10.1016/S0034-4257(02)00077-9)

Ressl, R., Lopez, G., Cruz, I., Colditz, R.R., Schmidt, M., Ressler, S. & Jiménez, R. 2009. Operational active fire mapping and burnt area identification applicable to Mexican Nature Protection Areas using MODIS and NOAA-AVHRR direct readout data. *Remote Sensing of Environment*. <https://doi.org/10.1016/j.rse.2008.10.016>

Restrepo, J.C., Ortíz, J.C., Pierini, J., Schrottke, K., Maza, M., Otero, L. & Aguirre, J. 2014. Freshwater discharge into the Caribbean Sea from the rivers of Northwestern South America (Colombia): Magnitude, variability and recent changes. *Journal of Hydrology*. <https://doi.org/10.1016/j.jhydrol.2013.11.045>

SAARC. 2012. Evaluating Energy Conservation Potential of Brick Kilns in SAARC Countries. South Asian Association for Regional Cooperation (SAARC) Energy Centre, Islamabad.

Saide, P.E., Spak, S.N., Pierce, R.B., Otkin, J.A., Schaack, T.K., Heidinger, A.K., Da Silva, A.M., Kacenelenbogen, M., Redemann, J. & Carmichael, G.R. 2015. Central American biomass burning smoke can increase tornado severity in the U.S. *Geophysical Research Letters*. <https://doi.org/10.1002/2014GL062826>

Salis, M., Ager, A.A., Finney, M.A., Arca, B. & Spano, D. 2014. Analyzing spatiotemporal changes in wildfire regime and exposure across a Mediterranean fire-prone area. *Natural Hazards*. <https://doi.org/10.1007/s11069-013-0951-0>

Samaa Web Desk. 2016. Fog, smog continue to disrupt life in Punjab—Samaa TV. Retrieved October 4, 2017, from <https://www.samaa.tv/pakistan/2016/11/fog-smog-continue-to-disrupt-life-in-punjab/>

Samina Bibi, Alam, K., Bibi, H., Khan, H.U. & Haq, B.S. 2015. Variation in Aerosol Optical Depth and its Impact on Longwave Radiative Properties in Northern Areas of Pakistan. *Journal of GeoSpace Science*.

Sánchez-Triana, E., Enriquez, S., Afzal, J., Nakagawa, A. & Khan, A.S. 2014. Cleaning Pakistan's Air: Policy Options to Address the Cost of Outdoor Air Pollution

Sarkar, S., Singh, R.P. & Chauhan, A. 2018. Crop Residue Burning in Northern India: Increasing Threat to Greater India. *Journal of Geophysical Research: Atmospheres*. <https://doi.org/10.1029/2018JD028428>

Sayer, A.M., Hsu, N.C., Bettenhausen, C. & Jeong, M.J. 2013. Validation and uncertainty estimate for MODIS Collection 6 “deep Blue” aerosol data. *Journal of Geophysical Research Atmospheres*. <https://doi.org/10.1002/jgrd.50600>

Sayer, A.M., Hsu, N.C., Bettenhausen, C., Lee, J., Redemann, J., Schmid, B. & Shinozuka, Y. 2016. Extending “deep blue” aerosol retrieval coverage to cases of absorbing aerosols above clouds: Sensitivity analysis and first case studies. *Journal of Geophysical Research*. <https://doi.org/10.1002/2015JD024729>

Schroeder, W., Giglio, L. & Aravéquia, J.A. 2009. Comment on “Reversal of trend of biomass burning in the Amazon” by Ilan Koren, Lorraine A. Remer, and Karla Longo

Schroeder, W., Csiszar, I., Giglio, L. & Schmidt, C.C. 2010. On the use of fire radiative power, area, and temperature estimates to characterize biomass burning via moderate to coarse spatial resolution remote sensing data in the Brazilian Amazon. *Journal of Geophysical Research Atmospheres*. <https://doi.org/10.1029/2009JD013769>

Schroeder, W., Oliva, P., Giglio, L. & Csiszar, I.A. 2014. The New VIIRS 375m active fire detection data product: Algorithm description and initial assessment. *Remote Sensing of Environment*. <https://doi.org/10.1016/j.rse.2013.12.008>

Semeniuk, T.A., Wise, M.E., Martin, S.T., Russell, L.M. & Buseck, P.R. 2007. Hygroscopic behavior of aerosol particles from biomass fires using environmental transmission electron microscopy. *Journal of Atmospheric Chemistry*. <https://doi.org/10.1007/s10874-006-9055-5>

Shahid, M.Z., Liao, H., Li, J., Shahid, I., Lodhi, A. & Mansha, M. 2015. Seasonal variations of aerosols in Pakistan: Contributions of domestic anthropogenic emissions and transboundary transport. *Aerosol and Air Quality Research*. <https://doi.org/10.4209/aaqr.2014.12.0332>

Sharif, F., Alam, K. & Afsar, S. 2015. Spatio-Temporal distribution of aerosol and cloud properties over Sindh using MODIS satellite data and a HYSPLIT model. *Aerosol and Air Quality Research*. <https://doi.org/10.4209/aaqr.2014.09.0200>

Sharma, A.R., Kharol, S.K., Badarinath, K.V.S. & Singh, D. 2010. Impact of agriculture crop residue burning on atmospheric aerosol loading — A study over Punjab State, India. *Annales Geophysicae*. <https://doi.org/10.5194/angeo-28-367-2010>

Sifakis, N.I., Soulakellis, A.A. & Paronis, D.K. 1998.

Quantitative mapping of air pollution density using Earth observations: A new processing method and application to an urban area. *International Journal of Remote Sensing*. <https://doi.org/10.1080/014311698213975>

Sillman, S. & Samson, P.J. 1995. Impact of temperature on oxidant photochemistry in urban polluted rural and remote environments. *Journal of Geophysical Research*. <https://doi.org/10.1029/94jd02146>

Sillman, S. 1999. The relation between ozone, NO(x) and hydrocarbons in urban and polluted rural environments

Singh, R.P. & Kaskaoutis, D.G. 2014. Crop residue burning: A threat to South Asian air quality. *Eos*. <https://doi.org/10.1002/2014E0370001>

Sisneros, M.A. 2014. Evaluation of O₃ Trends in Southern Doña Ana County, New Mexico Thru Wind Rose Analysis and Use of Noaa Hysplit Model. M.Sc. thesis. The University Of Texas At El Paso, Department of Civil Engineering, El Paso, Texas.

Smirnov, A., Holben, B.N., Eck, T.F., Dubovik, O. & Slutsker, I. 2000. Cloud—screening and quality control algorithms for the AERONET database. *Remote Sensing of Environment*. [https://doi.org/10.1016/S0034-4257\(00\)00109-7](https://doi.org/10.1016/S0034-4257(00)00109-7)

Smirnov, A., Holben, B.N., Kaufman, Y.J., Dubovik, O., Eck, F., Slutsker, I., Pietras, C. & Halthore, R.N. 2002. Optical properties of atmospheric aerosol in maritime environments. *Journal of the Atmospheric Sciences*. [https://doi.org/10.1175/1520-0469\(2002\)059<0501:opoaai>2.0.co;2](https://doi.org/10.1175/1520-0469(2002)059<0501:opoaai>2.0.co;2)

Soares Neto, T.G., Carvalho, J.A., Veras, C.A.G., Alvarado, E.C., Gielow, R., Lincoln, E.N., Christian, T.J., Yokelson, R.J. & Santos, J.C. 2009. Biomass consumption and CO₂, CO and main hydrocarbon gas emissions in an Amazonian forest clearing fire. *Atmospheric Environment*. <https://doi.org/10.1016/j.atmosenv.2008.07.063>

Sofiev, M., Vankevich, R., Lotjonen, M., Prank, M., Petukhov, V., Ermakova, T., Koskinen, J. & Kukkonen, J. 2009. An operational system for the assimilation of the satellite information on wild—land fires for the needs of air quality modelling and forecasting. *Atmospheric Chemistry and Physics*. <https://doi.org/10.5194/acp-9-6833-2009>

Stevenson, D.S., Young, P.J., Naik, V., Lamarque, J.F., Shindell, D.T., Voulgarakis, A., Skeie, R.B., Dalsoren, S.B., Myhre, G., Berntsen, T.K., Folberth, G.A., Rumbold, S.T., Collins, W.J., MacKenzie, I.A., Doherty, R.M., Zeng, G., Van Noije, T.P.C., Strunk, A., Bergmann, D., Cameron-Smith, P., Plummer, D.A., Strode, S.A., Horowitz, L., Lee, Y.H., Szopa, S., Sudo, K., Nagashima, T., Josse, B., Cionni, I., Righi, M., Eyring, V., Conley, A., Bowman, K.W., Wild, O. & Archibald, A. 2013. Tropospheric

ozone changes, radiative forcing and attribution to emissions in the Atmospheric Chemistry and Climate Model Intercomparison Project (ACCMIP). *Atmospheric Chemistry and Physics*. <https://doi.org/10.5194/acp-13-3063-2013>

Stocker, T.F., Qin, D., Plattner, G.K., Tignor, M.M.B., Allen, S.K., Boschung, J., Nauels, A., Xia, Y., Bex, V. & Midgley, P.M. 2013. Climate change 2013 the physical science basis: Working Group I contribution to the fifth assessment report of the intergovernmental panel on climate change.

Sukhinin, A.I., French, N.H.F., Kasischeke, E.S., Hewson, J.H., Soja, A.J., Csiszar, I.A., Hyer, E.J., Loboda, T., Conrad, S.G., Romasko, V.I., Pavlichenko, E.A., Miskiv, S.I. & Slinkina, O.A. 2004. AVHRR—based mapping of fires in Russia: New products for fire management and carbon cycle studies. *Remote Sensing of Environment*. <https://doi.org/10.1016/j.rse.2004.08.011>

Tariq, S. & Ali, M. 2015. Spatio—temporal distribution of absorbing aerosols over Pakistan retrieved from OMI onboard aura satellite. *Atmospheric Pollution Research*. <https://doi.org/10.5094/APR.2015.030>

Tariq, S., Zia, ul H. & Ali, M. 2016. Satellite and ground—based remote sensing of aerosols during intense haze event of October 2013 over Lahore, Pakistan. *Asia—Pacific Journal of Atmospheric Sciences*. <https://doi.org/10.1007/s13143-015-0084-3>

Torregrosa, A., Combs, C. & Peters, J. 2016. GOES—derived fog and low cloud indices for coastal north and central California ecological analyses. *Earth and Space Science*. <https://doi.org/10.1002/2015EA000119>

Turab Hussain, S., Khan, U., Zaheer Malik, K. & Faheem, A. 2012. The Constraints to Industry in Punjab, Pakistan. *THE LAHORE JOURNAL OF ECONOMICS*. <https://doi.org/10.35536/lje.2012.v17.isp.a7>

Ul—Haq, Z., Rana, A.D., Ali, M., Mahmood, K., Tariq, S. & Qayyum. 2015. Carbon monoxide (CO) emissions and its tropospheric variability over Pakistan using satellite—sensed data. *Advances in Space Research*. <https://doi.org/10.1016/j.asr.2015.04.026>

ul—Haq, Z., Tariq, S., Ali, M., Daud Rana, A. & Mahmood, K. 2017. Satellite—sensed tropospheric NO₂ patterns and anomalies over Indus, Ganges, Brahmaputra, and Meghna river basins. *International Journal of Remote Sensing*. <https://doi.org/10.1080/01431161.2017.1283071>

Vadrevu, K.P., Ellicott, E., Badarinath, K.V.S. & Vermote, E. 2011. MODIS derived fire characteristics and aerosol optical depth variations during the agricultural residue burning season, north India. *Environmental Pollution*. <https://doi.org/10.1016/j.envpol.2011.03.001>

Vadrevu, K.P., Ellicott, E., Giglio, L., Badarinath, K.V.S., Vermote,

E., Justice, C. & Lau, W.K.M. 2012. Vegetation fires in the himalayan region — Aerosol load, black carbon emissions and smoke plume heights. *Atmospheric Environment*. <https://doi.org/10.1016/j.atmosenv.2011.11.009>

Vaughan, M.A., Powell, K.A., Kuehn, R.E., Young, S.A., Winker, M., Hostetler, C.A., Hunt, W.H., Liu, Z., McGill, M.J. & Getzewich, B.J. 2009. Fully automated detection of cloud and aerosol layers in the CALIPSO lidar measurements. *Journal of Atmospheric and Oceanic Technology*. <https://doi.org/10.1175/2009JTECHA1228.1>

Wang, K., Dickinson, R.E. & Liang, S. 2009. Clear sky visibility has decreased over land globally from 1973 to 2007. *Science*. <https://doi.org/10.1126/science.1167549>

Waquet, F., Cornet, C., Deuzé, J.L., Dubovik, O., Ducos, F., Goloub, P., Herman, M., Lapyonok, T., Labonnote, L. C., Riedi, J., Tanré, D., Thieuleux, F. & Vanbauce, C. 2013. Retrieval of aerosol microphysical and optical properties above liquid clouds from POLDER/PARASOL polarization measurements. *Atmospheric Measurement Techniques*. <https://doi.org/10.5194/amt-6-991-2013>

Wen, X., Hu, D., Dong, X., Yu, F., Tan, D., Li, Z., Liang, Y., Xiang, D., Shen, S., Hu, C. & Cao, B. 2014. An object-oriented daytime land fog detection approach based on NDFI and fractal dimension using EOS/MODIS data. *International Journal of Remote Sensing*. <https://doi.org/10.1080/01431161.2014.930564>

Wiedinmyer, C., Akagi, S.K., Yokelson, R.J., Emmons, L.K., Al-Saadi, J.A., Orlando, J.J. & Soja, A.J. 2011. The Fire Inventory from NCAR (FINN): A high resolution global model to estimate the emissions from open burning. *Geoscientific Model Development*. <https://doi.org/10.5194/gmd-4-625-2011>

Winker, D.M., Vaughan, M.A., Omar, A., Hu, Y., Powell, K.A., Liu, Z., Hunt, W.H. & Young, S.A. 2009. Overview of the CALIPSO mission and CALIOP data processing algorithms. *Journal of Atmospheric and Oceanic Technology*. <https://doi.org/10.1175/2009JTECHA1281.1>

Wooster, M.J. 2002. Small-scale experimental testing of fire radiative energy for quantifying mass combusted in

natural vegetation fires. *Geophysical Research Letters*. <https://doi.org/10.1029/2002GL015487>

Wooster, M.J. & Zhang, Y.H. 2004. Boreal forest fires burn less intensely in Russia than in North America. *Geophysical Research Letters*. <https://doi.org/10.1029/2004GL020805>

Wooster, M.J., Roberts, G., Perry, G.L.W. & Kaufman, Y.J. 2005. Retrieval of biomass combustion rates and totals from fire radiative power observations: FRP derivation and calibration relationships between biomass consumption and fire radiative energy release. *Journal of Geophysical Research Atmospheres*. <https://doi.org/10.1029/2005JD006318>

Worton, B.J. 1989. Kernel methods for estimating the utilization distribution in home-range studies. *Ecology*. <https://doi.org/10.2307/1938423>

Yoon, J., Burrows, J.P., Vountas, M., Von Hoyningen-Huene, W., Chang, D.Y., Richter, A. & Hilboll, A. 2014. Changes in atmospheric aerosol loading retrieved from space-based measurements during the past decade. *Atmospheric Chemistry and Physics*. <https://doi.org/10.5194/acp-14-6881-2014>

Yasmeen, G., Rasul, G., Zahid, M. 2012. Impacts of aerosols on winter fog of Pakistan. *Pakistan Journal of Meteorology*

Zafar, Q., Zafar, S. & Holben, B. 2018. Seasonal assessment and classification of aerosols transported to Lahore using AERONET and MODIS deep blue retrievals. *International Journal of Climatology*. <https://doi.org/10.1002/joc.5230>

Zhang, H., Hu, J., Qi, Y., Li, C., Chen, J., Wang, X., He, J., Wang, S., Hao, J., Zhang, L., Zhang, L., Zhang, Y., Li, R., Wang, S. & Chai, F. 2017. Emission characterization, environmental impact, and control measure of PM_{2.5} emitted from agricultural crop residue burning in China. *Journal of Cleaner Production*. <https://doi.org/10.1016/j.jclepro.2017.02.092>

Zhao, T.X.P., Laszlo, I., Guo, W., Heidinger, A., Cao, C., Jelenak, A., Tarpley, D. & Sullivan, J. 2008. Study of long-term trend in aerosol optical thickness observed from operational AVHRR satellite instrument. *Journal of Geophysical Research Atmospheres*. <https://doi.org/10.1029/2007JD009061>

ul-Haq, Z., Tariq, S. & Ali, M. 2017. Spatiotemporal assessment of CO₂ emissions and its satellite remote sensing over Pakistan and neighboring regions. *Journal of Atmospheric and Solar-Terrestrial Physics*. <https://doi.org/10.1016/j.jastp.2016.11.001>

APPENDICES

APPENDIX A — NUMBER OF FOCUS GROUP DISCUSSIONS CONDUCTED BY TEHSIL AND DISTRICT

District	Tehsil	Number of FGDs Conducted
FAISALABAD	CHAK JHUMRA	2
	FAISALABAD	5
	JARANWALA	2
	SUMUNDARI	2
	TANDLIAN WALA	2
	Total	13
GUJRANWALA	GUJRANWALA	3
	KAMOKI	2
	NOSHERA VIRKA	3
	WAZIRABAD	3
	Total	11
GUJRAT	GUJRAT	6
	KHARIAN	3
	SARI—ALAMGIR	2
	Total	11
HAFIZABAD	HAFIZABAD	5
	PINDI BHATTIYAN	5
	Total	10
KASUR	CHUNIYAAN	1
	KASUR	2
	KOT RADHA KISHAN	3
	PATTOKI	3
	Total	9
LAHORE	LAHORE CANTT	5
	LAHORE CITY	7
	Total	12
MANDI BAHAUDDIN	MALIK WAL	3
	MB DIN	4
	PHALIA	5
	Total	12
NANKANA SAHIB	NANKANA SAHIB	6
	SANGLA HILL	3
	SHAHKOT	3
	Total	12



District	Tehsil	Number of FGDs Conducted
NAROWAL	NAROWAL	4
	NAROWAL/ZAFARWAL	2
	SHAKARGARH	4
	Total	10
SHEIKHUPURA	FEROZEWALA	1
	MURIDKE	3
	SAFDARABAD	2
	SHARAQPUR	2
	SHIEKHUPURA	3
	Total	11
SIALKOT	DASKA	3
	PASRUR	2
	SAMBRIAL	2
	SIALKOT	5
	Total	12
		123

APPENDIX B – LIST OF UNION COUNCILS SURVEYED DURING THE FOCUS GROUP DISCUSSIONS

District	Tehsil	Union Council
FAISALABAD	CHAK JHUMRA	126 RB
		146 RB
	FAISALABAD	208 R.B
		209 R.B
		202 R.B
		199 R.B
		229 RB.
		200 RB.
	JARANWALA	103 RB.
	SUMUNDARI	201
		228 GB
	TANDLIANWALA	416 GB
		MUNICIPAL COMETTI
GUJRANWALA	GUJRANWALA	KOT SHERA
		ARUP
		BUTRAN WALI
	KAMOKI	SADOKI
		CHAK RAMDAS
	NOSHERA VIRKA	ABIDABAD
		BUDHA GORAYA
		NO KHAR
		NAT KALAN
	WAZIRABAD	AHMED NAGAR
		MANSOOR WALI
GUJRAT	GUJRAT	KARIANWALA
		ANJALA
		MANGOWAL GHARBI
		FATEH PUR
		DAULAT NAGAR
		MURALA GUJRAN
	KHARIAN	KOTLA ARAB ALI
		SEKRALI
		DHORIA
	SARAI—ALAMGIR	BAGH NAGAR
		KHOHAR
HAFIZABAD	HAFIZABAD	SHAH JAMAL
		CHAK CHATA
		KALIKI MANDI



District	Tehsil	Union Council
		VANEEKY TARD
		KOLU TARD
	PINDI BHATTIYAN	BHALUPUR
		RASOOL PUR TARD
		KOT SARWAR
		SADHOKI
		KHURAM CHARIRA
KASUR	CHUNIYAAN	ALLA ABAD
	KASUR	BAHADUR PURA
		FATEH PUR
	KOT RADHA KISHAN	RAJOWAL
		MATTA
		ZAFAR KEY
	PATTOKI	AKBAR ABAD
		GHUMANKE
LAMBAY JAGIR		
LAHORE	LAHORE CANTT	BARKI
		HALLOKEE
		BHASEEN
		WARRAICH
		KAHANA NOH
	LAHORE CITY	SHAHPUR KANJРАН
		MARAKA
		ALI RAZA ABAD
		PAJIAN
		MANGAN
		CHUNG
		SHAMKI BHATTIAN
MANDI BAHAUDDIN	MALIK WAL	RUKKAN
		CHAK RAIB
		HARIA
	MANDI BAHAUDDIN	MIAN WALA
		MANGAT
		MOJIAN WALA
		DHOK KASIB
	PHALIA	DHUNNI KALAN
		BHEIKHO
		DHEREKAN KLAN
		JANO CHAK
PAHRIANWALI		

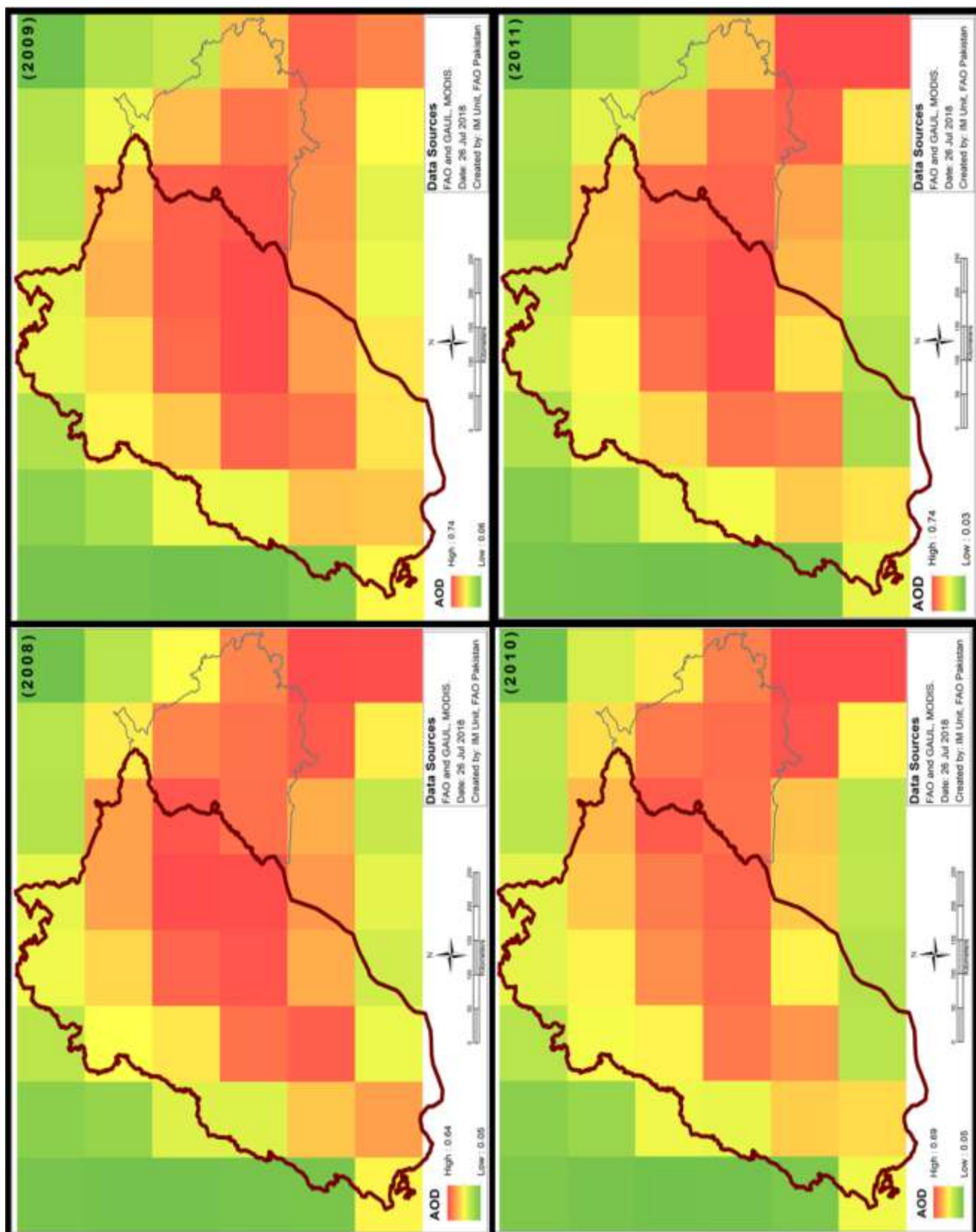


NANKANA SAHIB	NANKANA SAHIB	KOT HUSSAIN KHAN
		NABI PAR PIRAN
		MACHIRALA
		NO.63 SYED WALA
		U.C 34 KOT NAMDAR
		NATHA
	SANGLA HILL	BAHLIR CHAK
		NO.43 R.B
		MUD BALOCHAN
	SHAHKOT	U.C NO.176PANWAN
		CHAK 83 R.B DALA JARMIYAN
		KOT NIZAM DIN
NAROWAL	NAROWAL	TALWANDI BHINDRAN
		JASSAR
		CHANDOWAL
		DAM THAL
		JANDYALA
		DARA PUR
	SHAKARGARH	CHAK AMRO
		PHUL WARI
		ARA MANGA
		KOT NAINA
SHEIKHUPURA	FEROZEWALA	KHAN PUR
	MURIDKE	QILA SITAR SHAH
		LAMBRA
		KALA KHATAI
	SAFDARABAD	RATTI TIBI
		SALAR BHATIA
	SHARAQPUR	KOT MEHMOOD
		SAJOWAL
	SHIEKHUPURA	BAKHI
		JANDIAL SHER KHAN
		NOKHAR
	SIALKOT	DASKA
GALOTIAN KHURD		
SATRAH		
PASRUR		BADIANA
		SOKANVIND
SAMBRIAL		BADOKE CHEEMA
		HABIBPUR



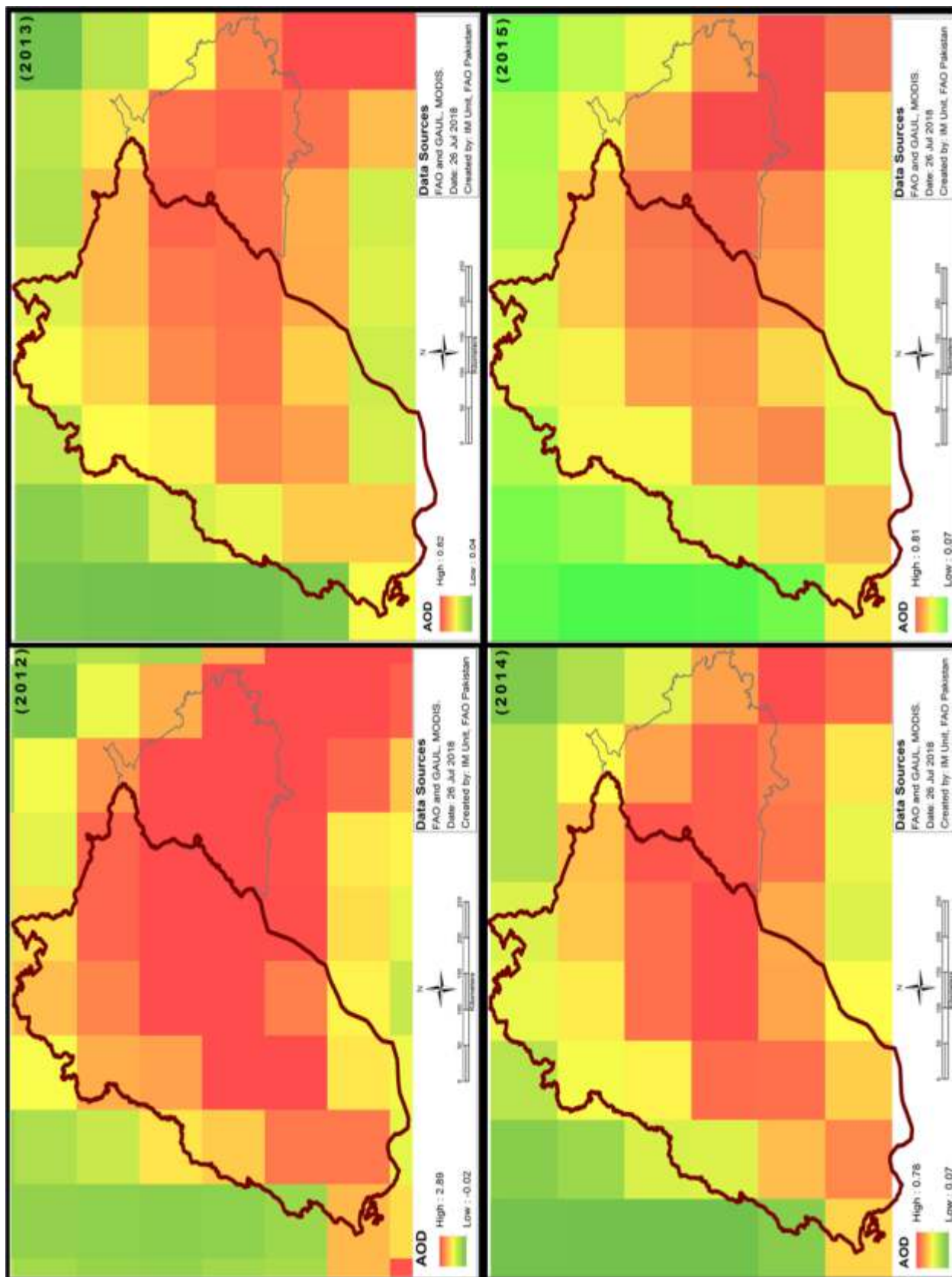
	SIALKOT	KAPOOR PUR
		MALKHAN WALA
		MARALA
		KOTLI COHARAN

APPENDIX C – YEAR WISE MAPPING OF AOD (2008–2018)



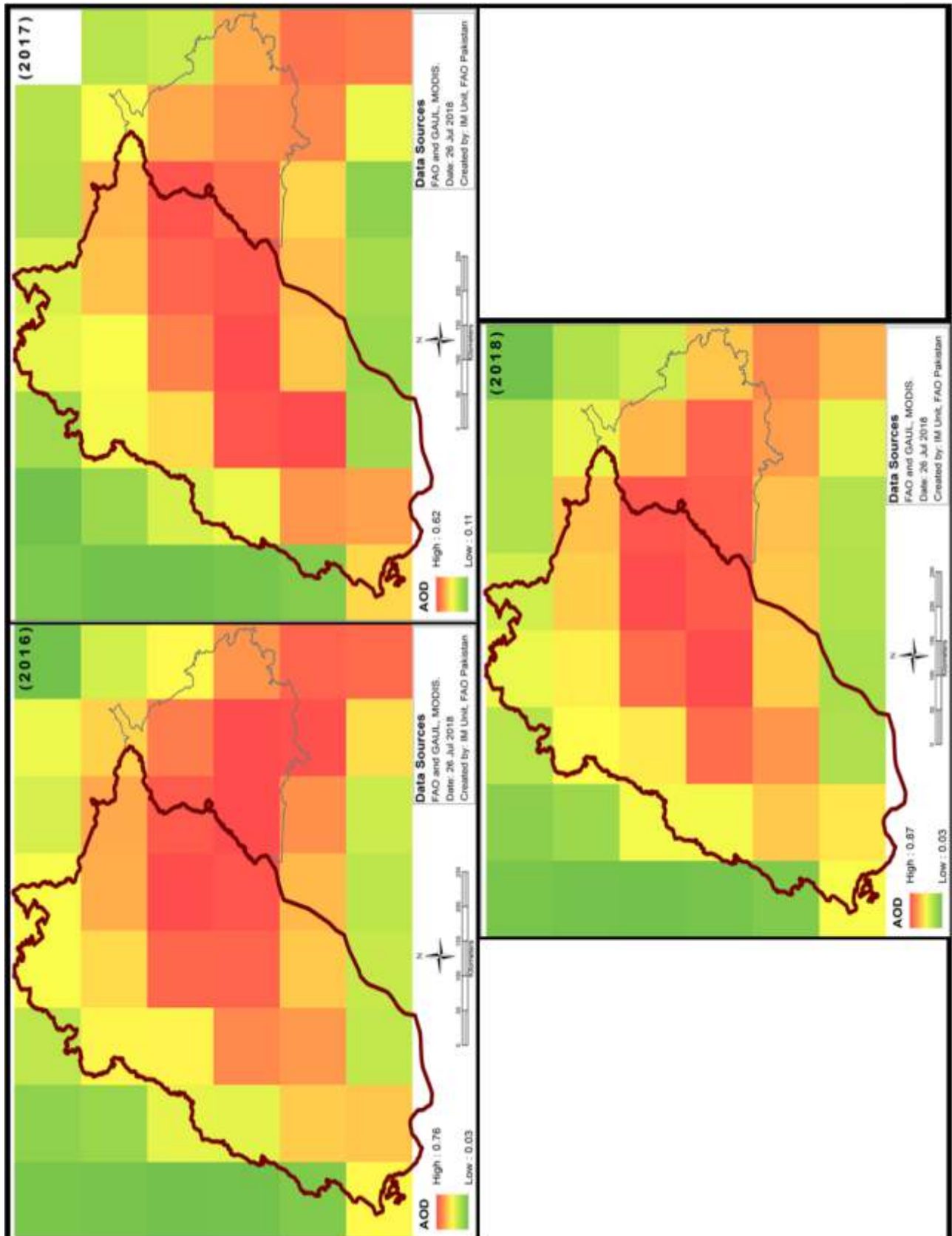
Disclaimer: The boundaries and names shown and the designation used on this map do not imply official endorsement or acceptance by the United Nations. Dotted line represents approximately the Line of Control in Jammu and Kashmir. The final status of Jammu and Kashmir has not yet been agreed upon by the parties.

Source: Adapted from United Nations World map, February 2020.



Disclaimer: The boundaries and names shown and the designation used on this map do not imply official endorsement or acceptance by the United Nations. Dotted line represents approximately the Line of Control in Jammu and Kashmir agreed upon by India and Pakistan. The final status of Jammu and Kashmir has not yet been agreed upon by the parties.

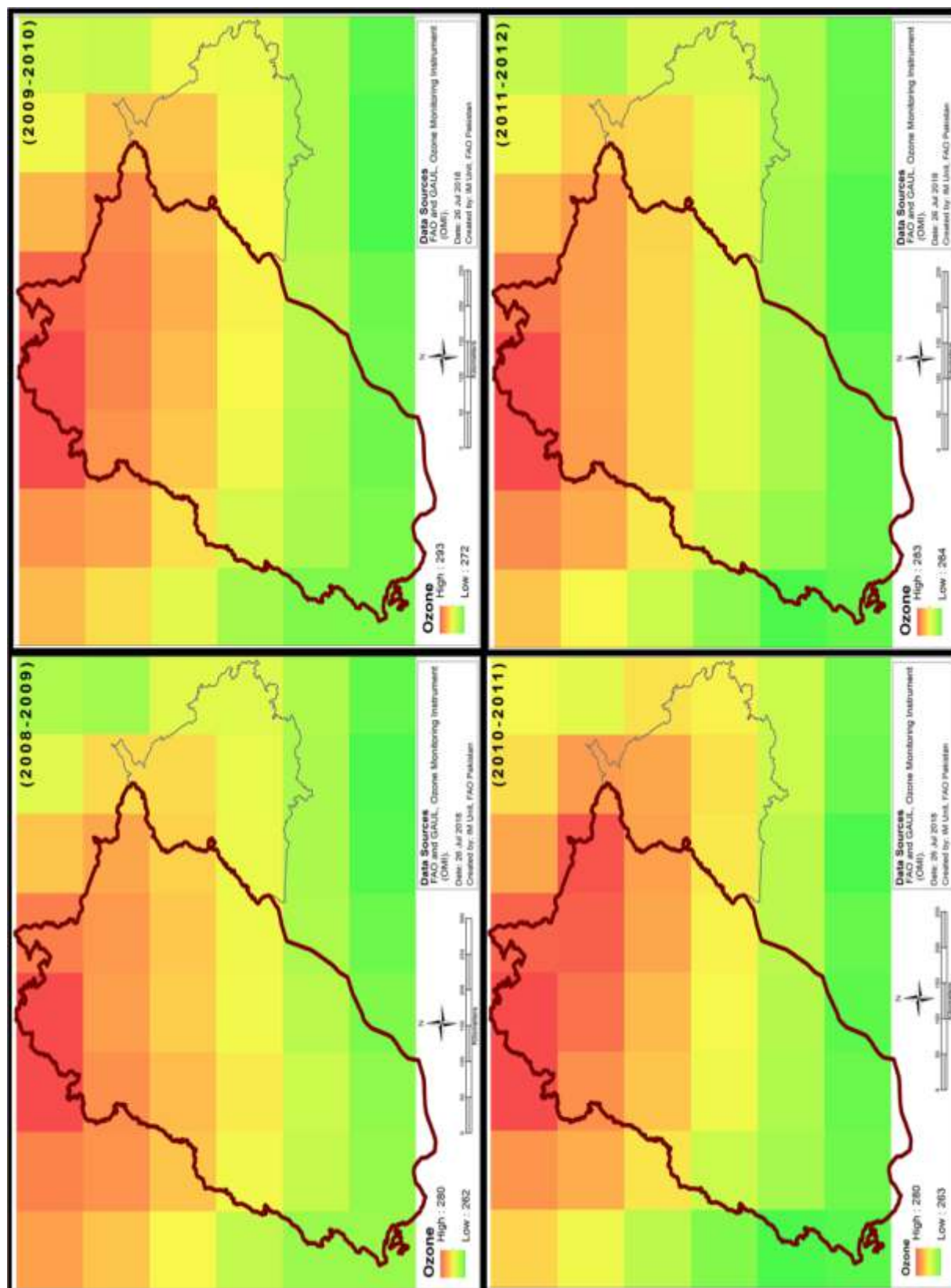
Source: Adapted from United Nations World map, February 2020.



Disclaimer: The boundaries and names shown and the designation used on this map do not imply official endorsement or acceptance by the United Nations. Dotted line represents approximately the Line of Control in Jammu and Kashmir agreed upon by India and Pakistan. The final status of Jammu and Kashmir has not yet been agreed upon by the parties

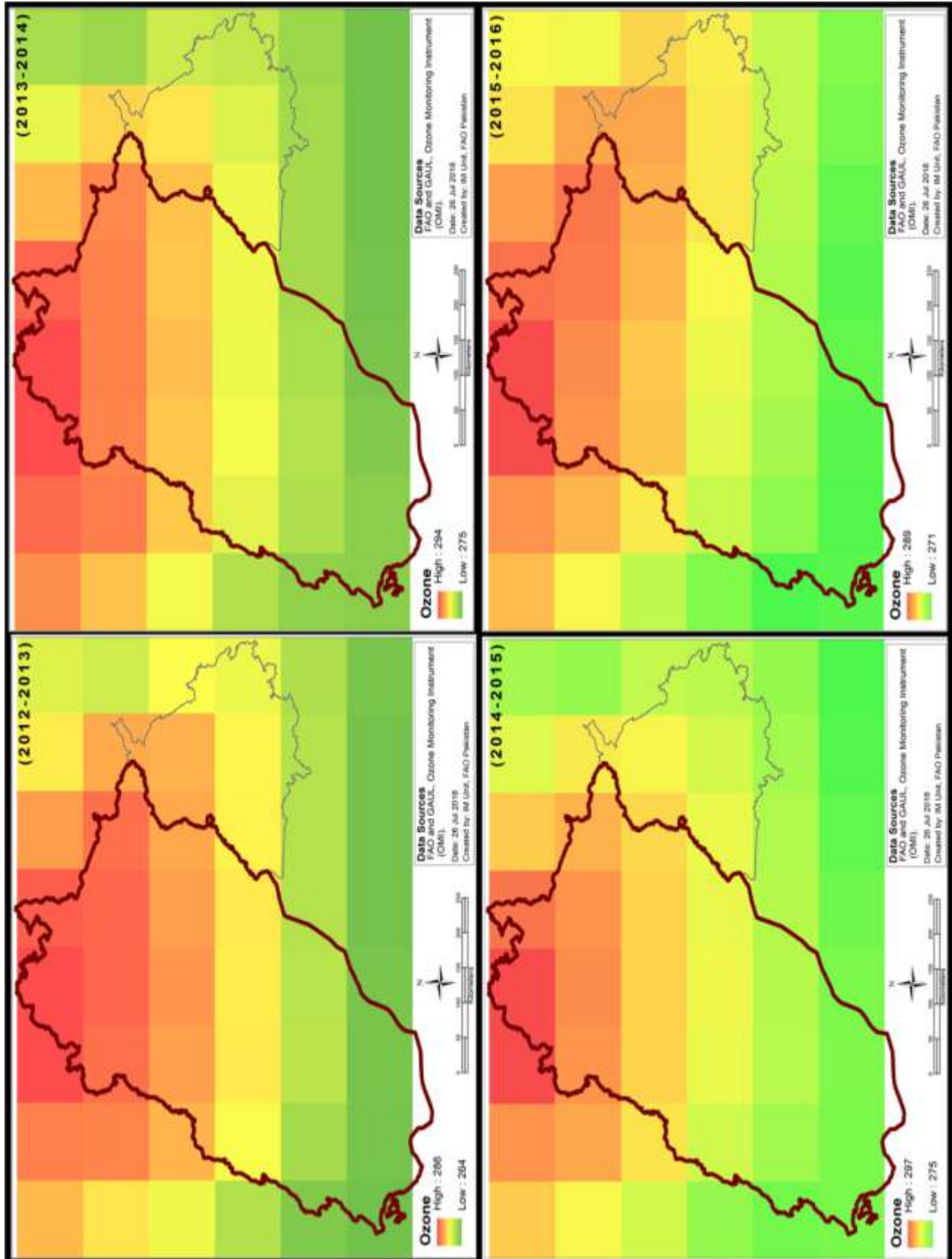
Source: Adapted from United Nations World map, February 2020.

APPENDIX D – YEAR WISE MAPPING OF OZONE (2008–2018)



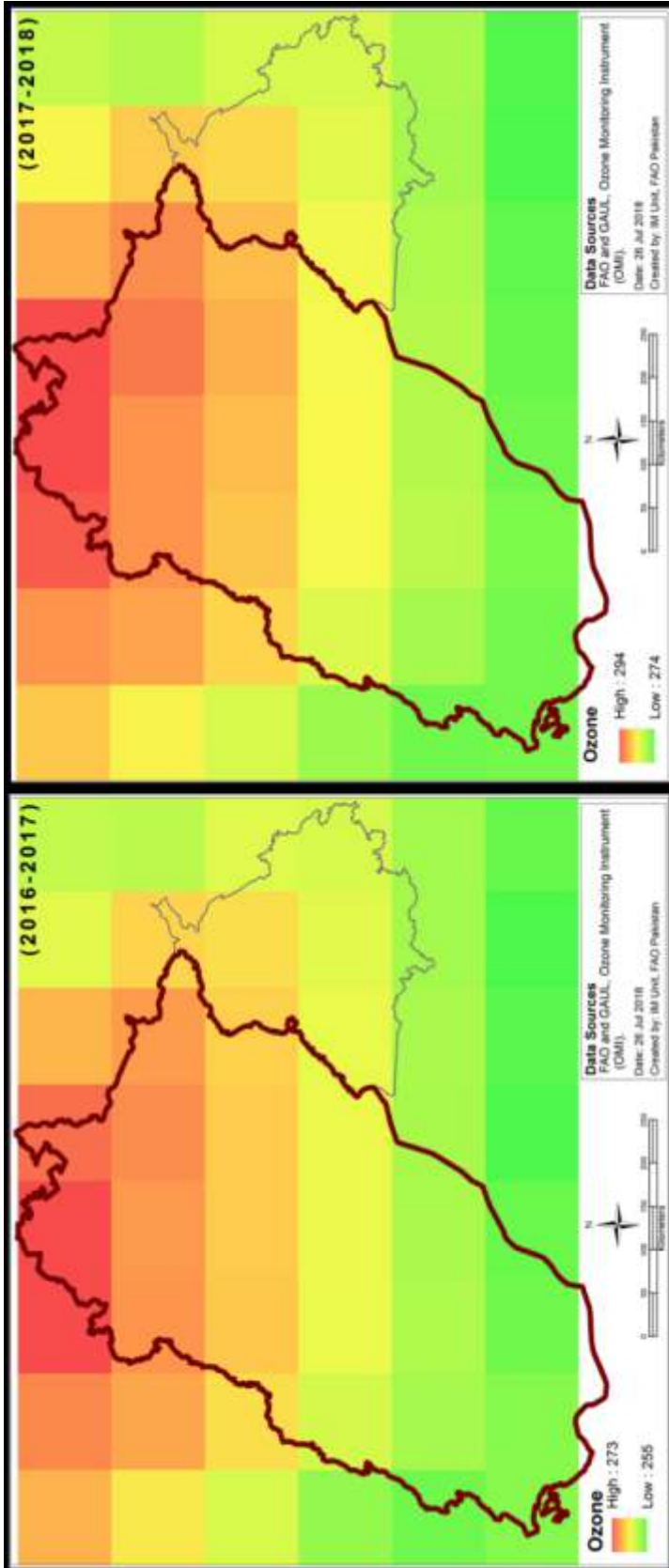
Source: Adapted from United Nations World map, February 2020.

Disclaimer: The boundaries and names shown and the designation used on this map do not imply official endorsement or acceptance by the United Nations. Dotted line represents approximately the Line of Control in Jammu and Kashmir agreed upon by India and Pakistan. The final status of Jammu and Kashmir has not yet been agreed upon by the parties.



Disclaimer: The boundaries and names shown and the designation used on this map do not imply official endorsement or acceptance by the United Nations. Dotted line represents approximately the Line of Control in Jammu and Kashmir agreed upon by India and Pakistan. The final status of Jammu and Kashmir has not yet been agreed upon by the parties.

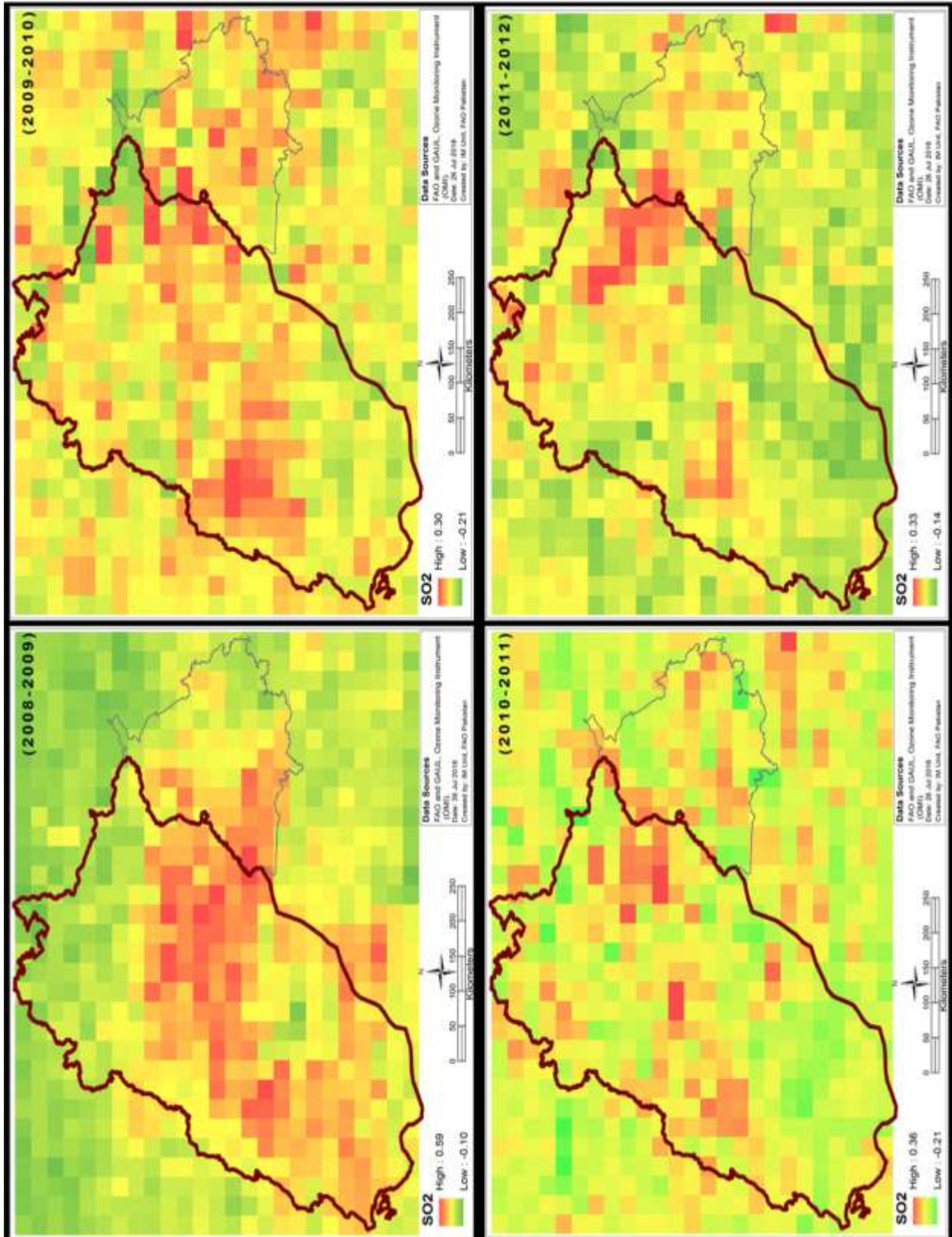
Source: Adapted from United Nations World map, February 2020.



Source: Adapted from United Nations World map, February 2020.

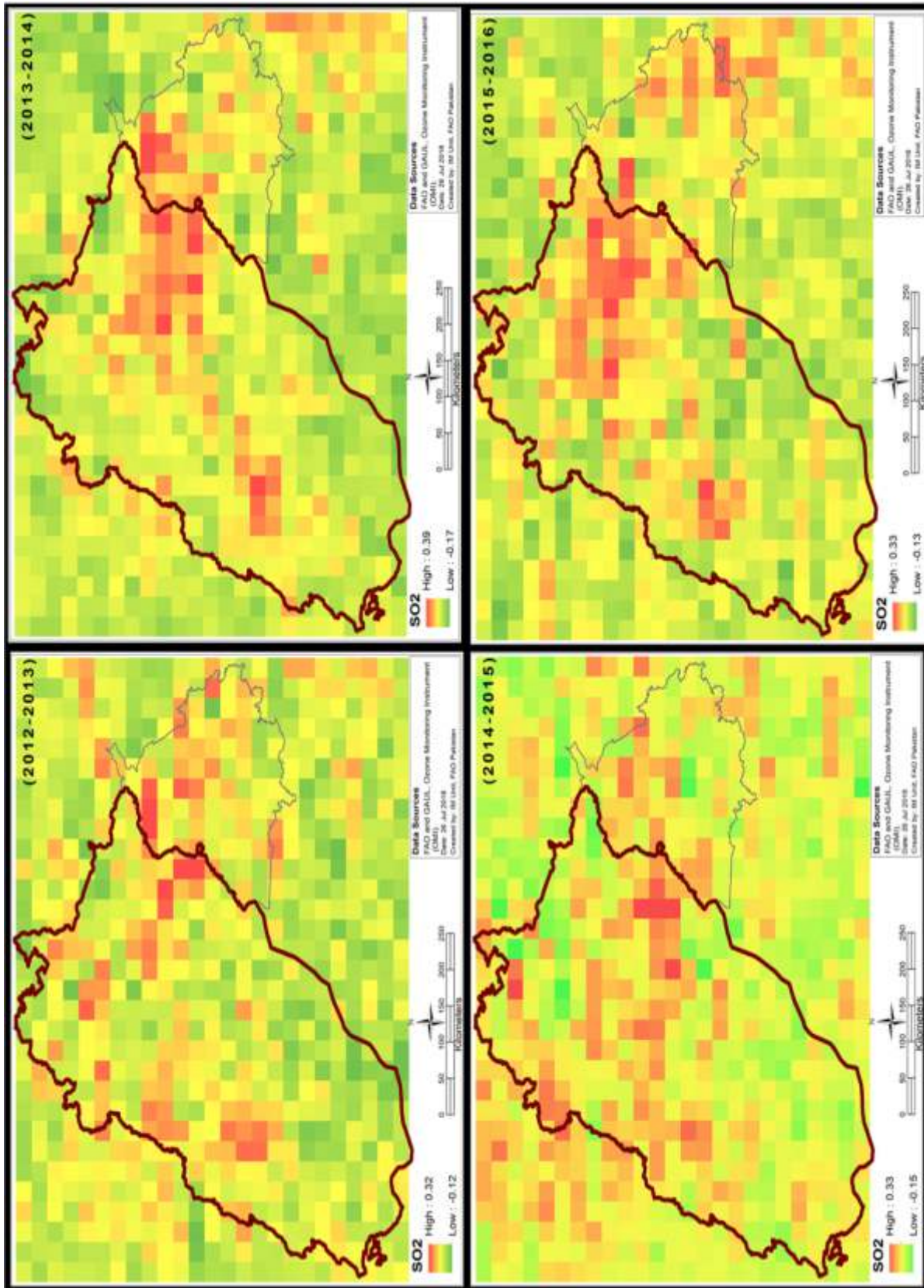
Disclaimer: The boundaries and names shown and the designation used on this map do not imply official endorsement or acceptance by the United Nations. Dotted line represents approximately the Line of Control in Jammu and Kashmir agreed upon by India and Pakistan. The final status of Jammu and Kashmir has not yet been agreed upon by the parties

APPENDIX E – YEAR WISE MAPPING OF SO₂ (2008–2018)



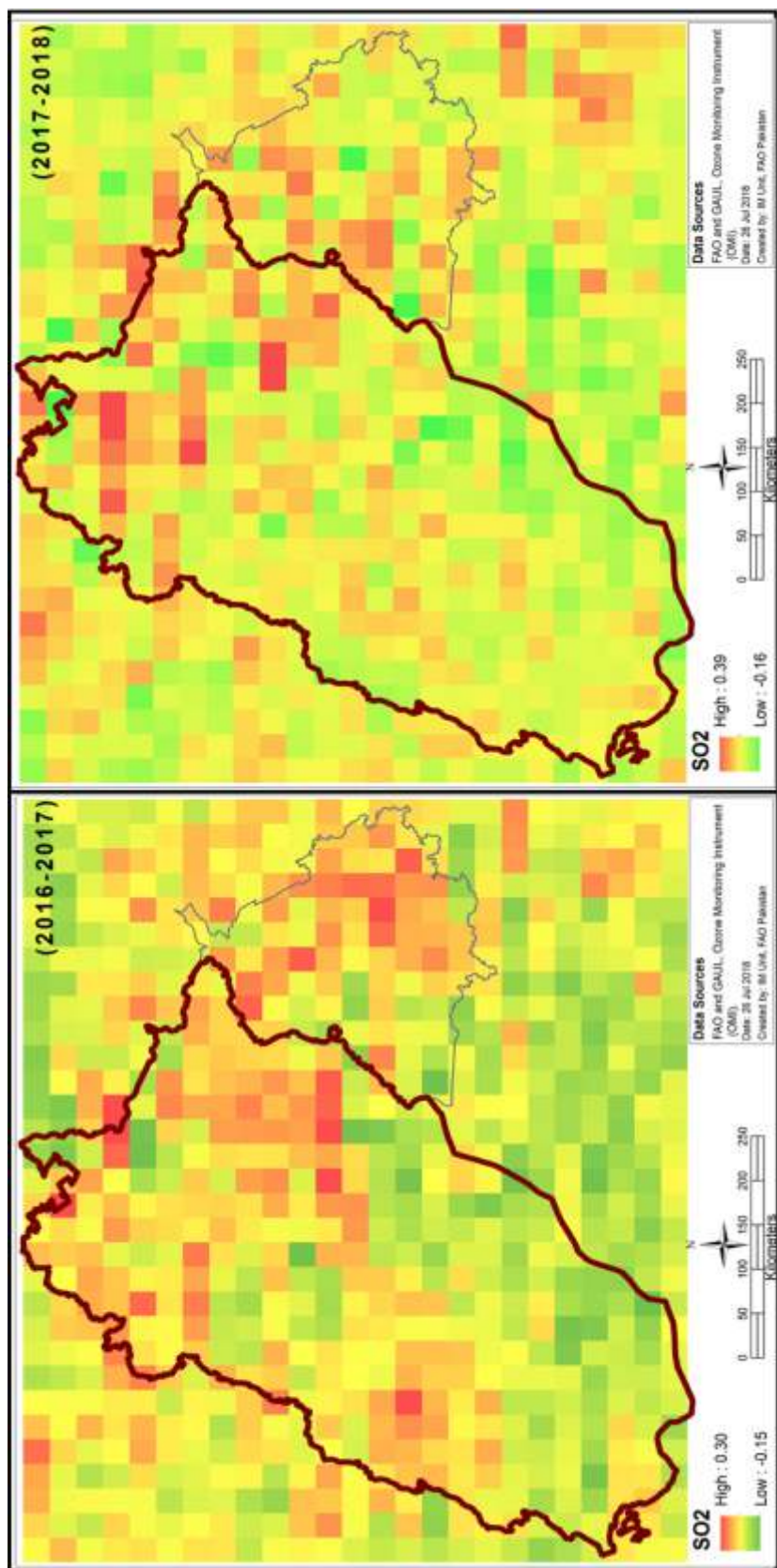
Disclaimer: The boundaries and names shown and the designation used on this map do not imply official endorsement or acceptance by the United Nations. Dotted line represents approximately the Line of Control in Jammu and Kashmir agreed upon by India and Pakistan. The final status of Jammu and Kashmir has not yet been agreed upon by the parties.

Source: Adapted from United Nations World map, February 2020.



Disclaimer: The boundaries and names shown and the designation used on this map do not imply official endorsement or acceptance by the United Nations. Dotted line represents approximately the Line of Control in Jammu and Kashmir agreed upon by India and Pakistan. The final status of Jammu and Kashmir has not yet been agreed upon by the parties.

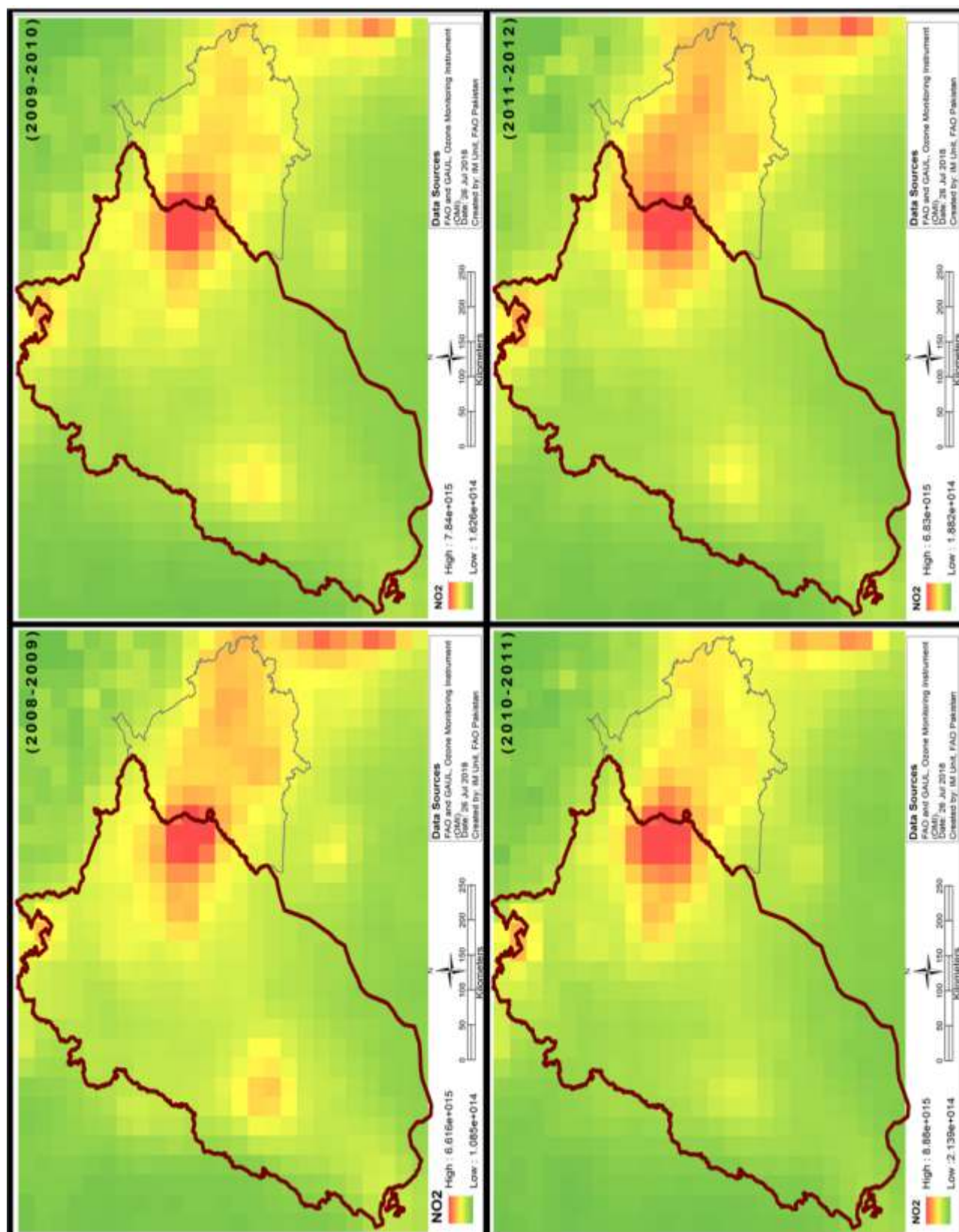
Source: Adapted from United Nations World map, February 2020.



Disclaimer: The boundaries and names shown and the designation used on this map do not imply official endorsement or acceptance by the United Nations. Dotted line represents approximately the Line of Control in Jammu and Kashmir agreed upon by India and Pakistan. The final status of Jammu and Kashmir has not yet been agreed upon by the parties

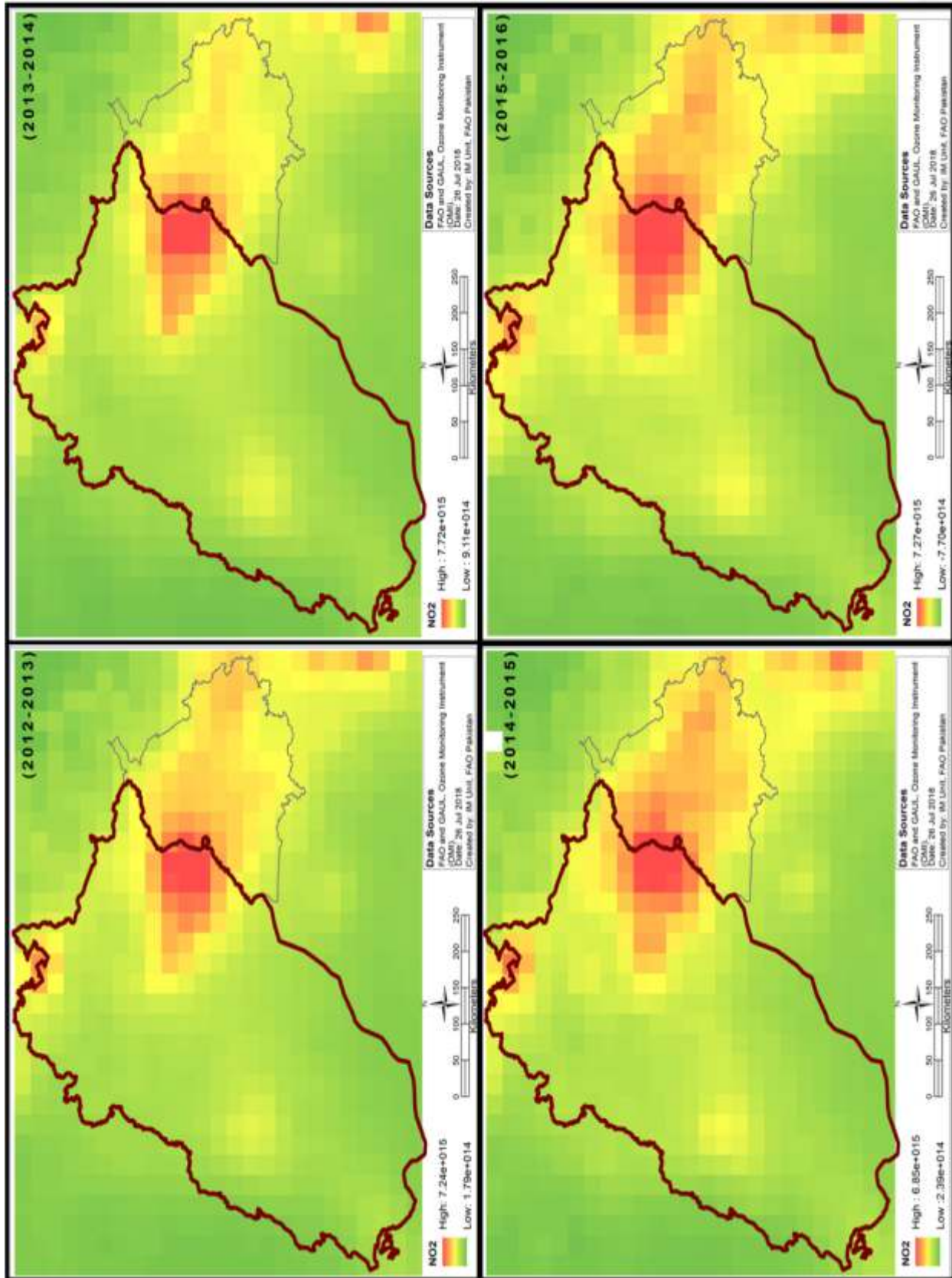
Source: Adapted from United Nations World map, February 2020.

APPENDIX F – YEAR WISE MAPPING OF NO₂ (2008–2018)



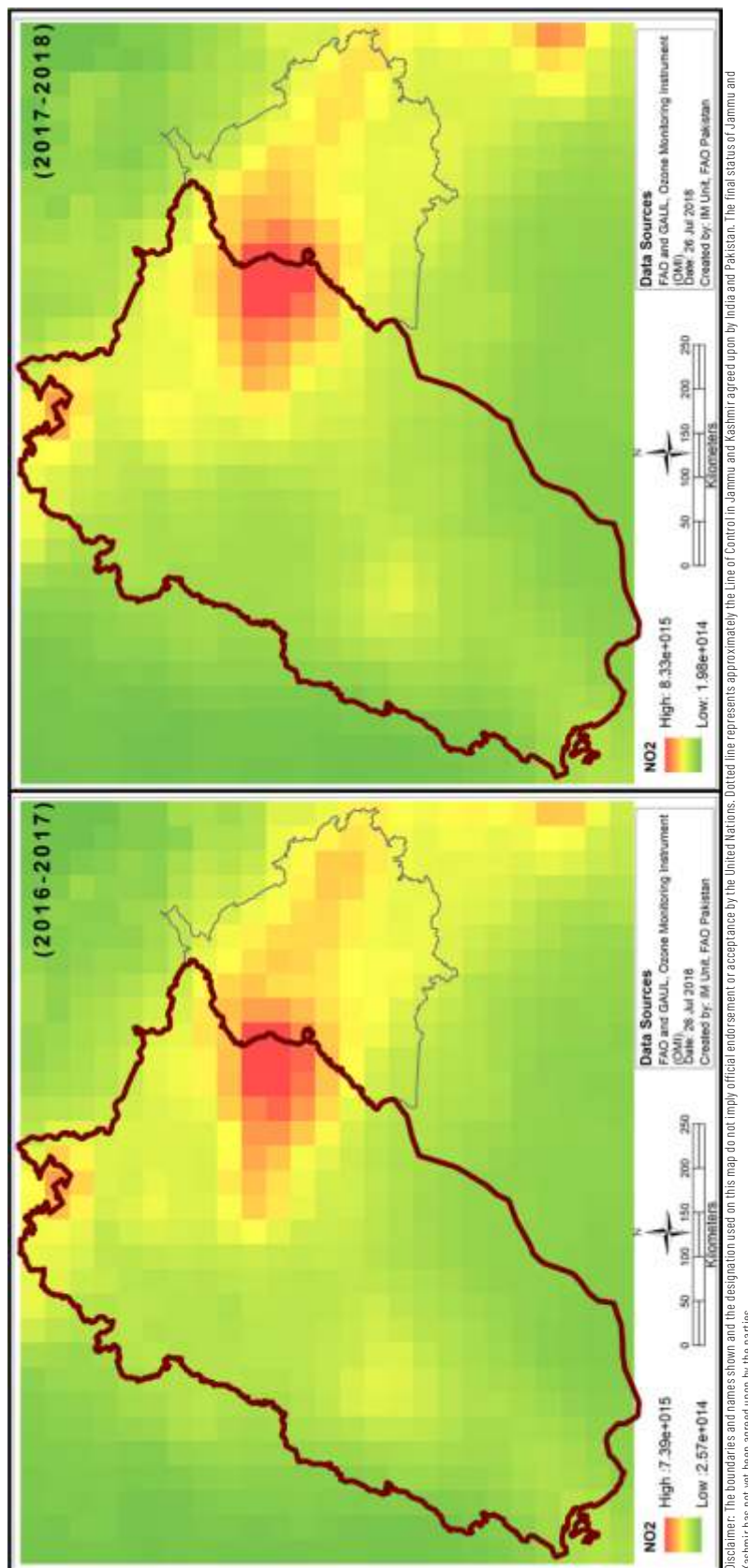
Source: Adapted from United Nations World map, February 2020.

Disclaimer: The boundaries and names shown and the designation used on this map do not imply official endorsement or acceptance by the United Nations. Dotted line represents approximately the Line of Control in Jammu and Kashmir agreed upon by India and Pakistan. The final status of Jammu and Kashmir has not yet been agreed upon by the parties.



Disclaimer: The boundaries and names shown and the designation used on this map do not imply official endorsement or acceptance by the United Nations. Dotted line represents approximately the Line of Control in Jammu and Kashmir agreed upon by India and Pakistan. The final status of Jammu and Kashmir has not yet been agreed upon by the parties

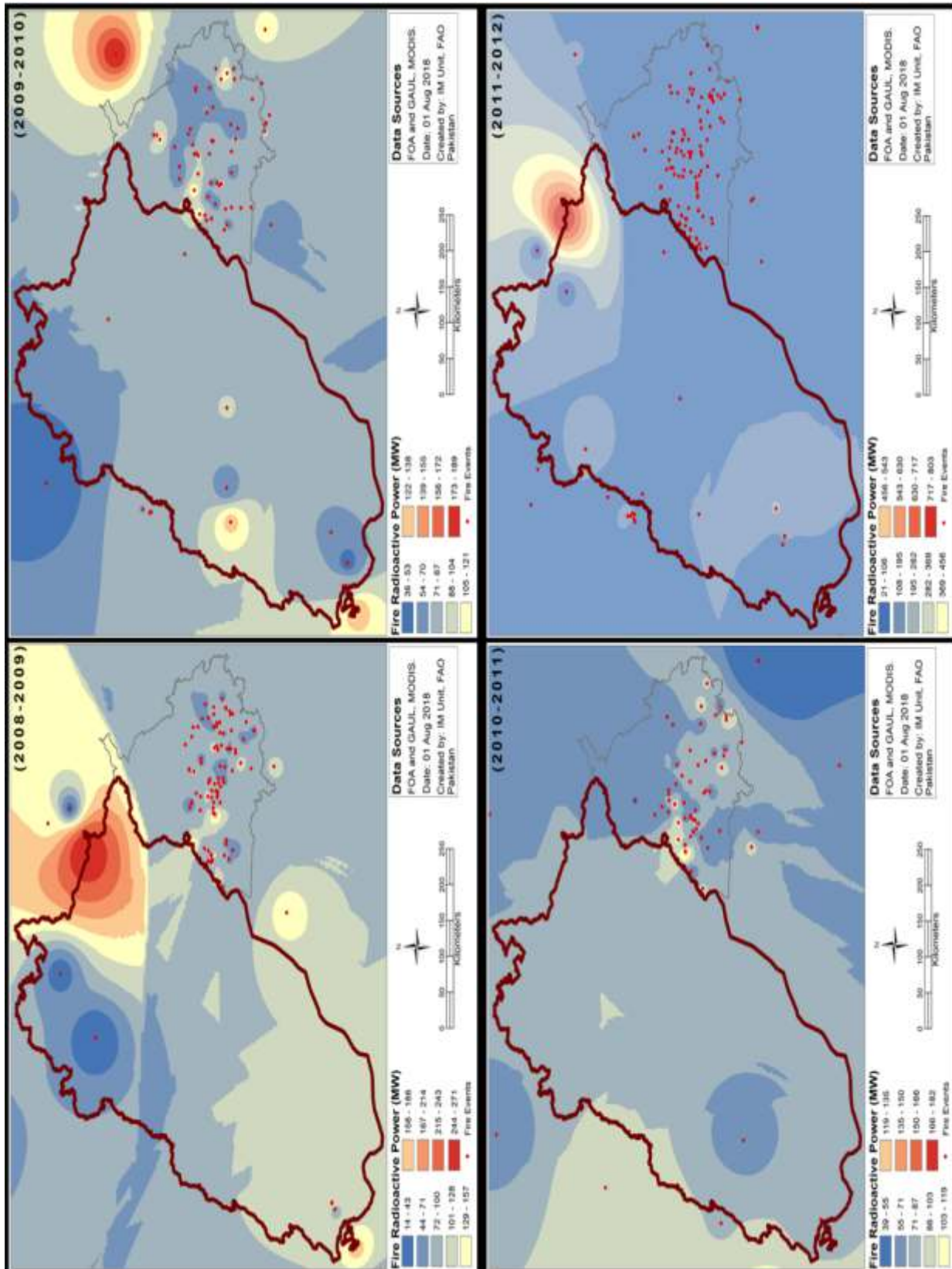
Source: Adapted from United Nations World map, February 2020.



Disclaimer: The boundaries and names shown and the designation used on this map do not imply official endorsement or acceptance by the United Nations. Dotted line represents approximately the Line of Control in Jammu and Kashmir agreed upon by India and Pakistan. The final status of Jammu and Kashmir has not yet been agreed upon by the parties

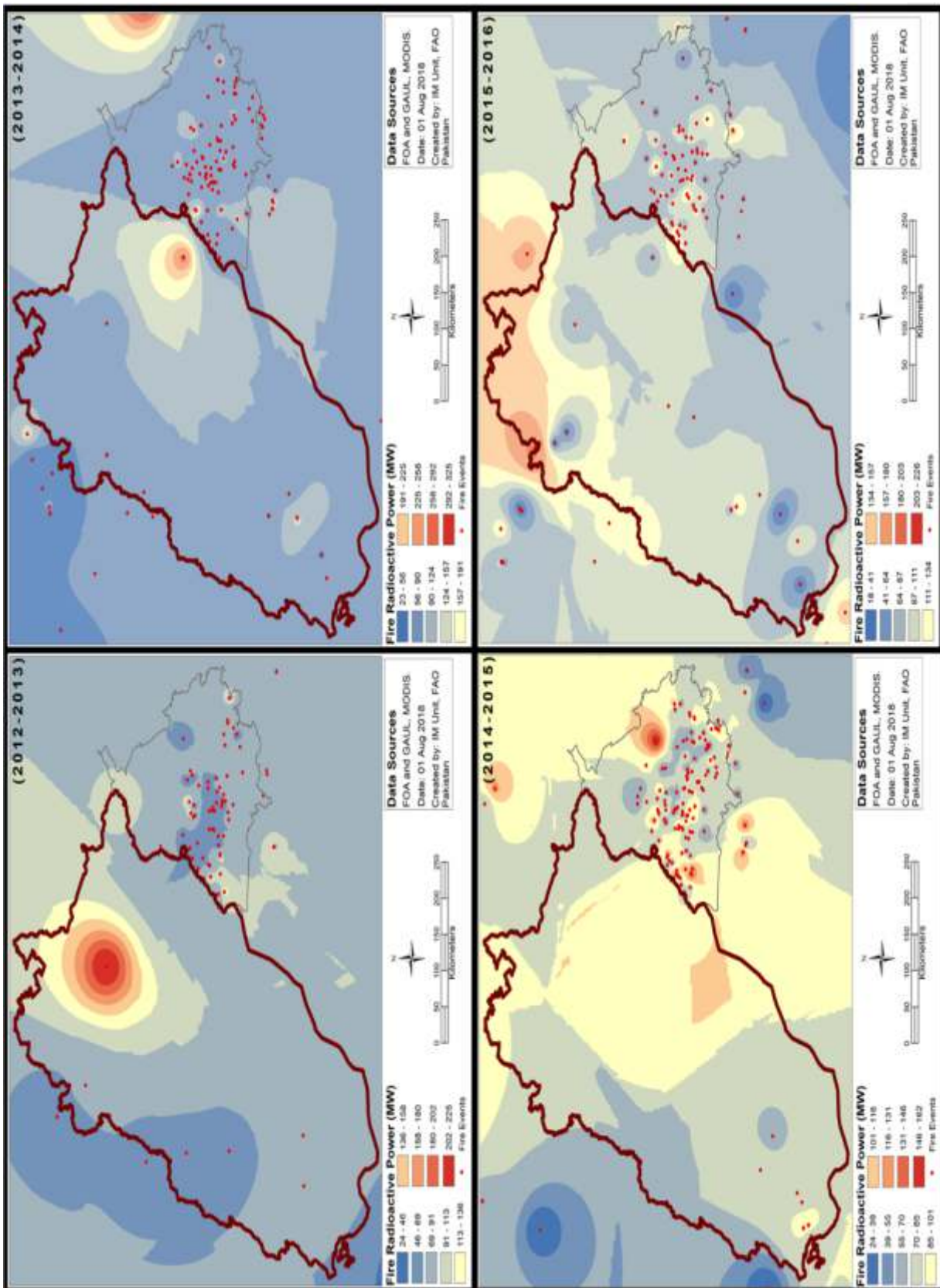
Source: Adapted from United Nations World map, February 2020.

APPENDIX G – YEAR WISE MAPPING OF FIRE EVENTS (2008–2018)



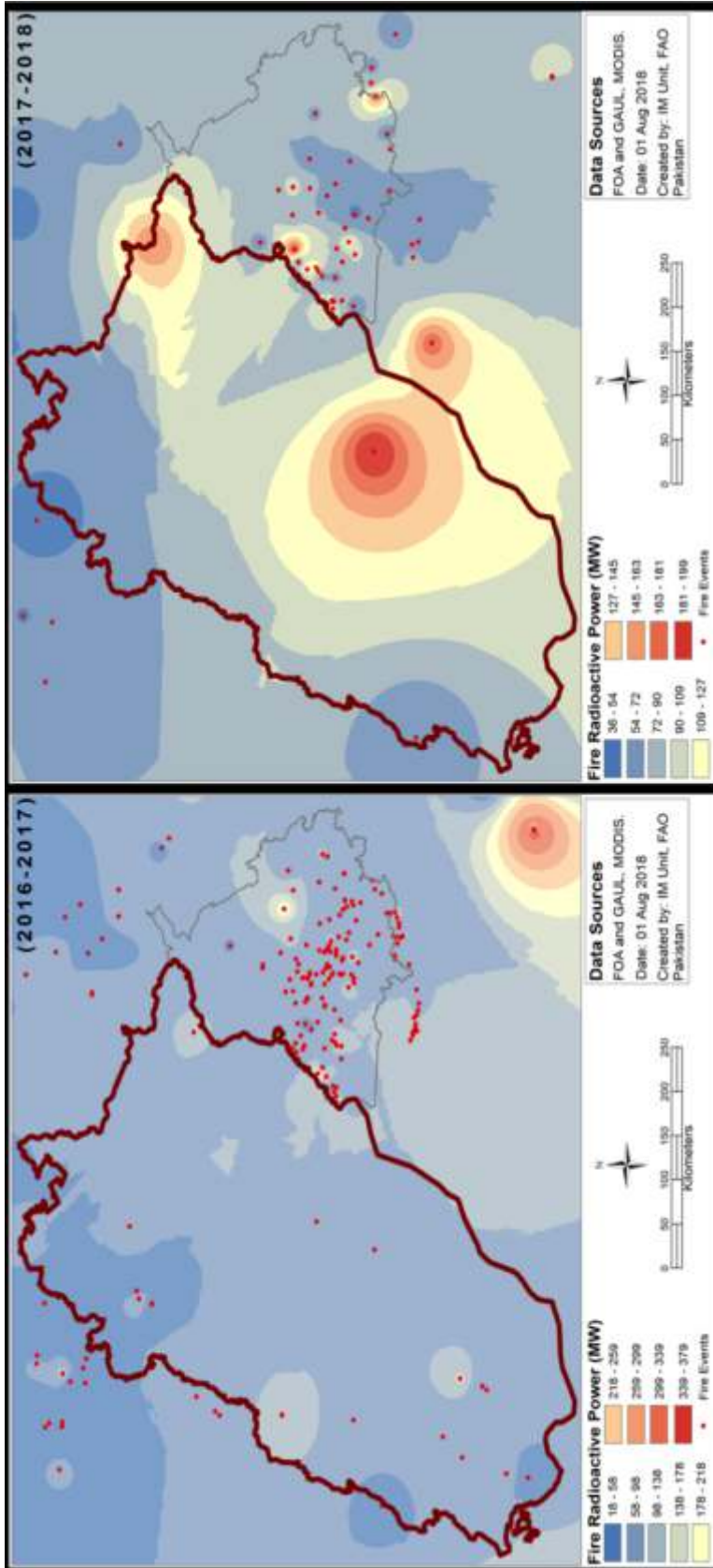
Disclaimer: The boundaries and names shown and the designation used on this map do not imply official endorsement or acceptance by the United Nations. Dotted line represents approximately the Line of Control in Jammu and Kashmir agreed upon by India and Pakistan. The final status of Jammu and Kashmir has not yet been agreed upon by the parties.

Source: Adapted from United Nations World map, February 2020.



Disclaimer: The boundaries and names shown and the designation used on this map do not imply official endorsement or acceptance by the United Nations. Dotted line represents approximately the Line of Control in Jammu and Kashmir agreed upon by India and Pakistan. The final status of Jammu and Kashmir has not yet been agreed upon by the parties.

Source: Adapted from United Nations World map, February 2020.



Disclaimer: The boundaries and names shown and the designation used on this map do not imply official endorsement or acceptance by the United Nations. Dotted line represents approximately the Line of Control in Jammu and Kashmir agreed upon by India and Pakistan. The final status of Jammu and Kashmir has not yet been agreed upon by the parties

Source: Adapted from United Nations World map, February 2020.

2019

REMOTE SENSING FOR SPACE-TIME MAPPING OF SMOG IN PUNJAB AND IDENTIFICATION OF THE UNDERLYING CAUSES USING GEOGRAPHIC INFORMATION SYSTEM (R-SMOG)

Food and Agriculture Organization of the United Nations, Pakistan initiated the Technical Cooperation Programme on Remote Sensing for Space-time mapping of Smog (R-SMOG) upon the request of the Government of Punjab. The R-SMOG evaluates the relationship between Smog and the rice residue burning practices by farmers in the Rice belt of Punjab. It is a comprehensive geospatial research which integrates Space-time mapping of smog viz-a-viz climatological modelling, study of seasonal trends and dynamics and estimates an inventory of sectoral emissions. The findings of the R-SMOG will assist to generate scientific evidences to study the causes of Smog in Punjab and to adopt adequate mitigation and adaptation strategies.

ISBN 978-92-5-131960-4



9 789251 319604

CA6989EN/1/03.20